IN VITRO EVALUATION OF EQUINE BONE MARROW-DERIVED MESENCHYMAL STROMAL CELLS TO COMBAT ORTHOPEDIC BIOFILM INFECTIONS

Sarah Marie Khatibzadeh

Dissertation submitted to the faculty of the Virginia Polytechnic Institute and State University in partial fulfillment of the requirements for the degree of

Doctor of Philosophy
In
Biomedical and Veterinary Sciences

Sophie H. Bogers, Co-Chair
Linda A. Dahlgren, Co-Chair
Clay C. Caswell
William A. Ducker

June 16, 2023
Blacksburg, VA

Keywords: biofilm, mesenchymal stromal cell, equine, orthopedic infection, regenerative medicine

IN VITRO EVALUATION OF EQUINE BONE MARROW-DERIVED MESENCHYMAL STROMAL CELLS TO COMBAT ORTHOPEDIC BIOFILM INFECTIONS

Sarah Marie Khatibzadeh

ACADEMIC ABSTRACT

Infections of fracture fixation implants and synovial structures are a primary cause of complications, increased treatment costs, and mortality in people and horses. Treatment failure is often due to biofilms that are communities of bacteria that are adhered to a surface or to each other and are surrounded in a self-secreted extracellular matrix. The biofilm matrix protects the indwelling bacteria from being killed by antibiotics and the immune system. Biofilms also stimulate chronic inflammation and tissue destruction, including peri-implant osteolysis and subsequent implant failure and chondromalacia with subsequent osteoarthritis. In horses, the resulting lameness, reduced athletic potential, and poor quality of life may necessitate euthanasia. Equine bone marrow-derived mesenchymal stromal cells (MSC) reduce inflammation and promote healing in musculoskeletal injuries and have recently been discovered to have antimicrobial properties. Equine MSC kill planktonic (free-floating) bacteria and prevent biofilm establishment in laboratory models. MSC from mice and people also promote the transition from acute inflammation to tissue regeneration (resolution of inflammation) by secretion of specialized pro-resolving lipid mediators (SPM). Whether equine MSC can disrupt established biofilms of orthopedic pathogens and modulate the inflammatory response to orthopedic biofilms is unknown.

Using a novel biofilm-MSC co-culture model, our objectives were two-fold. We investigated whether MSC alone or with amikacin sulfate, an antibiotic used to treat equine orthopedic infections, could reduce biomass, pellicle size, and live bacteria of biofilms of orthopedic infectious agents *S. aureus* and *E. coli*. Next, we investigated whether MSC could modulate immune response to *S. aureus* biofilms by reducing secretion of pro-inflammatory cytokines by peripheral blood mononuclear cells (PBMC) and by secreting SPM. MSC demonstrated partial ability to reduce biofilms but performed differently on *S. aureus* versus *E. coli* biofilms. Co-culture of biofilms with MSC significantly reduced pellicle area of biofilms of both bacteria, reduced biomass of *S. aureus* biofilms, and killed live *S. aureus* bacteria. MSC combined with amikacin also significantly reduced *S. aureus* biomass to a greater extent compared to amikacin alone. The resolution in detecting differences between groups for *E. coli* was diminished because of high variation between biofilms treated with MSC between different donors and between control biofilms between experiments.

Using the same experimental system, culture of *S. aureus* biofilms with MSC in the transwell inserts and PBMC in the bottom wells significantly reduced biofilm size compared to untreated biofilms. Co-culture of MSC and PBMC with *S. aureus* biofilms also significantly increased detection of multiple SPM on lipid chromatography-mass spectrometry compared to MSC or PBMC cultures alone. Using a commercial equine multiplex bead ELISA, multiple inflammatory cytokines and chemokines were increased when *S. aureus* biofilms were cultured with MSC and PBMC; however, these were not different from untreated biofilms. Our results indicate that the utility of MSC in combating orthopedic biofilm infections lies in their ability to disrupt the

biofilm matrix and promote inflammation resolution. These findings support continued investigation into and optimization of the anti-biofilm mechanisms of MSC.

IN VITRO EVALUATION OF EQUINE BONE MARROW-DERIVED MESENCHYMAL STROMAL CELLS TO COMBAT ORTHOPEDIC BIOFILM INFECTIONS

Sarah Marie Khatibzadeh

GENERAL AUDIENCE ABSTRACT

Biofilms are coating layers made by bacteria to protect them from being killed by antibiotics or the immune system. Biofilms result in untreatable infection, chronic inflammation and tissue destruction in people and horses with bone and joint infections. The resulting complications, including pain, reduced mobility, and poor quality of life, may result in horses being euthanized. Equine bone marrow-derived mesenchymal stromal cells (MSC) kill free floating bacteria in laboratory models and reduce inflammation in orthopedic injuries. Whether MSC can disrupt formed biofilms and reduce inflammation resulting from biofilm infections is unknown. Using a laboratory model, our objectives were to determine: 1) whether MSC alone or with an antibiotic used to treat orthopedic infections in horses can disrupt biofilms and kill indwelling live bacteria of orthopedic infectious agents *S. aureus* and *E. coli*, and 2) whether MSC can modify the immune response to *S. aureus* biofilms. MSC demonstrated some biofilm reducing ability but performed differently on *S. aureus* versus *E. coli* biofilms. Specifically, MSC reduced the size of biofilms of both bacteria, reduced the coating layer of *S. aureus* biofilms alone and to a greater extent when combined with the antibiotic, and killed live *S. aureus* bacteria. Using the same system, culture of MSC with *S. aureus* biofilms and peripheral blood mononuclear cells (PBMC), a type of white blood cell, reduced biofilm size compared to controls. The addition of

MSC and PBMC to *S. aureus* biofilms also increased detection of fatty acid-derived signals that promote resolution of inflammation, compared to controls. Multiple inflammatory cytokines and chemokines were increased with culture of MSC and PBMC with *S. aureus* biofilms but were not different from untreated biofilms. These results indicate that MSC may be useful to combat biofilm infections by breaking down the coating layer of biofilms and by promoting resolution of inflammation. Taken together, our results support continued investigation into the potential of MSC as a treatment for orthopedic biofilm infections. The potential of MSC to simultaneously break down biofilms and mitigate inflammation in orthopedic infections would improve cure rates and overall outcomes for horses and people afflicted with orthopedic biofilm infections.

DEDICATION

This dissertation is dedicated to our daughter, who is due on/around July 5, 2023 and has kept me pushing this body of work forward to completion. Gordon and I already love you so much and cannot wait to meet you!

ACKNOWLEDGEMENTS

I would like to express my sincere gratitude to my committee co-chairs, Dr. Sophie Bogers and Dr. Linda Dahlgren, for their continual support, guidance and mentorship in my PhD program and in my surgical residency. I would also like to thank my committee members, Dr. Clay Caswell and Dr. William Ducker, for their support and invaluable insight during my program. Many thanks to Dr. Stephen Werre for sharing your statistical wisdom with me over the years and for your contributions to this research. I have learned so much from each and every one of you and will strive to build on your teachings going forward!

A special acknowledgement to my funding sources: the Office of Research and Graduate Studies, the Regenerative Medicine Interdisciplinary Graduate Education Program, the Equine Research Competition at the VA-MD College of Veterinary Medicine, and the Morris Animal Foundation Large Animal Training Fellowship. Your generous support has made my program and this body of work possible.

I would also like to extend thanks to Dr. Ansar Ahmed, Dr. Jessica Crawford, and Andrea Green for helping me navigate the ins and outs of the graduate school during my MS and PhD programs. Special thanks to Nancy Tenpenny (Center for One Health Research) and Michelle Todd (Collaborative Multidisciplinary Research Laboratory) for their kind support and guidance with my experimentation over the years. I would like to include a shout-out to all of the undergraduate and DVM students who have contributed to this work and whom I have mentored. It has been a treat to work with you and watch you grow, and I wish you all the best in your

future endeavors. Additionally, a big thank you to all of the ACVS Diplomates and veterinarians who have trained, influenced, and inspired me over the years!

Many thanks to my parents, Dr. Mohammad Ali and Laura Khatibzadeh, my sisters, Drs. Natalie and Julia Khatibzadeh, my amazing friends and colleagues, and fur-babies past and present (Joker, Windsor, Coco) for their unconditional love and support over all of these years. I would not have made it to this point in my life without you. Much love and gratitude to my wonderful husband of 9 years and partner-in-crime of almost 16 years, Dr. Gordon Briggs. Words cannot express how fortunate I am to have you as my husband and as the father of our growing family.

TABLE OF CONTENTS

LIST OF FIGURES

.

LIST OF TABLES

ABBREVIATIONS

AA	Arachidonic acid
MSC	Equine bone marrow-derived mesenchymal stromal cell
CFU	Colony-forming unit
DHA	Docosahexaenoic acid
DiHETE	Dihydroxyeicosatetraenoic acid
DMEM	Dulbecco's modified Eagle's medium
DoHE	Dihydroxydocosahexaenoic acid
MSC	Equine bone marrow derived mesenchymal stem cell
E. coli	*Escherichia coli*
ELISA	Enzyme-linked immunosorbent assay
EPA	Eicosapentaenoic acid
EPS	Extracellular polymeric substance
FBS	Fetal bovine serum
FGF-2	Fibroblastic growth factor 2
G-CSF	Granulocyte colony stimulating factor
GM-CSF	Granulocyte-macrophage colony stimulating factor
GRO	Growth-regulated oncogene/keratinocyte chemoattractant
HEPE	Hydroxyeicosapentaenoic acid
HETE	Hydroxyeicosatetraenoic acid
IFN-γ	Interferon-gamma
IL-1α	Interleukin 1 alpha
IL-1β	Interleukin 1 beta
IL-2	Interleukin 2
IL-4	Interleukin 4
IL-5	Interleukin 5
IL-6	Interleukin 6
IL-8	Interleukin 8
IL-10	Interleukin 10
IL-12	Interleukin 12
IL-13	Interleukin 13
IL-17A	Interleukin 17A
IL-18	Interleukin 18
IP-10	INF-γ inducible protein 10
LC-MS	Lipid chromatography-mass spectrometry
LPS	Lipopolysaccharide
LB broth	Luria-Bertani broth
LTB_4	Leukotriene B4
LXA_4	Lipoxin A4
MaR	Maresin
MSC	Mesenchymal stromal cell
OD	Optical density
PBMC	Peripheral blood mononuclear cells

PBS	Phosphate buffered saline
PGE_2	Prostaglandin E2
PGF2 α	Prostaglandin F2 alpha
PD	Protectin
RANTES	Regulated Upon Activation, T cell Expressed, and Secreted
RvE1	Resolvin E1
RvE2	Resolvin E2
SPM	Specialized pro-resolving mediators
S. aureus	*Staphylococcus aureus*
TNF- α	Tumor necrosis factor alpha
TSA	Tryptic soy agar
TXB_2	Thromboxane B2

OVERVIEW OF DISSERTATION

Chapters 1 and 2 of this dissertation comprise the Literature Review. Chapter 1 discusses the impact of biofilms on clinical orthopedic infections in people and horses, and the need for an improved treatment for these infections. Biofilms in orthopedic infections protect bacteria from antimicrobials and the immune system, thereby causing persistent infection, chronic inflammation and secondary tissue damage. The resulting complications increase treatment duration, costs, complications, and mortality in people and horses. The remainder of Chapter 1 discusses biofilm biology in general and as applicable to orthopedic infections, and the mechanisms by which biofilms enhance antimicrobial resistance and inflammation-related tissue destruction.

Chapter 2 focuses on current diagnostic and treatment strategies for orthopedic biofilm infections, their limitations, and how mesenchymal stromal cells may improve treatment success. Additionally, Chapter 2 discusses current research models to evaluate biofilm reductions by novel treatments and the necessity for a simple *in vitro* model to evaluate paracrine biofilm-MSC interactions.

Chapters 3-5 comprise manuscripts targeted for publication that summarize the research objectives, approaches, and key findings of this dissertation. Our first objective, as described in Chapter 3, describes development of an *in vitro* transwell co-culture model to quantify MSC-mediated reduction of established biofilms of two orthopedic biofilm pathogens, *S. aureus* and *E. coli*. Our model was developed to allow assessment of interaction between biofilms and MSC alone or combined with amikacin sulfate, an aminoglycoside antimicrobial commonly used to

treat equine orthopedic infections. Furthermore, our model permits ready quantification of reductions in established biofilm biomass, pellicle size, and live bacteria following co-culture with MSC with or without amikacin.

Using the model described in Chapter 3, Chapter 4 describes evaluation of equine bone marrow-derived MSC-mediated reduction of biomass, pellicle size, and live bacteria of established biofilms of *S. aureus* and *E. coli.* Results from this study demonstrated that MSC reduced biofilm organization and pellicle size of both bacteria, with reduced *S. aureus* biomass. Live bacterial counts and reduction of *E. coli* biofilms were more variable. Chapter 4 provides a foundation for continued investigation into the antibiofilm mechanisms of MSC.

The potential for MSC to have multi-modal activity in biofilm infections led us to investigate the immunomodulatory properties of MSC in response to biofilms (Chapter 5). Using the same model, the final experimental chapter describes evaluation of the potential of MSC to modulate the immune cytokine/chemokine response of peripheral blood mononuclear cells to *S. aureus* biofilms and to promote resolution of inflammation via secretion of specialized pro-resolving lipid mediators. This experiment demonstrated increased lipid mediators when MSC were added to a co-culture system, with more variable results for cytokines and chemokines. This study suggests that secretion of SPM may be a key mechanism by which MSC modulate the immune response to biofilms.

Finally, Chapter 6 summarizes the key conclusions of this dissertation and a discussion of areas of future investigation into the antibiofilm potential of MSC.

CHAPTER 1: THE THREAT OF BIOFILMS IN ORTHOPEDIC INFECTIONS

Introduction

The advent of surgical techniques to repair fractures by placement of indwelling metallic implants (internal fixation), replace diseased joints with prostheses (arthroplasty), and treat infected synovial structures (joints, tendon sheaths, bursae) represent a monumental advance in human and veterinary medicine over the last century [1-10]. However, orthopedic infections, including infections of fracture fixation or arthroplasty implants and synovial structures, remain a significant challenge to patients, their treating clinicians, and the healthcare system. In the United States alone, over 2% of arthroplasties in people become infected at an annual cost of $1.62 billion/year [11]. Additionally, 20-30% of fracture repairs in people become infected, with medical costs being 2-6.5 times greater than for non-infected repairs [12, 13]. Horses likewise suffer from natural orthopedic infections, with current rates of fracture fixation infections ranging from 11-28% [1, 14, 15]. Septic synovitis also represents one of the most common emergencies encountered in equine medicine [7, 10, 16-18] and is often acquired following penetrating wounds in adults [17, 19, 20] or via hematogenous (blood-borne) spread from other sites of infection in foals [9, 10, 18].

One of the greatest hurdles encountered in resolving orthopedic infections in people and horses is the formation of bacterial biofilms on metallic fracture fixation implants [12, 14, 15], arthroplasties [11, 21, 22], and on and within the adjacent bones [23-26], soft tissues [25], and synovial fluid [27-31]. *Staphylococcus aureus* (*S. aureus*), a Gram-positive coccus, and

Escherichia coli (*E. coli*), a Gram-negative bacillus, are two common orthopedic infectious agents isolated from people [32-35] and horses [10, 14, 15, 17]. *S. aureus* and *E. coli* readily form biofilms on metallic implants and bones [14, 36-39], and as floating aggregates within synovial fluid [27-31, 40]. The formation of biofilms protects indwelling bacteria against antimicrobials [28, 30, 41, 42] and the immune system [43-47], thereby enabling infections to persist in the face of treatment. Persistent biofilm infections simultaneously cause complications by stimulating a chronic inflammatory response and secondary tissue destruction [24, 48-50]. In infected implants, persistent inflammation leads to activation of osteoclasts with peri-implant osteolysis (bone dissolution) and subsequent implant loosening and failure [14, 24, 36, 51]. In infected synovial structures, release of matrix metalloproteinases from polymorphonuclear leukocytes causes chondromalacia (cartilage destruction) and osteoarthritis [7, 36], or tendon matrix degradation and development of painful adhesions between the tendon and the surrounding sheath [17, 19, 20].

The consequences of persistent biofilm infections and the associated inflammatory-mediated tissue damage are dire. While long-term antimicrobial therapy is a mainstay of orthopedic infection treatment [12, 33, 52], one-third of people with implant infections additionally need one or more surgeries to remove and replace infected implants, a process that can take over a year and reduce patient mobility, comfort, and quality of life [11, 33, 53, 54]. If surgery and antimicrobial therapy fail to resolve the infection, amputation of the affected limb becomes necessary [33, 55, 56]. Persistent biofilms are also a nidus for bacterial dissemination, which worsens persistence of the orthopedic infection via re-seeding of the original site and can cause life-threatening infections of vital organs or the bloodstream (sepsis) [22, 33, 42, 56]. Due to

these dangerous sequelae, 26-55% of people with orthopedic implant infections die within 5 years of diagnosis [12, 21, 33].

Horses with refractory orthopedic biofilms infections likewise suffer a markedly reduced prognosis due to persistent lameness and associated secondary complications, including support limb laminitis, loss of athletic ability, poor quality of life, and treatment costs that exceed the ability of clients to pay [17, 36, 57]. As such, 6-56% of horses with orthopedic infections are subjected to euthanasia due to failure to respond to treatment [1, 14, 15, 17]. The development of an orthopedic infection reduces prognosis for horse survival to hospital discharge; only 59% of horses with infected fracture repairs survived to discharge, compared to 92% of horses without infected repairs [14]. In another retrospective study, horses with fracture fixation surgical site infections were 12 times less likely to survive to discharge than horses without infections [15]. The risk of developing implant-associated infection in fracture repairs increases, and prognosis decreases, with fractures open to the environment (bone fragments penetrating the skin) versus closed fractures [14]. Horses with open fractures were 4.23 times more likely to develop an implant-associated infection, and 4.59 times less likely to survive to hospital discharge, compared to horses with closed fractures [14].

Given the grim economic and patient welfare outcomes associated with orthopedic biofilm infections, there is an urgent need to develop treatment that will disrupt orthopedic biofilms, reduce the inflammatory response to these biofilms, and improve the success of surgery and antimicrobials.

Biofilm Biology in Orthopedic Infections

Biofilm definition and structure

A biofilm consists of bacteria adhered to a surface or to each other and encased in a self-secreted extracellular polymeric substance (EPS), also known as the biofilm matrix (Fig 1.1) [46, 58-60]. The core of the biofilm is relatively hypoxic [61, 62], nutrient-poor [63], and rich in waste products [42, 64] compared to the biofilm periphery. The oxygen and nutrient gradients have important implications for antimicrobial resistance [63, 65]. The matrix is primarily composed of bacterial-secreted carbohydrates [66, 67], proteins [60, 68], extracellular DNA (eDNA) [46, 69, 70], and lipids [47, 58]. The majority of biofilm matrix eDNA is derived from autolysis of indwelling bacteria [46, 70] and is important for initial bacterial attachment to surfaces [70] and stabilization of the biofilm matrix [46, 70].

The composition of biofilm matrix components varies between bacterial species and reflects adaptation to colonization of specific biological niches. Both *S. aureus* and *E. coli* biofilms contain *N*-acetyl glucosamine as a primary carbohydrate source [71, 72]. However, a polymer of *N*-acetyl glucosamine residues called polysaccharide intercellular adhesin (PIA) comprises the majority of matrix carbohydrate in the *S. aureus* biofilm [71], whereas the *E. coli* biofilm matrix also contains cellulose [66]. The primary protein components of *S. aureus* biofilms are microbial surface components recognizing adhesive matrix molecules (MSCRAMM) [60], a set of adhesion proteins that recognize and bind host extracellular matrix proteins, with amyloid fibrils making a smaller contribution [73]. The protein composition of the *S. aureus* biofilm thereby enables *S. aureus* to readily colonize and form biofilm on host tissues, including wound surfaces

[74] and bones [75]. In comparison, *E. coli* biofilms are rich in curli, a fimbrial amyloid protein [68, 76, 77]. Curli facilitates *E. coli* attachment to abiotic surfaces, such as those found on medical devices [77-79], and to host fibronectin [80]. Additionally, the tertiary structure of curli consists of tightly packed, parallel β-sheets that confer rigidity to the biofilm matrix and resistance to overlying fluid shear stresses [68, 76]. Type I fimbrial proteins known as pili also facilitate initial *E. coli* attachment to abiotic surfaces [81].

In contrast to matrix eDNA, carbohydrates and proteins, the roles of lipids in the matrix of *S. aureus* and *E. coli* biofilms are less understood but may be important in biofilm formation. The O-antigen of lipopolysaccharide (LPS) is derived from the outer membrane of *E. coli* and is important in cell adhesion and biofilm matrix synthesis [82]. The matrix of early *S. aureus* biofilms is lipid-rich, which may protect against diffusion of antimicrobials or other environmental threats into the interior of the biofilm [83]. It was recently discovered that the lipid component of *S. aureus* biofilm is primarily comprised of phospholipids that are stratified by chain length along the oxygen gradient in the matrix, the function of which is unknown [84].

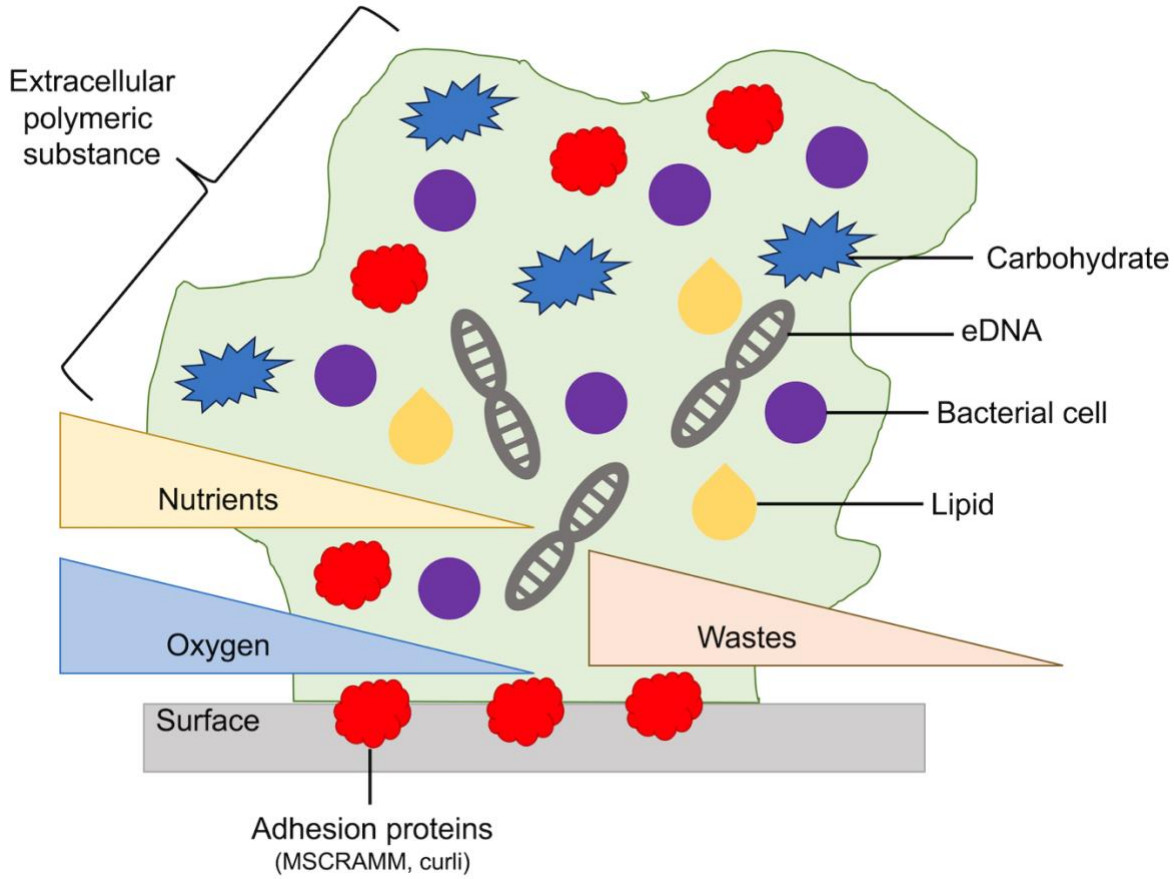

Figure 1.1: Biofilm structure. Biofilms consists of bacterial cells adhered to a surface or to each other and encased in a self-secreted matrix of carbohydrates, proteins, eDNA, and lipids. The concentrations of oxygen and nutrients are lowest, and the concentration of wastes are highest, in the biofilm core.

As often depicted in scientific illustrations, biofilms grown in static *in vitro* culture systems typically form pellicles, which are globular structures adhered to the base of the container and extending vertically to the liquid-air interface at the site of highest oxygen concentration [85]. However, biofilms in natural environments can also form as floating aggregates in fluid media [27-31], adhered small aggregates on surfaces [74, 86, 87], or sheet-like structures [85, 88, 89]. The environmental nutrient concentration [72, 77, 85, 90], material surface properties [32, 78,

91, 92], medium viscosity [29, 40], and shear stress applied by the medium in conditions of active overlying fluid movement [90, 93-95] can influence the degree of biofilm formation and the final morphology.

Polymicrobial biofilms

While biofilms of single bacterial species are often studied in experimental conditions [87, 89, 90, 96-98], biofilms in natural infections of multiple body systems often contain multiple co-existing bacterial species (polymicrobial) [38, 67, 99-101]. The formation of polymicrobial biofilms can provide unique opportunities for resource sharing between [102], and mutual protection of, the indwelling bacteria via enhanced adhesion [103, 104], matrix production [67] and inter-species transfer of mobile genetic elements encoding antimicrobial resistance genes [102]. The relative hypoxia in the biofilm core also favors co-existence of anaerobic organisms alongside aerobic organisms [62]. While standard bacterial culture/susceptibility testing often grows the most abundant organism in the sample [10, 17, 105, 106], genetic-based techniques including polymerase chain reaction and next generation sequencing have more recently been utilized to diagnose polymicrobial orthopedic infections in people [38] and horses [17, 99, 107]. The potential for polymicrobial biofilm infections in equine orthopedic infections likewise warrants further exploration, particularly in septic synovitis caused by penetrating wounds with environmental contamination [17, 19, 36].

Phases of biofilm formation

Biofilm formation follows 4 phases (Fig. 1.2), beginning with initial temporary interactions with the target surface, including electrostatic [70, 108] and van der Waals interactions [109]. For *E.*

coli, flagella-powered swimming motility is also important for initial surface colonization, with eventual biofilm formation directly proportional to the motility of a given strain [110]. Next, bacteria form irreversible attachments to the surface via secretion of adhesion proteins [60, 78]. The ability of *S. aureus* and *E. coli* to secrete adhesion proteins that target abiotic surfaces [78, 111] and host extracellular matrix proteins [60, 75, 80] facilitates biofilm formation on orthopedic implants and tissues. Examples of target host proteins include fibronectin [60, 80], fibrinogen [80], collagen [75], von Willebrand factor [95], and bone sialoprotein [75]. Once attached, bacteria replicate and secrete the biofilm extracellular matrix components [71, 87, 89, 94, 112]. The regulatory mechanisms for bacterial attachment and matrix secretion involve multi-gene units (operons) that are specific to bacterial species [59, 113, 114]. For *S. aureus*, production of matrix PIA is regulated by the *icaADBC* operon [113], which encodes the enzymes that synthesize PIA. For *E. coli*, cellulose production is regulated by the *bscA* operon [59], while matrix proteins *curli* is encoded by the *csgBAC* operon and pili are encoded by *fim* genes [114]. Once synthesized, the biofilm matrix undergoes additional maturation, including conformational changes in eDNA that confer additional matrix stability [46] and formation of pores and channels that distribute nutrients, water, and waste products throughout the matrix [64, 115].

.

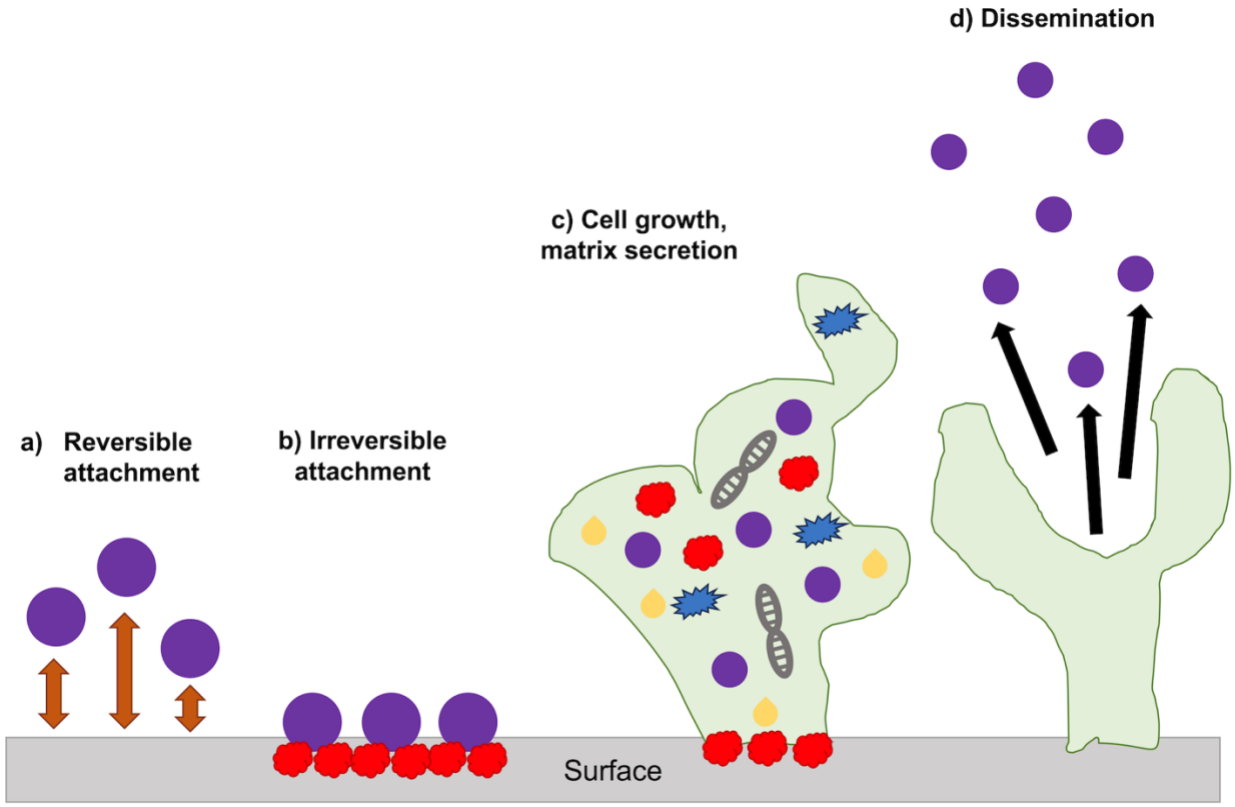

Figure 1.2: Stages of biofilm formation. Biofilm formation requires attachment of bacteria to a surface or to each other via a) initial temporary surface interactions, b) irreversible attachment, and c) cell growth and matrix secretion. Biofilm dissemination d) follows when bacterial cell density within the biofilm reaches a threshold and allows bacterial colonization of distant sites.

The final stage of biofilm formation is dissemination. Endogenous proteases and endonucleases dissolve the matrix and liberate the indwelling bacteria, which subsequently colonize other sites. The transition between matrix production and dissemination is regulated by quorum sensing, a process through which bacteria regulate gene expression and biofilm formation proportionate to their population density [115-118]. Quorum sensing systems rely on production of an autocrine

signal, the levels of which reflect bacterial population density [119, 120]. Upon detection of this signal at a threshold concentration, downstream intracellular signaling cascades reduce expression of genes important in biofilm matrix formation genes and increase expression of genes that promote matrix dissolution and bacterial motility to disperse the biofilm [59, 116, 117].

In *S. aureus*, the accessory gene regulatory (*agr*) system is the primary driver of quorum sensing in biofilm formation and dispersion [116]. The autocrine signal is an autoinducer peptide (AIP) with a thiolactone ring structure [119]. This system consists of 4 genes that regulate and encode the AIP synthesizing and modifying enzymes, receptor, and response regulator that modify biofilm synthesis according to cell density (Fig 1.3) [121, 122]. During bacterial attachment and biofilm matrix production, AIP is synthesized by AgrD and is modified by AgrB [119]. When *S. aureus* population density within the biofilm reaches a threshold concentration, AIP binds AgrC, which phosphorylates AgrA [119]. The phosphorylated AgrA then stimulates transcription of regulatory RNA III to increase transcription of proteases and phenol-soluble modulins, small amphipathic proteins that disrupt the biofilm matrix in a detergent-like manner [121, 122]. Simultaneous repression of biofilm matrix protein expression, including fibronectin binding proteins, is achieved through interaction of AgrA with the separate *sarA* locus [123].

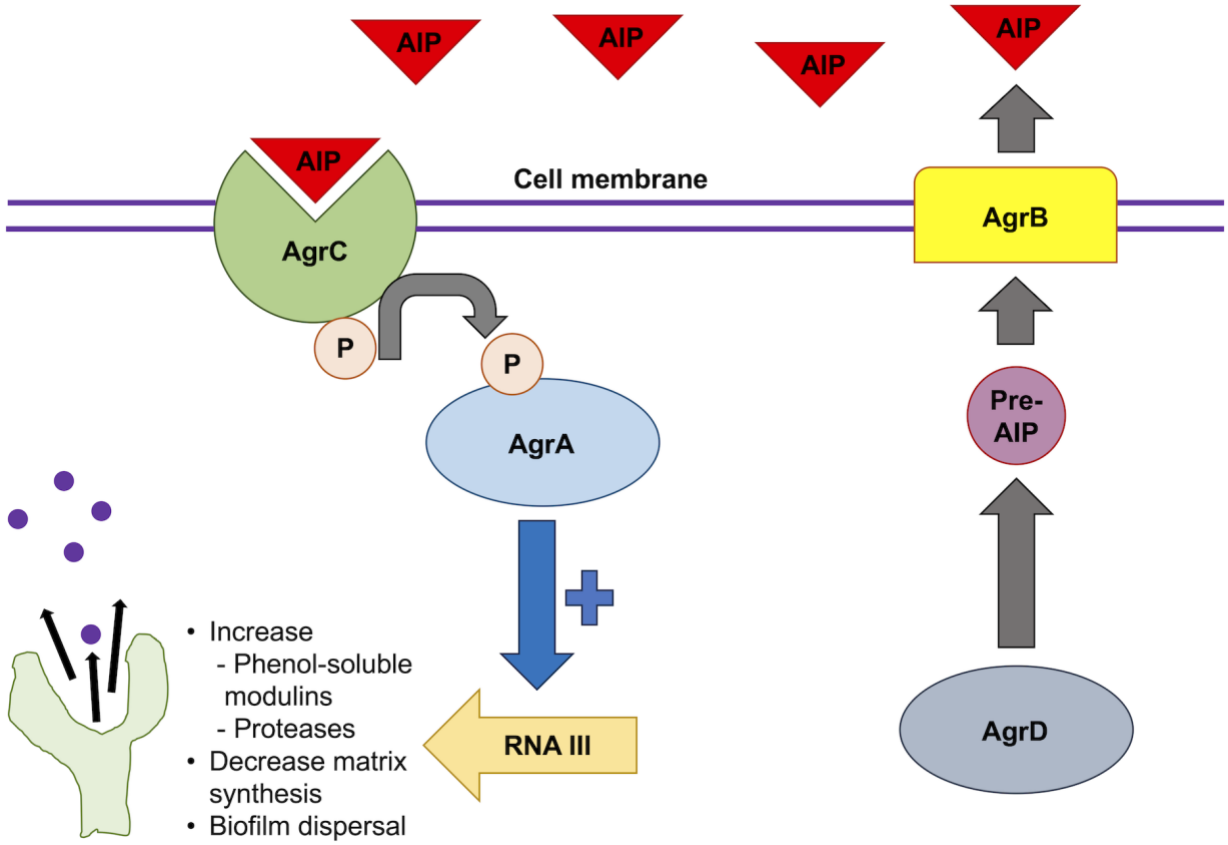

Figure 1.3: The *agr* system of quorum sensing in *S. aureus* regulates biofilm formation and dispersal. This system consists of 4 genes controlled by a regulatory RNA: *agrD* encodes the autoinducer peptide. *agrB* encodes a membrane-bound enzyme that post-translationally the AIP. *agrC* encodes the membrane-bound AIP receptor. *agrA* encodes the DNA binding protein response regulator. AgrC and AgrA form a 2-component system that detects levels of the autocrine signal AIP and modifies synthesis versus disruption of biofilm matrix according to cell density within the biofilm [122].

In comparison to *S. aureus*, Gram-negative organisms utilize the AI-1 quorum sensing system in regulating biofilm formation and dispersal (Fig 1.4) [59, 116]. The autocrine signal in this system is the acyl homoserine lactone molecule, which is synthesized by AI-1 synthase (encoded by *luxI*) and is detected by the AI-1 response regulator (encoded by *luxR*) once bacterial density reaches a threshold [120]. While *E. coli* cannot synthesize acyl homoserine lactone, it encodes a *luxR* homolog through the *sdiA* gene, which detects homoserine lactone molecules produced by other bacterial species. Binding of homoserine lactones to SdiA upregulates expression of genes that promote fimbrial expression [124], flagellar motion and bacterial motility through the Motility QS regulator (MqsR) and the *flhDC* regulon [125] to promote bacterial dispersal from the biofilm.

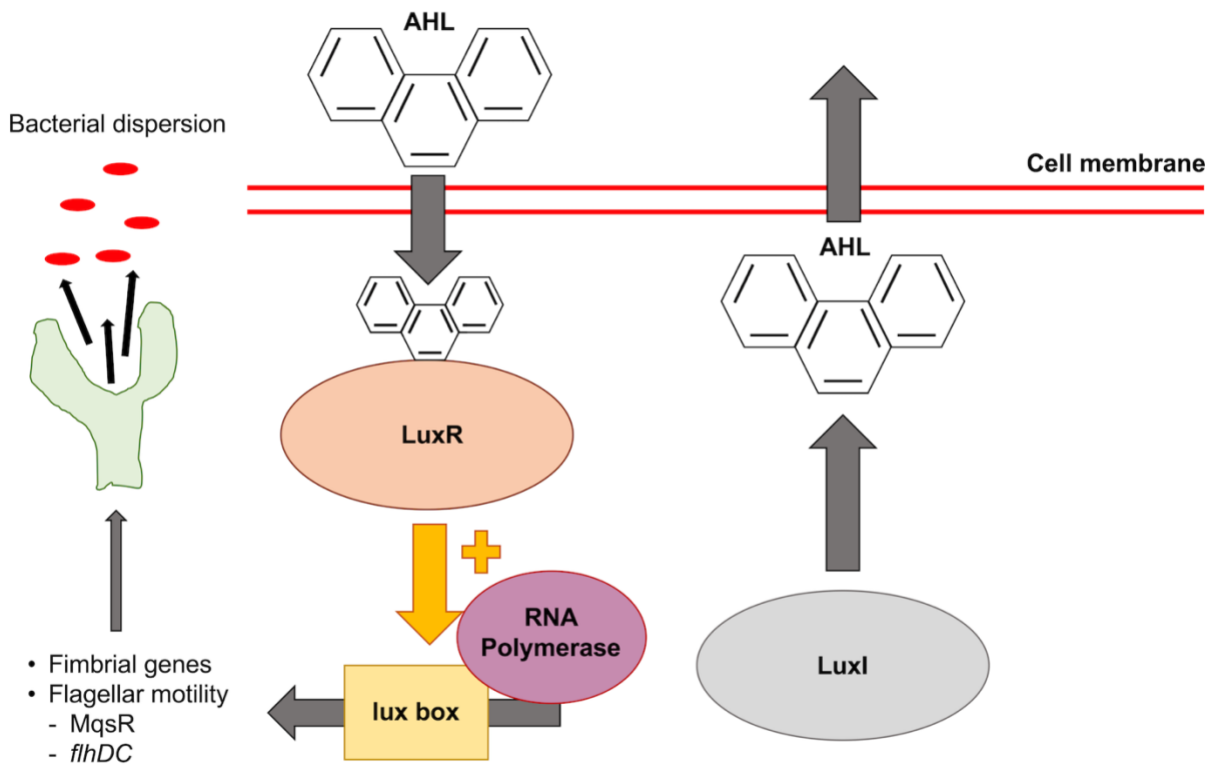

Figure 1.4: The AI-1 quorum sensing system in Gram-negative organisms.

LuxI generates the acyl homoserine lactone (AHL) signal. Acyl homoserine lactone is detected by LuxR when cell density reaches a threshold, leading to expression of genes that encode fimbiral proteins and regulate bacterial motility to promote biofilm dispersion. In *E. coli*, a luxR homolog SdiA detects homoserine lactones released by other bacterial species.

Biofilm formation within the orthopedic environment: unique niches for establishment and persistence of infections

Metallic implants: the "race for the surface"

Fracture fixation and arthroplasty implants provide an ideal environment for biofilm formation as they are designed to promote rapid integration with host tissues [32, 43, 126-128]. Orthopedic implants are minimally immunogenic [127, 129, 130] and promote cell attachment [32, 127]. Implants are also rapidly coated in host proteins following placement, a process known as "conditioning," which further facilitates bacterial attachment [32, 75, 128]. Successful implant integration and fracture healing requires formation of new bone via direct primary healing between osteons [131] or secondary ossification of a cartilaginous soft callus [131] and can take a minimum of 12 weeks in the absence of infection and interfragmentary motion [1, 14, 15, 130, 131]. Progression of appropriate healing before bacteria can form biofilms on implants and surrounding bone has thereby been dubbed a "race for the surface" [128].

Bone and soft tissues

Bones provide a multitude of surfaces and privileged sites for bacterial attachment and biofilm formation. The periosteum, endosteum, and the canaliculi are examples of such sites of attachment (Fig 1.5) [23, 24, 26, 132, 133]. Biofilms can form within abscesses in the soft tissues surrounding bones and joints [25, 134] and provide an additional reservoir of persistent infection in septic osteomyelitis and synovitis cases. As discussed in Chapter 2, surgical removal of infected implants, bone and soft tissue aims to eliminate these sources of biofilm infection.

However, the inability to diagnose and remove all microscopic reservoirs of infection intraoperatively can complicate eradication of infection and lead to infection persistence [36, 56].

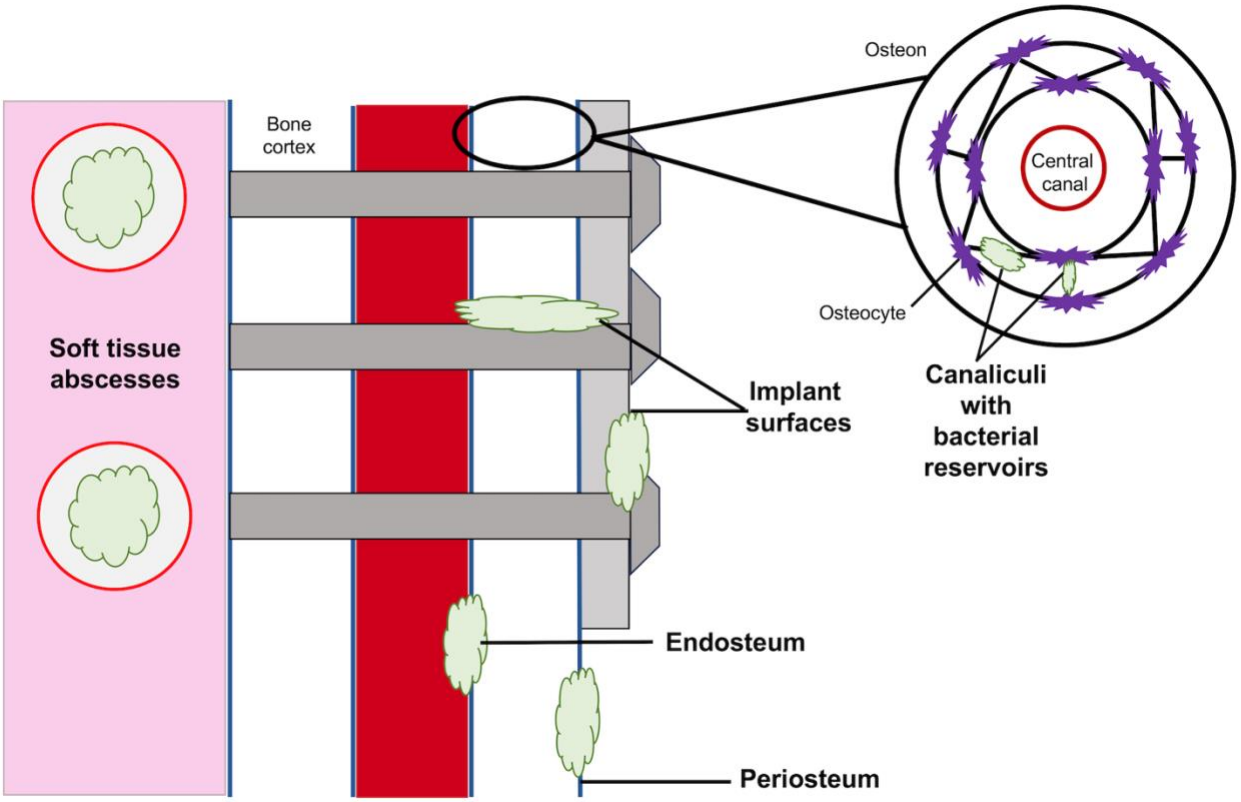

Figure 1.5: Longitudinal and cross-sections of a long bone to demonstrate sites for biofilm formation in an implant-associated infection. The surface of implants (e.g., plates and screws), the periosteum, endosteum, canaliculi, and surrounding soft tissues provide reservoirs for persistent biofilm infection.

Synovial fluid

Synovial fluid itself promotes bacterial cell-cell adhesion and formation of floating biofilm aggregates by Gram-positive and Gram-negative species [27-31, 40, 135]. The mechanisms by which synovial fluid promotes biofilm aggregate formation are further enhanced in an inflammatory environment following surgical intervention or establishment of infection [28, 136, 137]. Synovial proteins fibrinogen and fibronectin promote bacteria aggregation and matrix formation [27, 30], a phenomenon which is enhanced by elevations in these proteins during inflammation [28, 136]. Hyaluronan, a non-sulfated glycosaminoglycan molecule that is abundant in synovial fluid, also encourages bacterial aggregation and is incorporated into the biofilm matrix [29]. Reductions in synovial fluid viscosity with infection [138] and/or post-surgical inflammation [137] also encourage bacterial aggregation and bridging of biofilm matrix polymers [40]. The inflamed synovial structure thereby represents an optimal environment for formation of biofilms and a reservoir of persistent infection.

How Biofilms Cause Treatment Failure in Orthopedic Infections

Antimicrobial resistance

One of the overarching causes of treatment failure of orthopedic biofilm infections is the ability of these infections to resist antimicrobial therapy. The biofilm matrix itself inhibits penetration of antimicrobial drugs and prevents their access to the indwelling bacteria [28, 65, 139]. Bacteria within biofilms also undergo metabolic downregulation [68, 87, 140], particularly in the central, relatively hypoxic and nutrient-poor region of the biofilm [87]. The hypometabolic state confers additional resistance to currently available antimicrobial drugs that target bacterial cell

replication pathways, including protein synthesis, cell wall synthesis, and DNA replication [28, 30, 41, 141]. Bacteria within biofilms also express [41] and exchange antimicrobial resistance genes [142] at a higher rate than in planktonic cultures. These phenomena may be enhanced in multispecies biofilms as compared to single species biofilms [143]. The hypoxic environment in the biofilm core can also promote antimicrobial resistance by increasing expression of genes encoding antimicrobial efflux pumps [61]. Additionally, the biofilm matrix can provide a reservoir for bacterial antimicrobial resistance factors by sequestering enzymes that degrade antimicrobials, such as beta-lactamases [144].

As a result of the multiple antimicrobial resistance mechanisms enabled by the biofilm, the minimum inhibitory concentrations (MIC) of commonly used antimicrobials for indwelling biofilm bacteria can be increased from hundreds [30, 145] to several thousands of times [28, 146] the MIC of planktonic cultures. Exposure of biofilm-bound bacteria to sub-therapeutic concentrations of antimicrobials can, in turn, enhance biofilm formation [147]. Exposure of 15 strains of *S. aureus* to low concentrations of beta-lactamase antimicrobials increased biofilm matrix formation up to 10-fold compared to non-exposed strains via release of eDNA from lysed bacterial cells [147]. Increased biofilm maturity can likewise augment resistance to antimicrobials due to continued reductions in indwelling bacterial metabolism with biofilm aging [35]. Taken together, the effective antimicrobial resistance of biofilm-bound bacterial strains genetically susceptible to all or most antimicrobials in their planktonic form can equal the resistance levels of multi-drug resistant strains [146]. This scenario poses a frustrating conundrum to clinicians in choosing appropriate antimicrobial drugs, concentrations and delivery

routes based on routine susceptibility testing of clinical samples, which measure antimicrobial MIC for planktonic forms of isolates [41, 105, 146, 148].

Biofilm-immune system interactions

The biofilm matrix physically shields the indwelling bacteria against the host immune response by multiple mechanisms [44, 46, 47, 149, 150]. The matrix protects bacteria against phagocytosis [149, 151] and killing by neutrophil extracellular traps (NETs), webs of host extracellular DNA and antimicrobial proteins that destabilize bacterial cell membranes [44, 45, 150]. Conformational changes in matrix eDNA [46] or formulation of insoluble amyloid fibers [73] as biofilms mature further increases resistance to phagocytosis [149] and to host DNases and proteases [46]. The presence of orthopedic implant infections can indirectly reduce the ability of immune system to clear biofilms. Wear particles released from metallic implants over time can trigger a chronic, low-grade foreign body response, ultimately leading to a phenomenon called "immune exhaustion" [152]. The result is that the implant site is vulnerable to biofilm establishment and persistence [152].

In addition to avoiding host immunity, *S. aureus* and *E. coli* biofilms also directly trigger the host inflammatory response by stimulating host pattern recognition receptors and enhancing recruitment and activation of inflammatory cells. *S. aureus* biofilms stimulate inflammatory cytokine release [151], neutrophil chemotaxis and phagocytosis [151], and activation of Th1/Th17 T-lymphocytes [49]. Additionally, *S. aureus* implant-associated infections produce a marked inflammatory cell influx [132] and increased gene expression of inflammatory cytokines interleukin (IL)-1β and -6 and toll-like receptor (TLR)-2 [24]. Moreover, *S. aureus* biofilms

increase expression of nuclear factor kappa-B (NF-κB) ligand (RANKL) on osteoclasts [24], leading to osteoclast activation and peri-implant osteolysis [23, 24, 133]. LPS in the *E. coli* biofilm matrix also stimulate inflammation by binding TLR-4 on host immune cells and increasing expression of IL-1β, -6 and -8 [153]. The *E. coli* biofilm matrix adhesion protein curli also stimulates inflammatory cytokine gene expression by binding host TLR-2 and subsequent activating the NF-κB pathway [154].

Aggravation of the immune response by biofilms can promote further biofilm formation in a vicious cycle. Biofilms utilize the host immune response to their advantage through mechanisms that enable them to persist. For example, *S. aureus* uses host fibrin to form biofilm aggregates in synovial fluid [27, 30] and incorporates platelets and NETs into biofilms on cardiac valves [155]. The opportunistic pathogen *Pseudomonas aeruginosa* incorporates eDNA from host neutrophil extracellular traps into its biofilm matrix in cystic fibrosis patients [69]. Release of pro-inflammatory cytokines from host immune cells promote biofilm formation [49, 50, 156]. In particular, inflammatory cytokines IL-1β, IL-6, interferon (IFN)-γ, and tumor necrosis factor (TNF)-α promote *S. aureus* biofilm formation on bone implants in mice [49, 157]. Gene expression of IL-1β, IL-6, and TNF-α are also positively correlated with *S. aureus* biofilm formation on skin lesions in human patients with atopic dermatitis [50].

Biofilm infections ultimately lead to failure in host tissues due exacerbation of inflammation. In orthopedic implant infections, stimulation of inflammatory cytokine expression and Th1 T-lymphocytes leads to activation of osteoclasts [24, 36, 133, 158, 159]. Chronic activation of osteoclasts leads to peri-implant osteolysis, implant loosening and subsequent implant failure

[12, 24, 33, 36, 133]. In septic arthritis, expression of inflammatory cytokines causes release of MMPs from polymorphonuclear leukocytes recruited to the infected joint [9, 160]. These MMPs digest the articular cartilage extracellular matrix and ultimately lead to osteoarthritis and/or osteomyelitis via extension of the infection into the subchondral bone [9, 17, 160, 161].

The extent of inflammation triggered by the biofilm and associated tissue damage may vary between bacterial strains. The methicillin-resistant *S. aureus* strain *USA300* induced greater osteomyelitis and tibial implant loosening compared to a methicillin-sensitive *S. epidermidis* strain in mice [24]. However, it is unknown whether variation between individuals in their inflammatory responses may also influence the severity of biofilm persistence or subsequent tissue damage. For example, BALB/c mice secreted higher levels of the regulatory cytokines IL-4 and IL-10 in response to *S. aureus* implant biofilm infections, and resisted development of chronic infection, as compared to C57BL/6 mice [49]. The potential for variation between clinical patients in their response to orthopedic biofilm infections should be investigated and may support a need for more personalized approach to treatment.

Summary

Biofilms in orthopedic infections reduce treatment success and contribute to increased treatment costs, complications, and mortality in people and horses. The process of biofilm formation involves bacterial adhesion to a substrate or cell-cell aggregation, followed by secretion of extracellular polymeric substance (matrix). Orthopedic niches, including bones, implants, and synovial fluid, provide optimal environments for biofilm formation by multiple mechanisms. The

presence of biofilms in orthopedic infections promotes antimicrobial and immune resistance, chronic inflammation and tissue destruction. Furthermore, the immune response to biofilms can directly contribute to further biofilm formation or enhance biofilm persistence. Investigation of novel therapeutics for orthopedic biofilm formations should thereby focus on treatments that can disrupt biofilms and modulate the immune response to biofilms.

BIBLIOGRAPHY

1. Jacobs CC, Levine DG, Richardson DW. Use of locking compression plates in ulnar fractures of 18 horses. Vet Surg. 2017;46:242-8.
2. Kurum B. A Short Story of Veterinary Orthopedic Surgery. Int J Vet An Res. 2020;3:74-8.
3. Auer JA, Pohler O, Schlunder M, Kasa F, Olmstead M, von Salis B, Fackelman GE. History of AOVET: The First 40 Years. AOVET. 2013:1-96.
4. Knight SR, Aujla R, Biswas SP. Total hip arthroplasty- over 100 years of operative history. Orthop Rev. 2011;3:72-4.
5. Matter P. History of the AO and its global effect on operative fracture treatment. Clin Orthop Relat Res. 1998:11-8.
6. Anderson JR, Smagul A, Simpson D, Clegg PD, Rubio-Martinez LM, Peffers MJ. The synovial fluid proteome differentiates between septic and nonseptic articular pathologies. J Proteomics. 2019;202:103370.
7. Bertone AL. Update on infectious arthritis in horses. Equine Vet Educ. 1999;11:143-52.
8. Ludwig EK, Brandon Wiese R, Graham MR, Tyler AJ, Settlage JM, Werre SR, et al. Serum and Synovial Fluid Serum Amyloid A Response in Equine Models of Synovitis and Septic Arthritis. Vet Surg. 2016;45:859-67.
9. Hall MS, Pollock PJ, Russell T. Surgical treatment of septic physitis in 17 foals. Aust Vet J. 2012;90:479-84.

10. Rinnovati R, Butina BB, Lanci A, Mariella J. Diagnosis, Treatment, Surgical Management, and Outcome of Septic Arthritis of Tarsocrural Joint in 16 Foals. J Equine Vet Sci. 2018;67:128-32.

11. Kurtz SM, Lau E, Watson H, Schmier JK, Parvizi J. Economic burden of periprosthetic joint infection in the United States. J Arthroplasty. 2012;27:61-5.

12. Pollmann CT, Dahl FA, Rotterud JHM, Gjertsen JE, Aroen A. Surgical site infection after hip fracture - mortality and risk factors: an observational cohort study of 1,709 patients. Acta Orthop. 2020;91:347-52.

13. Thakore RV, Greenberg SE, Shi H, Foxx AM, Francois EL, Prablek MA, et al. Surgical site infection in orthopedic trauma: A case-control study evaluating risk factors and cost. J Clin Orthop Trauma. 2015;6:220-6.

14. Ahern BJ, Richardson DW, Boston RC, Schaer TP. Orthopedic infections in equine long bone fractures and arthrodeses treated by internal fixation: 192 cases (1990-2006). Vet Surg. 2010;39:588-93.

15. Curtiss AL, Stefanovski D, Richardson DW. Surgical site infection associated with equine orthopedic internal fixation: 155 cases (2008-2016). Vet Surg. 2019;48:685-93.

16. LaPointe JM, Laverty S, Lavoie JP. Septic arthritis in 15 Standardbred racehorses after intra-articular injection. Equine Vet J. 1992;24:430-4.

17. Schneider RK, Bramlage LR, Moore RN, Mecklenburg LM, Kohn KW, Gabel AA. A retrospective of 192 horses affected with septic arthritis/tenosynovitis. Equine Vet J. 1992;24:436-42.

18. Hepworth-Warren KL, Wong DM, Fulkerson CV, Wang C, Sun Y. Bacterial isolates, antimicrobial susceptibility patterns, and factors associated with infection and outcome in foals with septic arthritis: 83 cases (1998–2013). J Am Vet Med Assoc. 2015;246:785-93.

19. Straticò P, Varasano V, Suriano R, Sciarrini C, Petrizzi L. Traumatic Septic Tenosynovitis of the Tarsal Sheath with Fragmentation of the Sustentaculum Tali: Surgical Treatment and Outcome in 3 Horses. J Equine Vet Sci. 2014;34:538-43.

20. Marsh CA, Watkins JP, Schneider RK. Intrathecal deep digital flexor tenectomy for treatment of septic tendonitis/tenosynovitis in four horses. Vet Surg. 2011;40:284-90.

21. Zmistowski B, Karam JA, Durinka JB, Casper DS, Parvizi J. Periprosthetic joint infection increases the risk of one-year mortality. J Bone Joint Surg Am. 2013;95:2177-84.

22. Shukla SK, Ward JP, Jacofsky MC, Sporer SM, Paprosky WG, Della Valle CJ. Perioperative testing for persistent sepsis following resection arthroplasty of the hip for periprosthetic infection. J Arthroplasty. 2010;25:87-91.

23. Nishitani K, Sutipornpalangkul W, de Mesy Bentley KL, Varrone JJ, Bello-Irizarry SN, Ito H, et al. Quantifying the natural history of biofilm formation in vivo during the establishment of chronic implant-associated *Staphylococcus aureus* osteomyelitis in mice to identify critical pathogen and host factors. J Orthop Res. 2015;33:1311-9.

24. Tomizawa T, Ishikawa M, Bello-Irizarry SN, de Mesy Bentley KL, Ito H, Kates SL, et al. Biofilm Producing *Staphylococcus epidermidis* (RP62A Strain) Inhibits Osseous Integration Without Osteolysis and Histopathology in a Murine Septic Implant Model. J Orthop Res. 2020;38:852-60.

25. Masters EA, Trombetta RP, de Mesy Bentley KL, Boyce BF, Gill AL, Gill SR, et al. Evolving concepts in bone infection: redefining "biofilm," "acute vs. chronic

osteomyelitis," "the immune proteome," and "local antibiotic therapy." Bone Res. 2019;7:20.

26. de Mesy Bentley KL, Trombetta R, Nishitani K, Bello-Irizarry SN, Ninomiya M, Zhang L, et al. Evidence of *Staphylococcus Aureus* Deformation, Proliferation, and Migration in Canaliculi of Live Cortical Bone in Murine Models of Osteomyelitis. J Bone Miner Res. 2017;32:985-90.

27. Pestrak MJ, Gupta TT, Dusane DH, Guzior DV, Staats A, Harro J, et al. Investigation of synovial fluid induced *Staphylococcus aureus* aggregate development and its impact on surface attachment and biofilm formation. PLoS One. 2020;15:e0231791.

28. Bidossi A, Bottagisio M, Savadori P, De Vecchi E. Identification and Characterization of Planktonic Biofilm-Like Aggregates in Infected Synovial Fluids From Joint Infections. Front Microbiol. 2020;11:1368.

29. Ibberson CB, Parlet CP, Kwiecinski J, Crosby HA, Meyerholz DK, Horswill AR. Hyaluronan Modulation Impacts *Staphylococcus aureus* Biofilm Infection. Infect Immun. 2016;84:1917-29.

30. Gilbertie JM, Schnabel LV, Hickok NJ, Jacob ME, Conlon BP, Shapiro IM, et al. Equine or porcine synovial fluid as a novel *ex vivo* model for the study of bacterial free-floating biofilms that form in human joint infections. PLoS One. 2019;14:e0221012.

31. Perez K, Patel R. Biofilm-like aggregation of *Staphylococcus epidermidis* in synovial fluid. J Infect Dis. 2015;212:335-6.

32. Gomez-Barrena E, Esteban J, Medel F, Molina-Manso D, Ortiz-Perez A, Cordero-Ampuero J, et al. Bacterial adherence to separated modular components in joint prosthesis: a clinical study. J Orthop Res. 2012;30:1634-9.

33. Teterycz D, Ferry T, Lew D, Stern R, Assal M, Hoffmeyer P, et al. Outcome of orthopedic implant infections due to different staphylococci. Int J Infect Dis. 2010;14:e913-8.

34. Sreenivas T, Nataraj AR, Menon J. Acute hematogenous septic arthritis of the knee in adults. Eur J Orthop Surg Traumatol. 2013;23:803-7.

35. Babushkina IV, Mamonova IA, Ulyanov VY, Gladkova EV, Shpinyak SP. Antibiotic Susceptibility of *Staphylococcus aureus* Plankton and Biofilm Forms Isolated in Implant-Associated Infection. Bull Exp Biol Med. 2021;172:46-8.

36. Goodrich LR. Osteomyelitis in horses. Vet Clin North Am Equine Pract. 2006;22:389-417, viii-ix.

37. Trampuz A, Piper KE, Jacobson MJ, Hanssen AD, Unni KK, Osmon DR, Mandrekar JN, Cockerill FR, Steckelberg JM, Greenleaf JF, Patel R. Sonication of Removed Hip and Knee Prostheses for Diagnosis of Infection. N Engl J Med. 2007;357:654-63.

38. Gomez E, Cazanave C, Cunningham SA, Greenwood-Quaintance KE, Steckelberg JM, Uhl JR, et al. Prosthetic joint infection diagnosis using broad-range PCR of biofilms dislodged from knee and hip arthroplasty surfaces using sonication. J Clin Microbiol. 2012;50:3501-8.

39. Keeshen T, Case JB, Wellehan JF, Dujowich M. Bacterial recovery using sonication versus swabbing of titanium and stainless *steel implants inoculated with Staphylococcus pseudintermedius or Pseudomonas* aeruginosa. Vet Comp Orthop Traumatol. 2017;30:346-50.

40. Staats AB, Schwieters PW, Li AD, Sullivan A, Horswill AR, Stoodley P. Rapid Aggregation of *Staphylococcus aureus* in Synovial Fluid Is Influenced by Synovial Fluid

Concentration, Viscosity, and Fluid Dynamics, with Evidence of Polymer Bridging. mBio. 2022;13:1-15.

41. Crawford EC, Singh A, Gibson TW, Scott Weese J. Biofilm-Associated Gene Expression in *Staphylococcus pseudintermedius* on a Variety of Implant Materials. Vet Surg. 2016;45:499-506.

42. Bjarnsholt T, Alhede M, Alhede M, Eickhardt-Sorensen SR, Moser C, Kuhl M, et al. The *in vivo* biofilm. Trends Microbiol. 2013;21:466-74.

43. Arciola CR, Campoccia D, Montanaro L. Implant infections: adhesion, biofilm formation and immune evasion. Nat Rev Microbiol. 2018;16:397-409.

44. Bhattacharya M, Berends ETM, Chan R, Schwab E, Roy S, Sen CK, et al. *Staphylococcus aureus* biofilms release leukocidins to elicit extracellular trap formation and evade neutrophil-mediated killing. Proc Natl Acad Sci U S A. 2018;115:7416-21.

45. Berends ET, Horswill AR, Haste NM, Monestier M, Nizet V, von Kockritz-Blickwede M. Nuclease expression by *Staphylococcus aureus* facilitates escape from neutrophil extracellular traps. J Innate Immun. 2010;2:576-86.

46. Buzzo JR, Devaraj A, Gloag ES, Jurcisek JA, Robledo-Avila F, Kesler T, et al. Z-form extracellular DNA is a structural component of the bacterial biofilm matrix. Cell. 2021;184:5740-58 e17.

47. Le KY, Park MD, Otto M. Immune Evasion Mechanisms of *Staphylococcus epidermidis* Biofilm Infection. Front Microbiol. 2018;9:359.

48. Forestier C, Billard E, Milon G, Gueirard P. Unveiling and Characterizing Early Bilateral Interactions between Biofilm and the Mouse Innate Immune System. Front Microbiol. 2017;8:2309.

49. Prabhakara R, Harro JM, Leid JG, Keegan AD, Prior ML, Shirtliff ME. Suppression of the inflammatory immune response prevents the development of chronic biofilm infection due to methicillin-resistant *Staphylococcus aureus*. Infect Immun. 2011;79:5010-8.

50. Di Domenico EG, Cavallo I, Bordignon V, Prignano G, Sperduti I, Gurtner A, et al. Inflammatory cytokines and biofilm production sustain *Staphylococcus aureus* outgrowth and persistence: a pivotal interplay in the pathogenesis of atopic dermatitis. Sci Rep. 2018;8:9573.

51. Hoenders CS, Harmsen MC, van Luyn MJ. The local inflammatory environment and microorganisms in "aseptic" loosening of hip prostheses. J Biomed Mater Res B Appl Biomater. 2008;86:291-301.

52. Gieling F, Peters S, Erichsen C, Richards RG, Zeiter S, Moriarty TF. Bacterial osteomyelitis in veterinary orthopaedics: Pathophysiology, clinical presentation and advances in treatment across multiple species. Vet J. 2019;250:44-54.

53. Pietrocola G, Campoccia D, Motta C, Montanaro L, Arciola CR, Speziale P. Colonization and Infection of Indwelling Medical Devices by *Staphylococcus aureus* with an Emphasis on Orthopedic Implants. Int Journal Mol Sci. 2022;23.

54. Saeed K, McLaren AC, Schwarz EM, Antoci V, Arnold WV, Chen AF, et al. 2018 international consensus meeting on musculoskeletal infection: Summary from the biofilm workgroup and consensus on biofilm related musculoskeletal infections. J Orthop Res. 2019;37:1007-17.

55. Bezstarosti H, Van Lieshout EMM, Voskamp LW, Kortram K, Obremskey W, McNally MA, et al. Insights into treatment and outcome of fracture-related infection: a systematic literature review. Arch Orthop Trauma Surg. 2018;139:61-72.

56. Osmon DR, Berbari EF, Berendt AR, Lew D, Zimmerli W, Steckelberg JM, et al. Diagnosis and management of prosthetic joint infection: clinical practice guidelines by the Infectious Diseases Society of America. Clin Infect Dis. 2013;56:e1-e25.

57. Virgin JE, Goodrich LR, Baxter GM, Rao S. Incidence of support limb laminitis in horses treated with half limb, full limb or transfixation pin casts: a retrospective study of 113 horses (2000-2009). Equine Vet J Suppl. 2011:7-11.

58. Stiefel P, Rosenberg U, Schneider J, Mauerhofer S, Maniura-Weber K, Ren Q. Is biofilm removal properly assessed? Comparison of different quantification methods in a 96-well plate system. Appl Microbiol Biotechnol. 2016;100:4135-45.

59. Sharma G, Sharma S, Sharma P, Chandola D, Dang S, Gupta S, et al. *Escherichia coli* biofilm: development and therapeutic strategies. J Appl Microbiol. 2016;121:309-19.

60. Patti JM, Allen BL, McGavin MJ, Hook M. MSCRAMM-Mediated Adherence of Microorganisms to Host Tissues. Annu Rev Microbiol. 1994;48:585-617.

61. Hu D, Zou L, Yu W, Jia F, Han H, Yao K, et al. Relief of Biofilm Hypoxia Using an Oxygen Nanocarrier: A New Paradigm for Enhanced Antibiotic Therapy. Adv Sci (Weinh). 2020;7:2000398.

62. Wu Y, Klapper I, Stewart PS. Hypoxia arising from concerted oxygen consumption by neutrophils and microorganisms in biofilms. Pathog Dis. 2018;76.

63. Wood TK, Knabel SJ, Kwan BW. Bacterial persister cell formation and dormancy. Appl Environ Microbiol. 2013;79:7116-21.

64. Rooney LM, Amos WB, Hoskisson PA, McConnell G. Intra-colony channels in *E. coli* function as a nutrient uptake system. ISME J. 2020;14:2461-73.

65. Henry-Stanley MJ, Hess DJ, Wells CL. Aminoglycoside inhibition of *Staphylococcus aureus* biofilm formation is nutrient dependent. J Med Microbiol. 2014;63:861-9.

66. Nguyen MH, Ojima Y, Sakka M, Sakka K, Taya M. Probing of exopolysaccharides with green fluorescence protein-labeled carbohydrate-binding module in *Escherichia coli* biofilms and flocs induced by *bcsB* overexpression. J Biosci Bioeng. 2014;118:400-5.

67. Petruzzi B, Dickerman A, Lahmers K, Scarratt WK, Inzana TJ. Polymicrobial Biofilm Interaction Between *Histophilus somni* and *Pasteurella multocida*. Front Microbiol. 2020;11:1561.

68. Martin-Rodriguez AJ, Rhen M, Melican K, Richter-Dahlfors A. Nitrate Metabolism Modulates Biosynthesis of Biofilm Components in Uropathogenic *Escherichia coli* and Acts as a Fitness Factor During Experimental Urinary Tract Infection. Front Microbiol. 2020;11:26.

69. Alhede M, Alhede M, Qvortrup K, Kragh KN, Jensen PO, Stewart PS, et al. The origin of extracellular DNA in bacterial biofilm infections in vivo. Pathog Dis. 2020;78.

70. Whitchurch CB, Tolker-Nielsen T, Ragas PC, Mattick JS. Extracellular DNA is Required for Bacterial Biofilm Formation. Science. 2002;295:1487.

71. Wu S, Zhang J, Peng Q, Liu Y, Lei L, Zhang H. The Role of *Staphylococcus aureus YycFG* in Gene Regulation, Biofilm Organization and Drug Resistance. Antibiotics (Basel). 2021;10.

72. Cerca N, Jefferson KK. Effect of growth conditions on poly-*N*-acetylglucosamine expression and biofilm formation in *Escherichia coli*. FEMS Microbiol Lett. 2008;283:36-41.

73. Schwartz K, Syed AK, Stephenson RE, Rickard AH, Boles BR. Functional amyloids composed of phenol soluble modulins stabilize *Staphylococcus aureus* biofilms. PLoS Pathog. 2012;8:e1002744.

74. Jorgensen E, Bay L, Skovgaard LT, Bjarnsholt T, Jacobsen S. An Equine Wound Model to Study Effects of Bacterial Aggregates on Wound Healing. Adv Wound Care (New Rochelle). 2019;8:487-98.

75. Campoccia D, Speziale P, Ravaioli S, Cangini I, Rindi S, Pirini V, et al. The presence of both bone sialoprotein-binding protein gene and collagen adhesin gene as a typical virulence trait of the major epidemic cluster in isolates from orthopedic implant infections. Biomaterials. 2009;30:6621-8.

76. Jain N, Aden J, Nagamatsu K, Evans ML, Li X, McMichael B, et al. Inhibition of curli assembly and *Escherichia coli* biofilm formation by the human systemic amyloid precursor transthyretin. Proc Natl Acad Sci U S A. 2017;114:12184-9.

77. Leech J, Golub S, Allan W, Simmons MJH, Overton TW. Non-pathogenic *Escherichia coli* biofilms: effects of growth conditions and surface properties on structure and curli gene expression. Arch Microbiol. 2020;202:1517-27.

78. Pawar DM, Rossman ML, Chen J. Role of curli fimbriae in mediating the cells of enterohaemorrhagic *Escherichia coli* to attach to abiotic surfaces. J Appl Microbiol. 2005;99:418-25.

79. Trautner BW, Darouiche RO. Role of biofilm in catheter-associated urinary tract infection. Am J Infect Control. 2004;32:177-83.

80. Boden MK, Flock JI. Cloning and characterization of a gene for a 19 kDa fibrinogen-binding protein from *Staphylococcus aureus*. Mol Microbiol. 1994;12:599-606.

81. Wood TK. Insights on *Escherichia coli* biofilm formation and inhibition from whole-transcriptome profiling. Environ Microbiol. 2009;11:1-15.

82. Wang Z, Wang J, Ren G, Li Y, Wang X. Influence of Core Oligosaccharide of Lipopolysaccharide to Outer Membrane Behavior of *Escherichia coli*. Mar Drugs. 2015;13:3325-39.

83. Hess DJ, Henry-Stanley MJ, Wells CL. The Natural Surfactant Glycerol Monolaurate Significantly Reduces Development of *Staphylococcus aureus* and *Enterococcus faecalis* Biofilms. Surg Infect (Larchmt). 2015;16:538-42.

84. Rivera ES, Weiss A, Migas LG, Freiberg JA, Djambazova KV, Neumann EK, et al. Imaging mass spectrometry reveals complex lipid distributions across *Staphylococcus aureus* biofilm layers. J Mass Spectrom Adv Clin Lab. 2022;26:36-46.

85. Paytubi S, Cansado C, Madrid C, Balsalobre C. Nutrient Composition Promotes Switching between Pellicle and Bottom Biofilm in *Salmonella*. Front Microbiol. 2017;8:2160.

86. Johns BE, Purdy KJ, Tucker NP, Maddocks SE. Phenotypic and Genotypic Characteristics of Small Colony Variants and Their Role in Chronic Infection. Microbiol Insights. 2015;8:15-23.

87. Moormeier DE, Endres JL, Mann EE, Sadykov MR, Horswill AR, Rice KC, et al. Use of microfluidic technology to analyze gene expression during *Staphylococcus aureus* biofilm formation reveals distinct physiological niches. Appl Environ Microbiol. 2013;79:3413-24.

88. Marx C, Gardner S, Harman RM, Wagner B, Van de Walle GR. Mesenchymal stromal cell-secreted CCL2 promotes antibacterial defense mechanisms through increased

antimicrobial peptide expression in keratinocytes. Stem Cells Transl Med. 2021;10:1666-79.

89. Yawata Y, Toda K, Setoyama E, Fukuda J, Suzuki H, Uchiyama H, et al. Monitoring biofilm development in a microfluidic device using modified confocal reflection microscopy. J Biosci Bioeng. 2010;110:377-80.

90. Liu N, Skauge T, Landa-Marban D, Hovland B, Thorbjornsen B, Radu FA, et al. Microfluidic study of effects of flow velocity and nutrient concentration on biofilm accumulation and adhesive strength in the flowing and no-flowing microchannels. J Ind Microbiol Biotechnol. 2019;46:855-68.

91. Xu LC, Wo Y, Meyerhoff ME, Siedlecki CA. Inhibition of bacterial adhesion and biofilm formation by dual functional textured and nitric oxide releasing surfaces. Acta Biomater. 2017;51:53-65.

92. Zhang J, Huang J, Say C, Dorit RL, Queeney KT. Deconvoluting the effects of surface chemistry and nanoscale topography: *Pseudomonas aeruginosa* biofilm nucleation on Si-based substrates. J Colloid Interface Sci. 2018;519:203-13.

93. Lecuyer S, Rusconi R, Shen Y, Forsyth A, Vlamakis H, Kolter R, et al. Shear stress increases the residence time of adhesion of *Pseudomonas aeruginosa*. Biophys J. 2011;100:341-50.

94. Zhang XY, Sun K, Abulimiti A, Xu PP, Li ZY. Microfluidic System for Observation of Bacterial Culture and Effects on Biofilm Formation at Microscale. Micromachines (Basel). 2019;10.

95. Viela F, Prystopiuk V, Leprince A, Mahillon J, Speziale P, Pietrocola G, et al. Binding of *Staphylococcus aureus* Protein A to von Willebrand Factor Is Regulated by Mechanical Force. mBio. 2019;10.

96. Marx C, Gardner S, Harman RM, Van de Walle GR. The mesenchymal stromal cell secretome impairs methicillin-resistant *Staphylococcus aureus* biofilms via cysteine protease activity in the equine model. Stem Cells Transl Med. 2020.

97. Harman RM, Yang S, He MK, Van de Walle GR. Antimicrobial peptides secreted by equine mesenchymal stromal cells inhibit the growth of bacteria commonly found in skin wounds. Stem Cell Res Ther. 2017;8:157.

98. Goikoetxea E, Routkevitch D, de Weerdt A, Green JJ, Steenackers H, Braeken D. Impedimetric fingerprinting and structural analysis of isogenic *E. coli* biofilms using multielectrode arrays. Sensors and Actuators B: Chemical. 2018;263:319-26.

99. Lowman ME, Tipton CD, Labordere AL, Brown JA. Equine sinusitis aetiology is linked to sinus microbiome by amplicon sequencing. Equine Vet J. 2022.

100. Cunha E, Rebelo S, Carneiro C, Tavares L, Carreira LM, Oliveira M. A polymicrobial biofilm model for testing the antimicrobial potential of a nisin-biogel for canine periodontal disease control. BMC Vet Res. 2020;16:469.

101. Anju VT, Busi S, Imchen M, Kumavath R, Mohan MS, Salim SA, et al. Polymicrobial Infections and Biofilms: Clinical Significance and Eradication Strategies. Antibiotics (Basel). 2022;11.

102. Wolcott R, Costerton JW, Raoult D, Cutler SJ. The polymicrobial nature of biofilm infection. Clin Microbiol Infect. 2013;19:107-12.

103. Rickard AH, Gilbert P, High NJ, Kolenbrander PE, Handley PS. Bacterial coaggregation: an integral process in the development of multi-species biofilms. Trends Microbiol. 2003;11:94-100.

104. Elliott DR, Wilson M, Buckley CM, Spratt DA. Aggregative behavior of bacteria isolated from canine dental plaque. Appl Environ Microbiol. 2006;72:5211-7.

105. Drago L, Clerici P, Morelli I, Ashok J, Benzakour T, Bozhkova S, et al. The World Association against Infection in Orthopaedics and Trauma (WAIOT) procedures for Microbiological Sampling and Processing for Periprosthetic Joint Infections (PJIs) and other Implant-Related Infections. J Clin Med. 2019;8.

106. Schwarz EM, Parvizi J, Gehrke T, Aiyer A, Battenberg A, Brown SA, et al. 2018 International Consensus Meeting on Musculoskeletal Infection: Research Priorities from the General Assembly Questions. J Orthop Res. 2019;37:997-1006.

107. Snyder JR, Pascoe JR, Hirsch DC. Antimicrobial susceptibility of microorganisms isolated from equine orthopedic patients. Vet Surg. 1987;16:197-201.

108. Deev D, Rybkin I, Rijavec T, Lapanje A. When Beneficial Biofilm on Materials Is Needed: Electrostatic Attachment of Living Bacterial Cells Induces Biofilm Formation. Frontiers in Materials. 2021;8.

109. Zuki MF, Edyvean RGJ, Pourzolfaghar H, Kasim N. Modeling of the Van Der Waals Forces during the Adhesion of Capsule-Shaped Bacteria to Flat Surfaces. Biomimetics (Basel). 2021;6.

110. Wood TK, Gonzalez Barrios AF, Herzberg M, Lee J. Motility influences biofilm architecture in *Escherichia coli*. Appl Microbiol Biotechnol. 2006;72:361-7.

111. Niba ET, Naka Y, Nagase M, Mori H, Kitakawa M. A genome-wide approach to identify the genes involved in biofilm formation in *E. coli*. DNA Res. 2007;14:237-46.

112. Zhang Y, Li C, Wu Y, Zhang Y, Zhou Z, Cao B. A microfluidic gradient mixer-flow chamber as a new tool to study biofilm development under defined solute gradients. Biotechnol Bioeng. 2019;116:54-64.

113. Schwartbeck B, Birtel J, Treffon J, Langhanki L, Mellmann A, Kale D, et al. Dynamic *in vivo* mutations within the *ica* operon during persistence of *Staphylococcus aureus* in the airways of cystic fibrosis patients. PLoS Pathog. 2016;12:e1006024.

114. Pruss BM, Besemann C, Denton A, Wolfe AJ. A complex transcription network controls the early stages of biofilm development by *Escherichia coli*. J Bacteriol. 2006;188:3731-9.

115. Periasamy S, Joo HS, Duong AC, Bach TH, Tan VY, Chatterjee SS, et al. How *Staphylococcus aureus* biofilms develop their characteristic structure. Proc Natl Acad Sci USA. 2012;109:1281-6.

116. Kong KF, Vuong C, Otto M. *Staphylococcus* quorum sensing in biofilm formation and infection. Int J Med Microbiol. 2006;296:133-9.

117. Li Z, Nair SK. Quorum sensing: how bacteria can coordinate activity and synchronize their response to external signals? Protein Sci. 2012;21:1403-17.

118. Solano C, Echeverz M, Lasa I. Biofilm dispersion and quorum sensing. Curr Opin Microbiol. 2014;18:96-104.

119. Ji G, Beavis RC, Novick RP. Cell density control of staphylococcal virulence mediated by an octapeptide pheromone. Proc Natl Acad Sci U S A. 1995;92:12055-9.

120. Swift S, Winson MK, Chan PF, Bainton NJ, Birdsall M, Reeves PJ, et al. A novel strategy for the isolation of *luxI* homologues: evidence for the widespread distribution of a LuxR:LuxI superfamily in enteric bacteria. Mol Microbiol. 1993;10:511-20.

121. Novick RP, Projan SJ, Kornblum J, Ross HF, Ji G, Kreiswirth B, et al. The *agr* P2 operon: an autocatalytic sensory transduction system in *Staphylococcus aureus*. Mol Gen Genet. 1995;248:446-58.

122. Morfeldt E, Taylor D, von Gabain A, Arvidson S. Activation of alpha-toxin translation in *Staphylococcus aureus* by the trans-encoded antisense RNA, RNAIII. EMBO J. 1995;14:4569-77.

123. Dunman PM, Murphy E, Haney S, Palacios D, Tucker-Kellogg G, Wu S, et al. Transcription profiling-based identification of *Staphylococcus aureus* genes regulated by the *agr* and/or *sarA* loci. J Bacteriol. 2001;183:7341-53.

124. Sturbelle RT, de Avila LF, Roos TB, Borchardt JL, da Conceicao Rde C, Dellagostin OA, et al. The role of quorum sensing in *Escherichia coli* (ETEC) virulence factors. Vet Microbiol. 2015;180:245-52.

125. Gonzalez Barrios AF, Zuo R, Hashimoto Y, Yang L, Bentley WE, Wood TK. Autoinducer 2 controls biofilm formation in *Escherichia coli* through a novel motility quorum-sensing regulator (MqsR, B3022). J Bacteriol. 2006;188:305-16.

126. Veerachamy S, Yarlagadda T, Manivasagam G, Yarlagadda PK. Bacterial adherence and biofilm formation on medical implants: a review. Proc Inst Mech Eng H. 2014;228:1083-99.

127. Croes M, Akhavan B, Sharifahmadian O, Fan H, Mertens R, Tan RP, et al. A multifaceted biomimetic interface to improve the longevity of orthopedic implants. Acta Biomater. 2020;110:266-79.

128. Gristina AG, Naylor P, Myrvik Q. Infections from biomaterials and implants: a race for the surface. Med Prog Technol. 1988;14:205-24.

129. Tapscott DC, Wottowa C. Orthopedic Implant Materials. StatPearls Publishing, LLC. Treasure Island, Florida, USA. 2023.

130. Equine Surgery, 5th ed. Auer JA, Stick JA, Kummerle JM, Prange T, ed. Saunders Elsevier. Philadelphia, Pennsylvania, USA. 2019.

131. Equine Fracture Repair, 2nd ed. Nixon AJ, ed. Wiley Blackwell, Ltd. Hoboken, New Jersey, USA. 2020.

132. Johnson V, Webb T, Norman A, Coy J, Kurihara J, Regan D, et al. Activated Mesenchymal Stem Cells Interact with Antibiotics and Host Innate Immune Responses to Control Chronic Bacterial Infections. Sci Rep. 2017;7:9575.

133. Yamamuro Y, Kabata T, Nojima T, Hayashi K, Tokoro M, Kajino Y, et al. Combined adipose-derived mesenchymal stem cell and antibiotic therapy can effectively treat periprosthetic joint infection in rats. Sci Rep. 2023;13:3949.

134. McConoughey SJ, Howlin R, Granger JF, Manring MM, Calhoun JH, Shirtliff M, et al. Biofilms in periprosthetic orthopedic infections. Future Microbiol. 2014;9:987-1007.

135. Gilbertie JM, Schaer TP, Schubert AG, Jacob ME, Menegatti S, Ashton Lavoie R, et al. Platelet-rich plasma lysate displays antibiofilm properties and restores antimicrobial activity against synovial fluid biofilms *in vitro*. J Orthop Res. 2020.

136. Andreassen SM, Vinther AML, Nielsen SS, Andersen PH, Tnibar A, Kristensen AT, Jacobsen S. Changes in concentrations of haemostatic and inflammatory biomarkers in synovial fluid after intra-rticular injection of lipopolysaccharide in horses. BMC Vet Res. 2017;13:1-17.

137. Watkins A, Fasanello D, Stefanovski D, Schurer S, Caracappa K, D'Agostino A, et al. Investigation of synovial fluid lubricants and inflammatory cytokines in the horse: a comparison of recombinant equine interleukin 1 beta-induced synovitis and joint lavage models. BMC Vet Res. 2021;17:189.

138. Rejno S. Viscosity of equine synovial fluid. Acta Vet Scand 1976;17:169–77.

139. Chiang WC, Nilsson M, Jensen PO, Hoiby N, Nielsen TE, Givskov M, et al. Extracellular DNA shields against aminoglycosides in *Pseudomonas aeruginosa* biofilms. Antimicrob Agents Chemother. 2013;57:2352-61.

140. Lu H, Que Y, Wu X, Guan T, Guo H. Metabolomics Deciphered Metabolic Reprogramming Required for Biofilm Formation. Sci Rep. 2019;9:13160.

141. Veterinary Pharmacology and Therapeutics, 10th ed. Riviere JE, Papich MG, ed. Hoboken, New Jersey, USA. Wiley-Blackwell. 2017.

142. Yang D, Zhang Z. Biofilm-forming *Klebsiella pneumoniae* strains have greater likelihood of producing extended-spectrum beta-lactamases. J Hosp Infect. 2008;68:369-71.

143. Joshi RV, Gunawan C, Mann R. We Are One: Multispecies Metabolism of a Biofilm Consortium and Their Treatment Strategies. Front Microbiol. 2021;12:635432.

144. Hengzhuang W, Ciofu O, Yang L, Wu H, Song Z, Oliver A, et al. High beta-lactamase levels change the pharmacodynamics of beta-lactam antibiotics in *Pseudomonas aeruginosa* biofilms. Antimicrob Agents Chemother. 2013;57:196-204.

145. Mandell JB, Orr S, Koch J, Nourie B, Ma D, Bonar DD, et al. Large variations in clinical antibiotic activity against *Staphylococcus aureus* biofilms of periprosthetic joint infection isolates. J Orthop Res. 2019;37:1604-9.

146. Walker M, Singh A, Nazarali A, Gibson TW, Rousseau J, Weese JS. Evaluation of the Impact of Methicillin-Resistant *Staphylococcus pseudintermedius* Biofilm Formation on Antimicrobial Susceptibility. Vet Surg. 2016;45:968-71.

147. Kaplan JB, Izano EA, Gopal P, Karwacki MT, Kim S, Bose JL, et al. Low levels of beta-lactam antibiotics induce extracellular DNA release and biofilm formation in *Staphylococcus aureus.* mBio. 2012;3:e00198-12.

148. Lewis JS, Weinstein MP, Bobenchik AM, Campeau S, Cullen SK, Dingel T, Galas MF, Humphries RM. CLSI M100-ED33: 2023 Performance Standards for Antimicrobial Susceptibility Testing, 33rd Ed. CLSI. 2023.

149. Gunther F, Wabnitz GH, Stroh P, Prior B, Obst U, Samstag Y, et al. Host defence against *Staphylococcus aureus* biofilms infection: phagocytosis of biofilms by polymorphonuclear neutrophils (PMN). Mol Immunol. 2009;46:1805-13.

150. Sultan AR, Hoppenbrouwers T, Lemmens-den Toom NA, Snijders SV, van Neck JW, Verbon A, et al. During the Early Stages of *Staphylococcus aureus* Biofilm Formation, Induced Neutrophil Extracellular Traps Are Degraded by Autologous Thermonuclease. Infect Immun. 2019;87.

151. Leid JG, Shirtliff ME, Costerton JW, Stoodley P. Human leukocytes adhere to, penetrate, and respond to *Staphylococcus aureus* biofilms. Infect Immun. 2002;70:6339-45.

152. Gibon E, Cordova LA, Lu L, Lin TH, Yao Z, Hamadouche M, et al. The biological response to orthopedic implants for joint replacement. II: Polyethylene, ceramics, PMMA, and the foreign body reaction. J Biomed Mater Res B Appl Biomater. 2017;105:1685-91.

153. Vedrine M, Berthault C, Leroux C, Reperant-Ferter M, Gitton C, Barbey S, et al. Sensing of *Escherichia coli* and LPS by mammary epithelial cells is modulated by O-antigen chain and CD14. PLoS One. 2018;13:e0202664.

154. Tukel C, Nishimori JH, Wilson RP, Winter MG, Keestra AM, van Putten JP, et al. Toll-like receptors 1 and 2 cooperatively mediate immune responses to curli, a common amyloid from enterobacterial biofilms. Cell Microbiol. 2010;12:1495-505.

155. Hsu CC, Hsu RB, Ohniwa RL, Chen JW, Yuan CT, Chia JS, et al. Neutrophil Extracellular Traps Enhance *Staphylococcus Aureus* Vegetation Formation through Interaction with Platelets in Infective Endocarditis. Thromb Haemost. 2019;119:786-96.

156. Velsko IM, Cruz-Almeida Y, Huang H, Wallet SM, Shaddox LM. Cytokine response patterns to complex biofilms by mononuclear cells discriminate patient disease status and biofilm dysbiosis. J Oral Microbiol. 2017;9:1330645.

157. Gutierrez Jauregui R, Fleige H, Bubke A, Rohde M, Weiss S, Forster R. IL-1 beta Promotes *Staphylococcus aureus* Biofilms on Implants *in vivo*. Front Immunol. 2019;10:1082.

158. Smeltzer MS, Thomas JR, Hickraon SG, Skinner RA, Nelson CL, Griffith D, et al. Characterization of a rabbit model of staphylococcal osteomyelitis. Journal of orthopaedic research. 1997;15:414-21.

159. Luthje FL, Jensen LK, Jensen HE, Skovgaard K. The inflammatory response to bone infection - a review based on animal models and human patients. APMIS. 2020;128:275-86.

160. O'Brien TJ, Rosanowski SM, Mitchell KD, Carrick JB, Butt TD, Adkins AR. Factors associated with survival and racing performance of 114 Thoroughbred foals with septic arthritis compared with maternal siblings (2009-2015). Equine Vet J. 2021;53:935-43.

161. Jacobsen S, Mortensen CD, Hoj EA, Vinther AM, Berg LC, Adler DMT, et al. Neutrophil Gelatinase-Associated Lipocalin in Synovial Fluid from Horses with and without Septic Arthritis. Animals (Basel). 2022;13.

CHAPTER 2:

COMBATING ORTHOPEDIC BIOFILM INFECTIONS:

CURRENT LIMITATIONS AND FUTURE THERAPEUTIC OPTIONS

Diagnostic Testing

Physical examination and imaging

The diagnosis of orthopedic biofilm infections requires a multimodal approach to localize the infection, determine its chronicity, and identify the causative agents. Clinical diagnosis of orthopedic infections in people and horses involves documenting variable pain and gait changes in the affected limb. This is identified from patient history and on physical examination by gait assessment in addition to the presence of swelling, pain on palpation, and draining tracts over the affected structure(s) [1-5]. Diagnostic imaging, including radiography [5-7], ultrasonography [1, 8, 9], computed tomography [4, 10], or magnetic resonance imaging [11, 12] is then performed to document and localize evidence of infection over the affected bones or synovial structures and to guide sampling for bacteriologic testing. Although nuclear scintigraphy demonstrates increased radiopharmaceutical uptake in the area of infection due to increased osteoblast activity, higher-resolution imaging techniques are required to localize and evaluate the extent of infection [8, 10]. Signs of implant-associated infection include reduced bone density around implants due to peri-implant osteolysis, disorganized new bone proliferation, swelling of the surrounding soft tissues, and the presence of fluid tracts adjacent to the infected hardware [2, 3, 13]. Infected synovial structures manifest as synovial effusion, synovial membrane thickening, heterogenous

synovial fluid appearance due to the presence of cellular infiltrates, and fibrinous loculations [1, 14, 15].

Bacteriologic testing

Bacteriologic testing to document the species present in orthopedic infections and their antimicrobial sensitivity is essential to guide antimicrobial therapy. For accurate analysis, samples of synovial fluid from joints or fluid pockets surrounding infected implants are obtained aseptically prior to surgical intervention [1, 2, 10, 16, 17]. Additional biopsies of infected bone, soft tissues and/or infected implants may be taken intraoperatively [18-20]. Samples are then submitted for aerobic and anaerobic bacterial culture with antimicrobial susceptibility [2, 3, 16, 17, 21-23].

Standard cultures provide important information on the presence and species of bacteria in a sample. However, cultures can yield false negative results in an average of 50% of cases due to low organism numbers, uneven organism distribution within the sample, or sequestration of organisms within biofilms [16, 17, 21, 23, 24]. Sensitivity of bacterial culture can be improved by sample incubation in blood culture medium prior to plating (77.6%) [21] and by sonication of infected implants to dislodge adherent biofilm-bound bacteria (72.6%) [18-20]. Concurrent Gram-staining and cytologic evaluation of fluid samples may also confirm infection and give information on bacterial morphology [8]. Polymerase chain reaction (PCR) to detect bacterial 16s ribosomal RNA sequences has been utilized more recently to improve speed and sensitivity of bacterial detection (70.4-89.5% sensitivity, 90-97.8% specificity) compared to standard culture techniques [18, 21, 25]. PCR may be performed alone or combined with next generation

sequencing to identify the presence and relative abundances of multiple bacterial species and antimicrobial resistance genes. This approach is advantageous for diagnosing and managing polymicrobial infections [26-28].

Other clinicopathologic testing

Routine hematology and serum biochemistry are often performed to evaluate for signs of systemic inflammation due to an orthopedic infection and to evaluate general systemic status prior to initiating antimicrobial therapy or performing surgical treatment under general anesthesia [10, 29]. Patients with orthopedic infections may show elevations in total white blood cell count, neutrophil count, or the presence of band neutrophils due to rapid release from bone marrow [10, 29, 30]. Alterations in plasma proteins, including depressions in serum albumin and/or elevations in serum globulins, secondary to systemic inflammation may also be observed. Additionally, elevations in circulating acute phase proteins, including C-reactive protein in people [31, 32] or fibrinogen [8, 33] or serum amyloid A in horses [33-35], can document inflammation due to infection and their rapid decline is useful to monitor response to treatment. In septic synovitis, elevations in synovial fluid total nucleated cell count (TNNC) ($\geq$ 30,000 cells/µL), total protein ($\geq$ 4.0 g/dL), and percentage of neutrophils ($\geq$ 80%) are also consistent with infection [8, 10]. However, alterations in synovial cytologic parameters are variably specific to diagnose sepsis as they may be less markedly elevated with chronic infections [8] or may be elevated in non-septic inflammation [34].

Current treatments for orthopedic infections and their limitations

Antimicrobial therapy

Broad-spectrum antimicrobial therapy delivered systemically and regionally is a mainstay of the treatment of orthopedic infections [4-7]. The choice of antimicrobial(s) is initially empirical and is based on the most common organisms isolated from orthopedic infections, and is subsequently adjusted based on bacteriologic testing results [4, 7]. Regional intravenous limb perfusion is standard of care for equine orthopedic infections and involves application of a torniquet to a limb with direct antimicrobial injection into the vein distal to the torniquet [36, 37]. The tourniquet is left in place for a fixed time period following the injection to allow the antimicrobial to accumulate in the target tissues [38-41]. The purposes of regional antimicrobial therapy are to achieve drug concentrations at the infection site that are higher than those achieved through systemic administration and to use antimicrobials that are effective against common orthopedic pathogens but are not feasible to administer systemically [36, 38, 41-45]. Antimicrobials can also be administered into local circulation via intraosseous infusion [46] or, in the case of septic synovitis, via direct intrasynovial injection [8, 47, 48]. Placement of intrasynovial catheters facilitates repeated lavage of the affected structure and antimicrobial administration without repeated injections [42]. For implant-associated osteomyelitis, biodegradable antimicrobial-impregnated devices, such as polymethylmethacrylate [43, 49, 50] or Plaster of Paris [45] can be prepared and placed within the infection site or prophylactically around implants (“luting”) in open fracture cases for sustained drug delivery.

Regionally-delivered antimicrobials are selected by their spectrum of action against the target pathogen(s) and their pharmacokinetic properties. Antimicrobials used in regional delivery systems preferably have concentration-dependent versus time-dependent efficacy to maximize the dosing interval and thereby minimize the dosing frequency [51]. Concentration-dependent antimicrobials include aminoglycosides [38, 42, 45] and fluoroquinolones [39, 50]. The aminoglycoside amikacin sulfate is the most commonly used antimicrobial for regional treatment of orthopedic infections in horses [1, 3, 44, 52, 53] given its broad spectrum of activity against common equine orthopedic pathogens [51]. Gentamicin sulfate, another aminoglycoside, is also commonly used as a treatment in slow-release delivery systems [43, 45]. A summary of clinically-used antimicrobial classes and their mechanisms of actions is presented below (Table 2.1).

Table 2.1: Common antimicrobial drug classes used clinically and their mechanisms of action [54, 55].

Drug Class	Mechanism of Action	Examples
Aminoglycoside	Inhibits bacterial protein synthesis: binds 16sRNA of bacterial 30S ribosomal subunit	Amikacin sulfate, gentamicin sulfate, neomycin sulfate
Beta-lactam	Inhibits bacterial cell wall synthesis: bind penicillin binding proteins to inhibit peptidoglycan cross-linking	Ampicillin, amoxicillin, ampicillin, carbapenem, imipenem
Fluoroquinolone	Inhibits bacterial DNA replication: DNA gyrase	Enrofloxacin, ciprofloxacin, marbofloxacin, ofloxacin
Glycopeptide	Inhibits bacterial cell wall synthesis: inhibit lipid II and recycling of lipid transporter required for peptidoglycan and teichoic acid synthesis (bactoprenol)	Vancomycin
Nitroimidazole	Disrupts bacterial DNA via formation of nitroso radicals	Metronidazole
phenicol	Inhibits bacterial protein synthesis: binds bacterial 50S ribosomal subunit	Chloramphenicol
Polypeptide	Disrupts bacterial cell membranes via detergent-like action	Polymyxin B, bacitracin
Rifamycin	Binds and inhibits bacterial DNA-dependent RNA polymerase	Rifampin
Sulfonamides	Inhibit bacterial tetrahydrofolic acid synthesis: competitive inhibitor of dihydropteroate synthase	Sulfamethoxazole (combined with trimethoprim), sulfadiazine, sulfadimethoxine
Tetracyclines	Inhibits bacterial protein synthesis: inhibits aminoacyl-tRNA binding on 30S ribosomal subunit	Doxycycline, minocycline, oxytetracycline

Despite the overall positive impact of multimodal antimicrobial therapy on outcomes for horses with orthopedic infections, barriers to successful treatment still exist in the context of biofilm-associated infections. Concentration-dependent antimicrobials are maximally effective when their peak concentration reaches $\geq$ 10 times the MIC for target organism(s) [54]. While synovial concentrations of amikacin achieved *in vivo* surpass the MIC for common infections agents following regional administration [38, 40, 41, 48, 56], the presence of biofilms can increase antimicrobial MIC from several hundred [57, 58] to several thousand times [59, 60] the planktonic MIC and thereby reduce local antimicrobial efficacy. Synovial inflammation may also reduce antimicrobial efficacy by increasing antimicrobial uptake from the synovial vasculature. The peak amikacin concentration in experimentally inflamed equine joints was significantly lower than the concentration in non-inflamed joints [47]. In implant-associated infections, sustained antimicrobial release devices may fail to eradicate all biofilm-bound bacteria due to limited diffusion through the biofilm matrix [7, 59], even in the face of initial rapid elution of antimicrobial from the device [43, 45].

Surgical removal of biofilm

Surgery to identify and remove infected tissues and implants is often required to resolve orthopedic biofilm infections because antimicrobials alone may not be able to penetrate biofilms and eradicate all live bacteria [4, 15, 29, 44, 61, 62]. In cases of infected synovial structures in horses, arthroscopy remains the procedure of choice for detailed examination and visual documentation of infection and secondary chondromalacia in chronic cases [1, 9, 15, 63, 64]. Synovial membrane biopsies can also be obtained intraoperatively for bacteriologic testing to isolate the causative agent(s) [64]. High-volume fluid lavage and endoscopic instruments are

utilized to remove floating biofilm aggregates, fibrin and inflammatory cells and mediators [35, 42, 64]. Biofilm adhered to the synovial membrane and intrasynovial adhesions can also be debrided using motorized synovial resectors [64]. In chronically infected tendon sheaths that have not responded to previous treatment, open debridement, lavage of the sheath, with or without resection of infected tendon (tenectomy), can be performed through a large incision [15]. In chronic cases, the synovial structure can be sutured closed or left open for drainage with or without concurrent placement of an indwelling drain [8, 15]. Repeat post-operative lavage through synoviocentesis or an intrasynovial catheter placed intraoperatively can be performed [42].

In cases of infected fracture fixation implants and prosthetic joints, removal of the infected implants and debridement of the surrounding infected bone and soft tissue is performed to remove as many sources of biofilm as possible [13, 29, 65]. Tissue biopsies are collected and submitted along with the infected implants for bacteriologic testing [5, 29, 66]. Placement of passive or active suction drains to prevent post-operative seroma development can be performed as for chronically infected synovial structures. [10, 15, 67]. Negative pressure wound therapy can also be applied to remove accumulated fluid and reduce surgical site bacterial loads [68, 69]. Depending on the importance of the implant for bone healing and mobility of the affected limb, implant replacement can be performed once no signs of infection are detected on repeat physical examination, imaging, and clinicopathologic testing [5, 8, 29].

Several novel treatments to inhibit formation or prevent recurrence of implant-associated infections have recently been evaluated *in vitro* [70-74]. Implant surface modifications, including

coating with antimicrobials [70-72], synthetic antimicrobial peptides [75-77], or microscopic topographical modifications [73, 74, 78], show promise in inhibiting bacterial adherence. Local bacteriophage therapy has also been investigated as a technique to limit biofilm formation on implants by reducing live bacterial counts [79, 80]. Ultrasonic debridement of indwelling implants has shown superior *S. aureus* biofilm removal compared to standard pulsed lavage [65]. However, clinical translation of these novel treatments has yet to be achieved.

Even with attentive surgical debridement, accurate identification of infected tissues for removal remains a challenge [4, 61, 81]. Determining the extent of infection relies on pre-operative imaging and intra-operative visual examination, which may miss microscopic residual sources of biofilm that can cause local recurrence of infection or life-threatening dissemination infection dissemination to vital organs or the bloodstream [4, 29, 82]. Colorimetric, non-toxic stains that grossly highlight necrotic tissue and biofilm, such as methylene blue [61, 81, 83], have been evaluated as a tool to guide surgical debridement. However, methylene blue can also non-specifically stain healthy articular cartilage and meniscus tissue, and biofilm stain uptake can vary between doses and bacterial species [83]. Fluorescence-guided debridement of necrotic and infected tissue showed promise in a rat model of high-energy open fracture but has yet to be evaluated in clinical patients [62]. Intraoperative techniques to accurately and efficiently detect residual microscopic biofilm reservoirs within bone or infected synovial structures are thereby an unmet need.

Despite the current treatments available for biofilm infection, persistent biofilm infections continue to be a clinical challenge and cause significant patient morbidity. Adequate infection

clearance following combined therapy may take several weeks to months to achieve, during which time the patient may suffer pain and instability in the absence of the initial implant [84-87]. The recurrence rate for implant-associated infections in people ranges from 8-35%, even with two-stage implant removal and replacement [86-88]. While infected implants can be removed in horses [2, 3], the ability to perform two-stage radical implant removal and replacement is limited by the need to maintain fracture reduction for adequate healing given the large patient size and their inability to remain non-weight bearing for long periods. Additionally, no techniques currently exist to prosthetically replace joints with end-stage cartilage destruction secondary to chronic infection in horses. As such, persistent orthopedic infections often result in euthanasia due to a combination of high costs associated with continued treatment [52] and a poor prognosis for athleticism and quality of life [1, 17, 63, 89].

Summary of treatment options and limitations

While surgical removal of infected implants and tissues and long-term antimicrobial therapy aim to remove all sources of biofilm, residual biofilm reservoirs may persist that lead to re-infection or infection dissemination. The presence of chronic biofilm infections also aggravates inflammation that leads to bone and cartilage destruction that cause implant failure, pain, reduced quality of life, and can require euthanasia in horses. There is a desperate need for a treatment that can disrupt biofilms to facilitate antimicrobial access to indwelling bacteria and modulate the immune response to reduce inflammation-associated tissue damage and complications. Mesenchymal stromal cells (MSC) are a promising candidate to treat orthopedic biofilms given their dual antimicrobial and immunomodulatory properties. However, equine MSC require rigorous *in vitro* investigation prior to translation into a pre-clinical model.

The evidence for MSC as a potential therapy for orthopedic infections

Mesenchymal stromal cells as a therapeutic

Mesenchymal stromal cells are a heterogenous population of multipotent cells that can differentiate into multiple specialized mature cell types and guide tissue regeneration and repair in a paracrine fashion [90-92]. Equine MSC are typically isolated from bone marrow collected from the sternum [93, 94] or tuber coxae [95] or from adipose tissue [96-98]. MSC isolated from blood [99-101], placenta [102], and umbilical cord [103-106] have also been evaluated for their therapeutic potential. To-date, MSC have primarily been harnessed as a treatment to improve healing and return to function following musculoskeletal injuries in people [107-109] and horses [110-113]. MSC therapy has improved quality of healing and outcomes in tendinopathies [96, 98, 107, 110, 111], meniscal injuries [108, 112, 113], and osteoarthritis [97, 109, 114]. MSC used therapeutically are most commonly administered as intralesional [96, 110] or intrasynovial injections [97, 112, 113], although the feasibility of administration via regional limb perfusion has also been evaluated in horses [115-117].

MSC are typically isolated from and administered to the same patient (autologous) to avoid the risk of an immune reaction [110, 118, 119]. However, isolation and expansion of MSC from a patient can take a minimum of 3 weeks to obtain adequate cell numbers for treatment [120], delaying treatment. While the safety of administering MSC isolated from one individual into another individual of the same species (allogeneic) has been evaluated with variable results [105, 121-124], future advancements in the ability to administer allogeneic, banked MSC without

inducing an immune response would avoid delays associated with MSC isolation. Immediate availability is particularly important when treating orthopedic infections.

Antimicrobial properties

The primary antimicrobial mechanism of MSC is secretion of antimicrobial peptides (AMP), including those of the cathelicidin family [125-128], β-defensins [129, 130], elafins [99, 101], and cystatins [99]. These AMP have a dual hydrophobic-hydrophilic (amphipathic) structure and disrupt bacterial cell membranes in a detergent-like fashion [99, 125-127, 129]. MSC also secrete AMP that inhibit bacterial growth by interfering with metabolism of required nutrients, such as iron [102, 131] or the amino acid tryptophan [132]. Equine blood-derived MSC have also been shown to secrete cysteine proteases as an anti-biofilm defense [100]. Together, MSC-secreted AMP reduce live bacterial counts [99, 100, 125, 126, 128] and inhibit biofilm formation [99, 100, 128] from planktonic cultures. In addition to their inherent antimicrobial mechanisms, MSC synergize with antimicrobials and achieve better bacterial killing than MSC or antimicrobials alone [126, 127, 133].

MSC-mediated AMP secretion is stimulated in a paracrine fashion by binding of bacterial pathogen-associated molecular patterns (PAMP), such as LPS from Gram-negative outer membranes, cell wall teichoic acid, or bacterial nucleic acids to pattern recognition receptors (PRR) expressed on MSC membranes [102, 128, 129]. MSC specifically express TLR-2 [129], -3 [128, 134], -4 [102, 129, 134], and nucleotide-binding oligomerization domain (NOD)-like receptors [128]. Importantly, pre-stimulation of MSC with PRR ligands prior to exposure to bacteria enhances AMP synthesis and bacterial killing compared to unstimulated MSC [102, 126,

128]. In a mouse model of *S. aureus* mesh implant infection, the combination of antimicrobials and MSC pre-stimulated with a TLR-3 ligand achieved the greatest bacterial reduction [126], suggesting that pre-stimulation of MSC may enhance synergy with antimicrobials in bacterial killing. MSC also exert indirect antibacterial effects, including enhancing phagocytosis of planktonic bacteria by neutrophils [128] and AMP synthesis in keratinocytes [101]. These indirect mechanisms are driven by release of pro-inflammatory chemokines CCL-2 [101], macrophage chemotactic protein-1, and IL-8 [128] and are likewise enhanced by MSC pre-stimulation with PRR ligands [128].

MSC antimicrobial properties may vary between tissue sources [99-102, 125-128, 135, 136]. Equine endometrial-derived MSC secreted higher levels of AMP and reduced planktonic *E. coli* counts to a greater extent than bone marrow-derived or adipose-derived MSC [102]. Similarly, cysteine proteases have been detected in conditioned medium from equine blood-derived MSC [100] but have not been described in MSC from other tissues. The specific AMP profiles secreted by MSC from the same tissue source also varies between species. Human bone marrow-derived MSC secrete indoleamine 2,3 dioxygenase, an AMP that interferes with tryptophan metabolism, but murine bone marrow-derived MSC do not [132]. Further comparisons of MSC antimicrobial properties within and across species are therefore warranted prior to clinical translation as a treatment for orthopedic infections.

The ability of MSC to kill bacteria and inhibit biofilm formation via AMP secretion, and to synergize with antimicrobials in bacterial reduction, makes them a promising candidate for further evaluation as a treatment for orthopedic biofilm infections. One limitation of published

literature on MSC antimicrobial properties is that bacterial reduction is often evaluated following incubation with MSC conditioned medium. The conditioned medium, which contains the secreted antimicrobial proteins, is often generated by prior MSC stimulation with a specific PRR ligand [99-102, 128]. This approach may generate a more limited anti-bacterial response versus direct incubation with bacteria that would stimulate multiple PRR on MSC and thereby reflect how MSC would respond to an *in vivo* infection. Additionally, the antimicrobial ability of MSC is often measured by reduction of planktonic bacterial counts and prevention of biofilm formation from planktonic cultures [99-102, 128]. However, patients may present with orthopedic biofilm infections that have been present for several days to weeks [6, 137]. These long-standing biofilms would consist of adhered bacteria with a mature extracellular matrix and may be more resistant to MSC-mediated reduction than planktonic bacteria. Whether MSC can reduce established orthopedic biofilms in an *in vitro* system that allows interaction between MSC and biofilms requires investigation.

MSC immunomodulation: reduction versus resolution of inflammation

In addition to their antimicrobial properties, the ability of MSC to modulate inflammation [124, 138-141] and promote tissue healing in orthopedic injuries [96, 98, 108, 139] make MSC a promising therapy for orthopedic biofilm infections. MSC may reduce inflammation-associated tissue damage in orthopedic infections by directly suppressing inflammation [104, 124, 140] and by promoting *resolution* of inflammation [139, 142-144]. Resolution of inflammation is defined as the active transition from the inflammatory state to the reparative state and a return to tissue homeostasis (Fig 2.1) [30, 145-148]. The key requirement for inflammation resolution is synthesis of specialized pro-resolving lipid mediators (SPM) by regulatory macrophages and progenitor cells [139, 147, 149]. Stimulation of SPM synthesis, in turn, requires an initial inflammatory response. Binding of inflammatory cytokines and PAMP to target cells stimulates concurrent synthesis of pro-inflammatory lipid mediators and SPM [147, 149-153]. Resolution of inflammation by SPM synthesis is thereby an endogenous regulatory mechanism to prevent development of chronic, uncontrolled inflammation that results in tissue damage and loss-of-function [145].

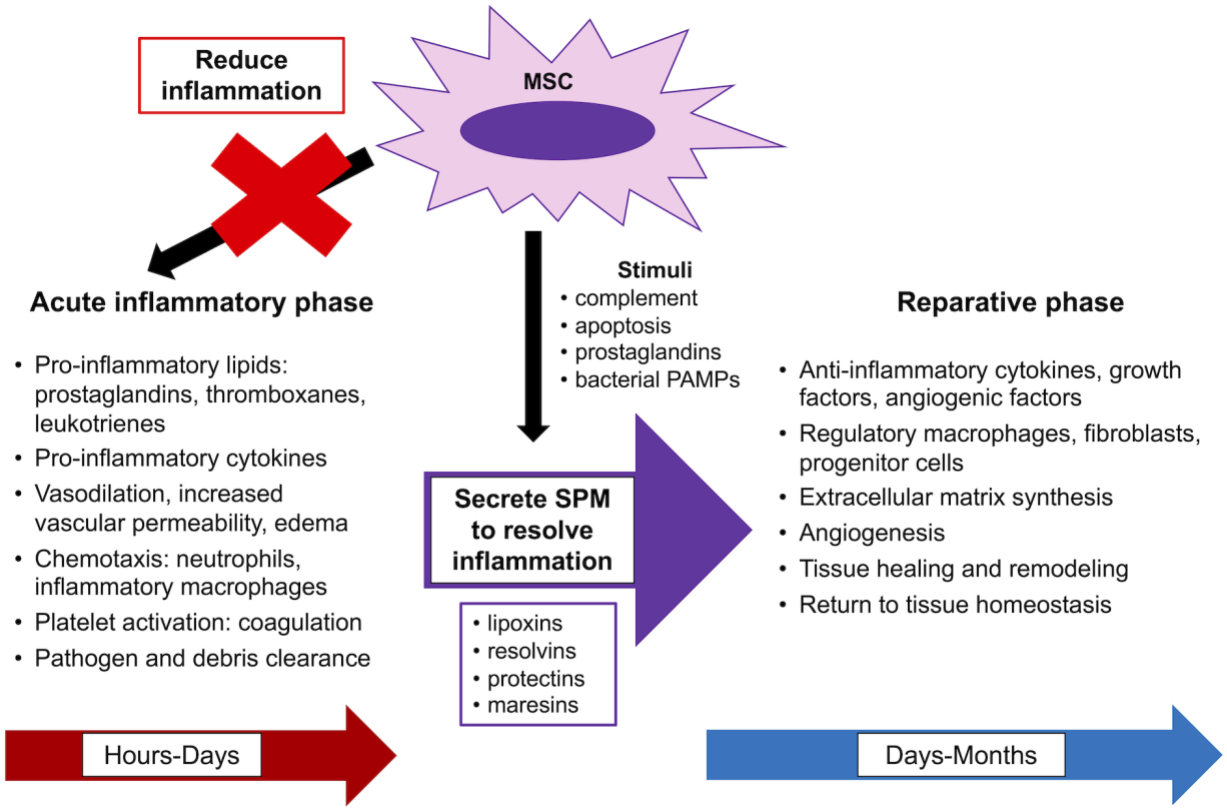

Figure 2.1: MSC reduce and promote resolution of inflammation.

MSC in mice and people modulate the immune response to infection by reducing inflammation and by promoting resolution of inflammation via SPM secretion. SPM simultaneously inflammatory signaling pathways and enhance pathways involved in tissue repair and homeostasis [111, 139, 154, 155].

Phases and resolution of inflammation

The acute inflammatory phase begins immediately following onset of inflammatory stimulus and can last for hours to days, depending on the strength and persistence of the stimulus (Fig 2.1) [10]. In a bacterial infection, the goal of the acute inflammatory phase is to remove the causative pathogen and tissue debris in preparation for tissue healing. During acute inflammation, neutrophils and inflammatory phenotype macrophages release pro-inflammatory lipid mediators, including prostaglandins, thromboxanes, and leukotrienes [150, 153, 154, 156]. These mediators promote vasodilation, increased vascular permeability, edema formation, and activation of hemostatic pathways [149, 154, 157, 158]. Prostaglandins and binding of bacterial PAMPs to PRR on host cells (e.g., TLR) also promote expression of pro-inflammatory cytokines, including IL-1, -6, -8, and -17, TNF, and interferons (INF), and activate Th1 and Th17 lymphocytes [159, 160]. These pathways result in further leukocyte recruitment to the site and stimulate bacterial killing by phagocytosis and release of antimicrobial extracellular traps and proteases [161-165].

The resolution of inflammation is triggered by enzymatic conversion of the ω-6 fatty acid arachidonic acid and the ω-3 fatty acids eicosapentaenoic acid (EPA) and docosahexaenoic acid (DHA) into SPM (Fig 2.2) [139, 146, 147]. SPM are synthesized by leukocytes and progenitor cells in response to complement [153], prostaglandins [149], and apoptosis [166]. In biofilm infections, binding of bacterial products such as LPS [150] and *Staphylococcal* toxins [152] to PRR also stimulate SPM synthesis. SPM bind G protein-coupled receptors on target cells to trigger production of anti-inflammatory cytokines and growth factors [139, 151], recruit progenitor cells to the site [139, 152], and stimulate polarization of macrophages to a regulatory phenotype [153]. SPM simultaneously reduce infiltration of neutrophils [147, 149], expression of

pro-inflammatory cytokines [152, 153], and macrophage polarization to an inflammatory phenotype [153]. Together, the actions of SPM on local cellular phenotype and signaling limit the duration and severity of the inflammatory response and allow transition into the reparative phase.

While both pro-inflammatory mediators (prostaglandins, thromboxanes, leukotrienes) and pro-resolving mediators (lipoxins) are derived from arachidonic acid, only pro-resolving mediators (resolvins, protectins, maresins) are derived from EPA and DHA (Fig 2.2) [139, 146, 147, 167, 168]. The function of the arachidonic acid-derived mediators also depends on the target cell. For example, the immunomodulatory functions of MSC are largely driven by prostaglandin (PG)E_2, including suppression of T-lymphocyte proliferation [104, 124], secretion of anti-inflammatory cytokines [140, 169], and reduction of pro-inflammatory cytokines [104]. The intermediate metabolites of SPM synthesis pathways may also have direct pro-resolving effects, including support of physiologic tissue remodeling [170] and inhibition of neutrophil function [171].

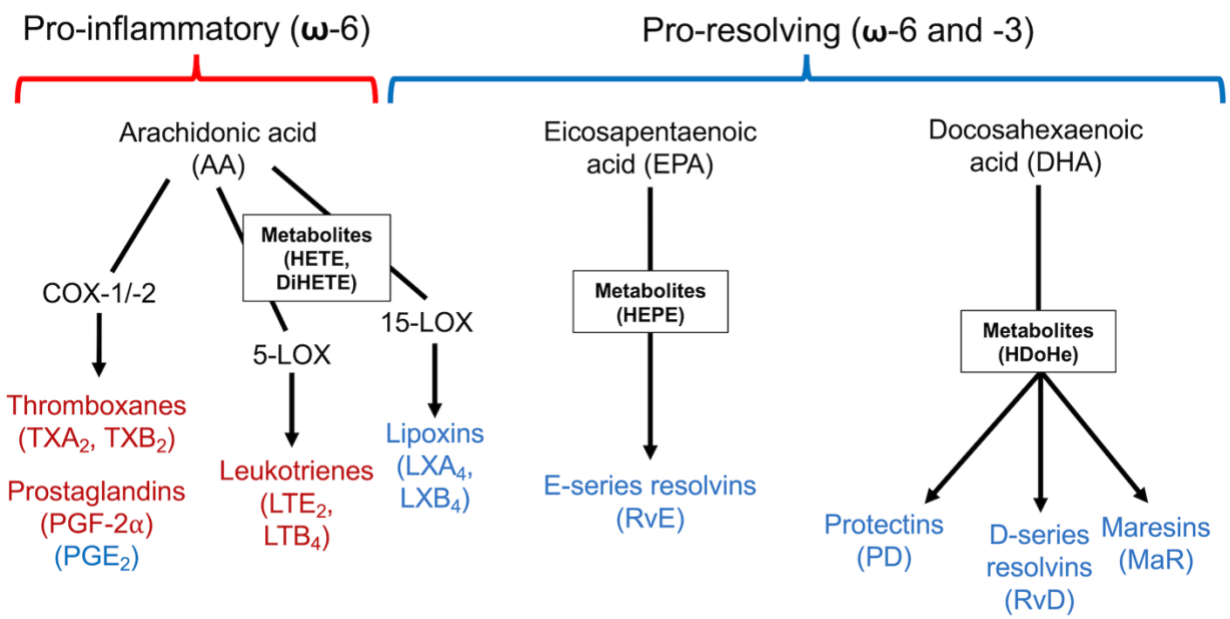

Figure 2.2: SPM synthesis from ω-6 and ω-3 fatty acids. Pro-inflammatory mediators are listed in red and pro-resolving mediators are listed in blue. Note that arachidonic acid can be metabolized to generate pro-inflammatory and pro-resolving mediators. COX = cyclooxygenase. LOX = lipoxygenase.

Following resolution of inflammation, the reparative phase can last weeks to months and is dominated by regulatory phenotype macrophages, fibroblasts, progenitor cells, anti-inflammatory cytokines, and angiogenic and anabolic growth factors (Fig 2.1) [139, 154, 155, 172]. Progenitor cells divide, differentiate, and recruit other progenitor cells to the site to promote angiogenesis and extracellular matrix synthesis [111, 139, 146, 173]. Regulatory macrophages also promote new tissue synthesis and remodeling by releasing anti-inflammatory cytokines and growth factors [154, 172, 174]. While SPM levels peak in serum at 1-8 hours post-inflammatory stimulus [149, 150] and are rapidly metabolized in target tissues [175, 176], SPM can be detected in sera from mice up to 14 days post-inflammatory challenge [177]. SPM may therefore have ongoing roles in promoting tissue repair and homeostasis following inflammation resolution.

Failure to resolve inflammation causes tissue damage in orthopedic biofilm infections

Inflammation in and of itself is not pathologic. A finite acute inflammatory response is necessary to remove pathogens and cellular debris prior to healing. However, persistent inflammation due the presence of biofilms in orthopedic infections causes secondary tissue damage, loss of function, and failure of appropriate tissue repair [127, 178, 179]. When implants become infected, inflammatory cytokines and Th1 lymphocytes promote osteoclast differentiation and activation, leading to bone matrix resorption and implant failure [178, 179]. In infected synovial structures, neutrophils and inflammatory macrophages release MMPs that degrade two key components of the cartilage extracellular matrix, aggrecan and type II collagen, leading to irreversible cartilage degradation and osteoarthritis [180, 181]. The goal of preventing these

complications is not only to reduce the magnitude of the inflammatory response, but to also promote resolution of inflammation such tissue repair can occur and homeostasis achieved [182].

The potential of MSC to modulate inflammation in orthopedic infections

The immunomodulatory potential of MSC in orthopedic infections is two-fold: reduction of inflammation [121, 124, 140, 183] and promotion of inflammation resolution via release of SPM (Fig 2.2) [138, 139, 142, 155]. MSC reduce expression of pro-inflammatory cytokines [103, 124, 133, 140, 141], express anti-inflammatory cytokines [140, 141, 183], and suppress lymphocyte proliferation [104, 121, 184]. MSC from people [139, 144, 150, 155] and mice [147, 185] also secrete multiple SPM that promote inflammation resolution. MSC-secreted SPM have promoted inflammation resolution in models of diabetic nephropathy [142], periodontitis [139, 155], peritonitis [147, 153], and neoplasia [186]. Administration of MSC-derived SPM has also been associated with inflammatory resolution in COVID-19 patients [187]. MSC from people additionally express membrane-bound SPM receptors that enhance the ability of MSC to migrate to and proliferate at the injury site [139, 143]. The dual ability to secrete and respond to SPM suggest that MSC can promote inflammation resolution via paracrine or autocrine pathways. While the equine SPM lipidome has yet to be fully investigated, one of the key mechanisms by which MSC modulate the inflammatory response is via production of arachidonic acid-derived lipid mediator PGE_2 [104, 124, 138, 140, 141]. The extent to which equine MSC produce and respond to a range of SPM, and promote resolution of inflammation in response to orthopedic biofilms, requires investigation.

MSC as a dual anti-biofilm and immune-modulating treatment

MSC therapy has shown promise in resolving infection-associated inflammation, in addition to reducing bacterial loads, in *in vivo* infection models. MSC administered intratracheally reduced lung edema, bacterial counts, and improved survival in a mouse model of *E. coli* pneumonia [131]. Intravenous MSC honed to the site of infection, reduced bacterial counts and promoted macrophage polarization to a regulatory M2 phenotype in a *S. aureus* subcutaneous mesh infection mouse model and in cutaneous wounds in dogs [126]. A recent study utilizing a rat model of *S. aureus* coxofemoral prosthetic joint infection revealed that MSC, combined with an antimicrobial, reduced bone bacterial loads, implant site osteolysis, and gene expression of inflammatory cytokines IL-6 and TNF-α compared to antimicrobials or MSC alone [127].

While reports of a potential dual ability of MSC to combat bacterial infections while reducing immune-mediated tissue destruction are promising, the extent to which MSC-mediated bacterial reductions versus direct immune modulation contributed to the improved outcomes is unclear, particularly when antimicrobials were co-administered. The mechanisms by which MSC ameliorated inflammation and promoted healing in these models, whether by direct reduction of inflammation versus promoting resolution of inflammation via SPM release, are also not understood. To evaluate the dual potential of equine MSC to reduce establish orthopedic biofilms and modulate the immune response to biofilms, a co-culture system in which MSC can interact in a paracrine or direct fashion with biofilms, with or without immune cells, must be developed. This system should also allow quantification of biofilm reduction by multiple methods following co-culture.

Models to grow and quantify biofilm reduction by novel treatments

Biofilm growth models

In vitro and *ex vivo* models of biofilm infections are an essential initial step for evaluation of novel pharmacologic and orthobiologic treatments (Table 2.2). Biofilm growth in cell culture plates remains the simplest and most cost-effective method for initial screening of treatment efficacy by multiple methods [99, 100, 188, 189]. However, microfluidic (flow-cell) models [190-195] and the CDC biofilm reactor [83, 196-198] allow more precise evaluation of biofilm growth under diverse conditions [83, 191, 193, 195, 196, 198]. The ability to evaluate biofilm growth on a variety of surfaces [196-198], over longer timespans [191, 193, 195], and under shear stress [192, 199] in these systems may more accurately model orthopedic biofilm growth *in vivo* compared to growth in cell culture plates. *Ex vivo* biofilm growth in synovial fluid [57, 200-202], on skin [101] and on bone explants [66] may provide more biologically relevant methods to measure biofilm response to novel treatments by providing physiologically organized tissue layers and tissue-specific host extracellular matrix proteins for biofilm attachment [66, 101, 203]. Results from *in vitro* and *ex vivo* biofilm growth models eventually require translation to *in vivo* models prior to clinical patient testing [203, 204].

In vivo models of orthopedic biofilm infections allow evaluation of orthopedic infection pathophysiology and response to novel treatments prior to evaluation in the species of interest. These models most often utilize inbred rodents [82, 178, 205] or rabbits [206-211] that enable repeatable establishment of biofilm formation, evaluation of the infection sequelae, and response to treatments of interest. Rodent models of implant-associated infections have improved our

understanding of orthopedic biofilm infection pathophysiology [205, 212], including variations in disease severity between bacterial species [178], immune system evasion [82], and infection response to MSC treatment [126, 127]. While a model of equine implant-associated infection has yet to be developed, reported equine models of septic synovitis have provided valuable information on the immune response to sepsis [34] and efficacy of orthobiologic therapies [213] that are directly translatable into clinical patients and document expected variations in outcomes in heterogeneous individuals [213].

Table 2.2: *In vitro* and *ex vivo* models of biofilm growth and reduction by treatments of interest.

Category	Model	Advantages and Disadvantages	References
In vitro	Growth in cell culture plates	Technically simple, repeatable, and cost-effective Multiple applicable biofilm quantification techniques Simultaneously screen multiple treatments Difficulty in separating planktonic cells vs. biofilm (alternate = Calgary peg model) Limited to static cultures	99, 100, 128, 188, 195, 214, 215
	Microfluidic (flow-cell) models	Real-time monitoring of biofilm formation on time-lapse microscopy Continuous in-flow of nutrients and removal of wastes and planktonic cells Evaluate polymicrobial biofilms and interspecies bacterial interactions Evaluate the role of quorum sensing in biofilm formation Small volume medium usage facilitates long-term experiments Confocal image resolution varies between microscopes and cell setup High cost, limited access to microscopy equipment Variable access to materials/working knowledge of microfluidic cell design	25, 190, 192-195, 216, 217
	CDC Biofilm Reactor	Simultaneously evaluate biofilm growth on multiple, customizable surfaces, including orthopedic implant materials Evaluate polymicrobial biofilms Evaluate growth under shear fluid stresses Can combine with staining or microscopic quantification techniques Cost/limited access to reactors and/or working knowledge	83, 196-198
Ex vivo	Direct synovial fluid inoculation	Relatively technically simple Biological relevance to clinical septic synovitis cases Cannot evaluate interaction with host immune cells Need to isolate synovial fluid from live animals	201, 202, 218
	Skin explant model	Biological relevance to clinical skin wounds Cannot evaluate interaction with host immune cells Need to isolate skin samples from live animals	101
	Bone explant model	Biological relevance to clinical implant-associated osteomyelitis cases Advantages/disadvantages as for other explant models	66

Biofilm quantification techniques

Biofilm quantification techniques can be broadly divided into matrix staining [99, 100, 188, 219], live bacterial quantification [188, 200, 220], or microscopic evaluation [57, 100, 178, 205] (Table 2.3). Colorimetric and fluorescent stains detect total biofilm biomass (all cells and matrix in the biofilm) and specific matrix components [57, 188, 219]. The crystal violet assay is relatively non-specific in that it stains negatively charged molecules [215]; however, it remains widely utilized as a tool to quantify changes in biofilm biomass [99, 100, 188, 219, 221]. The specificity of other staining techniques also varies. For example, the intercalating DNA stain STYO-9 detects double-stranded (dsDNA) but can be considered a biomass stain since it detects DNA in live bacteria and biofilm matrix eDNA [189]. In contrast, DNA stains that cannot penetrate live cells, such as propidium iodide, can specifically measure matrix eDNA [219]. Live bacterial quantification is commonly performed via enumeration of live colonies following enzymatic matrix digestion, serial dilution and agar plating [188, 200]. Alternatively, live bacteria can be quantified with fluorescent DNA stains that specifically penetrate live bacterial cells, such as 4′,6-diamidino-2-phenylindole [219] or by using combined live/dead DNA stain kits that simultaneously delineate live bacteria versus matrix eDNA [128]. Live bacterial counts are also indirectly quantified via colorimetric or fluorescent reduction of a substrate through cellular respiration [188, 220, 222].

While more technically challenging and costly, advanced microscopic techniques can give valuable information on changes in biofilm formation under specific growth conditions [25, 100, 205, 216, 217] and treatments [57, 100]. Electron microscopy can provide detailed three-

dimensional information on biofilm architecture [82, 205]. Confocal microscopy can be performed following fluorescent biofilm matrix staining to evaluate biofilm reduction in response to treatments [57, 100]. Alternatively, confocal microscopy can be combined with microfluidic models to allow real-time monitoring of biofilm formation [192, 194, 223, 224] and interactions between bacterial species or between bacteria and immune cells [164, 225]. Measurement of biofilm-associated gene expression by PCR is also used to document biofilm formation in laboratory models [193, 205, 226] and in clinical samples [18, 227, 228].

Table 2.3: Techniques to quantify biofilm reduction *in vitro*. All stains referenced are trademarked to Thermo-Fisher Scientific.

Abs = absorbance wavelength of colorimetric stains. Ex/Em = excitation and emission wavelengths of fluorescent stains.

Target	**Technique**	**Mechanism**	**References**
Biomass	Crystal violet	Basic dye, stains negatively charged molecules, including protein, DNA, polysaccharides; colorimetric, purple (Abs 595 nm)	99, 100, 188, 214, 215, 229
	Safranin O	As for crystal violet; colorimetric, red (Abs 530 nm)	99, 221
	SYTO™-9	Stains dsDNA, green fluorescence (ex/em 458/498 nm)	188, 230
Matrix DNA	SYTO™-9	Stains dsDNA, green fluorescence (ex/em 458/498 nm)	57, 188
	Acridine orange	Stains dsDNA, green fluorescence (ex/em 485/528 nm)	189
	4′,6-diamidino-2-phenylindole (DAPI)	Stains intracellular ds DNA to highlight live bacteria, blue fluorescence (ex/em 461/358 nm)	100, 219
	Propidium iodide	Stains extracellular ds DNA in matrix, red fluorescence (ex/em 528/617 nm)	219
Matrix protein	SYPRO™ Ruby	Stains proteins via noncovalent, hydrophobic, and electrostatic interactions; red fluorescence (ex/em 450/610 nm)	57, 100
	Congo Red	Stains amyloid, colorimetric, red (Abs 490 nm)	231, 232
Matrix carbohydrate	Wheat germ agglutinin (WGA)-Alexa Fluor™ 488	Stains *N*-acetylglucosamine and sialic acid residues, green fluorescence (ex/em 495/519 nm)	57, 214
	1, 9-dimethylmethylene blue (DMMB)	Stains polysulfated glycosaminoglycans, metachromatic (Abs 525 nm)	188, 222
	Alcian blue	Stains sulfated and carboxylated mucopolysaccharides, colorimetric (Abs 620 nm)	230

	Concanavalin-A	Stains glycoproteins, α-mannopyranosyl and α-glucopyranosyl residues, fluorescent, ex/em varies on conjugate molecule	219
Live bacteria	Colony-forming unit (CFU) quantification	Enumerates live biofilm-bound bacteria on agar	128, 200, 215
	Tetrazolium salt (XTT) reduction assay	Measures mitochondrial respiratory chain activity, colorimetric (Abs 490 nm)	188, 220
	Resazurin reduction assay	Phenoxazine dye, measures mitochondrial respiratory chain activity, fluorescent (ex/em 530/580-580 nm)	188, 222
	LIVE™/DEAD™ staining	Calcein AM quantifies intracellular esterase activity of live cells, green fluorescence (ex/em 494/517 nm); PI stains DNA of dead bacterial cells, red fluorescence (ex/em 528/617 nm)	128
Biofilm architecture	Confocal microscopy	Qualitative and quantitative evaluation of bacterial attachment to surfaces or aggregation, matrix production, biofilm formation over time in microfluidics systems	57, 100, 194, 224, 225
	Scanning electron microscopy	Qualitative evaluation of bacterial attachment to surfaces, matrix architecture and thickness	178, 205
Biofilm gene expression	Polymerase chain reaction (PCR)	Measures expression of genes important in bacterial adhesion and matrix synthesis	193, 233, 234
Other	Fluorescent *in situ* hybridization (FISH)	Evaluate intercellular interactions within polymicrobial biofilms or between biofilm bacteria and eukaryotic cells	164, 225

Applying current techniques to evaluation of MSC as an anti-biofilm therapy

Given that each method of biofilm quantification targets different aspects of biofilm formation and has unique advantages and disadvantages, a combination of techniques should be utilized to provide the most comprehensive evaluation of biofilm reduction [100, 188, 189, 220]. It is unclear which techniques can be successfully utilized to quantify biofilm reduction in a model that allows interaction between MSC and biofilms. It is also unclear whether the inclusion of antimicrobials that are used to treat clinical equine orthopedic infections, such as amikacin sulfate, would interfere with quantification methods, particularly staining techniques. In order to evaluate the ability of equine MSC alone or with clinically relevant antimicrobials to break down, and modulate the immune response to, orthopedic biofilms, development of an *in vitro* MSC-biofilm co-culture system that allows MSC-biofilm interactions and biofilm quantification by multiple methods is required.

Summary

Current treatment of orthopedic biofilm infections involves aggressive, multi-stage surgical removal of infected implants and tissues combined with prolonged systemic and local antimicrobial therapy. The inability to eliminate biofilms despite this multimodal approach can lead to infection recurrence and dissemination to vital organs, persistent pain/lameness, and morbidity. The ideal therapy for orthopedic biofilm infections would be able to disrupt biofilms and improve success of antimicrobial therapy and modulate biofilm-associated inflammation to mitigate secondary tissue damage and complications. MSC show promise as a treatment for orthopedic biofilm infections due to their abilities to kill planktonic bacteria, prevent

establishment of biofilms, synergize with antimicrobials, and regulate inflammation. The ability of MSC to disrupt established biofilms of orthopedic pathogens, and to modulate the immune response to orthopedic biofilms, is currently unknown. In order to evaluate whether equine MSC could fulfill either or both of these roles, there is an initial need to develop an *in vitro* model that allows a) interaction between equine MSC and biofilms of orthopedic pathogens and b) subsequent quantification of biofilm reduction by equine MSC by multiple techniques. That model would then be utilized to answer two questions:

1. Can MSC alone or combined with clinically relevant antimicrobials reduce biofilms of orthopedic pathogens in the aforementioned *in vitro* co-culture model?

2. Can MSC modulate the host immune response to orthopedic biofilms, either by reducing inflammation or promoting resolution of inflammation via SPM?

BIBLIOGRAPHY

1. O'Brien TJ, Rosanowski SM, Mitchell KD, Carrick JB, Butt TD, Adkins AR. Factors associated with survival and racing performance of 114 Thoroughbred foals with septic arthritis compared with maternal siblings (2009-2015). Equine Vet J. 2021;53:935-43.
2. Ahern BJ, Richardson DW, Boston RC, Schaer TP. Orthopedic infections in equine long bone fractures and arthrodeses treated by internal fixation: 192 cases (1990-2006). Vet Surg. 2010;39:588-93.
3. Curtiss AL, Stefanovski D, Richardson DW. Surgical site infection associated with equine orthopedic internal fixation: 155 cases (2008-2016). Vet Surg. 2019;48:685-93.
4. Masters EA, Trombetta RP, de Mesy Bentley KL, Boyce BF, Gill AL, Gill SR, et al. Evolving concepts in bone infection: redefining "biofilm," "acute vs. chronic osteomyelitis," "the immune proteome," and "local antibiotic therapy." Bone Res. 2019;7:20.
5. Gieling F, Peters S, Erichsen C, Richards RG, Zeiter S, Moriarty TF. Bacterial osteomyelitis in veterinary orthopaedics: Pathophysiology, clinical presentation and advances in treatment across multiple species. Vet J. 2019;250:44-54.
6. Goodrich LR. Osteomyelitis in horses. Vet Clin North Am Equine Pract. 2006;22:389-417, viii-ix.
7. Saeed K, McLaren AC, Schwarz EM, Antoci V, Arnold WV, Chen AF, et al. 2018 international consensus meeting on musculoskeletal infection: Summary from the biofilm workgroup and consensus on biofilm related musculoskeletal infections. J Orthop Res. 2019;37:1007-17.

8. Bertone AL. Update on infectious arthritis in horses. Equine Vet Educ. 1999;11:143-52.

9. Straticò P, Varasano V, Suriano R, Sciarrini C, Petrizzi L. Traumatic Septic Tenosynovitis of the Tarsal Sheath with Fragmentation of the Sustentaculum Tali: Surgical Treatment and Outcome in 3 Horses. J Equine Vet Sci. 2014;34:538-43.

10. Equine Surgery, 5th ed. Auer JA, Stick JA, Kummerle JM, Prange T, ed. Saunders Elsevier. Philadelphia, Pennsylvania, USA. 2019.

11. Easley JT, Brokken MT, Zubrod CJ, Morton AJ, Garrett KS, Holmes SP. Magnetic resonance imaging findings in horses with septic arthritis. Vet Radiol Ultrasound. 2011;52:402-8.

12. Lalam RK, Cassar-Pullicino VN, Tins BJ. Magnetic resonance imaging of appendicular musculoskeletal infection. Top Magn Reson Imaging. 2007;18:177-91.

13. Equine Fracture Repair, 2nd ed. Nixon AJ, ed. Wiley Blackwell, Ltd. Hoboken, New Jersey, USA. 2020.

14. Beccati F, Gialletti R, Passamonti F, Nannarone S, Di Meo A, Pepe M. Ultrasonographic findings in 38 horses with septic arthritis/tenosynovitis. Vet Radiol Ultrasound. 2015;56:68-76.

15. Marsh CA, Watkins JP, Schneider RK. Intrathecal deep digital flexor tenectomy for treatment of septic tendonitis/tenosynovitis in four horses. Vet Surg. 2011;40:284-90.

16. Drago L, Clerici P, Morelli I, Ashok J, Benzakour T, Bozhkova S, et al. The World Association against Infection in Orthopaedics and Trauma (WAIOT) procedures for Microbiological Sampling and Processing for Periprosthetic Joint Infections (PJIs) and other Implant-Related Infections. J Clin Med. 2019;8.

17. Schneider RK, Bramlage LR, Moore RN, Mecklenburg LM, Kohn KW, Gabel AA. A retrospective of 192 horses affected with septic arthritis/tenosynovitis. Equine Vet J. 1992;24:436-42.

18. Gomez E, Cazanave C, Cunningham SA, Greenwood-Quaintance KE, Steckelberg JM, Uhl JR, et al. Prosthetic joint infection diagnosis using broad-range PCR of biofilms dislodged from knee and hip arthroplasty surfaces using sonication. J Clin Microbiol. 2012;50:3501-8.

19. Keeshen T, Case JB, Wellehan JF, Dujowich M. Bacterial recovery using sonication versus swabbing of titanium and stainless steel implants inoculated with *Staphylococcus pseudintermedius* or *Pseudomonas aeruginosa*. Vet Comp Orthop Traumatol. 2017;30:346-50.

20. Trampuz A, Piper, K. E., Jacobson, M. J., , Hanssen AD, Unni, K. K., Osmon, D. R., Mandrekar, J. N., Cockerill, F. R.,, Steckelberg JM, Greenleaf, J. F., Patel, R. Sonication of Removed Hip and Knee Prostheses for Diagnosis of Infection. N Engl J Med. 2007;357:654-63.

21. Pille F, Martens A, Schouls LM, Dewulf J, Decostere A, Vogelaers D, et al. Broad range 16S rRNA gene PCR compared to bacterial culture to confirm presumed synovial infection in horses. Vet J. 2007;173:73-8.

22. Sreenivas T, Nataraj AR, Menon J. Acute hematogenous septic arthritis of the knee in adults. Eur J Orthop Surg Traumatol. 2013;23:803-7.

23. Rinnovati R, Butina BB, Lanci A, Mariella J. Diagnosis, Treatment, Surgical Management, and Outcome of Septic Arthritis of Tarsocrural Joint in 16 Foals. J Equine Vet Sci. 2018;67:128-32.

24. Schwarz EM, Parvizi J, Gehrke T, Aiyer A, Battenberg A, Brown SA, et al. 2018 International Consensus Meeting on Musculoskeletal Infection: Research Priorities from the General Assembly Questions. J Orthop Res. 2019;37:997-1006.

25. Liu TH, Cheng SS, You HL, Lee MS, Lee GB. Bacterial detection and identification from human synovial fluids on an integrated microfluidic system. Analyst. 2019;144:1210-22.

26. Lowman ME, Tipton CD, Labordere AL, Brown JA. Equine sinusitis aetiology is linked to sinus microbiome by amplicon sequencing. Equine Vet J. 2022.

27. Anis E, Ilha, M. R. S., Engiles, J. B., Wilkes, R. P. Evaluation of targeted next-generation sequencing for detection of equine pathogens in clinical samples. J Vet Diag Invest. 2021;33:227-34.

28. He W, Wu C, Zhong Y, Li J, Wang G, Yu B, et al. Case Report: Therapeutic Strategy With Delayed Debridement for Culture-Negative Invasive Group A Streptococcal Infections Diagnosed by Metagenomic Next-Generation Sequencing. Front Public Health. 2022;10:899077.

29. Osmon DR, Berbari EF, Berendt AR, Lew D, Zimmerli W, Steckelberg JM, et al. Diagnosis and management of prosthetic joint infection: clinical practice guidelines by the Infectious Diseases Society of America. Clin Infect Dis. 2013;56:e1-e25.

30. Tizard I. Veterinary Immunology, 10th ed. Saunders Elsevier, Ltd. Philadelphia, Pennsylvania, USA. 2017.

31. Ettinger M, Calliess T, Kielstein JT, Sibai J, Bruckner T, Lichtinghagen R, et al. Circulating biomarkers for discrimination between aseptic joint failure, low-grade infection, and high-grade septic failure. Clin Infect Dis. 2015;61:332-41.

32. Shukla SK, Ward JP, Jacofsky MC, Sporer SM, Paprosky WG, Della Valle CJ. Perioperative testing for persistent sepsis following resection arthroplasty of the hip for periprosthetic infection. J Arthroplasty. 2010;25:87-91.

33. Thurston CC, Stefanovski D, MacKinnon MC, Chapman HS, Richardson DW, Levine DG. Serum amyloid A and fibrinogen as markers for early detection of surgical site infection associated with internal fixation in the horse. Front Vet Sci. 2022;9:960865.

34. Ludwig EK, Brandon Wiese R, Graham MR, Tyler AJ, Settlage JM, Werre SR, et al. Serum and Synovial Fluid Serum Amyloid A Response in Equine Models of Synovitis and Septic Arthritis. Vet Surg. 2016;45:859-67.

35. Muller AC, Buttner K, Rocken M. Systemic serum amyloid A in early (<24 h) diagnosis of acute synovial structure involvement in horses with penetrating limb injuries. Vet J. 2021;277:105759.

36. Biasutti SA, Cox E, Jeffcott LB, Dart AJ. A review of regional limb perfusion for distal limb infections in the horse. Equine Vet Educ. 2020;33:263-77.

37. Redding LE, Elzer EJ, Ortved KF. Effects of regional limb perfusion technique on concentrations of antibiotic achieved at the target site: A meta-analysis. PLoS One. 2022;17:e0265971.

38. Harvey A, Kilcoyne I, Byrne BA, Nieto J. Effect of Dose on Intra-Articular Amikacin Sulfate Concentrations Following Intravenous Regional Limb Perfusion in Horses. Vet Surg. 2016;45:1077-82.

39. Parra-Sanchez A, Lugo J, Boothe DM, Gaughan EM, Hanson RR, Duran S, Belknap JK. Pharmacokinetics and pharmacodynamics of enrofloxacin and a low dose of amikacin

administered via regional intravenous limb perfusion in standing horses. Am J Vet Res. 2006;67:1687-95.

40. Moser DK, Schoonover MJ, Holbrook TC, Payton ME. Effect of Regional Intravenous Limb Perfusate Volume on Synovial Fluid Concentration of Amikacin and Local Venous Blood Pressure in the Horse. Vet Surg. 2016;45:851-8.

41. Oreff GL, Dahan R, Tatz AJ, Raz T, Britzi M, Kelmer G. The Effect of Perfusate Volume on Amikacin Concentration in the Metacarpophalangeal Joint Following Cephalic Regional Limb Perfusion in Standing Horses. Vet Surg. 2016;45:625-30.

42. Stewart AA, Goodrich LR, Byron CR, Evans RB, Stewart MC. Antimicrobial delivery by intrasynovial catheterisation with systemic administration for equine synovial trauma and sepsis. Aust Vet J. 2010;88:115-23.

43. Farnsworth KD, White NA, 2nd, Robertson J. The effect of implanting gentamicin-impregnated polymethylmethacrylate beads in the tarsocrural joint of the horse. Vet Surg. 2001;30:126-31.

44. Hall MS, Pollock PJ, Russell T. Surgical treatment of septic physitis in 17 foals. Aust Vet J. 2012;90:479-84.

45. Santschi EM, McGarvey L. *In vitro* elution of gentamicin from Plaster of Paris beads. Vet Surg. 2003;32:128-33.

46. Scheuch BC, Van Hoogmoed LM, Wilson WD, Snyder JR, MacDonald MH, Watson ZE, Steffey EP. Comparison of intraosseous or intravenous infusion for delivery of amikacin sulfate to the tibiotarsal joint of horses. Am J Vet Res. 2002;63:374-80.

47. Taintor J, Schumacher J, DeGraves F. Comparison of amikacin concentrations in normal and inflamed joints of horses following intra-articular administration. Equine Vet J. 2006;38:189-91.

48. Sedrish SA, Moore RM, Barker SA. Pharmacokinetics of single dose intra-articular administration of amikacin in the radiocarpal joints of normal horses. Am College of Vet Surgeons Annual Summit. Chicago, Illinois, USA. 1994. p. 437.

49. Zmistowski B, Karam JA, Durinka JB, Casper DS, Parvizi J. Periprosthetic joint infection increases the risk of one-year mortality. J Bone Joint Surg Am. 2013;95:2177-84.

50. DiMaio FR, O'Halloran JJ, Quale JM. *In vitro* elution of ciprofloxacin from polymethylmethacrylate cement beads. J Orthop Res. 1994;12:79-82.

51. Moore RM, Schneider RK, Kowalski J, Bramlage LR, Mecklenburg LM, Kohn CW. Antimicrobial susceptibility of bacterial isolates from 233 horses with musculoskeletal infection during 1979–1989. Equine Vet J. 1992;24:450-56.

52. Jacobs CC, Levine DG, Richardson DW. Use of locking compression plates in ulnar fractures of 18 horses. Vet Surg. 2017;46:242-8.

53. Levine DG, Epstein KL, Neelis DA, Ross MW. Effect of topical application of 1% diclofenac sodium liposomal cream on inflammation in healthy horses undergoing intravenous regional limb perfusion with amikacin sulfate. Am J Vet Res. 2009;70:1323-5.

54. Veterinary Pharmacology and Therapeutics, 10th ed. Riviere JE, Papich MG, ed. Hoboken, New Jersey, USA. Wiley-Blackwell. 2017.

55. Singh M, Chang J, Coffman L, Kim SJ. Hidden Mode of Action of Glycopeptide Antibiotics: Inhibition of Wall Teichoic Acid Biosynthesis. J Phys Chem B. 2017;121:3925-32.

56. McKellar OA, Bruni SFS. Jones DG. Pharmacokinetic/pharmacodynamic relationships of antimicrobial drugs used in veterinary medicine. J Vet Pharmacol Therap. 2004;27:503-14.

57. Gilbertie JM, Schnabel LV, Hickok NJ, Jacob ME, Conlon BP, Shapiro IM, et al. Equine or porcine synovial fluid as a novel *ex vivo* model for the study of bacterial free-floating biofilms that form in human joint infections. PLoS One. 2019;14:e0221012.

58. Bidossi A, Bottagisio M, Savadori P, De Vecchi E. Identification and Characterization of Planktonic Biofilm-Like Aggregates in Infected Synovial Fluids From Joint Infections. Front Microbiol. 2020;11:1368.

59. Walker M, Singh A, Nazarali A, Gibson TW, Rousseau J, Weese JS. Evaluation of the Impact of Methicillin-Resistant *Staphylococcus pseudintermedius* Biofilm Formation on Antimicrobial Susceptibility. Vet Surg. 2016;45:968-71.

60. Babushkina IV, Mamonova IA, Ulyanov VY, Gladkova EV, Shpinyak SP. Antibiotic Susceptibility of *Staphylococcus aureus* Plankton and Biofilm Forms Isolated in Implant-Associated Infection. Bull Exp Biol Med. 2021;172:46-8.

61. Shaw JD, Miller S, Plourde A, Shaw DL, Wustrack R, Hansen EN. Methylene Blue-Guided Debridement as an Intraoperative Adjunct for the Surgical Treatment of Periprosthetic Joint Infection. J Arthroplasty. 2017;32:3718-23.

62. Elliott JT, Henderson E, Streeter SS, Demidov V, Han X, Tang Y, et al. Fluorescence-guided and molecularly-guided debridement: identifying devitalized and infected tissue in orthopaedic trauma. Proc SPIE Int Soc Opt Eng. 2023;12361.

63. Hepworth-Warren KL, Wong DM, Fulkerson CV, Wang C, Sun Y. Bacterial isolates, antimicrobial susceptibility patterns, and factors associated with infection and outcome in foals with septic arthritis: 83 cases (1998–2013). J Am Vet Med Assoc. 2015;246:785-93.

64. McIlwraith CW, Nixon, AJ, Wright IM. Diagnostic and Surgical Arthroscopy of the Horse, 4th Ed. Saunders-Elsevier, Ltd. Philadelphia, Pennsylvania, USA. 2015.

65. Russo A, Gatti A, Felici S, Gambardella A, Fini M, Neri MP, et al. Piezoelectric ultrasonic debridement as new tool for biofilm removal from orthopedic implants: A study *in vitro*. J Orthop Res. 2023.

66. Lamret F, Lemaire A, Lagoutte M, Varin-Simon J, Abraham L, Colin M, et al. Approaching prosthesis infection environment: Development of an innovative *in vitro Staphylococcus aureus* biofilm model. Biofilm. 2023;5:100120.

67. Clifton R, Haleem S, McKee A, Parker MJ. Closed suction surgical wound drainage after hip fracture surgery: a systematic review and meta-analysis of randomised controlled trials. Int Orthop. 2008;32:723-7.

68. Stichling M, Wiessner A, Kikhney J, Gatzer R, Muller M, Scheuermann-Poley C, et al. Is There a Wound Recontamination by Eluates with High Bacterial Load in Negative-Pressure Wound Therapy with Instillation and Dwell Time? Plast Reconstr Surg. 2023;151:136e-47e.

69. Launois T, Moor PL, Berthier A, Merlin N, Rieu F, Schlotterer C, et al. Use of Negative Pressure Wound Therapy in the Treatment of Limb Wounds: A Case Series of 42 Horses. J Equine Vet Sci. 2021;106:103725.

70. Kwan JC, Flannagan RS, Vasquez Pena M, Heinrichs DE, Holdsworth DW, Gillies ER. Induction Heating Triggers Antibiotic Release and Synergistic Bacterial Killing on Polymer-Coated Titanium Surfaces. Adv Healthc Mater. 2023:e2202807.

71. Choi S, Lee H, Hong R, Jo B, Jo S. Application of Multi-Layered Temperature-Responsive Polymer Brushes Coating on Titanium Surface to Inhibit Biofilm Associated Infection in Orthopedic Surgery. Polymers (Basel). 2022;15.

72. Karacan I, Ben-Nissan B, Santos J, Yiu S, Bradbury P, Valenzuela SM, et al. *In vitro* testing and efficacy of poly-lactic acid coating incorporating antibiotic loaded coralline bioceramic on Ti6Al4V implant against *Staphylococcus aureus*. J Tissue Eng Regen Med. 2022;16:1149-62.

73. Shi K, Zhang H, Gu Y, Liang Z, Zhou H, Liu H, et al. Electric Spark Deposition of Antibacterial Silver Coating on Microstructured Titanium Surfaces with a Novel Flexible Brush Electrode. ACS Omega. 2022;7:47108-19.

74. Rawat N, Bencina M, Gongadze E, Junkar I, Iglic A. Fabrication of Antibacterial TiO(2) Nanostructured Surfaces Using the Hydrothermal Method. ACS Omega. 2022;7:47070-7.

75. Gao W, Han X, Sun D, Li Y, Liu X, Yang S, et al. Antibacterial properties of antimicrobial peptide HHC36 modified polyetheretherketone. Front Microbiol. 2023;14:1103956.

76. Lallukka M, Gamna F, Gobbo VA, Prato M, Najmi Z, Cochis A, et al. Surface Functionalization of Ti6Al4V-ELI Alloy with Antimicrobial Peptide Nisin. Nanomaterials (Basel). 2022;12.

77. Wei J, Cao X, Qian J, Liu Z, Wang X, Su Q, et al. Evaluation of antimicrobial peptide LL-37 for treatment of *Staphylococcus aureus* biofilm on titanium plate. Medicine (Baltimore). 2021;100:e27426.

78. Erdogan YK, Ercan B. Anodized Nanostructured 316L Stainless Steel Enhances Osteoblast Functions and Exhibits Anti-Fouling Properties. ACS Biomater Sci Eng. 2023;9:693-704.

79. Ragupathi NKD, Muthuirulandi Sethuvel DP, Gopikrishnan M, Dwarakanathan HT, Murugan D, Biswas I, et al. Phage-based therapy against biofilm producers in gram-negative ESKAPE pathogens. Microb Pathog. 2023;178:106064.

80. Joo H, Wu SM, Soni I, Wang-Crocker C, Matern T, Beck JP, et al. Phage and Antibiotic Combinations Reduce *Staphylococcus aureus* in Static and Dynamic Biofilms Grown on an Implant Material. Viruses. 2023;15.

81. Dorafshar AH, Gitman M, Henry G, Agarwal S, Gottlieb LJ. Guided surgical debridement: staining tissues with methylene blue. J Burn Care Res. 2010;31:791-4.

82. de Mesy Bentley KL, Trombetta R, Nishitani K, Bello-Irizarry SN, Ninomiya M, Zhang L, et al. Evidence of *Staphylococcus Aureus* Deformation, Proliferation, and Migration in Canaliculi of Live Cortical Bone in Murine Models of Osteomyelitis. J Bone Miner Res. 2017;32:985-90.

83. Shaw JD, Brodke DS, Williams DL, Ashton NN. Methylene Blue Is an Effective Disclosing Agent for Identifying Bacterial Biofilms on Orthopaedic Implants. J Bone Joint Surg Am. 2020;102:1784-91.

84. Cahill JL, Shadbolt B, Scarvell JM, Smith PN. Quality of life after infection in total joint replacement. J Orthop Surg (Hong Kong). 2008;16:58-65.

85. Kurtz SM, Lau E, Watson H, Schmier JK, Parvizi J. Economic burden of periprosthetic joint infection in the United States. J Arthroplasty. 2012;27:61-5 e1.

86. Kunutsor SK, Whitehouse MR, Blom AW, Board T, Kay P, Wroblewski BM, et al. One- and two-stage surgical revision of peri-prosthetic joint infection of the hip: a pooled individual participant data analysis of 44 cohort studies. Eur J Epidemiol. 2018;33:933-46.

87. van den Kieboom J, Tirumala V, Klemt C, Kwon YM. Outcome of Two-Stage Revision Total Hip and Knee Arthroplasty as a Salvage Procedure for Deep Infection of Peri-Articular Fracture Fixation: Propensity Score-Matched Study. Arch Bone Jt Surg. 2022;10:576-84.

88. Kunutsor SK, Whitehouse MR, Blom AW, Beswick AD, Team I. Re-Infection Outcomes following One- and Two-Stage Surgical Revision of Infected Hip Prosthesis: A Systematic Review and Meta-Analysis. PLoS One. 2015;10:e0139166.

89. LaPointe JM, Laverty S, Lavoie JP. Septic arthritis in 15 Standardbred racehorses after intra-articular injection. Equine Vet J. 1992;24:430-4.

90. Mocchi M, Dotti S, Bue MD, Villa R, Bari E, Perteghella S, et al. Veterinary Regenerative Medicine for Musculoskeletal Disorders: Can Mesenchymal Stem/Stromal Cells and Their Secretome Be the New Frontier? Cells. 2020;9.

91. Kupcova Skalnikova H. Proteomic techniques for characterisation of mesenchymal stem cell secretome. Biochimie. 2013;95:2196-211.

92. Bogers SH. Cell-Based Therapies for Joint Disease in Veterinary Medicine: What We Have Learned and What We Need to Know. Front Vet Sci. 2018;5:70.

93. Bourzac C, Smith LC, Vincent P, Beauchamp G, Lavoie JP, Laverty S. Isolation of equine bone marrow-derived mesenchymal stem cells: a comparison between three protocols. Equine Vet J. 2010;42:519-27.

94. Kasashima Y, Ueno T, Tomita A, Goodship AE, Smith RK. Optimisation of bone marrow aspiration from the equine sternum for the safe recovery of mesenchymal stem cells. Equine Vet J. 2011;43:288-94.

95. Delling U, Lindner K, Ribitsch I, Julke H, Brehm W. Comparison of bone marrow aspiration at the sternum and the tuber coxae in middle-aged horses. Can J Vet Res. 2012;76:52-6.

96. Nixon AJ, Dahlgren LA, Haupt JL, Yeager AE, Ward DL. Effect of adipose-derived nucleated cell fractions on tendon repair in horses with collagenase-induced tendinitis. Am J Vet Res. 2008;69:928-37.

97. Frisbie DD, Kisiday JD, Kawcak CE, Werpy NM, McIlwraith CW. Evaluation of adipose-derived stromal vascular fraction or bone marrow-derived mesenchymal stem cells for treatment of osteoarthritis. J Orthop Res. 2009;27:1675-80.

98. Polly SS, Nichols AEC, Donnini E, Inman DJ, Scott TJ, Apple SM, et al. Adipose-Derived Stromal Vascular Fraction and Cultured Stromal Cells as Trophic Mediators for Tendon Healing. J Orthop Res. 2019;37:1429-39.

99. Harman RM, Yang S, He MK, Van de Walle GR. Antimicrobial peptides secreted by equine mesenchymal stromal cells inhibit the growth of bacteria commonly found in skin wounds. Stem Cell Res Ther. 2017;8:157.

100. Marx C, Gardner S, Harman RM, Van de Walle GR. The mesenchymal stromal cell secretome impairs methicillin-resistant *Staphylococcus aureus* biofilms via cysteine protease activity in the equine model. Stem Cells Transl Med. 2020.

101. Marx C, Gardner S, Harman RM, Wagner B, Van de Walle GR. Mesenchymal stromal cell-secreted CCL2 promotes antibacterial defense mechanisms through increased antimicrobial peptide expression in keratinocytes. Stem Cells Transl Med. 2021;10:1666-79.

102. Cortes-Araya Y, Amilon K, Rink BE, Black G, Lisowski Z, Donadeu FX, et al. Comparison of Antibacterial and Immunological Properties of Mesenchymal Stem/Stromal Cells from Equine Bone Marrow, Endometrium, and Adipose Tissue. Stem Cells Dev. 2018;27:1518-25.

103. Carrade DD, Lame MW, Kent MS, Clark KC, Walker NJ, Borjesson DL. Comparative Analysis of the Immunomodulatory Properties of Equine Adult-Derived Mesenchymal Stem Cells. Cell Med. 2012;4:1-11.

104. Carrade Holt DD, Wood JA, Granick JL, Walker NJ, Clark KC, Borjesson DL. Equine mesenchymal stem cells inhibit T cell proliferation through different mechanisms depending on tissue source. Stem Cells Dev. 2014;23:1258-65.

105. Williams LB, Koenig JB, Black B, Gibson TW, Sharif S, Koch TG. Equine allogeneic umbilical cord blood derived mesenchymal stromal cells reduce synovial fluid nucleated cell count and induce mild self-limiting inflammation when evaluated in an lipopolysaccharide induced synovitis model. Equine Vet J. 2016;48:619-25.

106. Punzon E, Salguero R, Totusaus X, Mesa-Sanchez C, Badiella L, Garcia-Castillo M, et al. Equine umbilical cord mesenchymal stem cells demonstrate safety and efficacy in the treatment of canine osteoarthritis: a randomized placebo-controlled trial. J Am Vet Med Assoc. 2022;260:1947-55.

107. Young M. Stem cell applications in tendon disorders: a clinical perspective. Stem Cells Int. 2012;2012:637836.

108. Centeno CJ, Busse D, Kisiday J, Keohan C, Freeman M, Karli D. Regeneration of meniscus cartilage in a knee treated with percutaneously implanted autologous mesenchymal stem cells. Med Hypotheses. 2008;71:900-8.

109. Koh YG, Jo SB, Kwon OR, Suh DS, Lee SW, Park SH, et al. Mesenchymal stem cell injections improve symptoms of knee osteoarthritis. Arthroscopy. 2013;29:748-55.

110. Salz RO, Elliott CRB, Zuffa T, Bennet ED, Ahern BJ. Treatment of racehorse superficial digital flexor tendonitis: A comparison of stem cell treatments to controlled exercise rehabilitation in 213 cases. Equine Vet J. 2023.

111. Depuydt E, Broeckx SY, Van Hecke L, Chiers K, Van Brantegem L, van Schie H, et al. The Evaluation of Equine Allogeneic Tenogenic Primed Mesenchymal Stem Cells in a Surgically Induced Superficial Digital Flexor Tendon Lesion Model. Front Vet Sci. 2021;8:641441.

112. McCoy AM, Smith RL, Herrera S, Kawcak CE, McIlwraith CW, Goodrich LR. Long-term outcome after stifle arthroscopy in 82 Western performance horses (2003-2010). Vet Surg. 2019;48:956-65.

113. Ferris DJ, Frisbie DD, Kisiday JD, McIlwraith CW, Hague BA, Major MD, et al. Clinical Outcome After Intra-Articular Administration of Bone Marrow Derived Mesenchymal Stem Cells in 33 Horses With Stifle Injury. Vet Surg 2014;43:255-65.

114. Broeckx SY, Martens AM, Bertone AL, Van Brantegem L, Duchateau L, Van Hecke L, et al. The use of equine chondrogenic-induced mesenchymal stem cells as a treatment for osteoarthritis: A randomised, double-blinded, placebo-controlled proof-of-concept study. Equine Vet J. 2019;51:787-94.

115. Sole A, Spriet M, Galuppo LD, Padgett KA, Borjesson DL, Wisner ER, et al. Scintigraphic evaluation of intra-arterial and intravenous regional limb perfusion of allogeneic bone marrow-derived mesenchymal stem cells in the normal equine distal limb using (99m) Tc-HMPAO. Equine Vet J. 2012;44:594-9.

116. Sole A, Spriet M, Padgett KA, Vaughan B, Galuppo LD, Borjesson DL, et al. Distribution and persistence of technetium-99 hexamethyl propylene amine oxime-labelled bone marrow-derived mesenchymal stem cells in experimentally induced tendon lesions after intratendinous injection and regional perfusion of the equine distal limb. Equine Vet J. 2013;45:726-31.

117. Trela JM, Spriet M, Padgett KA, Galuppo LD, Vaughan B, Vidal MA. Scintigraphic comparison of intra-arterial injection and distal intravenous regional limb perfusion for administration of mesenchymal stem cells to the equine foot. Equine Vet J. 2014;46:479-83.

118. Frisbie DD, Kawcak CE, Werpy NM, Park RD, McIlwraith CW. Clinical, biochemical, and histologic effects of intra-articular administration of autologous conditioned serum in horses with experimentally induced osteoarthritis. Am J Vet Res. 2007;68:290-6.

119. Crovace A, Lacitignola L, Rossi G, Francioso E. Histological and immunohistochemical evaluation of autologous cultured bone marrow mesenchymal stem cells and bone marrow mononucleated cells in collagenase-induced tendinitis of equine superficial digital flexor tendon. Vet Med Int. 2010;2010:250978.

120. Fortier LN, AJ; Williams, J; Cable, CS. Isolation and chondrocytic differentiation of equine bone marrow-derived mesenchymal stem cells. Am J Vet Res. 1998;59:1182-7.

121. Ranera B, Antczak D, Miller D, Doroshenkova T, Ryan A, McIlwraith CW, et al. Donor-derived equine mesenchymal stem cells suppress proliferation of mismatched lymphocytes. Equine Vet J. 2016;48:253-60.

122. Schnabel L, Pezzanite L, Antczak D, Felippe J, Fortier L. Equine bone marrow-derived mesenchymal stromal cells are heterogenous in MHC class II expression and capable of inciting an immune response *in vitro*. Stem Cell Res Ther. 2014;5.

123. Joswig AJ, Mitchell A, Cummings KJ, Levine GJ, Gregory CA, Smith R, 3rd, et al. Repeated intra-articular injection of allogeneic mesenchymal stem cells causes an adverse response compared to autologous cells in the equine model. Stem Cell Res Ther. 2017;8:42.

124. Colbath AC, Dow SW, Phillips JN, McIlwraith CW, Goodrich LR. Autologous and Allogeneic Equine Mesenchymal Stem Cells Exhibit Equivalent Immunomodulatory Properties *In Vitro*. Stem Cells Dev. 2017;26:503-11.

125. Krasnodembskaya A, Song Y, Fang X, Gupta N, Serikov V, Lee JW, et al. Antibacterial effect of human mesenchymal stem cells is mediated in part from secretion of the antimicrobial peptide LL-37. Stem Cells. 2010;28:2229-38.

126. Johnson V, Webb T, Norman A, Coy J, Kurihara J, Regan D, et al. Activated Mesenchymal Stem Cells Interact with Antibiotics and Host Innate Immune Responses to Control Chronic Bacterial Infections. Sci Rep. 2017;7:9575.

127. Yamamuro Y, Kabata T, Nojima T, Hayashi K, Tokoro M, Kajino Y, et al. Combined adipose-derived mesenchymal stem cell and antibiotic therapy can effectively treat periprosthetic joint infection in rats. Sci Rep. 2023;13:3949.

128. Pezzanite LM, Chow L, Johnson V, Griffenhagen GM, Goodrich L, Dow S. Toll-like receptor activation of equine mesenchymal stromal cells to enhance antibacterial activity and immunomodulatory cytokine secretion. Vet Surg. 2021;50:858-71.

129. Sung DK, Chang YS, Sung SI, Yoo HS, Ahn SY, Park WS. Antibacterial effect of mesenchymal stem cells against *Escherichia coli* is mediated by secretion of beta-defensin-2 via toll-like receptor 4 signalling. Cell Microbiol. 2016;18:424-36.

130. Varoga D, Klostermeier E, Paulsen F, Wruck C, Lippross S, Brandenburg LO, et al. The antimicrobial peptide HBD-2 and the Toll-like receptors-2 and -4 are induced in synovial membranes in case of septic arthritis. Virchows Arch. 2009;454:685-94.

131. Gupta N, Krasnodembskaya A, Kapetanaki M, Mouded M, Tan X, Serikov V, et al. Mesenchymal stem cells enhance survival and bacterial clearance in murine *Escherichia coli* pneumonia. Thorax. 2012;67:533-9.

132. Meisel R, Brockers S, Heseler K, Degistirici Ö, Bülle H, Woite C, et al. Human but not murine multipotent mesenchymal stromal cells exhibit broad-spectrum antimicrobial effector function mediated by indoleamine 2, 3-dioxygenase. Leukemia. 2011;25:648-54.

133. Alcayaga-Miranda F, Cuenca J, Martin A, Contreras L, Figueroa FE, Khoury M. Combination therapy of menstrual derived mesenchymal stem cells and antibiotics ameliorates survival in sepsis. Stem Cell Res Ther. 2015;6:199.

134. Rashedi I, Gomez-Aristizabal A, Wang XH, Viswanathan S, Keating A. TLR3 or TLR4 Activation Enhances Mesenchymal Stromal Cell-Mediated Treg Induction via Notch Signaling. Stem Cells. 2017;35:265-75.

135. Sutton MT, Fletcher D, Ghosh SK, Weinberg A, van Heeckeren R, Kaur S, et al. Antimicrobial Properties of Mesenchymal Stem Cells: Therapeutic Potential for Cystic Fibrosis Infection, and Treatment. Stem Cells Int. 2016;2016:5303048.

136. Avellar HK, Lutter JD, Ganta CK, Beard W, Smith JR, Jonnalagadda N, et al. *In vitro* antimicrobial activity of equine platelet lysate and mesenchymal stromal cells against common clinical pathogens. Can J Vet Res. 2022;86:59-64.

137. Hoenders CS, Harmsen MC, van Luyn MJ. The local inflammatory environment and microorganisms in "aseptic" loosening of hip prostheses. J Biomed Mater Res B Appl Biomater. 2008;86:291-301.

138. Holopainen M, Colas RA, Valkonen S, Tigistu-Sahle F, Hyvarinen K, Mazzacuva F, et al. Polyunsaturated fatty acids modify the extracellular vesicle membranes and increase the production of proresolving lipid mediators of human mesenchymal stromal cells. Biochim Biophys Acta Mol Cell Biol Lipids. 2019;1864:1350-62.

139. Cianci E, Recchiuti A, Trubiani O, Diomede F, Marchisio M, Miscia S, et al. Human Periodontal Stem Cells Release Specialized Proresolving Mediators and Carry Immunomodulatory and Prohealing Properties Regulated by Lipoxins. Stem Cells Transl Med. 2016;5:20-32.

140. Bogers SH, Barrett JG. Three-Dimensional Culture of Equine Bone Marrow-Derived Mesenchymal Stem Cells Enhances Anti-Inflammatory Properties in a Donor-Dependent Manner. Stem Cells Dev. 2022;31:777-86.

141. Aggarwal S, Pittenger MF. Human mesenchymal stem cells modulate allogeneic immune cell responses. Blood. 2005;105:1815-22.

142. Bai Y, Wang J, He Z, Yang M, Li L, Jiang H. Mesenchymal Stem Cells Reverse Diabetic Nephropathy Disease via Lipoxin A4 by Targeting Transforming Growth Factor beta (TGF-beta)/smad Pathway and Pro-Inflammatory Cytokines. Med Sci Monit. 2019;25:3069-76.

143. Gaudin A, Tolar M, Peters OA. Lipoxin A4 Attenuates the Inflammatory Response in Stem Cells of the Apical Papilla via ALX/FPR2. Sci Rep. 2018;8:8921.

144. Fang X, Abbott J, Cheng L, Colby JK, Lee JW, Levy BD, et al. Human Mesenchymal Stem (Stromal) Cells Promote the Resolution of Acute Lung Injury in Part through Lipoxin A4. J Immunol. 2015;195:875-81.

145. Sugimoto MA, Sousa LP, Pinho V, Perretti M, Teixeira MM. Resolution of Inflammation: What Controls Its Onset? Front Immunol. 2016;7:160.

146. Serhan CN, Chiang N, Dalli J. New pro-resolving n-3 mediators bridge resolution of infectious inflammation to tissue regeneration. Mol Aspects Med. 2018;64:1-17.

147. Schwab JM, Chiang N, Arita M, Serhan CN. Resolvin E1 and protectin D1 activate inflammation-resolution programmes. Nature. 2007;447:869-74.

148. Everett J. Bone marrow mononuclear cell therapy for equine joint disease. 66th Annual Convention, Am Assoc Equine Pract. Virtual. 2020. p. 226-7.

149. Levy BD, Clish, C. B., Schmidt, B., Gronert, K., Serhan, C. N. Lipid mediator class switching during acute inflammation: signals in resolution. Nat Immunol. 2001;2:612-9.

150. Norris PC, Skulas-Ray AC, Riley I, Richter CK, Kris-Etherton PM, Jensen GL, et al. Identification of specialized pro-resolving mediator clusters from healthy adults after intravenous low-dose endotoxin and omega-3 supplementation: a methodological validation. Sci Rep. 2018;8:18050.

151. Fiore S, Ryeom SW, Weller PF, Serhan CN. Lipoxin recognition sites. Specific binding of labeled lipoxin A4 with human neutrophils. Journal of Biological Chemistry. 1992;267:16168-76.

152. Jordan PM, Gerstmeier J, Pace S, Bilancia R, Rao Z, Borner F, et al. *Staphylococcus aureus*-Derived alpha-Hemolysin Evokes Generation of Specialized Pro-resolving Mediators Promoting Inflammation Resolution. Cell Rep. 2020;33:108247.

153. Liu T, Xiang A, Peng T, Doran AC, Tracey KJ, Barnes BJ, et al. HMGB1-C1q complexes regulate macrophage function by switching between leukotriene and specialized proresolving mediator biosynthesis. Proc Natl Acad Sci U S A. 2019;116:23254-63.

154. Menarim BC, Gillis KH, Oliver A, Mason C, Werre SR, Luo X, et al. Inflamed synovial fluid induces a homeostatic response in bone marrow mononuclear cells *in vitro*: Implications for joint therapy. FASEB J. 2020;34:4430-44.

155. Chen J, Xu H, Xia K, Cheng S, Zhang Q. Resolvin E1 accelerates pulp repair by regulating inflammation and stimulating dentin regeneration in dental pulp stem cells. Stem Cell Res Ther. 2021;12:75.

156. Mangal D, Uboh CE, Soma LR, Liu Y. Inhibitory effect of triamcinolone acetonide on synthesis of inflammatory mediators in the equine. Eur J Pharmacol. 2014;736:1-9.

157. Serhan CN, Brain SD, Buckley CD, Gilroy DW, Haslett C, O'Neill LAJ, et al. Resolution of inflammation: state of the art, definitions and terms. The FASEB Journal. 2006.

158. Kennedy A, Fearon U, Veale DJ, Godson C. Macrophages in synovial inflammation. Front Immunol. 2011;2:52.

159. Prabhakara R, Harro JM, Leid JG, Keegan AD, Prior ML, Shirtliff ME. Suppression of the inflammatory immune response prevents the development of chronic biofilm infection due to methicillin-resistant *Staphylococcus aureus*. Infect Immun. 2011;79:5010-8.

160. Dufour JH, Dziejman M, Liu MT, Leung JH, Lane TE, Luster AD. IFN-gamma-inducible protein 10 (IP-10; CXCL10)-deficient mice reveal a role for IP-10 in effector T cell generation and trafficking. J Immunol. 2002;168:3195-204.

161. Leid JG, Shirtliff ME, Costerton JW, Stoodley P. Human leukocytes adhere to, penetrate, and respond to *Staphylococcus aureus* biofilms. Infect Immun. 2002;70:6339-45.

162. Buzás K, Megyeri A. Miczák AF, Degré M, Mándi Y, Rosztóczy I. Different Staphylococcal Strains Elicit Different Levels of Production of T-helper 1-inducing Cytokines. Acta Microbiol Immunol Hung. 2004;51:371-84.

163. Wang X, Du J, Zhao C. Bacterial biofilms are associated with inflammatory cells infiltration and the innate immunity in chronic rhinosinusitis with or without nasal polyps. Inflammation. 2014;37:871-9.

164. Alhede M, Alhede M, Qvortrup K, Kragh KN, Jensen PO, Stewart PS, et al. The origin of extracellular DNA in bacterial biofilm infections *in vivo*. Pathog Dis. 2020;78.

165. Bhattacharya M, Berends ETM, Chan R, Schwab E, Roy S, Sen CK, et al. *Staphylococcus aureus* biofilms release leukocidins to elicit extracellular trap formation and evade neutrophil-mediated killing. Proc Natl Acad Sci U S A. 2018;115:7416-21.

166. Dalli J, Gomez EA, Jouvene CC. Utility of the Specialized Pro-Resolving Mediators as Diagnostic and Prognostic Biomarkers in Disease. Biomolecules. 2022;12.

167. Hansen TV, Vik A, Serhan CN. The Protectin Family of Specialized Pro-resolving Mediators: Potent Immunoresolvents Enabling Innovative Approaches to Target Obesity and Diabetes. Front Pharmacol. 2018;9:1582.

168. Isobe Y, Arita M, Matsueda S, Iwamoto R, Fujihara T, Nakanishi H, et al. Identification and structure determination of novel anti-inflammatory mediator resolvin E3, 17,18-dihydroxyeicosapentaenoic acid. J Biol Chem. 2012;287:10525-34.

169. Hyvarinen K, Holopainen M, Skirdenko V, Ruhanen H, Lehenkari P, Korhonen M, et al. Mesenchymal Stromal Cells and Their Extracellular Vesicles Enhance the Anti-Inflammatory Phenotype of Regulatory Macrophages by Downregulating the Production of Interleukin (IL)-23 and IL-22. Front Immunol. 2018;9:771.

170. Endo J, Sano M, Isobe Y, Fukuda K, Kang JX, Arai H, et al. 18-HEPE, an n-3 fatty acid metabolite released by macrophages, prevents pressure overload-induced maladaptive cardiac remodeling. J Exp Med. 2014;211:1673-87.

171. von Schacky C, Marcus AJ, Safier LB, Ullman HL, Islam N, Broekman MJ, et al. Platelet-neutrophil interactions. 12S,20- and 5S,12S-dihydroxyeicosapentaenoic acids: two novel neutrophil metabolites from platelet-derived 12S-hydroxyeicosapentaenoic acid. Journal of Lipid Research. 1990;31:801-10.

172. Menarim BC, El-Sheikh Ali H, Loux SC, Scoggin KE, Kalbfleisch TS, MacLeod JN, et al. Transcriptional and Histochemical Signatures of Bone Marrow Mononuclear Cell-Mediated Resolution of Synovitis. Front Immunol. 2021;12:734322.

173. Mainka M, George S, Angioni C, Ebert R, Goebel T, Kampschulte N, et al. On the biosynthesis of specialized pro-resolving mediators in human neutrophils and the influence of cell integrity. Biochim Biophys Acta Mol Cell Biol Lipids. 2022;1867:159093.

174. Abreu SC, Antunes MA, de Castro JC, de Oliveira MV, Bandeira E, Ornellas DS, et al. Bone marrow-derived mononuclear cells vs. mesenchymal stromal cells in experimental allergic asthma. Respir Physiol Neurobiol. 2013;187:190-8.

175. Tiberi M, Chiurchiu V. Specialized Pro-resolving Lipid Mediators and Glial Cells: Emerging Candidates for Brain Homeostasis and Repair. Front Cell Neurosci. 2021;15:673549.

176. Clish CB, Levy BD, Chiang N, Tai HH, Serhan CN. Oxidoreductases in lipoxin A4 metabolic inactivation: a novel role for 15-onoprostaglandin 13-reductase/leukotriene B4 12-hydroxydehydrogenase in inflammation. J Biol Chem. 2000;275:25372-80.

177. Leiria LO, Wang CH, Lynes MD, Yang K, Shamsi F, Sato M, et al. 12-Lipoxygenase Regulates Cold Adaptation and Glucose Metabolism by Producing the Omega-3 Lipid 12-HEPE from Brown Fat. Cell Metab. 2019;30:768-83 e7.

178. Tomizawa T, Ishikawa M, Bello-Irizarry SN, de Mesy Bentley KL, Ito H, Kates SL, et al. Biofilm Producing *Staphylococcus epidermidis* (RP62A Strain) Inhibits Osseous Integration Without Osteolysis and Histopathology in a Murine Septic Implant Model. J Orthop Res. 2020;38:852-60.

179. Luthje FL, Jensen LK, Jensen HE, Skovgaard K. The inflammatory response to bone infection - a review based on animal models and human patients. APMIS. 2020;128:275-86.

180. Clark IM, Parker AE. Metalloproteinases: their role in arthritis and potential as therapeutic targets. Expert Opin Ther Targets. 2003;7:19-34.

181. Patwari P, Gao G, Lee JH, Grodzinsky AJ, Sandy JD. Analysis of ADAMTS4 and MT4-MMP indicates that both are involved in aggrecanolysis in interleukin-1-treated bovine cartilage. Osteoarthritis Cartilage. 2005;13:269-77.

182. Schebb NH, Kuhn H, Kahnt AS, Rund KM, O'Donnell VB, Flamand N, et al. Formation, Signaling and Occurrence of Specialized Pro-Resolving Lipid Mediators-What is the Evidence so far? Front Pharmacol. 2022;13:838782.

183. Bundgaard L, Stensballe A, Elbaek KJ, Berg LC. Mass spectrometric analysis of the *in vitro* secretome from equine bone marrow-derived mesenchymal stromal cells to assess the effect of chondrogenic differentiation on response to interleukin-1 beta treatment. Stem Cell Res Ther. 2020;11:187.

184. Tessier L, Bienzle D, Williams LB, Koch TG. Phenotypic and immunomodulatory properties of equine cord blood-derived mesenchymal stromal cells. PLoS One. 2015;10:e0122954.

185. Yamada T, Tani Y, Nakanishi H, Taguchi R, Arita M, Arai H. Eosinophils promote resolution of acute peritonitis by producing proresolving mediators in mice. FASEB J. 2011;25:561-8.

186. Lavy M, Gauttier V, Poirier N, Barille-Nion S, Blanquart C. Specialized Pro-Resolving Mediators Mitigate Cancer-Related Inflammation: Role of Tumor-Associated Macrophages and Therapeutic Opportunities. Front Immunol. 2021;12:702785.

187. Bai Y, Huang W, Li Y, Lai C, Huang S, Wang G, et al. Lipidomic alteration of plasma in cured COVID-19 patients using ultra high-performance liquid chromatography with high-resolution mass spectrometry. Biosci Rep. 2021;41.

188. Peeters E, Nelis HJ, Coenye T. Comparison of multiple methods for quantification of microbial biofilms grown in microtiter plates. J Microbiol Methods. 2008;72:157-65.

189. Stiefel P, Rosenberg U, Schneider J, Mauerhofer S, Maniura-Weber K, Ren Q. Is biofilm removal properly assessed? Comparison of different quantification methods in a 96-well plate system. Appl Microbiol Biotechnol. 2016;100:4135-45.

190. Zhang Y, Li C, Wu Y, Zhang Y, Zhou Z, Cao B. A microfluidic gradient mixer-flow chamber as a new tool to study biofilm development under defined solute gradients. Biotechnol Bioeng. 2019;116:54-64.

191. Kim J, Park HD, Chung S. Microfluidic approaches to bacterial biofilm formation. Molecules. 2012;17:9818-34.

192. Liu N, Skauge T, Landa-Marban D, Hovland B, Thorbjornsen B, Radu FA, et al. Microfluidic study of effects of flow velocity and nutrient concentration on biofilm accumulation and adhesive strength in the flowing and no-flowing microchannels. J Ind Microbiol Biotechnol. 2019;46:855-68.

193. Moormeier DE, Endres JL, Mann EE, Sadykov MR, Horswill AR, Rice KC, et al. Use of microfluidic technology to analyze gene expression during *Staphylococcus aureus* biofilm formation reveals distinct physiological niches. Appl Environ Microbiol. 2013;79:3413-24.

194. Yawata Y, Toda K, Setoyama E, Fukuda J, Suzuki H, Uchiyama H, et al. Monitoring biofilm development in a microfluidic device using modified confocal reflection microscopy. J Biosci Bioeng. 2010;110:377-80.

195. Pousti M, Zarabadi MP, Abbaszadeh Amirdehi M, Paquet-Mercier F, Greener J. Microfluidic bioanalytical flow cells for biofilm studies: a review. Analyst. 2018;144:68-86.

196. Kay W, Hunt C, Nehring L, Barnum B, Ashton N, Williams D. Biofilm Growth on Simulated Fracture Fixation Plates Using a Customized CDC Biofilm Reactor for a Sheep Model of Biofilm-Related Infection. Microorganisms. 2022;10.

197. Manville E, Kaya EC, Yucel U, Boyle D, Trinetta V. Evaluation of *Listeria monocytogenes* biofilms attachment and formation on different surfaces using a CDC biofilm reactor. Int J Food Microbiol. 2023;399:110251.

198. Williams DL, Woodbury KL, Haymond BS, Parker AE, Bloebaum RD. A modified CDC biofilm reactor to produce mature biofilms on the surface of peek membranes for an in vivo animal model application. Curr Microbiol. 2011;62:1657-63.

199. Lecuyer S, Rusconi R, Shen Y, Forsyth A, Vlamakis H, Kolter R, et al. Shear stress increases the residence time of adhesion of *Pseudomonas aeruginosa*. Biophys J. 2011;100:341-50.

200. Gilbertie JM, Schaer TP, Schubert AG, Jacob ME, Menegatti S, Ashton Lavoie R, et al. Platelet-rich plasma lysate displays antibiofilm properties and restores antimicrobial activity against synovial fluid biofilms *in vitro*. J Orthop Res. 2020.

201. Pestrak MJ, Gupta TT, Dusane DH, Guzior DV, Staats A, Harro J, et al. Investigation of synovial fluid induced *Staphylococcus aureus* aggregate development and its impact on surface attachment and biofilm formation. PLoS One. 2020;15:e0231791.

202. Staats AB, P. W.; Schwieters, A.; Li, D.; Sullivan, A.; Horswill, A. R.; Stoodley, P. Rapid Aggregation of *Staphylococcus aureus* in Synovial Fluid Is Influenced by Synovial Fluid Concentration, Viscosity, and Fluid Dynamics, with Evidence of Polymer Bridging. mBio. 2022;13:1-15.

203. Vyas HKN, Xia B, Mai-Prochnow A. Clinically relevant *in vitro* biofilm models: A need to mimic and recapitulate the host environment. Biofilm. 2022;4.

204. Coenye T, Nelis HJ. *In vitro* and *in vivo* model systems to study microbial biofilm formation. J Microbiol Methods. 2010;83:89-105.

205. Nishitani K, Sutipornpalangkul W, de Mesy Bentley KL, Varrone JJ, Bello-Irizarry SN, Ito H, et al. Quantifying the natural history of biofilm formation *in vivo* during the establishment of chronic implant-associated *Staphylococcus aureus* osteomyelitis in mice to identify critical pathogen and host factors. J Orthop Res. 2015;33:1311-9.

206. Smeltzer MS, Thomas JR, Hickraon SG, Skinner RA, Nelson CL, Griffith D, et al. Characterization of a rabbit model of staphylococcal osteomyelitis. J Orthop Res. 1997;15:414-21.

207. Faber C, Stallmann HP, Lyaruu DM, Joosten U, von Eiff C, van Nieuw Amerongen A, et al. Comparable efficacies of the antimicrobial peptide human lactoferrin 1-11 and gentamicin in a chronic methicillin-resistant *Staphylococcus aureus* osteomyelitis model. Antimicrob Agents Chemother. 2005;49:2438-44.

208. Yin LY, Lazzarini L, Li F, Stevens CM, Calhoun JH. Comparative evaluation of tigecycline and vancomycin, with and without rifampicin, in the treatment of methicillin-resistant *Staphylococcus aureus* experimental osteomyelitis in a rabbit model. J Antimicrob Chemother. 2005;55:995-1002.

209. Börzsei L, Mintál T, Koós Z, Kocsis B, Helyes Z, Kereskai L, et al. Examination of a novel, specified local antibiotic therapy through polymethylmethacrylate capsules in a rabbit osteomyelitis model. Chemotherapy. 2006;52:73-9.

210. Visperas A, Santana D, Ju M, Milbrandt NB, Tsai YH, Wickramasinghe S, et al. Standardized quantification of biofilm in a novel rabbit model of periprosthetic joint infection. J Bone Jt Infect. 2022;7:91-9.

211. Li H, Hamza T, Tidwell JE, Clovis N, Li B. Unique antimicrobial effects of platelet-rich plasma and its efficacy as a prophylaxis to prevent implant-associated spinal infection. Adv Healthc Mater. 2013;2:1277-84.

212. Wang Y, Cheng LI, Helfer DR, Ashbaugh AG, Miller RJ, Tzomides AJ, et al. Mouse model of hematogenous implant-related *Staphylococcus aureus* biofilm infection reveals therapeutic targets. Proc Natl Acad Sci U S A. 2017;114:E5094-E102.

213. Gilbertie JM, Schaer TP, Engiles JB, Seiler GS, Deddens BL, Schubert AG, et al. A Platelet-Rich Plasma-Derived Biologic Clears *Staphylococcus aureus* Biofilms While Mitigating Cartilage Degeneration and Joint Inflammation in a Clinically Relevant Large Animal Infectious Arthritis Model. Front Cell Infect Microbiol. 2022;12:895022.

214. Burton E, Yakandawala N, LoVetri K, Madhyastha MS. A microplate spectrofluorometric assay for bacterial biofilms. J Ind Microbiol Biotechnol. 2007;34:1-4.

215. Merritt JH, Kadouri DE, O'Toole GA. Growing and analyzing static biofilms. Curr Protoc Microbiol. 2005;Chapter 1:Unit 1B

216. Zhang XY, Sun K, Abulimiti A, Xu PP, Li ZY. Microfluidic System for Observation of Bacterial Culture and Effects on Biofilm Formation at Microscale. Micromachines (Basel). 2019;10.

217. Goikoetxea E, Routkevitch D, de Weerdt A, Green JJ, Steenackers H, Braeken D. Impedimetric fingerprinting and structural analysis of isogenic *E. coli* biofilms using multielectrode arrays. Sensors and Actuators B: Chemical. 2018;263:319-26.

218. Perez K, Patel R. Biofilm-like aggregation of *Staphylococcus epidermidis* in synovial fluid. J Infect Dis. 2015;212:335-6.

219. Zatorska B, Groger M, Moser D, Diab-Elschahawi M, Lusignani LS, Presterl E. Does Extracellular DNA Production Vary in Staphylococcal Biofilms Isolated From Infected Implants versus Controls? Clin Orthop Relat Res. 2017;475:2105-13.

220. Xu Z, Liang Y, Lin S, Chen D, Li B, Li L, et al. Crystal Violet and XTT Assays on *Staphylococcus aureus* Biofilm Quantification. Curr Microbiol. 2016;73:474-82.

221. Ommen P, Zobek N, Meyer RL. Quantification of biofilm biomass by staining: Non-toxic safranin can replace the popular crystal violet. J Microbiol Methods. 2017;141:87-9.

222. Tote K, Vanden Berghe D, Maes L, Cos P. A new colorimetric microtitre model for the detection of *Staphylococcus aureus* biofilms. Lett Appl Microbiol. 2008;46:249-54.

223. Schlafer S, Meyer RL. Confocal microscopy imaging of the biofilm matrix. J Microbiol Methods. 2017;138:50-9.

224. Nguyen MH, Ojima Y, Sakka M, Sakka K, Taya M. Probing of exopolysaccharides with green fluorescence protein-labeled carbohydrate-binding module in *Escherichia coli* biofilms and flocs induced by bcsB overexpression. J Biosci Bioeng. 2014;118:400-5.

225. Petruzzi B, Dickerman A, Lahmers K, Scarratt WK, Inzana TJ. Polymicrobial Biofilm Interaction Between *Histophilus somni* and *Pasteurella multocida*. Front Microbiol. 2020;11:1561.

226. Gonzalez Barrios AF, Zuo R, Hashimoto Y, Yang L, Bentley WE, Wood TK. Autoinducer 2 controls biofilm formation in *Escherichia coli* through a novel motility quorum-sensing regulator (MqsR, B3022). J Bacteriol. 2006;188:305-16.

227. Uribe-Garcia A, Paniagua-Contreras GL, Monroy-Perez E, Bustos-Martinez J, Hamdan-Partida A, Garzon J, et al. Frequency and expression of genes involved in adhesion and biofilm formation in *Staphylococcus aureus* strains isolated from periodontal lesions. J Microbiol Immunol Infect. 2019.

228. Yu S, Jiang B, Jia C, Wu H, Shen J, Hu X, et al. Investigation of biofilm production and its association with genetic and phenotypic characteristics of OM (osteomyelitis) and non-OM orthopedic *Staphylococcus aureus*. Ann Clin Microbiol Antimicrob. 2020;19:10.

229. Pawar DM, Rossman ML, Chen J. Role of curli fimbriae in mediating the cells of enterohaemorrhagic *Escherichia coli* to attach to abiotic surfaces. J Appl Microbiol. 2005;99:418-25.

230. Jensen LK, Henriksen NL, Bjarnsholt T, Kragh KN, Jensen HE. Combined Staining Techniques for Demonstration of *Staphylococcus aureus* Biofilm in Routine Histopathology. J Bone Jt Infect. 2018;3:27-36.

231. Parai D, Banerjee M, Dey P, Mukherjee SK. Reserpine attenuates biofilm formation and virulence of *Staphylococcus aureus*. Microb Pathog. 2020;138:103790.

232. Thilakavathy P, Priyan RM, Jagatheeswari PA, Charles J, Dhanalakshmi V, Lallitha S, et al. Evaluation of *Ica* Gene in Comparison with Phenotypic Methods for Detection of Biofilm Production by Coagulase Negative *Staphylococci* in a Tertiary Care Hospital. J Clin Diagn Res. 2015;9:DC16-9.

233. Li C, Zhu C, Ren B, Yin X, Shim SH, Gao Y, et al. Two optimized antimicrobial peptides with therapeutic potential for clinical antibiotic-resistant *Staphylococcus aureus*. Eur J Med Chem. 2019;183:111686.

234. Shang D, Han X, Du W, Kou Z, Jiang F. Trp-Containing Antibacterial Peptides Impair Quorum Sensing and Biofilm Development in Multidrug-Resistant *Pseudomonas aeruginosa* and Exhibit Synergistic Effects With Antibiotics. Front Microbiol. 2021;12:611009.

CHAPTER 3: NOVEL *IN VITRO* CO-CULTURE SYSTEM ALLOWS ASSESSMENT OF MSC-MEDIATED MITIGATION OF BIOFILMS

To be submitted for publication as:

Sarah M. Khatibzadeh, Linda A. Dahlgren, Clayton C. Caswell, William A. Ducker, Stephen R. Werre, Sophie H. Bogers. Novel *in vitro* co-culture system allows assessment of MSC-mediated mitigation of biofilms. *J Microbial Methods*

ABSTRACT

Mesenchymal stromal cells (MSC) show promise as a therapy for biofilm infections given their abilities to reduce bacteria and prevent biofilm formation in a paracrine fashion. However, the ability of MSC alone or with clinically-relevant antimicrobials to disrupt established biofilms is unknown. A culture method to evaluate MSC efficacy at reducing established biofilms that allows direct MSC-biofilm interactions and biofilm quantification by multiple methods is needed. We describe development of a novel *in vitro* method of co-culturing established *S. aureus* and *E. coli* biofilms with equine bone marrow-derived MSC ± antimicrobials. Our method allows reliable downstream quantification of biofilm biomass, live bacterial counts, and pellicle size and may be used for future high-throughput evaluation of MSC as a treatment for biofilm infections.

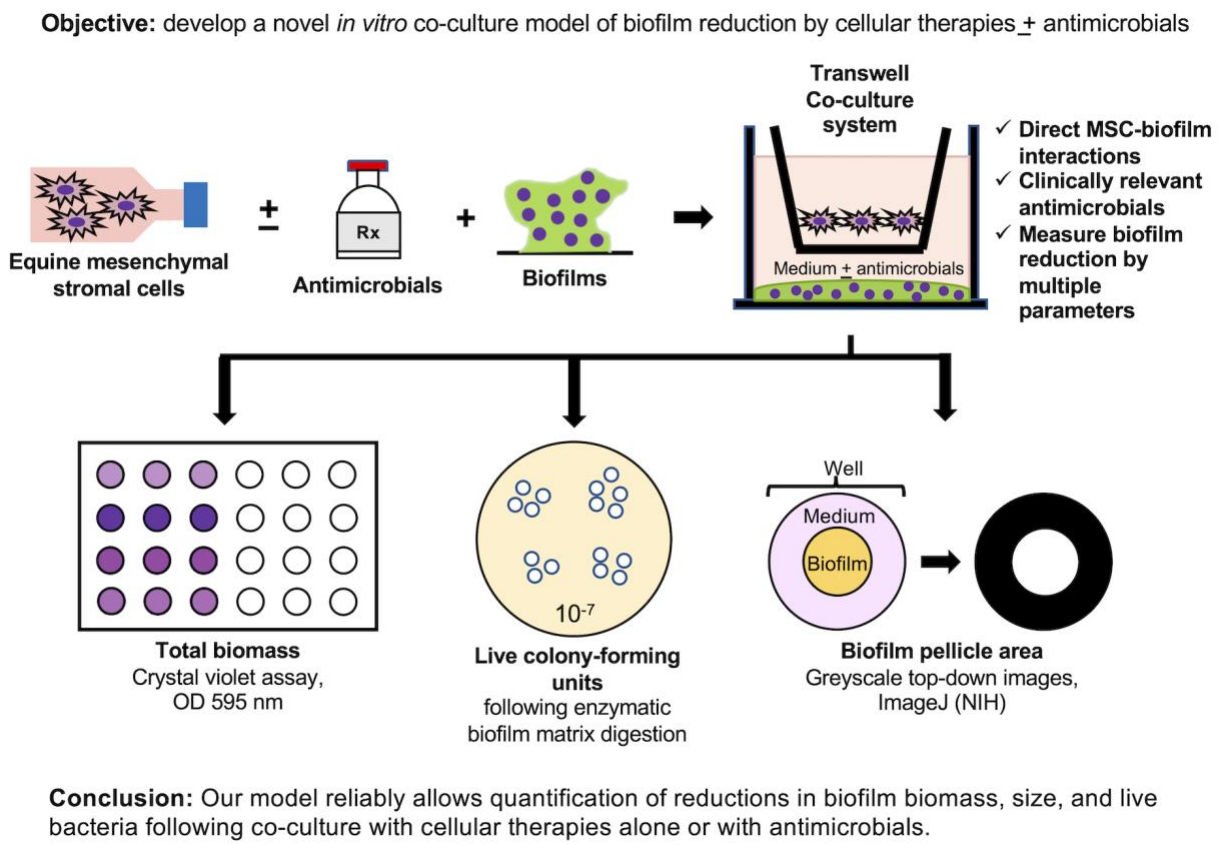

Figure 3.1: Graphical abstract. Co-culture of biofilms with equine MSC and antimicrobials in a transwell co-culture system facilitates MSC-biofilm interactions while maintaining spatial separation. This system allows ready evaluation of MSC antibiofilm efficacy via quantification of biofilm biomass, live bacterial counts, and biofilm pellicle area following co-culture.

Highlights:

1. Our system allows MSC-biofilm interactions while maintaining spatial separation.
2. Biofilm biomass, size and live bacteria are readily quantified post-co-culture.
3. Biofilm reduction by MSC can be evaluated prior to *in vivo* testing.

Keywords: *biofilm quantification, mesenchymal stromal cell, co-culture, biomass, live bacterial counts, matrix reduction*

INTRODUCTION

A biofilm is a community of bacteria that are adhered to each other or a solid surface and encased in a self-secreted extracellular matrix of carbohydrates, proteins, and extracellular DNA [1-4]. During orthopedic infections, biofilms protect the indwelling bacteria from antimicrobials [5-7] and the immune response [8, 9], which can lead to infection recurrence and dissemination to the bloodstream or vital organs [10-12]. Biofilms also exacerbate chronic inflammation and secondary tissue damage, including osteolysis and implant failure [13-15]. The resulting mortality rates for orthopedic infections are high, with 55% of people succumbing to these infections within 5 years of diagnosis [10-12] and up to 56% of affected horses requiring euthanasia [16-18]. Biological products, including mesenchymal stromal cells (MSC) [19-24], are being investigated to treat biofilm infections. MSC kill bacteria [20, 24, 25] and inhibit biofilm formation [20, 22] in a paracrine fashion via secretion of antimicrobial proteins [19, 20, 22, 24] and stimulation of host immune defenses [25, 26]. MSC antimicrobial activity is stimulated by activation of pattern recognition receptors on MSC by bacterial by-products or exogenous toll-like receptor (TLR) ligands [24, 25, 27] and may be synergistic with traditional antimicrobials [28-30].

One limitation of published methods to evaluate MSC-mediated antimicrobial effects is that bacteria are often cultured with MSC conditioned medium. Conditioned MSC medium contains secreted bioactive antimicrobial proteins that disrupt bacterial membranes and interfere with key nutrient metabolism [20, 24-26]. However, bacterial incubation with MSC conditioned medium does not allow the real-time paracrine signaling between MSC and biofilms present in natural

infections. Reported MSC antimicrobial effects include reductions in planktonic bacterial counts and prevention of biofilm formation from planktonic cultures [20, 24-26], but the ability of MSC to disrupt established biofilms with a mature extracellular matrix is unknown. Current techniques to evaluate biofilm reduction by MSC include crystal violet staining of total biofilm biomass (bacterial cells and matrix) [20, 31], staining of specific matrix components [32-34], enumeration of live biofilm-bound bacteria by colony forming unit (CFU) analysis [32, 33, 35], and three-dimensional microscopic techniques [7, 22, 36]. Although a combination of quantification techniques provides the most comprehensive evaluation of treatment efficacy [33], a model that simultaneously allows direct MSC-biofilm interactions and easy separation of biofilms post-culture for quantification by multiple techniques has not been reported. Furthermore, it is unknown if use of antimicrobials relevant to traditional treatment of biofilm infections [37, 38] would interfere with quantification techniques. Therefore, an *in vitro* co-culture model that allows MSC to interact with established biofilms and permits reliable and rapid downstream quantification of biofilm components by multiple methods is required to elucidate the anti-biofilm mechanisms of MSC and evaluate potential treatment efficacy.

The aims of this study were two-fold. We sought to develop a high throughput *in vitro* co-culture model that would allow paracrine interactions between biofilms and MSC alone or with antimicrobials. Using this model, we aimed to reliably quantify biofilm biomass by crystal violet assay, biofilm pellicle size by image analysis, and live bacterial counts by CFU analysis following co-culture. We specifically utilized biofilms of *S. aureus* or *E. coli* and equine bone marrow derived-MSC, with or without the addition of amikacin sulfate, in this report. We hypothesized that use of this model would allow: 1) Ready quantification of *S. aureus* and *E. coli*

biofilm biomass, live bacterial counts, and pellicle size after co-culture with MSC, 2) Use of amikacin sulfate to reduce established biofilms with no interference with biofilm quantification techniques, and 3) Survival of the majority (> 50% live cells after co-culture) of MSC after 48-hours of co-culture with *S. aureus* and *E. coli* biofilms.

METHODS

3.1 Experimental design

Biofilm isolation for biomass and live bacterial quantification, as well as amikacin concentration for use as a treatment group or positive control were optimized on *S. aureus* or *E. coli* biofilms grown in 96 well plates. Optimized parameters were then applied to biofilms co-cultured with MSC from healthy horses using a transwell plate system to confirm consistency of biofilm quantification techniques and to evaluate MSC viability.

3.2 Establishment of biofilms for use in co-culture model

Commercial strains of methicillin-sensitive *S. aureus* (ATCC® 23912, Biosafety Level -2) and *E. coli* (ATCC® 25992, Biosafety Level -1) were utilized for biofilm formation. Quality control testing was performed on both strains by broth microdilution using Sensititre™ plates (ThermoFisher™) to ensure that the minimum inhibitory concentration (MIC) of each drug fell within the expected ranges outlined in the Clinical Laboratory Standards Institute M100 (Table 3.1, 3.2) [39]. Cultures were established by isolation of pure colonies on tryptic soy agar (TSA), inoculation of 1 pure colony in Luria-Bertani (LB) broth, and overnight growth (37°C, 200 rpm, Fisherbrand™ Mini-shaker) into the exponential growth phase. Overnight cultures of *S. aureus*

and *E. coli* were serially diluted in LB broth to an optical density (OD) at 600 nm of 0.05. For initial optimization of biomass and live bacterial quantification techniques and the positive control for biofilm removal, *S. aureus* and *E. coli* biofilms were formed by inoculation of 5×10^4 colony-forming units (CFU) per well in 96-well plates and growth at 37°C, 5% CO_2, 95% humidity for 24 hours to allow adequate bacterial attachment and matrix production [40, 41]. Optimization of the final transwell plate co-culture model was performed following growth of 24-hour *S. aureus* and *E. coli* biofilms from a starting inoculum of 2×10^5 CFU per well in 24-well tissue culture-treated plates under the same culture conditions.

Table 3.1: Minimum inhibitory concentrations (MIC) of *S. aureus* ATCC29213

measured by antimicrobial susceptibility testing on broth microdilution

Antimicrobial	**MIC (µg/mL)**	**Interpretation**
Amikacin	≤ 4	In range
Amoxicillin/clavulanic acid	≤ 0.25	In range
Ampicillin	≤ 0.25	In range
Cefazolin	≤ 2	In range
Cefovecin	1	In range
Cefpodoxime	≤ 2	In range
Cephalothin	≤ 2	In range
Chloramphenicol	≤ 8	In range
Clindamycin	≤ 0.5	In range
Doxycycline	0.25	In range
Enrofloxacin	≤ 0.25	In range
Erythromycin	0.5	In range
Gentamicin	≤ 4	In range
Imipenem	≤ 1	In range
Marbofloxacin	≤ 1	In range
Minocycline	≤ 0.5	In range
Nitrofuratonin	≤ 16	In range
Oxacillin 2 + 2% NaCl	≤ 0.25	In range
Penicillin	0.5	In range
Pradofloxacin	≤ 0.25	No interpretation
Rifampin	≤ 1	In range
Tetracycline	0.5	In range
Trimethoprim/Sulfamethoxazole	≤ 2	In range
Vancomycin	≤ 1	In range

Table 3.2: Minimum inhibitory concentrations (MIC) of *E. coli* ATCC25922

measured by antimicrobial susceptibility testing on broth microdilution

Antimicrobial	**MIC (µg/mL)**	**Interpretation**
Amikacin	≤ 4	In range
Amoxicillin/clavulanic acid	4	In range
Ampicillin	4	In range
Cefalexin	8	In range
Cefazolin	2	In range
Cefovecin	1	In range
Cefpodoxime	≤ 1	In range
Ceftazidime	≤ 4	In range
Chloramphenicol	4	In range
Doxycycline	1	In range
Enrofloxacin	≤ 0.12	In range
Gentamicin	0.5	In range
Imipenem	≤ 1	In range
Marbofloxacin	≤ 0.12	In range
Orbifloxacin	≤ 1	In range
Piperacillin/Tazobactam	≤ 8	In range
Pradofloxacin	≤ 0.25	No interpretation
Rifampin	≤ 1	In range
Tetracycline	≤ 4	In range
Trimethoprim/Sulfamethoxazole	≤ 0.5	In range

3.3 Evaluation of physiologic amikacin sulfate and SDS for use in biofilm-MSC co-culture model

24-hour *S. aureus* and *E. coli* biofilms were incubated with 30 µg/mL amikacin sulfate, a physiologic concentration achieved *in vivo* following regional administration for treatment of clinical orthopedic infections [37, 38, 42]. To investigate an appropriate positive control, biofilms were simultaneously incubated with two supraphysiologic concentrations of amikacin sulfate (500 and 50,000 µg/mL) and a range of concentrations (0.5-8%) of sodium dodecyl sulfate (SDS), an anionic surfactant that inhibits biofilm formation [43, 44]. All treatments were incubated with biofilms for 48 hours to mimic a clinical scenario [45] and biofilm reduction was

then quantified via crystal violet staining and biofilm-bound CFU enumeration as described below. Successful positive control was defined as reduction of CFU to within threshold of contamination control samples.

3.4 Establishing MSC-biofilm co-cultures

3.4.1 MSC isolation

Under standing sedation and local anesthesia, marrow aspirates were harvested from the sternum of 6 healthy Thoroughbred horses (Table 3.3) using protocols approved by the Virginia Tech Institutional Animal Care and Use Committee. Bone marrow mononuclear cells (MNC) were isolated by density gradient centrifugation (Ficoll® Paque PLUS, Cytivia™) and cryopreserved in fetal bovine serum (FBS) with 10% dimethyl sulfoxide until use [46-48]. Cryopreserved MNC were thawed in a 37°C water bath and stained with Trypan Blue (Gibco™) diluted 1:8 in PBS, at a volumetric suspension: stain ratio of 1:10 to determine baseline viability. Live (colorless) versus dead (blue) cells were quantified under phase contrast microscopy (Olympus CKX41, EVIDENT©) at 10x magnification using a hemacytometer (Fisher Scientific™). Live MNC were plated at 350,000 MNC/cm^2 in 175 cm^2 tissue culture flasks [49-51] in MSC medium: low-glucose GlutaMax DMEM with 110 µg/mL sodium pyruvate (Gibco™), 100 U/mL sodium penicillin, 100 µg/mL streptomycin sulfate (Sigma Aldrich®), and 10% FBS (Corning®). A 50% medium exchange was performed every 48 hours and resulting mesenchymal stromal cells (MSC) passaged at 70-80% confluency to passage 1 prior to cryopreservation at 1 x 10^7 cells/mL (Synth-a-freeze™, Life Technologies, Inc) in liquid nitrogen, vapor phase.

Table 3.3: Bone marrow-derived MSC donor horse information

Donor	Breed	Sex	Age
1	TB	M	2 months
2	TB	MC	5 years
3	TB	MC	7 years
4	TB	F	3 years
5	TB	F	5 years
6	TB	MC	7 years

Abbreviations: TB = Thoroughbred, M = Male, C = castrate, F = Female

3.4.2 MSC expansion and acclimation to transwell inserts

In preparation for co-culture with biofilms, cryopreserved passage 1 MSC were thawed in a water bath at 37°C and expanded at passage 2 in antibiotic-free MSC medium + 10% FBS. Passage 2 MSC were trypsinized at 70-80% confluence, baseline viability assessed via Trypan Blue staining, and 1.0 x 10^6 live MSC seeded at passage 3 into the upper insert of a 24-well transwell plate (6.5 mm diameter, 0.4 µm pore diameter, polyester, Corning®) in antibiotic-free MSC medium + 5% FBS. MSC were acclimated overnight at 37ºC, 5% CO_2, and 95% humidity.

3.4.3 Co-culture setup

24-hour old *S. aureus* and *E. coli* biofilms were prepared for use in the co-culture system by centrifugation at 1,400 x g, 23ºC, 10 minutes, and the overlying LB broth was aspirated. MSC medium with 5% FBS ± 30 µg/mL amikacin sulfate (400 µL/well) was added to the lower wells and inserts containing passage 3 MSC in 100 µL MSC medium were transferred to the wells (500 µL total system volume). Control biofilms without MSC had 500 µL MSC medium with 5% FBS alone ± 30 µg/mL amikacin sulfate added per well. Co-cultures were maintained for up to 48 hours.

3.5 Biofilm quantification techniques for co-culture model

3.5.1 Biomass

Following co-culture and removal of transwell inserts containing MSC, biofilms were centrifuged at 1,400 x g, 10 minutes at room temperature, rinsed twice with distilled water, fixed in reagent-grade methanol, and stained with 0.2% aqueous crystal violet for 15 minutes at room temperature [20, 31, 32]. Excess stain was then aspirated, biofilms rinsed twice with distilled water to remove excess stain, and biofilm-bound stain eluted with 70% ethanol. Eluted stain was quantified at OD at 595 nm using a spectrophotometric plate reader (BioTek H1 Synergy™, Agilent Technologies, Inc) and software (Gen5™, Agilent Technologies, Inc).

3.5.2 Live bacterial counts

Live biofilm-bound CFU were quantified following matrix digestion *in situ* with 20 µg/mL Proteinase K (Life Technologies, Inc) for 30 minutes at 37 ºC, 150 rpm on a shaking incubator (Incubating Mini-Shaker, Fisher Scientific™) [35]. We confirmed this minimum required Proteinase K concentration to liberate CFU from the biofilm matrix without inadvertent CFU reduction. Digested biofilm well contents were serially diluted in sterile phosphate buffered saline (PBS), plated in triplicate on TSA, and incubated overnight at 37ºC. Live colonies were counted, divided by the dilution factor, and the quotient multiplied by well volume to calculate live bacteria/well system (CFU/biofilm):

$$\text{CFU/biofilm} = (\text{Live colonies} / \text{dilution factor}) \times \text{well volume in mL}$$

3.5.3 Biofilm pellicle area measurement

Following co-culture with MSC from 5 adult horses (Horses 2-6, Table 3.3), inserts containing MSC were removed and biofilms were grossly examined and photographed digitally (iPhone XR, Apple, Inc) using a commercial ring LED photography booth with a black backdrop and lens set to an object distance of 19 cm (PULUZ®). High resolution JPEG images were imported to ImageJ (NIH), converted to 8-bit greyscale, and images showing biofilm pellicles as white areas on a black background were obtained via default algorithm histogram thresholding (Fig 3.2). The number of white pixels (value 255) were recorded in an oval region of interest (ROI) that incorporated the pellicle. Triplicate technical replicates were measured and the mean used for statistical analysis. Four independent reviewers (Kayla Hackler, Jacq Field, Hannah Elshafie, Sidney Schumaker) were trained to review pellicle area using Image J. Each reviewer assessed images from all horses within a randomly assigned bacterial strain and time point. Then, reviewers were randomly assigned to a different bacterial strain and time point for review so that each set of images was reviewed by two independent reviewers. Random allocation by time point and bacteria grouping was chosen as not direct comparisons between time point or bacteria were performed in final analysis. Pixel size was calibrated to reference lines of known distance in mm and final pellicle area in mm^2 was calculated prior to statistical analysis.

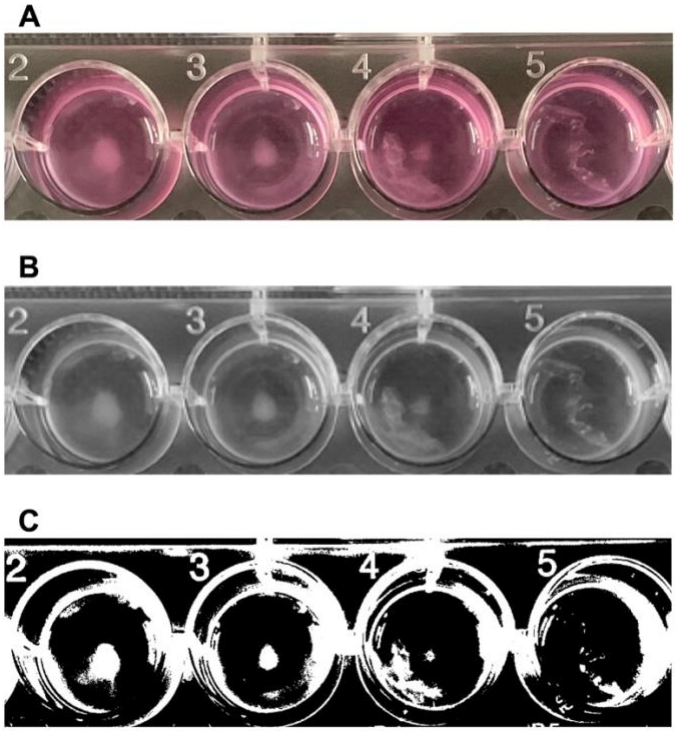

Figure 3.2: Biofilm image processing for pellicle area measurement in ImageJ (NIH) software. Raw images (A) were converted into greyscale images (B) and subsequently converted into black and white images (C) where biofilm pellicle area could be quantified by number of white pixels and standardized to plate measurements to get final area in mm^2.

3.6 Confirming MSC viability following co-culture

MSC from 1 horse (Horse 1, Table 3.3) were cultured as described in *3.4.1*, dissociated from culture flasks with trypsin EDTA 0.25% (Thermo-Fisher Scientific™) for 5 minutes at 37°C, resuspended in MSC medium with 5% FBS, and baseline viability assessed via Trypan Blue staining. MSC viability following co-culture with *S. aureus* or *E. coli* biofilms for 48 hours was

performed following trypsinization of MSC in transwell inserts, resuspension, and Trypan Blue staining.

3.7 Statistical analysis

Data distribution was assessed using normal probability plots, summarized as means ± standard deviations if normally distributed, and effects of treatment on outcomes analyzed using one-way analysis of variance. Where appropriate, *p*-values were adjusted for multiple comparisons using Tukey's procedure. Inter-observer agreement in biofilm pellicle area measurement was calculated using Pearson's r coefficient. Statistical significance was set to $p < 0.05$. All analyses were performed using SAS v. 9.4 (Cary, NC).

RESULTS AND DISCUSSION

3.1 Establishment of MSC-biofilm co-cultures was technically simple and allowed reliable quantification of biomass and live bacteria

Biofilm-MSC co-cultures were technically simple to establish and allowed for simultaneous co-culture of multiple technical replicates for each donor cell-line. No technical challenges were faced when transferring inserts containing MSC to the biofilm wells or upon removal following co-culture. The transwell system allowed quantification of biomass by crystal violet and CFU analysis on separate biofilms. For 5 horses, the range of untreated biofilm technical replicates for biomass quantification by crystal violet staining was 1.01-2.02 (minimum-maximum) for *S. aureus* (Fig 3.3A) and 0.41–3.76 for *E. coli* (Fig 3.3B). For CFU analysis, the technical

replicates ranged from 5.75 x 10^7-1.30 x 10^8 CFU for *S. aureus* (Fig 3.4A) and from 1.70 x 10^7-8.50 x 10^7 CFU for *E. coli* (Fig 3.4B).

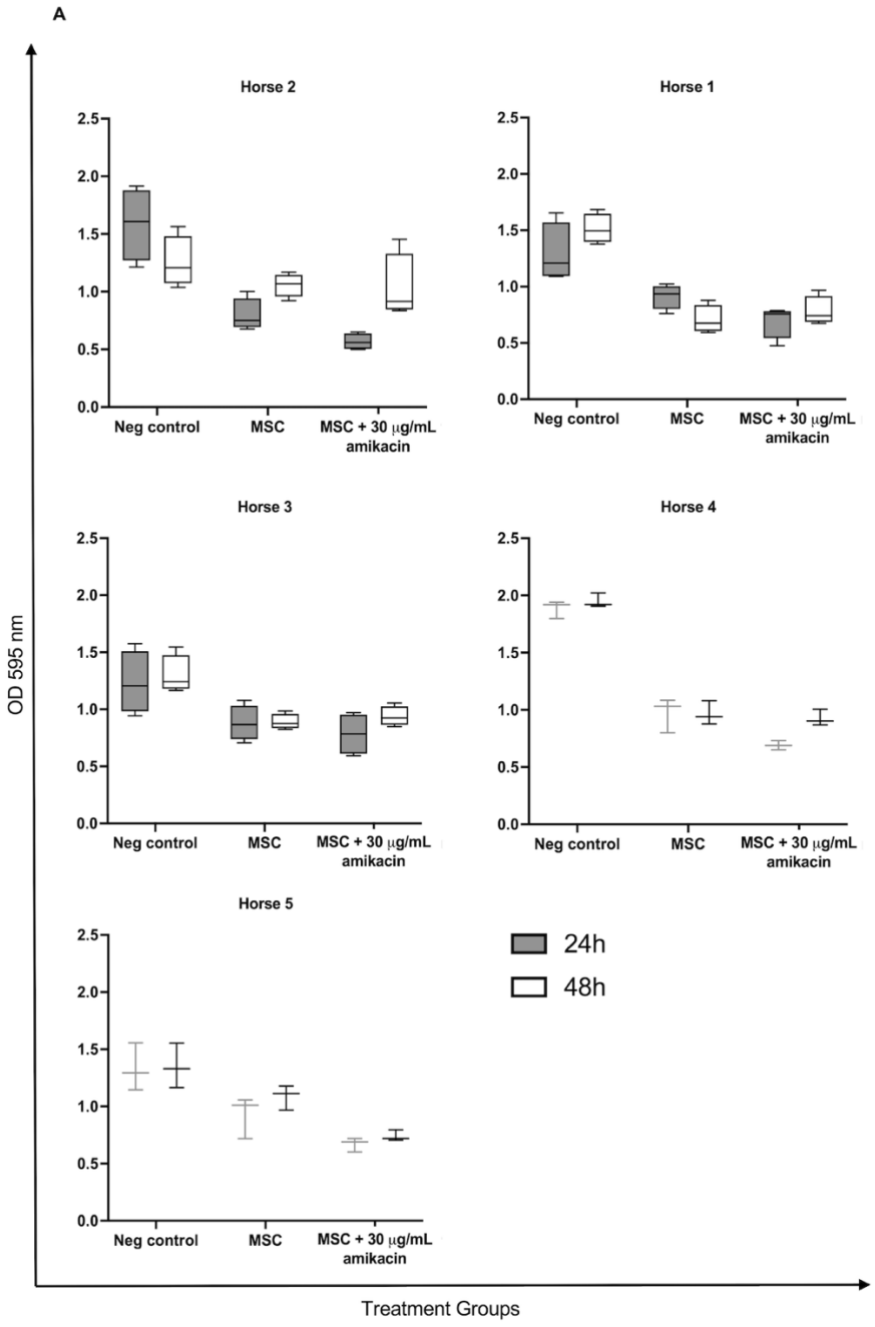

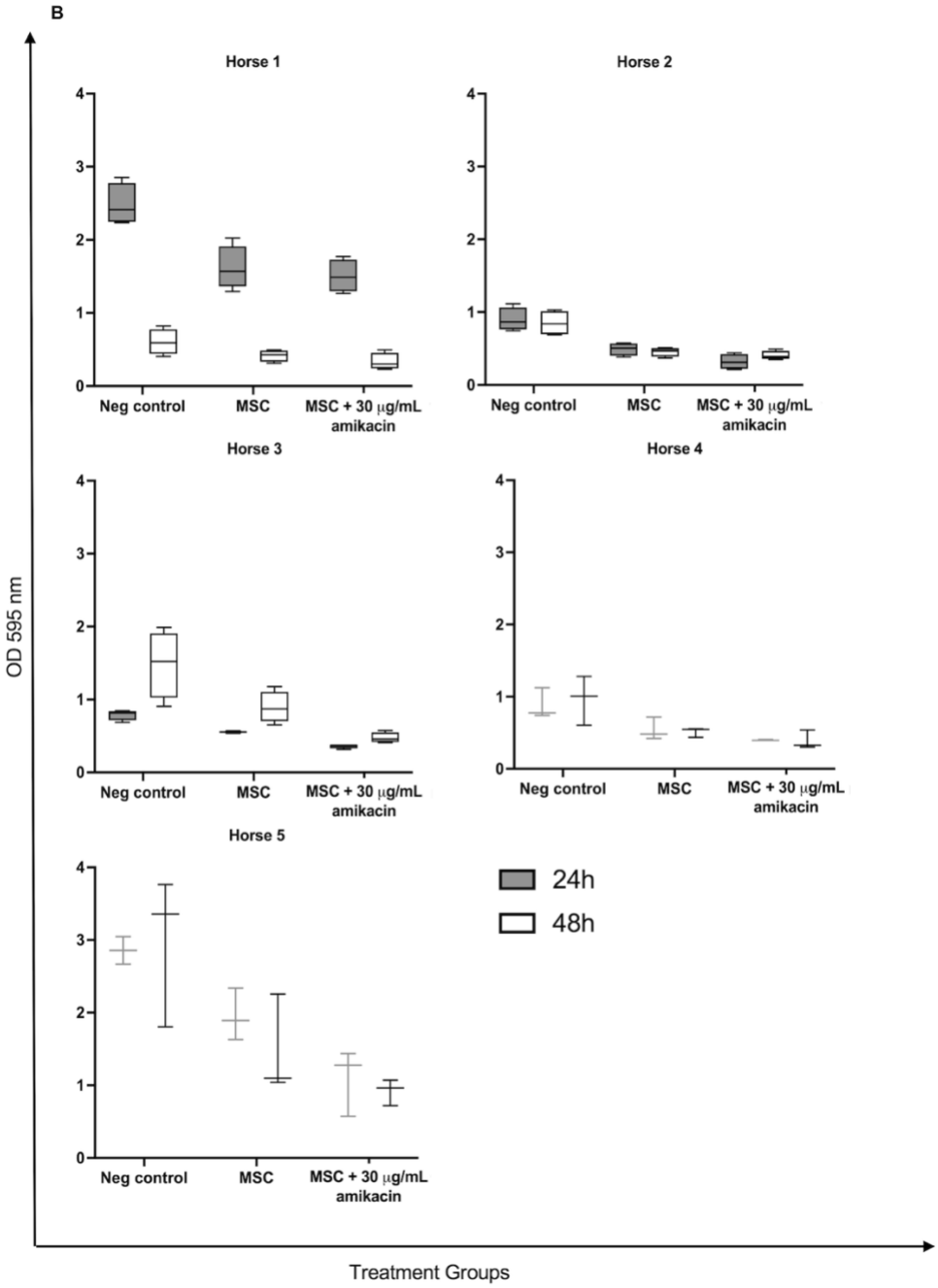

Figure 3.3: Crystal violet-stained biomass (OD 595 nm) of *S. aureus* (A) or *E. coli* (B) biofilms following no treatment (neg control) or co-culture with MSC or MSC + physiologic (30 µg/mL) amikacin sulfate from 5 horses for 24 (grey) or 48 hours (white + black lines). Boxes represent means (center lines), 5th and 95th percentiles (lower and upper limits), and minimum and maximum values (whiskers) from 3 technical replicates per horse and treatment.

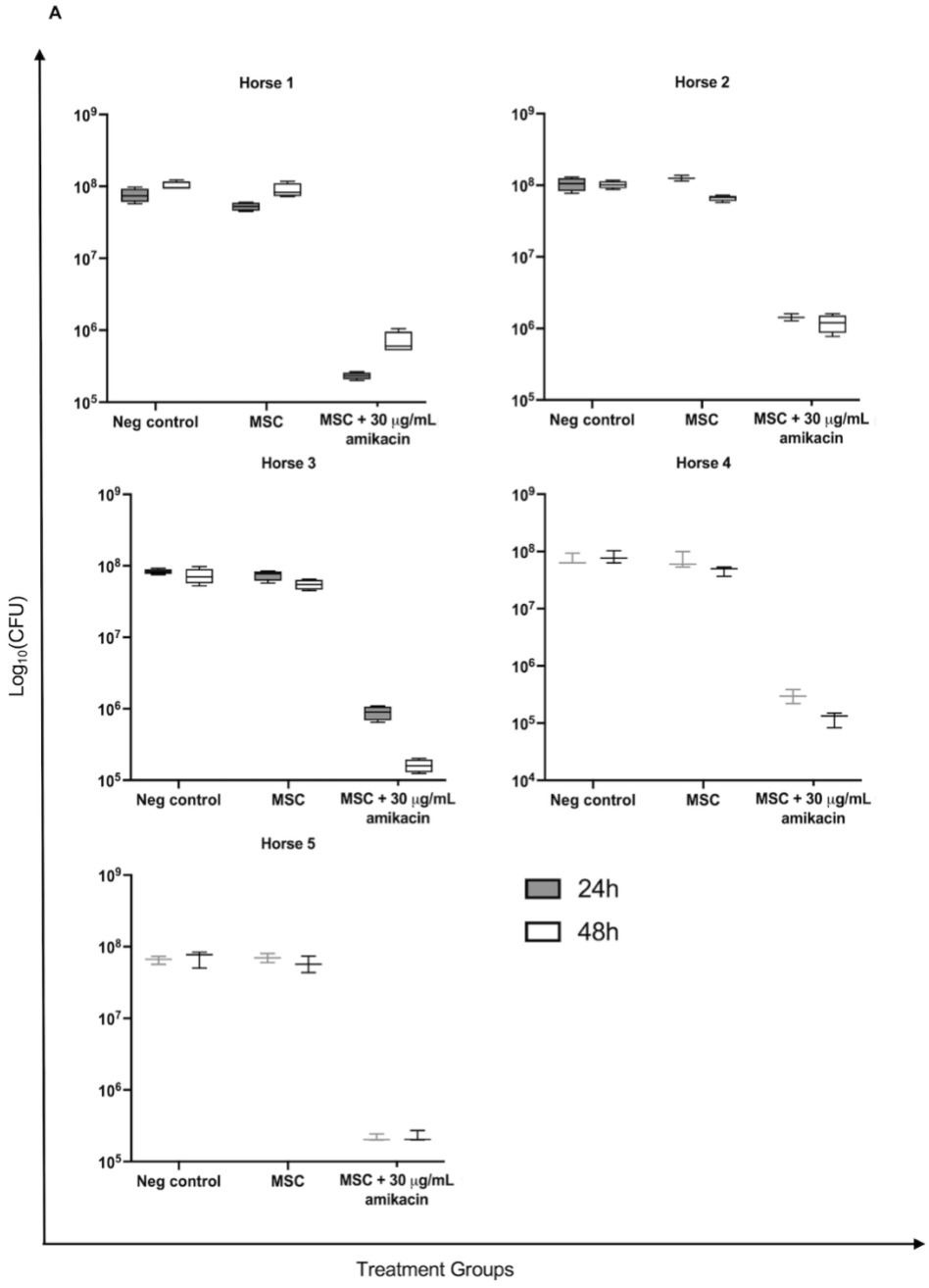
A
Horse 1
Horse 2
Horse 3
Horse 4
Horse 5
Neg control
MSC
MSC + 30 μg/mL amikacin
24h
48h
Log10(CFU)
Treatment Groups

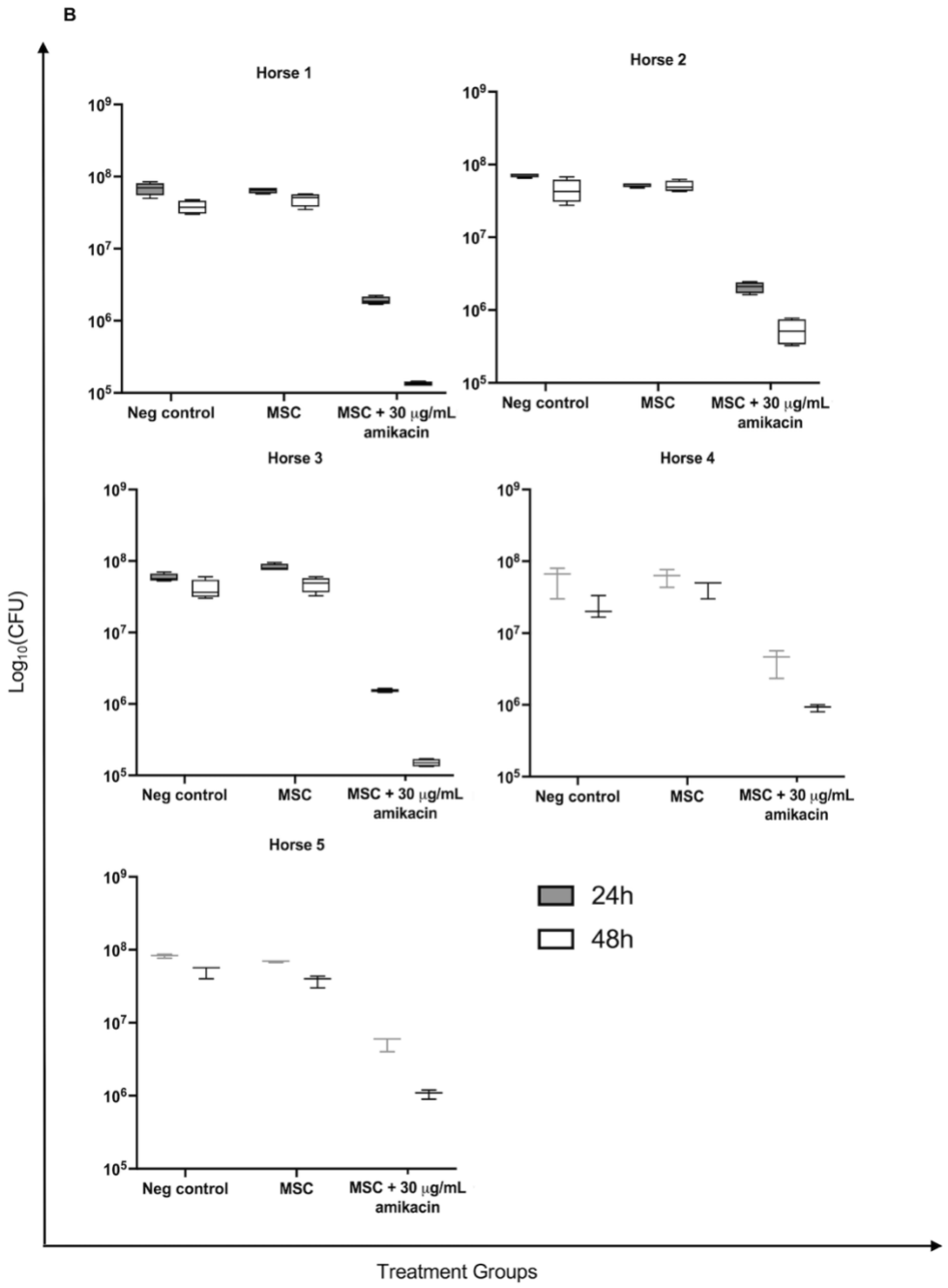

Figure 3.4: Live bacterial counts (log_{10}-transformed CFU) of *S. aureus* (A) or *E. coli* (B) biofilms following no treatment (neg control) or co-culture with MSC or MSC + physiologic (30 µg/mL) amikacin sulfate from 5 horses for 24 (grey) or 48 hours (white + black lines). Boxes represent means (center lines), 5th and 95th percentiles (lower and upper limits), and minimum and maximum values (whiskers) from 3 technical replicates per horse and treatment.

3.2 Quantification of biofilm pellicle reduction on digital photograph analysis provided a cost-effective tool to quantify biofilm pellicle size in a co-culture model

Quantification of pixels for biofilm pellicle size in ImageJ software (Fig 3.2), successfully reflected biofilm pellicle area following MSC co-culture with good agreement between independent observers (Pearson's r = 0.91, $P < 0.01$). We chose to measure the pellicle area by quantifying the number of white pixels in the ROI on black-and-white converted images, and then standardizing pixels to known plate distances. Pixel quantification minimizes potential inter-observer variation associated with manually encircling the pellicle on unmanipulated images. While confocal and electron microscopy provide detailed, three-dimensional visual [7, 36] and quantitative information [22] on biofilm reduction by cellular therapies, substantial financial and time investments may be required to refine microscopic techniques, and access to the required microscopes and software may be limited to specific core facilities. Quantification of reductions in visible biofilm area on digital photographs may thereby serve as a useful intermediary step to document biofilm disruption as a potential mechanism of action of cellular therapies and as a justification to further investigate the biofilm disruption on advanced microscopic imaging.

3.3. Reductions in S. aureus and E. coli biofilm biomass and CFU by physiologic amikacin sulfate were consistently quantified

Incubation of *S. aureus* and *E. coli* biofilms with amikacin sulfate at all concentrations grossly reduced biofilms compared to no treatment (Fig 3.5). A physiologic concentration of amikacin sulfate (30 µg/mL) reduced biofilm biomass of *S. aureus* by 25% ($P = 0.04$) (Fig 3.3A) and of *E. coli* by 75% ($P < 0.01$) (Fig 3.3B) on crystal violet staining compared to untreated biofilms. 30

µg/mL amikacin sulfate also reduced CFU of *S. aureus* ($P < 0.01$) (Fig 3.4C) and *E. coli* ($P < 0.01$) (Fig 3.4D) biofilms by 1 $\log_{10}$-fold compared to no treatment. Similar reductions in biomass and CFU were achieved with 30 µg/mL amikacin sulfate treatment in the final transwell model (Khatibzadeh *PLoS One*, in press) The efficacy of amikacin sulfate at physiologic concentration (30 µg/mL) in the co-culture model supports our second hypothesis. While the MIC for planktonic cultures of our *S. aureus* and *E. coli* strains was $\leq$ 4 µg/mL (Tables 3.1 and 3.2), the MIC for common antimicrobials against biofilm-bound bacteria can be up to 2,000 times greater than that for planktonic bacteria [5-7]. The significant but partial reductions in biomass and CFU seen in this study are thereby consistent with the expected increase in MIC for biofilm-bound bacteria. The significant reduction in biofilm parameters by 30 µg/mL amikacin also confirm that this concentration is a relevant comparison for evaluation of MSC anti-biofilm properties in this model. Addition of antimicrobials to MSC treatment is relevant to the potential use of MSC as an adjunct rather than alternative to traditional antimicrobial therapy, and the previously described synergy demonstrated for MSC with antimicrobials [28, 29].

3.4. A combination of 500 µg/mL amikacin sulfate with 2% SDS eliminates CFU from S. aureus and E. coli biofilms without interfering with biomass staining techniques

Incubation of *S. aureus* and *E. coli* biofilms with both supraphysiologic concentrations (500 and 50,000 µg/ mL) of amikacin sulfate for 48 hours visibly reduced biofilms, with subjectively more reduction seen with 50,000 µg/ mL amikacin treatment (Fig 3.5). However, only 500 µg/mL amikacin reduced biomass by crystal violet staining compared to no treatment (Fig 3.6A and B) (*S. aureus* $P = 0.01$; *E. coli* $P < 0.01$). The lack of change in biomass staining following

treatment with 50,000 ug/mL amikacin versus no treatment (*S. aureus* $P = 0.90$; *E. coli* $P > 0.99$), despite visible biofilm reduction, partially refuted our second hypothesis.

The discrepancy between visible biofilm reduction by 50,000 µg/mL amikacin and the lack of reduction in crystal violet staining compared to untreated biofilms suggests interference between crystal violet staining and amikacin at that concentration. While interference between crystal violet and aminoglycoside antimicrobials has not been reported, it is possible that the amino or carbohydrate groups in the amikacin molecule [52] may be stained by crystal violet, which non-specifically stains all biofilm components [31, 33]. Testing of stains for specific matrix components in our model, including wheat germ agglutinin for carbohydrates, yielded increased stain uptake across all amikacin concentrations despite visible biofilm reduction (Supplement 3.1), further supporting that amikacin may by non-specifically stained by certain matrix stains. Aminoglycoside antimicrobials have also been reported to bind biofilm matrix components [53, 54]. Retention of amikacin in the matrix of biofilms in this study, particularly at the highest tested concentration of 50,000 µg/mL, may thereby have falsely elevated crystal violet stain uptake despite thorough pre- and post-stain rinsing. Based on these findings, 500 µg/mL amikacin sulfate was selected for further evaluation with SDS as a positive control for biofilm removal.

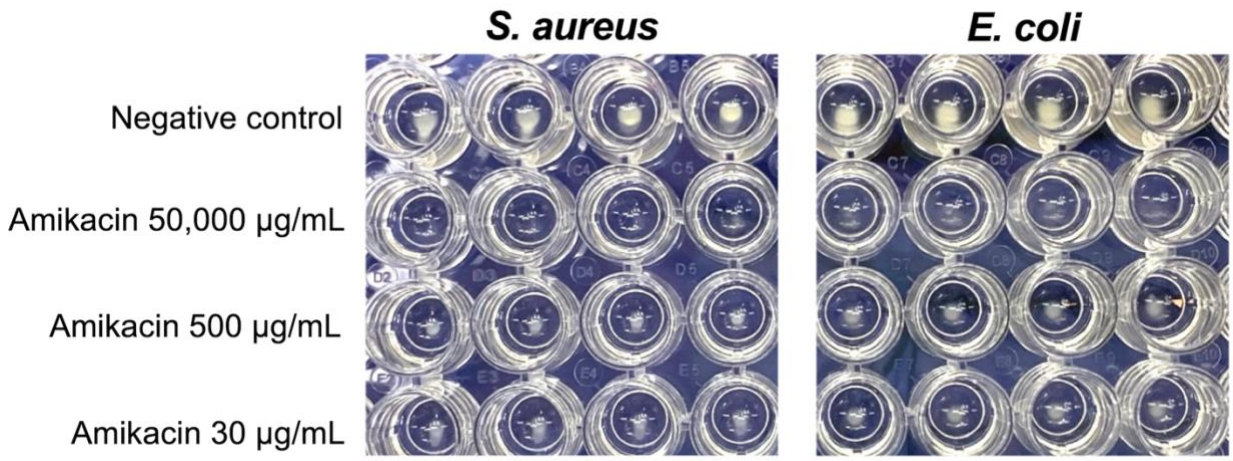

Figure 3.5: Visual *S. aureus* and *E. coli* biofilm reduction by amikacin sulfate. From top to bottom are untreated (negative control) biofilms and biofilms following treatment with supraphysiologic (50,000 and 500 µg/mL) or physiologic (30 µg/mL) concentrations of amikacin sulfate for 48 hours in 96-well plates. Note almost complete elimination of visual biofilm by 50,000 µg/mL amikacin for both bacteria.

While incubation of *S. aureus* and *E. coli* biofilms with all SDS concentrations (0.5-8%) reduced biomass on crystal violet staining comparable to growth medium alone (Supplement 3.2), 2% SDS was selected for further evaluation as a positive control to avoid pipetting difficulties associated with increased viscosity at higher concentrations. A combination of 500 µg/mL amikacin with 2% SDS eliminated CFU from *S. aureus* (Fig 3.6C) and *E. coli* biofilms (Fig 3.6D), confirming this combination as an effective positive control for biofilm elimination.

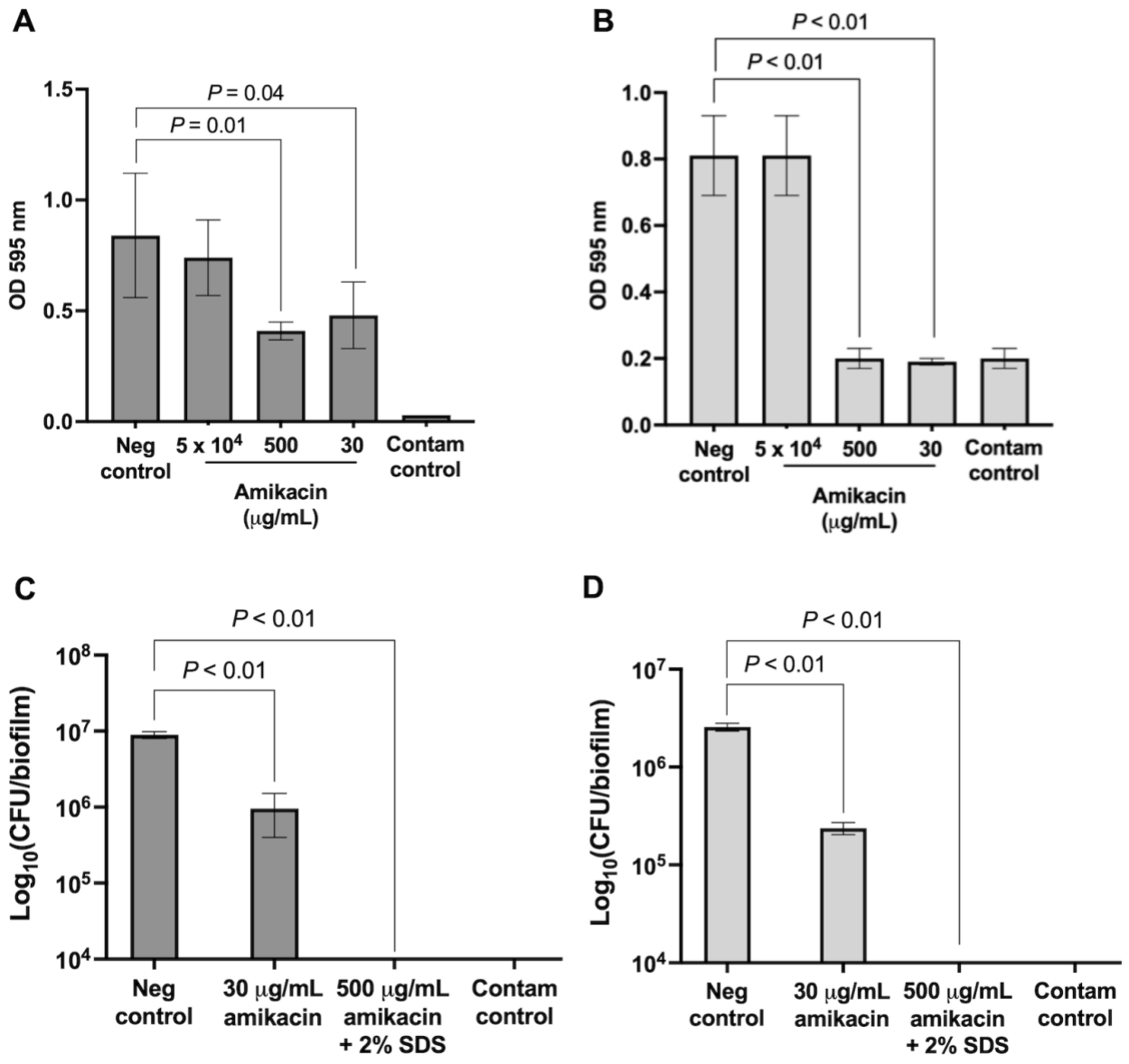

Figure 3.6: Evaluation of amikacin sulfate as a comparison treatment for MSC co-culture and for development of a positive control for biofilm removal. Biomass of *S. aureus* (A) or *E. coli* biofilms (B) in 96-well plates following no treatment (neg control) or 48-hour treatment with supraphysiologic (50,000 or 500 µg/mL) or physiologic (30 µg/mL) concentrations of amikacin. Live bacterial counts ($\log_{10}$(CFU)) of *S. aureus* (C) and *E. coli* biofilms (D) in 96-well plates following no treatment (neg control) or 48-hour treatment with 30 µg/mL amikacin or the

positive control candidate (500 µg/mL amikacin + 2% SDS). The contamination control is growth medium alone. Bars represent mean ± standard deviation of 3 technical replicates. Brackets indicate significant ($p < 0.05$) post-hoc differences between groups.

3.5. The majority of MSC survive co-culture with established S. aureus and E. coli biofilms

Baseline MSC viability prior to seeding in transwell inserts for co-culture was 99%. Seventy percent (70%) of seeded MSC were viable following 48-hour co-culture with *S. aureus* biofilms, while 75% of seeded MSC were alive following 48-hour co-culture with *E. coli* biofilms (Fig 3.7). These finding support our final hypothesis that a minimum of 50% of MSC would survive co-culture with biofilms of both bacteria. Given that our model allowed MSC to interact with biofilms, and that MSC viability following co-culture with bacteria has not been reported, it was necessary to confirm that the majority of MSC would survive biofilm exposure as a basis for interpreting biofilm reduction by MSC in downstream experimentation. While MSC from 5 subsequent horses demonstrated biofilm matrix reduction in our co-culture system (Khatibzadeh *PLoS One*, in press), confirmation of MSC viability post-co-culture from additional horses is needed to further evaluate MSC as an anti-biofilm treatment prior to testing *in vivo.*

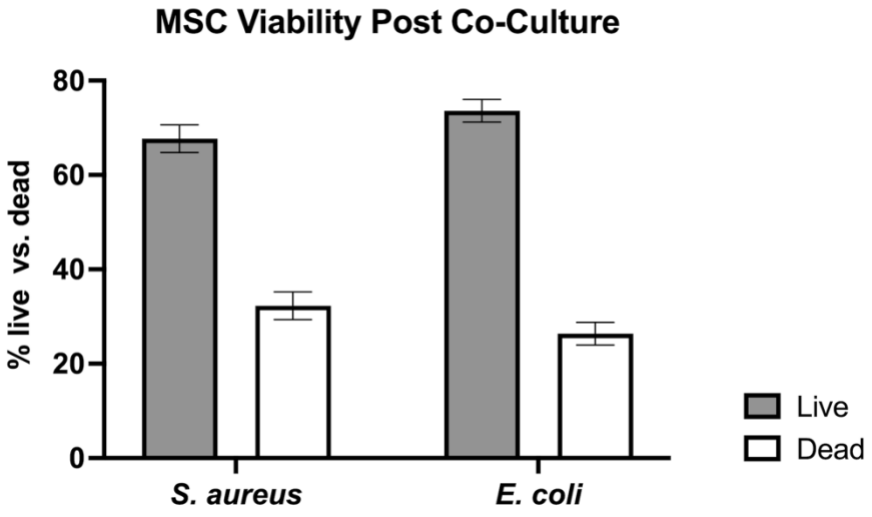

Figure 3.7: MSC viability following transwell co-culture with biofilms.

MSC were trypsinized *in situ*, resuspended, and stained with Trypan Blue following 48-hour co-culture with established *S. aureus* or *E. coli* biofilms. Bars represent mean ± standard deviation of 3 technical replicates from MSC from Horse 1 (Table 3.3).

CONCLUSIONS

Our model of biofilm co-culture with MSC ± a physiologic concentration of amikacin sulfate allows reliable quantification of biofilm reduction by biomass staining, CFU enumeration, and biofilm pellicle area on image analysis, and preserves viability of the majority of MSC. The model offers a viable *in vitro* technique to assess the effect of MSC on biofilms and can be used to screen different treatment parameters using a high-throughput design. This approach can be used to screen MSC from multiple donors, synergy between different antimicrobials, varying MSC doses, and MSC pre-stimulation with PRR agonists [24, 25] or culture conditions that stimulate MSC immunomodulatory properties [55-59]. Future areas for improved biofilm analysis in this model include three-dimensional microscopic techniques for biofilm quantification, comparison of biofilm-bound versus planktonic CFU fractions in the biofilm well system, and measurement of changes in biofilm matrix mechanical properties (e.g., using elastography) [41]. The model represents an easily accessible route to further investigate and refine MSC antibiofilm responses and thereby represents a valuable pre-clinical step in optimizing MSC as a therapy for orthopedic biofilm infections.

Acknowledgements

The authors would like to acknowledge Dr. Bruno Menarim (Gluck Equine Research Center, University of Kentucky) and Dr. James Blake Everett (Equine Surgical Center, Murfreesboro, Tennessee) for their efforts in isolating and cryopreserving the equine bone marrow mononuclear cells used for MSC isolation. The authors would like to thank Dr. Tessa LeCuyer, Dr. Jessica Gilbertie, the technical specialists at the Center for One Health Research (Nancy Tenpenny) and the Collaborative Multidisciplinary Research Laboratory (Michelle Todd), members of the Caswell Laboratory (Tristan Stoyanof, Dr. Mitchell Caudill), and numerous undergraduate students (Elanagh Smith, Kayla Hackler, Jacq Field, Hannah Elshafie, Sidney Schumaker, Jane Perkins), for their invaluable assistance and support.

Funding sources

This work was supported by the Morris Animal Foundation Large Animal Training Fellowship, the Interdisciplinary Graduate Education Program in Regenerative Medicine and the Office of Research and Graduate Studies (Virginia Tech), and the Equine Research Competition (Virginia-Maryland College of Veterinary Medicine).

Supplemental information

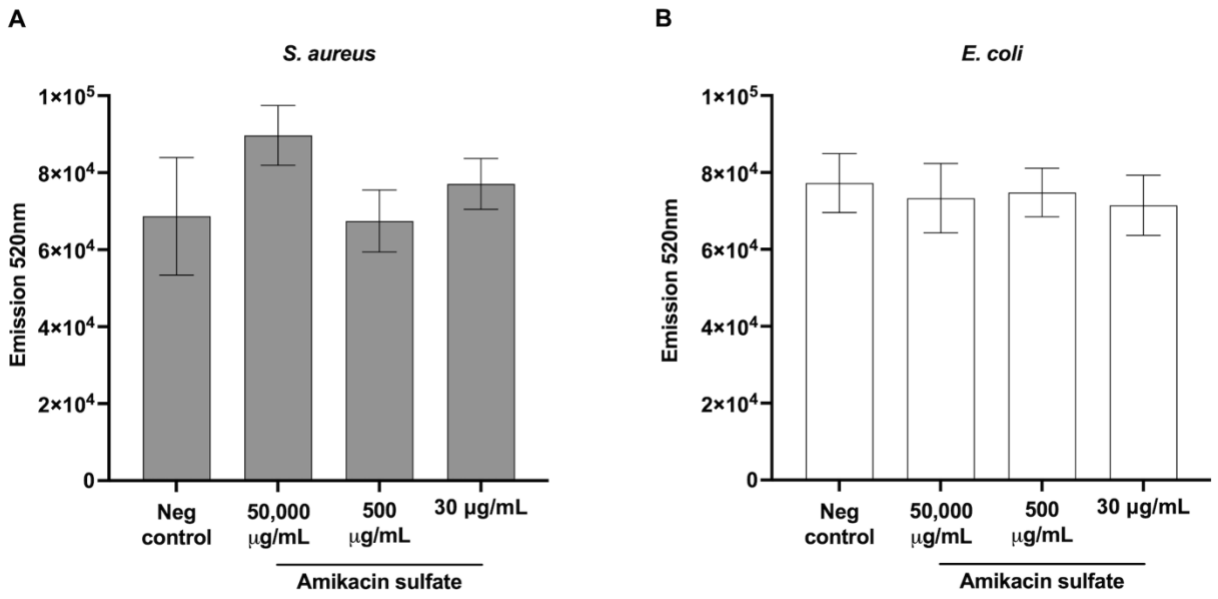

Supplement 3.1: Biofilm matrix carbohydrate staining following amikacin sulfate treatment. Matrix carbohydrate staining by wheat germ agglutinin (emission 520 nm) of *S. aureus* (A) or *E. coli* (B) biofilms following treatment with supraphysiologic (50,000 and 500 µg/mL) or physiologic (30 µg/mL) concentrations of amikacin sulfate for 48 hours. Bars represent mean ± standard deviation of 3 technical replicates.

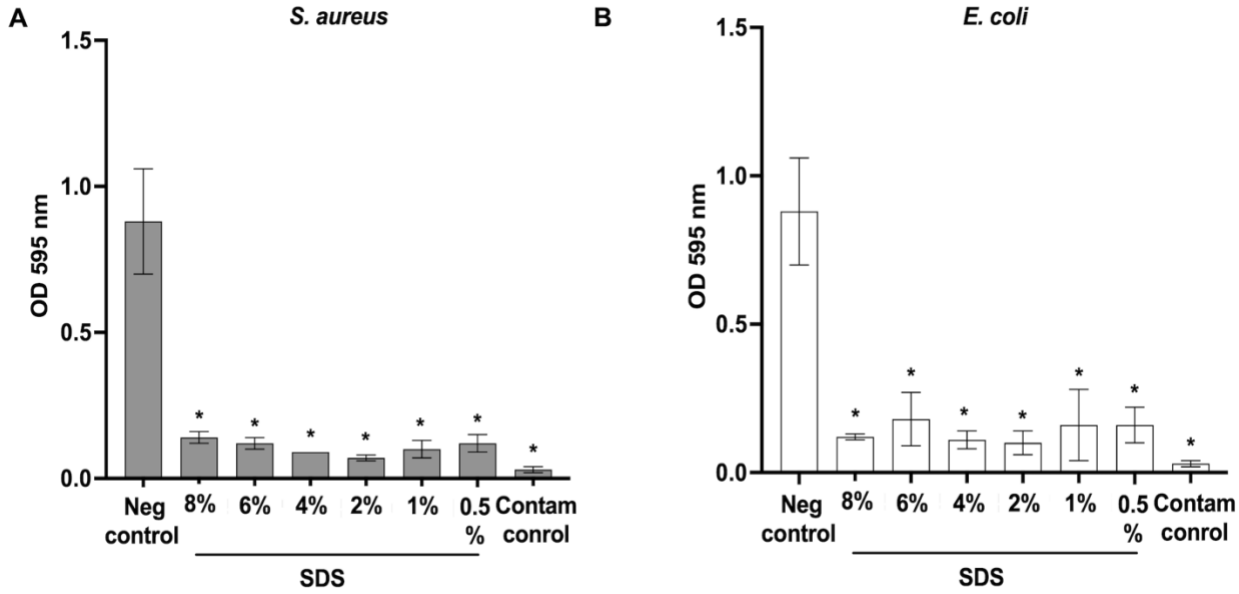

Supplement 3.2: Biofilm biomass reduction by sodium dodecyl sulfate (SDS). Biomass of crystal violet-stained *S. aureus* (A) or *E. coli* biofilms (B) in 96-well plates following no treatment (neg control) or 48-hour treatment with a range of SDS concentrations. The contamination control is growth medium alone. Bars represent mean ± standard deviation of 3 technical replicates. Asterisks indicate significant ($p < 0.05$) post-hoc differences compared to the untreated control, with no differences between SDS concentrations or between SDS treatment and the contamination control.

BIBLIOGRAPHY

1. Bjarnsholt T, Alhede M, Alhede M, Eickhardt-Sorensen SR, Moser C, Kuhl M, et al. The *in vivo* biofilm. Trends Microbiol. 2013;21:466-74.
2. Alhede M, Alhede M, Qvortrup K, Kragh KN, Jensen PO, Stewart PS, et al. The origin of extracellular DNA in bacterial biofilm infections *in vivo*. Pathog Dis. 2020;78.
3. Patti JM, Allen BL, McGavin MJ, Hook M. MSCRAMM -Mediated Adherence of Microorganisms to Host Tissues. Annu Rev Microbiol. 1994;48:585-617.
4. Nguyen MH, Ojima Y, Sakka M, Sakka K, Taya M. Probing of exopolysaccharides with green fluorescence protein-labeled carbohydrate-binding module in *Escherichia coli* biofilms and flocs induced by bcsB overexpression. J Biosci Bioeng. 2014;118:400-5.
5. Walker M, Singh A, Nazarali A, Gibson TW, Rousseau J, Weese JS. Evaluation of the Impact of Methicillin-Resistant *Staphylococcus pseudintermedius* Biofilm Formation on Antimicrobial Susceptibility. Vet Surg. 2016;45:968-71.
6. Mandell JB, Orr S, Koch J, Nourie B, Ma D, Bonar DD, et al. Large variations in clinical antibiotic activity against *Staphylococcus aureus* biofilms of periprosthetic joint infection isolates. J Orthop Res. 2019;37:1604-9.
7. Gilbertie JM, Schnabel LV, Hickok NJ, Jacob ME, Conlon BP, Shapiro IM, et al. Equine or porcine synovial fluid as a novel *ex vivo* model for the study of bacterial free-floating biofilms that form in human joint infections. PLoS One. 2019;14:e0221012.
8. Arciola CR, Campoccia D, Montanaro L. Implant infections: adhesion, biofilm formation and immune evasion. Nat Rev Microbiol. 2018;16:397-409.

9. Bhardwaj RG, Al-Khabbaz A, Karched M. Cytokine induction of peripheral blood mononuclear cells by biofilms and biofilm supernatants of *Granulicatella* and *Abiotrophia spp*. Microb Pathog. 2018;114:90-4.
10. Pollmann CT, Dahl FA, Rotterud JHM, Gjertsen JE, Aroen A. Surgical site infection after hip fracture - mortality and risk factors: an observational cohort study of 1,709 patients. Acta Orthop. 2020;91:347-52.
11. Zmistowski B, Karam JA, Durinka JB, Casper DS, Parvizi J. Periprosthetic joint infection increases the risk of one-year mortality. J Bone Joint Surg Am. 2013;95:2177-84.
12. Teterycz D, Ferry T, Lew D, Stern R, Assal M, Hoffmeyer P, et al. Outcome of orthopedic implant infections due to different *staphylococci*. Int J Infect Dis. 2010;14:e913-8.
13. Tomizawa T, Ishikawa M, Bello-Irizarry SN, de Mesy Bentley KL, Ito H, Kates SL, et al. Biofilm Producing *Staphylococcus epidermidis* (RP62A Strain) Inhibits Osseous Integration Without Osteolysis and Histopathology in a Murine Septic Implant Model. J Orthop Res. 2020;38:852-60.
14. Prabhakara R, Harro JM, Leid JG, Keegan AD, Prior ML, Shirtliff ME. Suppression of the inflammatory immune response prevents the development of chronic biofilm infection due to methicillin-resistant *Staphylococcus aureus*. Infect Immun. 2011;79:5010-8.
15. Leid JG, Shirtliff ME, Costerton JW, Stoodley P. Human leukocytes adhere to, penetrate, and respond to *Staphylococcus aureus* biofilms. Infect Immun. 2002;70:6339-45.
16. Ahern BJ, Richardson DW, Boston RC, Schaer TP. Orthopedic infections in equine long bone fractures and arthrodeses treated by internal fixation: 192 cases (1990-2006). Vet Surg. 2010;39:588-93.

17. Curtiss AL, Stefanovski D, Richardson DW. Surgical site infection associated with equine orthopedic internal fixation: 155 cases (2008-2016). Vet Surg. 2019;48:685-93.

18. Hall MS, Pollock PJ, Russell T. Surgical treatment of septic physitis in 17 foals. Aust Vet J. 2012;90:479-84.

19. Krasnodembskaya A, Song Y, Fang X, Gupta N, Serikov V, Lee JW, et al. Antibacterial effect of human mesenchymal stem cells is mediated in part from secretion of the antimicrobial peptide LL-37. Stem Cells. 2010;28:2229-38.

20. Harman RM, Yang S, He MK, Van de Walle GR. Antimicrobial peptides secreted by equine mesenchymal stromal cells inhibit the growth of bacteria commonly found in skin wounds. Stem Cell Res Ther. 2017;8:157.

21. Gupta N, Krasnodembskaya A, Kapetanaki M, Mouded M, Tan X, Serikov V, et al. Mesenchymal stem cells enhance survival and bacterial clearance in murine *Escherichia coli* pneumonia. Thorax. 2012;67:533-9.

22. Marx C, Gardner S, Harman RM, Van de Walle GR. The mesenchymal stromal cell secretome impairs methicillin-resistant *Staphylococcus aureus* biofilms via cysteine protease activity in the equine model. Stem Cells Transl Med. 2020.

23. Avellar HK, Lutter JD, Ganta CK, Beard W, Smith JR, Jonnalagadda N, et al. *In vitro* antimicrobial activity of equine platelet lysate and mesenchymal stromal cells against common clinical pathogens. Can J Vet Res. 2022;86:59-64.

24. Cortes-Araya Y, Amilon K, Rink BE, Black G, Lisowski Z, Donadeu FX, et al. Comparison of Antibacterial and Immunological Properties of Mesenchymal Stem/Stromal Cells from Equine Bone Marrow, Endometrium, and Adipose Tissue. Stem Cells Dev. 2018;27:1518-25.

25. Pezzanite LM, Chow L, Johnson V, Griffenhagen GM, Goodrich L, Dow S. Toll-like receptor activation of equine mesenchymal stromal cells to enhance antibacterial activity and immunomodulatory cytokine secretion. Vet Surg. 2021;50:858-71.
26. Marx C, Gardner S, Harman RM, Wagner B, Van de Walle GR. Mesenchymal stromal cell-secreted CCL2 promotes antibacterial defense mechanisms through increased antimicrobial peptide expression in keratinocytes. Stem Cells Transl Med. 2021;10:1666-79.
27. Gupta N, Sinha R, Krasnodembskaya A, Xu X, Nizet V, Matthay MA, et al. The TLR4-PAR1 Axis Regulates Bone Marrow Mesenchymal Stromal Cell Survival and Therapeutic Capacity in Experimental Bacterial Pneumonia. Stem Cells. 2018;36:796-806.
28. Johnson V, Webb T, Norman A, Coy J, Kurihara J, Regan D, et al. Activated Mesenchymal Stem Cells Interact with Antibiotics and Host Innate Immune Responses to Control Chronic Bacterial Infections. Sci Rep. 2017;7:9575.
29. Yamamuro Y, Kabata T, Nojima T, Hayashi K, Tokoro M, Kajino Y, et al. Combined adipose-derived mesenchymal stem cell and antibiotic therapy can effectively treat periprosthetic joint infection in rats. Sci Rep. 2023;13:3949.
30. Alcayaga-Miranda F, Cuenca J, Martin A, Contreras L, Figueroa FE, Khoury M. Combination therapy of menstrual derived mesenchymal stem cells and antibiotics ameliorates survival in sepsis. Stem Cell Res Ther. 2015;6:199.
31. Merritt JH, Kadouri DE, O'Toole GA. Growing and analyzing static biofilms. Curr Protoc Microbiol. 2005;Chapter 1:Unit 1B
32. Peeters E, Nelis HJ, Coenye T. Comparison of multiple methods for quantification of microbial biofilms grown in microtiter plates. J Microbiol Methods. 2008;72:157-65.

33. Stiefel P, Rosenberg U, Schneider J, Mauerhofer S, Maniura-Weber K, Ren Q. Is biofilm removal properly assessed? Comparison of different quantification methods in a 96-well plate system. Appl Microbiol Biotechnol. 2016;100:4135-45.

34. Tote K, Vanden Berghe D, Maes L, Cos P. A new colorimetric microtitre model for the detection of *Staphylococcus aureus* biofilms. Lett Appl Microbiol. 2008;46:249-54.

35. Gilbertie JM, Schaer TP, Schubert AG, Jacob ME, Menegatti S, Ashton Lavoie R, et al. Platelet-rich plasma lysate displays antibiofilm properties and restores antimicrobial activity against synovial fluid biofilms *in vitro*. J Orthop Res. 2020.

36. Nishitani K, Sutipornpalangkul W, de Mesy Bentley KL, Varrone JJ, Bello-Irizarry SN, Ito H, et al. Quantifying the natural history of biofilm formation *in vivo* during the establishment of chronic implant-associated *Staphylococcus aureus* osteomyelitis in mice to identify critical pathogen and host factors. J Orthop Res. 2015;33:1311-9.

37. Harvey A, Kilcoyne I, Byrne BA, Nieto J. Effect of Dose on Intra-Articular Amikacin Sulfate Concentrations Following Intravenous Regional Limb Perfusion in Horses. Vet Surg. 2016;45:1077-82.

38. Oreff GL, Dahan R, Tatz AJ, Raz T, Britzi M, Kelmer G. The Effect of Perfusate Volume on Amikacin Concentration in the Metacarpophalangeal Joint Following Cephalic Regional Limb Perfusion in Standing Horses. Vet Surg. 2016;45:625-30.

39. Lewis JS, Weinstein MP, Bobenchik AM, Campeau S, Cullen SK, Dingel T, Galas MF, Humphries RM. CLSI M100-ED33: 2023 Performance Standards for Antimicrobial Susceptibility Testing, 33rd Ed. CLSI. 2023.

40. Zhang XY, Sun K, Abulimiti A, Xu PP, Li ZY. Microfluidic System for Observation of Bacterial Culture and Effects on Biofilm Formation at Microscale. Micromachines (Basel). 2019;10.

41. Buzzo JR, Devaraj A, Gloag ES, Jurcisek JA, Robledo-Avila F, Kesler T, et al. Z-form extracellular DNA is a structural component of the bacterial biofilm matrix. Cell. 2021;184:5740-58 e17.

42. Moser DK, Schoonover MJ, Holbrook TC, Payton ME. Effect of Regional Intravenous Limb Perfusate Volume on Synovial Fluid Concentration of Amikacin and Local Venous Blood Pressure in the Horse. Vet Surg. 2016;45:851-8.

43. Diaz De Rienzo MA, Stevenson P, Marchant R, Banat IM. Antibacterial properties of biosurfactants against selected Gram-positive and -negative bacteria. FEMS Microbiol Lett. 2016;363:fnv224.

44. Li L, Molin S, Yang L, Ndoni S. Sodium Dodecyl Sulfate (SDS)-Loaded Nanoporous Polymer as Anti-Biofilm Surface Coating Material. Int J Mol Sci. 2013;14:3050-64.

45. Biasutti SA, Cox E, Jeffcott LB, Dart AJ. A review of regional limb perfusion for distal limb infections in the horse. Equine Vet Educ. 2020;33:263-77.

46. Correa F, Borlone C, Wittwer F, Bustamante H, Muller A, Ramirez A, et al. How to obtain and isolate equine sternal bone marrow mononuclear cells with limited resources. Arch Med Vet. 2014;46:471-6.

47. Menarim BC, Gillis KH, Oliver A, Mason C, Werre SR, Luo X, et al. Inflamed synovial fluid induces a homeostatic response in bone marrow mononuclear cells *in vitro*: Implications for joint therapy. FASEB J. 2020;34:4430-44.

48. Everett J. Bone marrow mononuclear cell therapy for equine joint disease. Proceedings: 66th Annual Convention, Am Assoc Equine Pract. Virtual. 2020. p. 226-7.

49. Fortier LN, Nixon AJ, Williams J, Cable CS. Isolation and chondrocytic differentiation of equine bone marrow-derived mesenchymal stem cells. Am J Vet Res. 1998;59:1182-7.

50. Bourzac C, Smith LC, Vincent P, Beauchamp G, Lavoie JP, Laverty S. Isolation of equine bone marrow-derived mesenchymal stem cells: a comparison between three protocols. Equine Vet J. 2010;42:519-27.

51. Zahedi M, Parham A, Dehghani H, Kazemi Mehrjerdi H. Equine bone marrow-derived mesenchymal stem cells: optimization of cell density in primary culture. Stem Cell Investig. 2018;5:31.

52. Amikacin sulfate. Daily Med Health. National Institutes of Health. 2022.

53. Chiang WC, Nilsson M, Jensen PO, Hoiby N, Nielsen TE, Givskov M, et al. Extracellular DNA shields against aminoglycosides in *Pseudomonas aeruginosa* biofilms. Antimicrob Agents Chemother. 2013;57:2352-61.

54. Ramphal R, Lhermitte, M., Filliat, M., Roussel, P. The binding of anti-pseudomonal antibiotics to macromolecules from cystic fibrosis sputum. J Antimicrob Chemother. 1988;22:483-90.

55. Wang D, Chen D, Yu J, Liu J, Shi X, Sun Y, et al. Impact of Oxygen Concentration on Metabolic Profile of Human Placenta-Derived Mesenchymal Stem Cells As Determined by Chemical Isotope Labeling LC-MS. J Proteome Res. 2018;17:1866-78.

56. Crisostomo PR, Wang Y, Markel TA, Wang M, Lahm T, Meldrum DR. Human mesenchymal stem cells stimulated by TNF-alpha, LPS, or hypoxia produce growth factors by an NF kappa B- but not JNK-dependent mechanism. Am J Physiol Cell Physiol. 2008;294:C675-82.

57. Ohnishi S, Yasuda T, Kitamura S, Nagaya N. Effect of hypoxia on gene expression of bone marrow-derived mesenchymal stem cells and mononuclear cells. Stem Cells. 2007;25:1166-77.

58. Bogers SH, Barrett JG. Three-Dimensional Culture of Equine Bone Marrow-Derived Mesenchymal Stem Cells Enhances Anti-Inflammatory Properties in a Donor-Dependent Manner. Stem Cells Dev. 2022;31:777-86.

59. Park MJ, Lee J, Byeon JS, Jeong DU, Gu NY, Cho IS, et al. Effects of three-dimensional spheroid culture on equine mesenchymal stem cell plasticity. Vet Res Commun. 2018;42:171-81.

CHAPTER 4: EQUINE BONE MARROW-DERIVED MESENCHYMAL STROMAL CELLS REDUCE ESTABLISHED *S. AUREUS* AND *E. COLI* BIOFILM MATRIX *IN VITRO.*

To be submitted for publication as:

Sarah M. Khatibzadeh, Linda A. Dahlgren, Clayton C. Caswell, William A. Ducker, Stephen R. Werre, Sophie H. Bogers. Equine bone marrow-derived mesenchymal stromal cells reduce established *S. aureus* and *E. coli* biofilm matrix *in vitro. PLoS One*

ABSTRACT

Biofilms reduce the efficacy of antibiotics and lead to complications and mortality in human and equine patients with orthopedic infections. Equine bone marrow-derived mesenchymal stromal cells (MSC) kill planktonic bacteria and prevent biofilm formation, but their ability to disrupt established orthopedic biofilms is unknown. Our objective was to evaluate the ability of MSC to reduce established *S. aureus* or *E. coli* biofilms *in vitro*. We hypothesized that MSC would reduce biofilm matrix and colony-forming units (CFU) compared to no treatment and that MSC combined with the antibiotic, amikacin sulfate, would reduce these components more than MSC or amikacin alone. MSC were isolated from 5 adult Thoroughbred horses in antibiotic-free medium. 24-hour *S. aureus* or *E. coli* biofilms were co-cultured in triplicate for 24 or 48 hours in a transwell plate system: untreated (negative) control, 30 µg/mL amikacin, 1 x 10^6 passage 3 MSC, MSC with 30 µg/mL amikacin. Treated biofilms were photographed and pellicle area quantified digitally, biomass was quantified via crystal violet staining, and CFU quantified

following enzymatic digestion. Data were analyzed using mixed model ANOVA with Tukey post-hoc comparisons ($p < 0.05$). MSC significantly reduced *S. aureus* pellicles at both timepoints and *E. coli* pellicle area at 48 hours compared to untreated controls. MSC with amikacin significantly reduced *S. aureus* pellicles versus amikacin and *E. coli* pellicles versus MSC at 48 hours. MSC significantly reduced *S. aureus* biomass at both timepoints and reduced *S. aureus* CFU at 48 hours versus untreated controls. MSC with amikacin significantly reduced *S. aureus* biomass versus amikacin at 24 hours and *S. aureus* and *E. coli* CFU versus MSC at both timepoints. MSC primarily disrupted the biofilm matrix but performed differently on *S. aureus* versus *E. coli.* Evaluation of biofilm-MSC interactions, MSC dose, and treatment time are warranted prior to testing *in vivo*.

INTRODUCTION

Biofilms are a common and critical problem in orthopedic infections, such as septic synovitis and implant-associated infections. Complications and resistance of biofilms to treatment contribute to increased treatment costs and treatment failure in human [1-3] and veterinary patients [4-7]. A biofilm is a community of bacteria adhered to a surface or to each other and encased in a self-secreted extracellular matrix of carbohydrates, proteins, and DNA [8-14]. Biofilms contribute to antimicrobial resistance in orthopedic infections by shielding indwelling bacteria from immune cells and antimicrobials [12, 15-18], facilitating bacterial metabolic downregulation [19, 20], and promoting exchange of antimicrobial resistance genes [7]. Resistance of biofilm-bound bacteria to antimicrobials and immune cells contributes to persistent infection in the face of parenteral and regional antimicrobial administration [6, 21-23]. Multi-stage surgical removal of infected implants and debridement of affected tissue are often required in conjunction with prolonged antimicrobial therapy for infection resolution [4, 5, 24].

Despite aggressive and prolonged medical and surgical therapy, sequalae of orthopedic infections involving biofilms include irreversible tissue damage due to chronic inflammation, such as osteolysis with subsequent implant failure [4, 25, 26] and chondromalacia in septic synovitis [6, 27]. Additionally, persistent biofilms serve as a nidus for dissemination of infection to the bloodstream and vital organs, which can be life-threatening [2, 28-31]. The complications related to biofilm infections are dire; 26-55% of people with orthopedic implant infections die within 5 years of initial diagnosis [29-31]. Persistent orthopedic biofilm infections are an equally significant problem in horses and are often caused by *Staphylococcus aureus* and *Escherichia coli*, which readily form biofilms on metallic orthopedic implants [7, 13, 32, 33] and in synovial

fluid as floating aggregates [12, 34-37]. The resulting chronic lameness, loss of athletic potential, and reduced quality of life due to chronic, unresolved orthopedic infections [4-6, 22, 24] make euthanasia ultimately necessary in up to 54% of horses [4, 5, 22, 38, 39]. A treatment that disrupts established orthopedic biofilms and improves success of antimicrobials and surgical intervention is desperately needed.

Mesenchymal stromal cells (MSC) support tissue regeneration and immunomodulation in people and veterinary species and are widely used for the treatment of musculoskeletal injuries in horses [40-46]. Recently, MSC have been demonstrated to have antimicrobial properties *in vitro* [47-51], *ex vivo* [52], and in animal models of infection [53-55]. Equine MSC exert antimicrobial effects in a paracrine manner, via secretion of antimicrobial peptides that depolarize bacterial cell membranes [48, 50] and interfere with bacterial metabolism of key nutrients [49]. Additionally, equine MSC enhance the host antibacterial response through stimulation of phagocytosis by neutrophils [51] and secretion of antimicrobial peptides from keratinocytes [52]. As a combination treatment, MSC with antimicrobials significantly reduced bacterial numbers, demonstrating therapeutic synergy [54-56].

To date, studies have primarily evaluated the ability of MSC to prevent establishment of infection, including planktonic (free-floating) bacterial reduction and inhibition of biofilm formation [48-51]. Harman et al. demonstrated that conditioned medium from equine MSC prevented biofilm formation by planktonic cultures of *S. aureus* and *E. coli* [48]. However, it was unclear if the anti-biofilm properties were due to bacterial killing prior to biofilm establishment, or direct disruption of biofilm formation. The biofilm matrix physically protects

indwelling bacteria from killed by immune cells and can utilize host immune response to its advantage by incorporating secreted proteins [12, 36, 57] and DNA [58] into its matrix. Therefore, it is important to investigate of the ability of equine MSC to reduce established orthopedic biofilms that contain a mature extracellular matrix. It is also unknown whether equine MSC synergize with antimicrobials used clinically in equine orthopedic infections [21, 59, 60] and can reduce established orthopedic biofilms to a greater extent than MSC alone.

The objectives of this study were to 1) evaluate the ability of equine bone marrow-derived MSC to reduce biomass (total cells and matrix), biofilm size, and live bacterial counts of established *S. aureus* or *E. coli* biofilms *in vitro*, and 2) whether the combination of MSC and the antimicrobial amikacin sulfate would be more effective than either alone. We hypothesized that 1) MSC would reduce biomass, size, and live bacterial counts of *S. aureus* and *E. coli* biofilms compared to untreated controls, and 2) the combination of MSC with amikacin would reduce biomass, size, and live bacteria of *S. aureus* and *E. coli* biofilms more than MSC or amikacin alone.

METHODS

Overview: MSC were isolated from bone marrow from 5 horses and co-cultured at passage 3, alone or with a concentration of amikacin sulfate achieved *in vivo* [21, 61], with established 24-hour *S. aureus* or *E. coli* biofilms in a transwell plate system (Fig 4.1). This system allowed MSC and biofilms to interact in a paracrine manner during co-culture and facilitated easy biofilm separation after co-culture for imaging and quantification of biomass and live bacterial counts. Biofilm biomass, live bacterial counts, and pellicle area were quantified following 24 or 48 hours of co-culture.

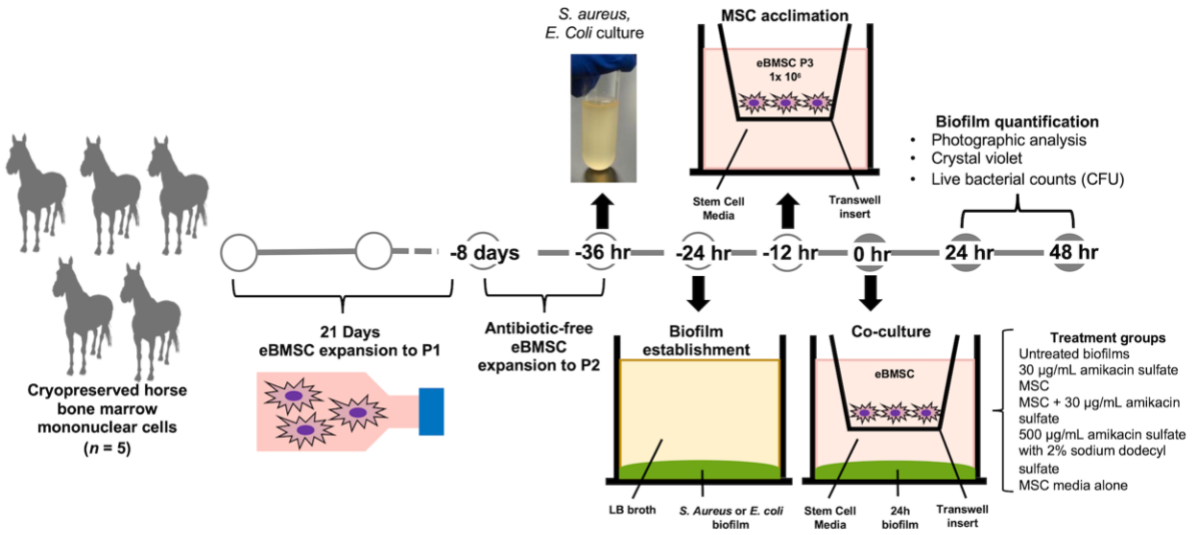

Figure 4.1: Experimental Workflow to Quantify Biofilm Reduction: MSC and biofilms of *S. aureus* or *E. coli* were prepared separately. Biofilms were established on 24-well tissue culture-treated plates for 24 hours and were co-cultured with 1 x 10^6 passage 3 MSC seeded in transwell inserts alone or with amikacin sulfate for an additional 24 or 48 hours. Biofilms that remained untreated for the co-culture period were the negative control. Open circles indicate preparatory

steps and solid circles indicate steps to establish co-cultures and perform biofilm quantification assays.

MSC isolation: Under standing sedation and local anesthesia, 60 mL bone marrow was aspirated into sodium heparinized syringes (200 units/mL marrow) from the 4th and 5th sternebrae of 5 adult Thoroughbred horses (Table 4.1). Bone marrow collection protocols were reviewed and approved by the Virginia Tech Institutional Animal Care and Use Committee. Bone marrow mononuclear cells were isolated using gradient density separation (Ficoll® Paque PLUS) and assessed by live-dead staining with Trypan blue (Gibco™) as previously described and cryopreserved at passage 0 in fetal bovine serum (FBS) with 10% dimethyl sulfoxide until use (Fig 4.1) [62-64]. Equine bone marrow stromal cells (MSC) were thawed in a 37°C water bath and plated at 350,000 live cells/cm^2 in 175 cm^2 tissue culture flasks in MSC medium: low-glucose (l/g) GlutaMax DMEM with 110 µg/mL sodium pyruvate (Gibco™), 100 U/mL sodium penicillin and 100 µg/mL streptomycin sulfate (Sigma Aldrich®), plus 10% MSC FBS (Gibco™) [65-67]. A 50% medium exchange was performed every 48 hours and MSC passaged at 70-80% to passage 1 prior to short-term cryopreservation (Synth-a-freeze™, Gibco™) in liquid nitrogen, vapor phase.

Table 4.1: Bone marrow-derived MSC donor horse information

DONOR	BREED	SEX	AGE (YEARS)
1	TB	MC	5
2	TB	MC	7
3	TB	F	3
4	TB	F	5
5	TB	MC	7

Abbreviations: TB = Thoroughbred, MC = Male castrate, F = Female

Biofilm growth: Quality control testing was performed on commercial strains of *S. aureus* (ATCC® 2913) or *E. coli* (ATCC® 25922) by broth microdilution (Sensititre™, ThermoFisher™) to ensure that the minimum inhibitory concentration (MIC) of each drug fell within the expected ranges as outlined in the Clinical Laboratory Standards Institute [68]. The MIC of amikacin was ≤ 4 µg/mL for *S. aureus* and *E. coli*. Planktonic cultures of *S. aureus* or *E. coli* were established by isolation of pure colonies on tryptic soy agar (TSA) and inoculation of one colony of either bacterium in Luria-Bertani (LB) broth. Cultures were grown overnight at 37ºC at 200 rpm on an orbital shaker (Fisherbrand™ Incubating Mini-Shaker, Fisher Scientific) to reach the exponential growth phase and then were serially diluted in LB broth to a final optical density of 0.05 at 600 nm. Biofilms were established by inoculation of 2 x 10^5 colony-forming units (CFU)/well in 24-well, tissue-culture treated plates and grown at 37ºC, 5% CO_2, and 95% humidity for 24 hours, to allow adequate bacterial attachment and matrix production (Fig 4.1) [13, 14].

Biofilm-MSC co-culture: Thawed MSC were expanded at passage 2 in in antibiotic-free MSC medium (l/g DMEM, 10% FBS), trypsinized at 70-80% confluency, baseline viability assessed via Trypan Blue staining, and seeded at passage 3 into inserts of 24-well transwell plates (6.5 mm insert diameter, 0.4 µm pore diameter, polyester, Corning®) at 1.0 x 10^6 live MSC/insert in antibiotic-free MSC medium with 5% FBS. MSC were acclimated to the inserts overnight at 37ºC, 5% CO_2, and 95% humidity prior to transfer to biofilm co-culture. At time = 0 hours, MSC-biofilm co-cultures were established (Fig 4.1). 24-hour-old *S. aureus* and *E. coli* biofilms were centrifuged at 1,400 x g, room temperature (RT) for 10 minutes to concentrate biomass in

the well bottom, the overlying LB broth aspirated, and 500 µL MSC medium with 5% FBS alone (negative control) or containing 30 µg/mL amikacin sulfate (amikacin group) added per well. Inserts containing MSC in 100 µL MSC medium were then transferred to wells containing biofilms with 400 µL/well of MSC medium with 5% FBS alone (MSC) or with 5% FBS and 30 µg/mL amikacin sulfate (MSC + amikacin). The bacterial CFU:MSC ratios at time 0 were 500 *S. aureus* CFU:1 MSC and 1,000 *E. coli* CFU:1 MSC.

Treatment groups: Triplicate biofilms of the following 6 groups were either left untreated (negative control) or treated as follows for 24 or 48 hours: 30 µg/mL amikacin sulfate (Avet Pharmaceuticals, Inc®, New Brunswick, NJ) [21, 61, 69]; MSC alone; MSC + 30 µg/mL amikacin sulfate; 500 µg/mL amikacin sulfate with 2% sodium dodecyl sulfate (positive control) [70-72]; and MSC medium alone (contamination control).

Photographic analysis: Following co-culture, inserts containing MSC were aseptically removed to allow downstream assays. Biofilms were examined grossly and digitally photographed (iPhone XR, Apple, Inc, Cupertino, CA) in a commercial ring LED photography booth with a black backdrop and lens set to an object distance of 19 cm (PULUZ®, Guangdong, China). High resolution JPEG images were imported to ImageJ (NIH) and converted to 8-bit greyscale. Binary images that showed biofilm pellicles as white areas on a black background were obtained via default algorithm histogram thresholding (black value 0, white value 255) and the number of white pixels was recorded in an oval region of interest that incorporated the entire biofilm pellicle. Triplicate technical replicates were measured and the mean used for statistical analysis. Four independent reviewers (Kayla Hackler, Jacq Field, Hannah Elshafie, Sidney Schumaker)

were trained to review pellicle area using Image J. Each reviewer assessed images from all horses within a randomly assigned bacterial strain and time point. Then, reviewers were randomly assigned to a different bacterial strain and time point for review so that each set of images was reviewed by two independent reviewers. Random allocation by time point and bacteria grouping was chosen as not direct comparisons between time point or bacteria were performed in final analysis. Pixel size was calibrated to reference lines of known distance in mm and final pellicle area in mm^2 was calculated prior to statistical analysis.

Biomass quantification: Following photography, total bacterial well contents were centrifuged at 1,400 x g, 10 minutes, RT, rinsed twice with distilled water and fixed with reagent grade methanol [73]. Well contents were stained with 0.2% aqueous crystal violet for 15 minutes at RT, excess stain aspirated, and unbound stain removed by rinsing with distilled water. Biomass-bound stain was eluted with 70% ethanol, 15 minutes at RT, then 100 µL/well of eluted stain were transferred to a 96-well microtiter plate and optical density at 595 nm quantified on a spectrophotometric plate reader (BioTek® Synergy H1 ™, Agilent Technologies, Inc, Santa Clara, CA) with commercial software (BioTek® Gen 5™) [48, 50, 73].

Live bacterial quantification: Total biofilm well contents were digested *in situ* with 20 µg/mL Proteinase K (Life Technologies, Inc, Carlsbad, CA) for 30 minutes at 37ºC on a rotary shaker at 150 rpm (Fisherbrand™ Incubating Mini-Shaker, Fisher Scientific™) [12]. Well digests were transferred to a sterile microfuge tube and wells were rinsed 3 times with sterile phosphate-buffered saline (PBS) to collect residual bacteria. Digests were serially diluted 10-fold in PBS, plated in triplicate on TSA, and incubated overnight at 37ºC. Live colonies were counted,

divided by the dilution factor, and the quotient multiplied by well volume to calculate live bacteria/well system (CFU/biofilm):

$$\text{CFU/biofilm} = (\text{Live colonies} / \text{dilution factor}) \times \text{well volume in mL}$$

Statistical analysis: Sample size was calculated using commercial software (G*Power, University of Düsseldorf, Netherlands) based on *in vitro* data on mean AMP synthesis and bacterial killing by equine bone marrow-derived MSC [48, 49] and using an effect size of 0.5, an alpha level of 0.05, and a power of 0.8. For pellicle area quantification, correlation between pixel measurements of the two independent investigators was assessed using Pearson's r coefficient. Data distribution was assessed using normal probability plots, summarized as mean $\pm$ standard deviation if normally distributed, and effects of treatment on outcomes were analyzed using a mixed model analysis of variance. CFU results were $\log_{10}$-transformed to normalize distribution prior to analysis. The generalized linear model specified treatment, time, and the interaction between treatment and time as fixed effects. Horse identification was specified as a random effect. The interaction between treatment and time was further analyzed to compare the treatment groups at each time point. Where appropriate, p-values were adjusted for multiple comparisons using Tukey's procedure. Statistical significance was set to $p < 0.05$. All analyses were performed using SAS version 9.4 (Cary, NC).

RESULTS

MSC reduced biofilm organization and pellicle area: MSC maintained 75% of baseline viability on Trypan Blue staining following co-culture with *S. aureus* biofilms and 70% following co-culture with *E. coli* biofilms for 48 hours. Established biofilms of each bacterial species that were co-cultured with MSC were visibly less organized and had smaller, less-defined central pellicles compared to untreated biofilms at both time points (Fig 4.2A and B). *E. coli* biofilms were less organized, with more expansive pellicles, than *S. aureus* biofilms across treatment groups. When placed under mechanical stress on the same rotary shaker used for enzymatic biofilm digestion at 200 rpm, MSC-treated biofilms subjectively dispersed more readily than untreated or amikacin-treated biofilms (Supplemental videos 4.1 and 4.2).

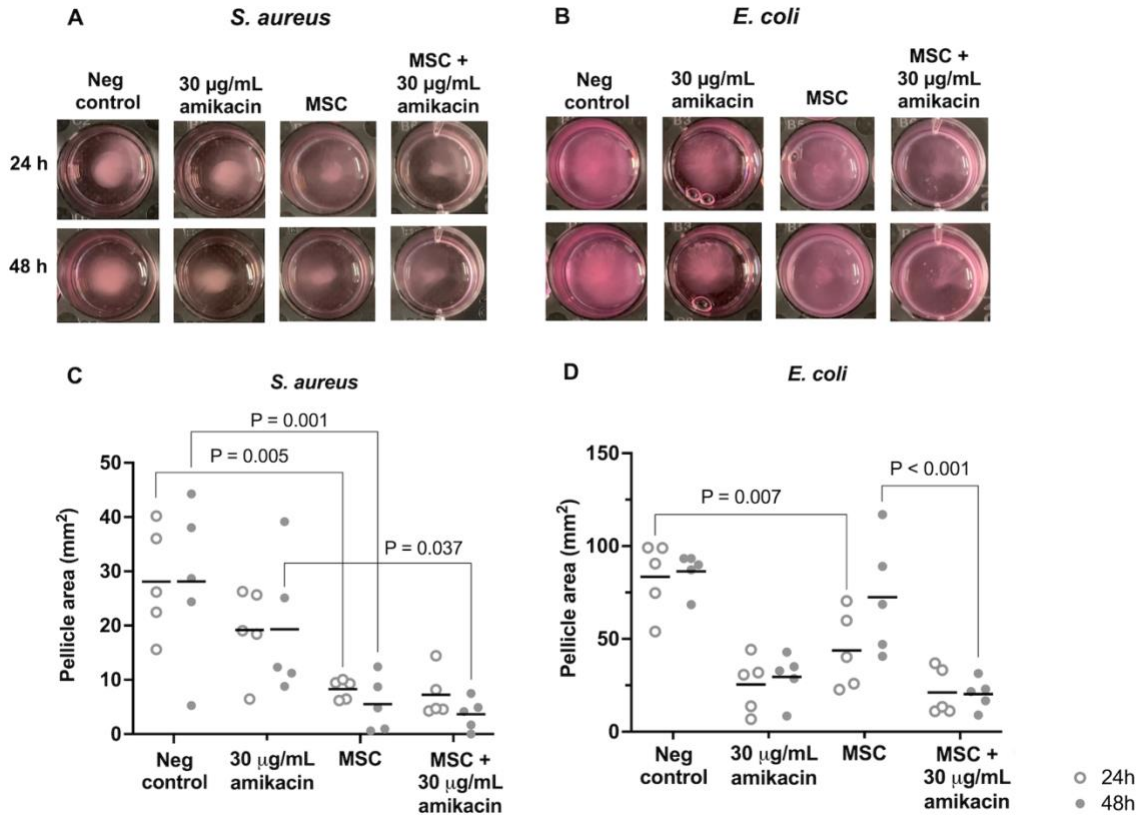

Figure 4.2: Effect of MSC ± amikacin on biofilm pellicle size. *In situ* digital images of biofilms from one representative horse for *S. aureus* (A) and *E. coli* (B) following 24 or 48 hours of treatment. The negative control was untreated biofilms. (C, D) Dot-plots of normalized biofilm pellicle area (mm^2) from n = 5 horses. Horizontal black lines indicate mean pellicle size across horses, and circles indicate mean pellicle size for each individual horse at 24 (open circles) or 48 hours (closed circles). Brackets and p-values indicate groups significantly different ($p < 0.05$) from each other.

Supplemental Videos S4.1 and S4.2: *S. aureus* (S4.1) and *E. coli* (S4.2) biofilms on a rotary shaker (Fisherbrand™ Incubating Mini-Shaker, Fisher Scientific) at 200 rpm after 48 hours of treatment demonstrate subjective biofilm dispersion under mechanical stress. Treatment groups from left-to-right are untreated biofilms (negative control) and biofilms treated with 30 ug/mL amikacin sulfate, MSC, or MSC + 30 ug/mL amikacin sulfate. Similar relative biofilm dispersion between treatment groups was seen after 24 hours of co-culture.

Inter-observer agreement of biofilm pellicle area using pixel thresholding was high, with a Pearson's r coefficient of 0.911 (95% CI 0.865-0.940, $p < 0.001$). *S. aureus* biofilm pellicle area was significantly affected by treatment ($F = 12.42$, $df = 3$, $p < 0.001$) only, whereas *E. coli* biofilm pellicle area was affected by treatment ($F = 16.46$, $df = 3$, $p < 0.001$) and time ($F = 7.81$, $df = 3$, $p = 0.013$), with a significant interaction between treatment and time ($F = 4.65$, $df = 1$, $p = 0.016$). MSC reduced *S. aureus* pellicle area compared to untreated biofilms at 24 hours ($p = 0.005$) and 48 hours ($p = 0.001$), while MSC + amikacin reduced *S. aureus* pellicle area compared to amikacin alone at 48 hours ($p = 0.037$) with no difference at 24 hours ($p = 0.154$) or compared to MSC alone at 48 hours ($p = 0.998$) (Fig 4.2C). MSC reduced *E. coli* pellicle area compared to untreated biofilms at 24 hours ($p = 0.007$) with no changes at 48 hours ($p = 0.606$) (Fig 4.2D). MSC + amikacin reduced *E. coli* pellicle area compared to MSC alone ($p < 0.001$) at 48 hours, with no changes at 24 hours ($p = 0.202$) or compared to amikacin at either timepoint ($p = 0.980$ at 24 hours; $p = 0.843$ at 48 hours).

Co-culture with MSC reduced total biomass of S. aureus biofilms: Co-culture with MSC reduced *S. aureus* biomass compared to untreated biofilms at 24 and 48 hours ($p < 0.001$ for both) (Fig

4.3A). MSC with amikacin reduced *S. aureus* biomass compared to amikacin alone at 24 hours (p = 0.014) and at 48 hours (p = 0.053). MSC + amikacin reduced biomass of *E. coli* biofilms compared to untreated controls (p = 0.032 at 24 hours; p = 0.023 at 48 hours) (Fig 4.3B). No other differences were detected between treatment groups.

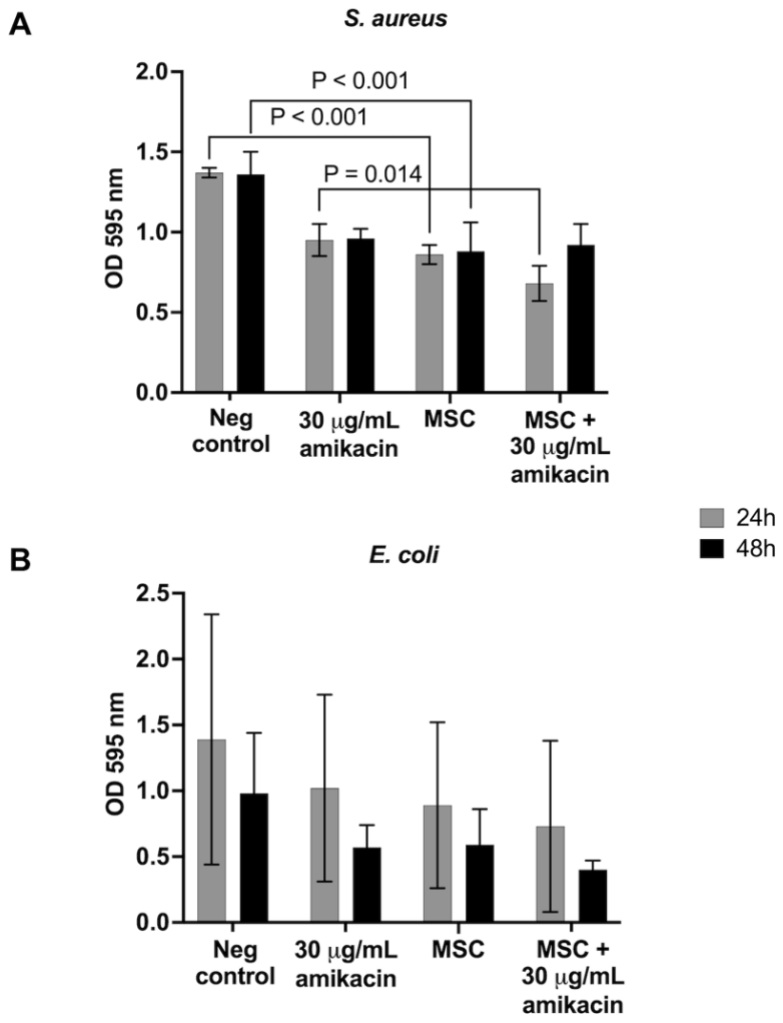

Figure 4.3: Biofilm biomass quantified by crystal violet staining for *S. aureus* and *E. coli.* Bars represent mean ± standard deviation from biofilms co-cultured with MSC from *n* = 5 horses at 24 (grey) or 48 hours (black). The negative control was untreated biofilms. Brackets and p-values indicate groups significantly different from each other.

Co-culture with MSC reduced S. aureus CFU at 48 hours, with no improvement in bacterial killing of either species by MSC + amikacin versus amikacin alone: CFU/biofilm of MSC-treated S. aureus biofilms was reduced by 0.5 $\log_{10}$-fold compared to untreated biofilms at 48 hours ($p = 0.036$), with no difference at 24 hours ($p = 0.997$) (Fig 4.4A). MSC + amikacin reduced CFU of *S. aureus* biofilms compared to MSC-treated biofilms by 2 $\log_{10}$-fold at both time points ($p < 0.001$). As for *S. aureus*, MSC + amikacin reduced *E. coli* CFU by 2 $\log_{10}$-fold compared to MSC alone at both timepoints ($p < 0.001$) (Fig 4.4B). However, reductions in CFU of both bacteria by MSC + amikacin were equivalent to reductions achieved by amikacin alone. Additionally, MSC + amikacin treatment reduced CFU of both bacteria by 2 $\log_{10}$-fold at both timepoints compared to untreated controls ($p < 0.001$). No other differences were detected between treatment groups.

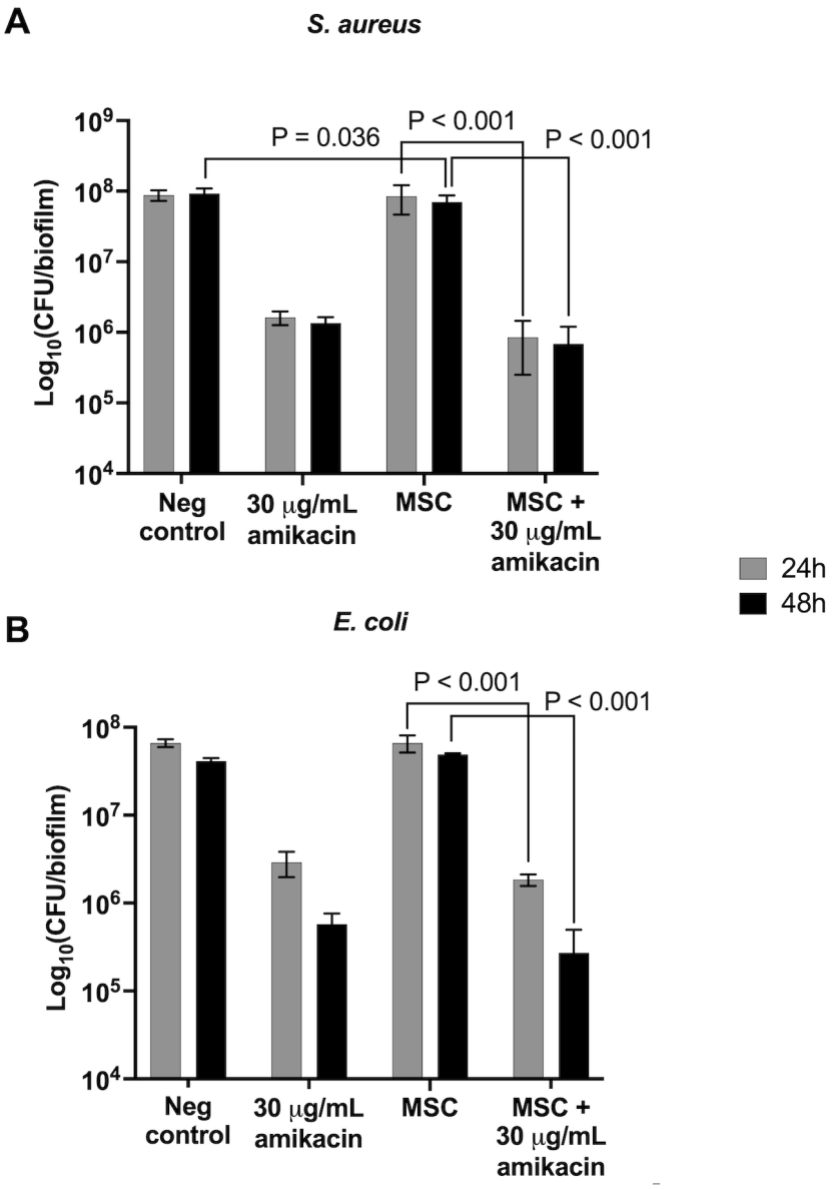

Figure 4.4: Live bacteria quantified by total colony forming units (CFU) per biofilm for *S. aureus* and *E. coli.* Bars represent mean ± standard deviation from biofilms co-cultured with MSC from *n* = 5 horses at 24 or 48 hours. The negative control was untreated biofilms. Brackets indicate groups significantly different from each other.

DISCUSSION

Our study demonstrates that equine bone marrow-derived MSC reduce biomass and pellicle area of established *S. aureus* biofilms, but that MSC + amikacin did not reduce biomass further compared to MSC alone. However, MSC + amikacin was effective at reducing *S. aureus* biofilm biomass compared to amikacin alone at 24 hours and at reducing pellicle area compared to amikacin alone at 48 hours. Taken together, our results are supportive of a potential synergy between amikacin and MSC in combatting *S. aureus* biofilms. In contrast, while *E. coli* biofilm pellicle area and visible biofilm organization were reduced by MSC at 24 hours and by MSC + amikacin at 48 hours compared to no treatment, neither MSC nor MSC + amikacin decreased *E. coli* biofilm biomass. With the exception of *S. aureus* following 48 hours of MSC treatment, MSC did not otherwise reduce live bacterial counts in our biofilms. Furthermore, MSC + amikacin reduced live counts of both bacteria equivalently to amikacin alone.

Co-culture of planktonic bacteria with either MSC or MSC conditioned medium have demonstrated that the MSC response is paracrine in nature [48-50]. Our transwell system enabled MSC-mediated antibacterial response through real-time paracrine feedback without allowing physical contact with the bacteria. This design isolated the MSC physically, but enabled their real-time response to the bacteria. MSC express pattern recognition receptors (PRR) [51, 74-76] that can be stimulated by bacterial pathogen-associated molecular patterns or synthetic ligands to enhance planktonic bacterial killing via antimicrobial peptide synthesis [47, 49, 51]. Although our co-culture design allowed for stimulation of MSC PRR stimulation by bacterial products, it is unclear why a more uniform antibiofilm MSC response was not observed. The *S. aureus* and

E. coli strains used in our study were selected because of their ability to form robust biofilms, their clinical relevance [77], and their susceptibility to amikacin sulfate [68]. However, evaluation of biofilm-forming strains that generate a strong inflammatory response, such as methicillin-resistant *USA300* [25, 50, 52], may stimulate a greater anti-biofilm MSC response than that seen in our study. Pre-treatment of MSC to increase their immunomodulatory properties prior to bacterial co-culture may also improve biofilm reduction. Possible candidates include PRR agonists [49, 51, 78], hypoxic exposure [78], or three-dimensional culture [79, 80]. Inclusion of immune cells in this model may have improved biofilm reduction and more closely captured the MSC antibiofilm potential that would occur *in vivo* [51, 54]. MSC may indirectly exert an antimicrobial effects through enhancement of the antibacterial responses of immune cells, such as macrophages, present in the infected tissues [54, 81].

Our study demonstrated a difference in the ability of MSC to combat established biofilms of *S. aureus* versus *E. coli*. These findings are consistent with greater reduction of live bacterial counts for Gram-positive versus Gram-negative organisms by equine adipose-derived MSC [82] and platelet lysate [34]. Greater variation in *E. coli* untreated (negative control) and amikacin-treated biofilms may have limited our ability to detect differences in biomass reduction between groups. Important differences in biofilm matrix composition between *S. aureus* and *E. coli* may also confer varying resistance to MSC-mediated disruption via varying resistance to MSC-secreted factors and/or a variable MSC-mediated PRR activation [51, 83, 84]. Such differences include those in the specific matrix carbohydrates [11, 85] and adhesion proteins [8, 10, 86] present in *S. aureus* versus *E. coli* biofilms. Donor-dependent variation in MSC anti-biofilm activities was observed with both bacterial strains but was more pronounced for *E. coli* and may have impacted

our ability to detect differences between treatment groups. It is widely known that MSC from different horses vary in their immunomodulatory properties [79, 80, 87], proliferation [88], differentiation [88], and cell yield on isolation from tissues [89]. The potential for inter-donor variation in overall MSC anti-biofilm function and in the ability of *E. coli* versus *S. aureus* to stimulate anti-biofilm responses requires further investigation. Donor screening [90, 91] or pooling of MSC-derived active factors from multiple horses [34, 35] may be required to minimize the impact of inter-donor variation.

The primary mechanism of action of MSC against established *S. aureus* and *E. coli* biofilms is likely dispersion of the biofilm matrix and liberation of biofilm-bound live bacteria based on observed reductions in *S. aureus* and *E. coli* biofilm pellicle size and *S. aureus* biofilm matrix components. MSC kill planktonic bacteria and prevent biofilm formation by disrupting bacterial cell membranes through secretion of amphipathic antimicrobial peptides [47, 48, 51] and cysteine proteases [50]. MSC antimicrobial proteins may disrupt the matrix of established biofilms in a similar fashion, causing reductions in biomass and pellicle area.

With the exception of *S. aureus* following a 48 hour co-culture, MSC did not reduce live bacteria of our biofilms compared to untreated biofilms, which did not correlate with biomass and pellicle reductions. This finding may be related to the measurement of CFU in the entire well (biofilm + medium) to quantify bacteria. MSC may have reduced CFU immediately following biofilm dispersion. However, ongoing multiplication of dispersed bacteria prior to quantification may have masked these immediate reductions, as planktonic bacteria divide more rapidly than biofilm-bound bacteria [16]. Three-dimensional imaging techniques, including confocal

microscopy [12] or scanning electron microscopy [26], may have captured MSC-specific biofilm reductions not seen with our techniques. While MSC-treated biofilms were subjectively easier to disperse under mechanical stress in our study, biomechanical testing would quantify changes in biofilm matrix physical properties, such as stiffness [14], following MSC treatment. The potential for MSC to disperse biofilm matrix may prove useful in a therapeutic context by increasing antimicrobial and immune cell access to live bacteria in biofilms, improving infection clearance. Biofilm matrix dispersion by MSC may also facilitate physical removal of biofilm intraoperatively by pulsatile lavage or ultrasonic debridement [92]. Staged treatment of biofilms with MSC to initially disperse the matrix, followed by surgical debridement to remove residual matrix and antimicrobials to kill liberated live bacteria, may be a useful tactic to improve the therapeutic utility of biofilm matrix dispersal.

Use of established biofilms with a mature matrix likely limited the ability of MSC and/or amikacin to penetrate the biofilm matrix compared to planktonic bacteria. Our MSC: bacteria ratio or the physiologic dose of amikacin sulfate chosen may have resulted in lower than expected live bacterial reductions [21, 61]. Ratios of MSC to live bacteria used in this study were similar to those reported for a 6-hour co-incubation of human MSC with planktonic *S. aureus* or *E. coli* in a transwell plate system [47] and were chosen to maximize the MSC dose while maintaining MSC survival during co-culture. The concentration of amikacin used in our study reflects that achieved in equine synovial fluid *in vivo* following regional administration [21, 61, 69], and was selected to be non-cytotoxic to MSC [93]. Our amikacin concentration was higher than the reported MIC of amikacin against planktonic bacteria for our *S. aureus* and *E. coli* strains ($\leq$ 4 µg/mL) but may have been insufficient in the face of established biofilms, as the

presence of a biofilm matrix increases the MIC of antimicrobials 100-2,000 times [12, 15] compared to planktonic bacteria. Furthermore, adaptive resistance to aminoglycoside antimicrobials *in vitro* can develop within 24 hours of constant antimicrobial exposure [94, 95] and could have limited live bacterial count reductions by MSC and our ability to detect synergy between MSC and amikacin [54-56]. In a clinical setting, patients often present with biofilm infections that may have enhanced resistance to MSC, including chronic infections containing mature biofilms [6, 96], following prolonged antimicrobial pre-treatment in which adaptive resistance develops [27], or polymicrobial infections [22, 28, 97]. The ability of MSC to disrupt biofilms with varying degrees of potential treatment resistance thereby requires rigorous investigation.

CONCLUSIONS

Our study documents MSC-mediated reductions in biomass for *S. aureus* biofilms and pellicle area for *S. aureus* and *E. coli* biofilms. The transwell co-culture model facilitated MSC-biofilm interactions and allowed evaluation of reduction of established biofilms that may be encountered in clinical orthopedic infections. Differing biomass reduction between bacterial species may be attributed to variations in biomass of untreated and amikacin-treated *E. coli* biofilms that limited our ability to detect changes with MSC treatment. Differences in resistance of *E. coli* biofilm matrix to MSC-mediated disruption, or in stimulation of an MSC antibiofilm response, compared to *S. aureus*, and/or inter-donor variability, may also have limited detection of biomass reduction. Combining amikacin sulfate with MSC reduces *S. aureus* biofilm biomass and pellicle area of both bacterial species compared to either treatment alone and warrants further

investigation. The lower-than-expected live bacterial reduction by MSC does not correlate with biofilm matrix reduction and may reflect limitations in quantification techniques or lack of pre-stimulation of MSC PRR prior to co-culture. Our results support further investigation of the mechanisms by which MSC disrupt biofilm matrix as well as differences in response to different bacterial strains or polymicrobial biofilms.

Acknowledgements

The authors acknowledge the Morris Animal Foundation Large Animal Training Fellowship, the Interdisciplinary Graduate Education Program in Regenerative Medicine (Virginia Tech), the Office of Research and Graduate Studies, and the Equine Research Competition (Virginia-Maryland College of Veterinary Medicine) for funding this research. The authors acknowledge Dr. Bruno Menarim (Gluck Equine Research Center, University of Kentucky) and Dr. James Blake Everett (Equine Surgical Center, Murfreesboro, Tennessee) for their efforts in isolating and cryopreserving the equine bone marrow mononuclear cells used for MSC isolation. The authors would also like to thank Dr. Tessa LeCuyer, Dr. Jessica Gilbertie, the technical specialists at the Center for One Health Research (Nancy Tenpenny) and the Collaborative Multidisciplinary Research Laboratory at the Virginia-Maryland College of Veterinary Medicine (Michelle Todd), members of the Caswell Laboratory (Tristan Stoyanof, Dr. Mitchell Caudill), and numerous undergraduate students (Elanagh Smith, Olivia Brown, Breanna Murray, Emma Stewart, Kayla Hackler, Jacq Field, Hannah Elshafie, Sidney Schumaker, Jane Perkins), for their invaluable assistance and support.

BIBLIOGRAPHY

1. Kurtz SM, Lau E, Watson H, Schmier JK, Parvizi J. Economic burden of periprosthetic joint infection in the United States. J Arthroplasty. 2012;27:61-5 e1.
2. Pollmann CT, Dahl FA, Rotterud JHM, Gjertsen JE, Aroen A. Surgical site infection after hip fracture - mortality and risk factors: an observational cohort study of 1,709 patients. Acta Orthop. 2020;91:347-52.
3. Thakore RV, Greenberg SE, Shi H, Foxx AM, Francois EL, Prablek MA, et al. Surgical site infection in orthopedic trauma: A case-control study evaluating risk factors and cost. J Clin Orthop Trauma. 2015;6:220-6.
4. Ahern BJ, Richardson DW, Boston RC, Schaer TP. Orthopedic infections in equine long bone fractures and arthrodeses treated by internal fixation: 192 cases (1990-2006). Vet Surg. 2010;39:588-93.
5. Curtiss AL, Stefanovski D, Richardson DW. Surgical site infection associated with equine orthopedic internal fixation: 155 cases (2008-2016). Vet Surg. 2019;48:685-93.
6. Goodrich LR. Osteomyelitis in horses. Vet Clin North Am Equine Pract. 2006;22:389-417, viii-ix.
7. Crawford EC, Singh A, Gibson TW, Scott Weese J. Biofilm-Associated Gene Expression in *Staphylococcus pseudintermedius* on a Variety of Implant Materials. Vet Surg. 2016;45:499-506.
8. Patti JM, Allen BL, McGavin MJ, Hook M. MSCRAMM -Mediated Adherence of Microorganisms to Host Tissues. Annu Rev Microbiol. 1994;48:585-617.

9. Schwartz K, Syed AK, Stephenson RE, Rickard AH, Boles BR. Functional amyloids composed of phenol soluble modulins stabilize *Staphylococcus aureus* biofilms. PLoS Pathog. 2012;8:e1002744.
10. Niba ET, Naka Y, Nagase M, Mori H, Kitakawa M. A genome-wide approach to identify the genes involved in biofilm formation in *E. coli*. DNA Res. 2007;14:237-46.
11. Nguyen MH, Ojima Y, Sakka M, Sakka K, Taya M. Probing of exopolysaccharides with green fluorescence protein-labeled carbohydrate-binding module in *Escherichia coli* biofilms and flocs induced by bcsB overexpression. J Biosci Bioeng. 2014;118:400-5.
12. Gilbertie JM, Schnabel LV, Hickok NJ, Jacob ME, Conlon BP, Shapiro IM, et al. Equine or porcine synovial fluid as a novel *ex vivo* model for the study of bacterial free-floating biofilms that form in human joint infections. PLoS One. 2019;14:e0221012.
13. Zhang XY, Sun K, Abulimiti A, Xu PP, Li ZY. Microfluidic System for Observation of Bacterial Culture and Effects on Biofilm Formation at Microscale. Micromachines (Basel). 2019;10.
14. Buzzo JR, Devaraj A, Gloag ES, Jurcisek JA, Robledo-Avila F, Kesler T, et al. Z-form extracellular DNA is a structural component of the bacterial biofilm matrix. Cell. 2021;184:5740-58 e17.
15. Walker M, Singh A, Nazarali A, Gibson TW, Rousseau J, Weese JS. Evaluation of the Impact of Methicillin-Resistant *Staphylococcus pseudintermedius* Biofilm Formation on Antimicrobial Susceptibility. Vet Surg. 2016;45:968-71.
16. Bjarnsholt T, Alhede M, Alhede M, Eickhardt-Sorensen SR, Moser C, Kuhl M, et al. The *in vivo* biofilm. Trends Microbiol. 2013;21:466-74.

17. Mandell JB, Orr S, Koch J, Nourie B, Ma D, Bonar DD, et al. Large variations in clinical antibiotic activity against *Staphylococcus aureus* biofilms of periprosthetic joint infection isolates. J Orthop Res. 2019;37:1604-9.
18. Leid JG, Shirtliff ME, Costerton JW, Stoodley P. Human leukocytes adhere to, penetrate, and respond to *Staphylococcus aureus* biofilms. Infect Immun. 2002;70:6339-45.
19. Martin-Rodriguez AJ, Rhen M, Melican K, Richter-Dahlfors A. Nitrate Metabolism Modulates Biosynthesis of Biofilm Components in Uropathogenic *Escherichia coli* and Acts as a Fitness Factor During Experimental Urinary Tract Infection. Front Microbiol. 2020;11:26.
20. Henry-Stanley MJ, Hess DJ, Wells CL. Aminoglycoside inhibition of *Staphylococcus aureus* biofilm formation is nutrient dependent. J Med Microbiol. 2014;63:861-9.
21. Harvey A, Kilcoyne I, Byrne BA, Nieto J. Effect of Dose on Intra-Articular Amikacin Sulfate Concentrations Following Intravenous Regional Limb Perfusion in Horses. Vet Surg. 2016;45:1077-82.
22. Schneider RK, Bramlage LR, Moore RN, Mecklenburg LM, Kohn KW, Gabel AA. A retrospective of 192 horses affected with septic arthritis/tenosynovitis. Equine Vet J. 1992;24:436-42.
23. Hepworth-Warren KL, Wong DM, Fulkerson CV, Wang C, Sun Y. Bacterial isolates, antimicrobial susceptibility patterns, and factors associated with infection and outcome in foals with septic arthritis: 83 cases (1998–2013). J Am Vet Med Assoc. 2015;246:785-93.
24. Rinnovati R, Butina BB, Lanci A, Mariella J. Diagnosis, Treatment, Surgical Management, and Outcome of Septic Arthritis of Tarsocrural Joint in 16 Foals. J Equine Vet Sci. 2018;67:128-32.

25. Tomizawa T, Ishikawa M, Bello-Irizarry SN, de Mesy Bentley KL, Ito H, Kates SL, et al. Biofilm Producing *Staphylococcus epidermidis* (RP62A Strain) Inhibits Osseous Integration Without Osteolysis and Histopathology in a Murine Septic Implant Model. J Orthop Res. 2020;38:852-60.
26. Nishitani K, Sutipornpalangkul W, de Mesy Bentley KL, Varrone JJ, Bello-Irizarry SN, Ito H, et al. Quantifying the natural history of biofilm formation *in vivo* during the establishment of chronic implant-associated *Staphylococcus aureus* osteomyelitis in mice to identify critical pathogen and host factors. J Orthop Res. 2015;33:1311-9.
27. Bertone AL. Update on infectious arthritis in horses. Equine Vet Educ. 1999;11:143-52.
28. Zmistowski B, Karam JA, Durinka JB, Casper DS, Parvizi J. Periprosthetic joint infection increases the risk of one-year mortality. J Bone Joint Surg Am. 2013;95:2177-84.
29. Osmon DR, Berbari EF, Berendt AR, Lew D, Zimmerli W, Steckelberg JM, et al. Diagnosis and management of prosthetic joint infection: clinical practice guidelines by the Infectious Diseases Society of America. Clin Infect Dis. 2013;56:e1-e25.
30. Shukla SK, Ward JP, Jacofsky MC, Sporer SM, Paprosky WG, Della Valle CJ. Perioperative testing for persistent sepsis following resection arthroplasty of the hip for periprosthetic infection. J Arthroplasty. 2010;25:87-91.
31. Teterycz D, Ferry T, Lew D, Stern R, Assal M, Hoffmeyer P, et al. Outcome of orthopedic implant infections due to different *Staphylococci*. Int J Infect Dis. 2010;14:e913-8.
32. Moormeier DE, Endres JL, Mann EE, Sadykov MR, Horswill AR, Rice KC, et al. Use of microfluidic technology to analyze gene expression during *Staphylococcus aureus* biofilm formation reveals distinct physiological niches. Appl Environ Microbiol. 2013;79:3413-24.

33. Gomez-Barrena E, Esteban J, Medel F, Molina-Manso D, Ortiz-Perez A, Cordero-Ampuero J, et al. Bacterial adherence to separated modular components in joint prosthesis: a clinical study. J Orthop Res. 2012;30:1634-9.

34. Gilbertie JM, Schaer TP, Schubert AG, Jacob ME, Menegatti S, Ashton Lavoie R, et al. Platelet-rich plasma lysate displays antibiofilm properties and restores antimicrobial activity against synovial fluid biofilms *in vitro*. J Orthop Res. 2020.

35. Gilbertie JM, Schaer TP, Engiles JB, Seiler GS, Deddens BL, Schubert AG, et al. A Platelet-Rich Plasma-Derived Biologic Clears *Staphylococcus aureus* Biofilms While Mitigating Cartilage Degeneration and Joint Inflammation in a Clinically Relevant Large Animal Infectious Arthritis Model. Front Cell Infect Microbiol. 2022;12:895022.

36. Pestrak MJ, Gupta TT, Dusane DH, Guzior DV, Staats A, Harro J, et al. Investigation of synovial fluid induced *Staphylococcus aureus* aggregate development and its impact on surface attachment and biofilm formation. PLoS One. 2020;15:e0231791.

37. Staats AB, Schwieters PW, Li AD, Sullivan A, Horswill AR, Stoodley P. Rapid Aggregation of *Staphylococcus aureus* in Synovial Fluid Is Influenced by Synovial Fluid Concentration, Viscosity, and Fluid Dynamics, with Evidence of Polymer Bridging. mBio. 2022;13:1-15.

38. Hall MS, Pollock PJ, Russell T. Surgical treatment of septic physitis in 17 foals. Aust Vet J. 2012;90:479-84.

39. Jacobs CC, Levine DG, Richardson DW. Use of locking compression plates in ulnar fractures of 18 horses. Vet Surg. 2017;46:242-8.

40. Bogers SH. Cell-Based Therapies for Joint Disease in Veterinary Medicine: What We Have Learned and What We Need to Know. Front Vet Sci. 2018;5:70.

41. Colbath AC, Dow SW, Phillips JN, McIlwraith CW, Goodrich LR. Autologous and Allogeneic Equine Mesenchymal Stem Cells Exhibit Equivalent Immunomodulatory Properties *In Vitro*. Stem Cells Dev. 2017;26:503-11.

42. Ranera B, Antczak D, Miller D, Doroshenkova T, Ryan A, McIlwraith CW, et al. Donor-derived equine mesenchymal stem cells suppress proliferation of mismatched lymphocytes. Equine Vet J. 2016;48:253-60.

43. Ferris DJ, Frisbie DD, Kisiday JD, McIlwraith CW, Hague BA, Major MD, et al. Clinical Outcome After Intra-Articular Administration of Bone Marrow Derived Mesenchymal Stem Cells in 33 Horses With Stifle Injury. Vet Surg 2014;43:255-65.

44. Frisbie DD, Kisiday JD, Kawcak CE, Werpy NM, McIlwraith CW. Evaluation of adipose-derived stromal vascular fraction or bone marrow-derived mesenchymal stem cells for treatment of osteoarthritis. J Orthop Res. 2009;27:1675-80.

45. McCoy AM, Smith RL, Herrera S, Kawcak CE, McIlwraith CW, Goodrich LR. Long-term outcome after stifle arthroscopy in 82 Western performance horses (2003-2010). Vet Surg. 2019;48:956-65.

46. Crovace A, Lacitignola L, Rossi G, Francioso E. Histological and immunohistochemical evaluation of autologous cultured bone marrow mesenchymal stem cells and bone marrow mononucleated cells in collagenase-induced tendinitis of equine superficial digital flexor tendon. Vet Med Int. 2010;2010:250978.

47. Krasnodembskaya A, Song Y, Fang X, Gupta N, Serikov V, Lee JW, et al. Antibacterial effect of human mesenchymal stem cells is mediated in part from secretion of the antimicrobial peptide LL-37. Stem Cells. 2010;28:2229-38.

48. Harman RM, Yang S, He MK, Van de Walle GR. Antimicrobial peptides secreted by equine mesenchymal stromal cells inhibit the growth of bacteria commonly found in skin wounds. Stem Cell Res Ther. 2017;8:157.

49. Cortes-Araya Y, Amilon K, Rink BE, Black G, Lisowski Z, Donadeu FX, et al. Comparison of Antibacterial and Immunological Properties of Mesenchymal Stem/Stromal Cells from Equine Bone Marrow, Endometrium, and Adipose Tissue. Stem Cells Dev. 2018;27:1518-25.

50. Marx C, Gardner S, Harman RM, Van de Walle GR. The mesenchymal stromal cell secretome impairs methicillin-resistant *Staphylococcus aureus* biofilms via cysteine protease activity in the equine model. Stem Cells Transl Med. 2020.

51. Pezzanite LM, Chow L, Johnson V, Griffenhagen GM, Goodrich L, Dow S. Toll-like receptor activation of equine mesenchymal stromal cells to enhance antibacterial activity and immunomodulatory cytokine secretion. Vet Surg. 2021;50:858-71.

52. Marx C, Gardner S, Harman RM, Wagner B, Van de Walle GR. Mesenchymal stromal cell-secreted CCL2 promotes antibacterial defense mechanisms through increased antimicrobial peptide expression in keratinocytes. Stem Cells Transl Med. 2021;10:1666-79.

53. Gupta N, Krasnodembskaya A, Kapetanaki M, Mouded M, Tan X, Serikov V, et al. Mesenchymal stem cells enhance survival and bacterial clearance in murine *Escherichia coli* pneumonia. Thorax. 2012;67:533-9.

54. Johnson V, Webb T, Norman A, Coy J, Kurihara J, Regan D, et al. Activated Mesenchymal Stem Cells Interact with Antibiotics and Host Innate Immune Responses to Control Chronic Bacterial Infections. Sci Rep. 2017;7:9575.

55. Yamamuro Y, Kabata T, Nojima T, Hayashi K, Tokoro M, Kajino Y, et al. Combined adipose-derived mesenchymal stem cell and antibiotic therapy can effectively treat periprosthetic joint infection in rats. Sci Rep. 2023;13:3949.

56. Alcayaga-Miranda F, Cuenca J, Martin A, Contreras L, Figueroa FE, Khoury M. Combination therapy of menstrual derived mesenchymal stem cells and antibiotics ameliorates survival in sepsis. Stem Cell Res Ther. 2015;6:199.

57. Bidossi A, Bottagisio M, Savadori P, De Vecchi E. Identification and Characterization of Planktonic Biofilm-Like Aggregates in Infected Synovial Fluids From Joint Infections. Front Microbiol. 2020;11:1368.

58. Alhede M, Alhede M, Qvortrup K, Kragh KN, Jensen PO, Stewart PS, et al. The origin of extracellular DNA in bacterial biofilm infections *in vivo*. Pathog Dis. 2020;78.

59. Taintor JS, Schumaker J, DeGraves F. Comparison of amikacin concentrations in normal and inflamed joints of horses following intra-articular administration. Equine Vet J. 2006;38:189-91.

60. Sedrish SA, Moore RM, Barker SA. Pharmacokinetics of single dose intra-articular administration of amikacin in the radiocarpal joints of normal horses. Am College of Vet Surgeons Annual Summit. Chicago, Illinois, USA. 1994. p. 437.

61. Oreff GL, Dahan R, Tatz AJ, Raz T, Britzi M, Kelmer G. The Effect of Perfusate Volume on Amikacin Concentration in the Metacarpophalangeal Joint Following Cephalic Regional Limb Perfusion in Standing Horses. Vet Surg. 2016;45:625-30.

62. Côrrea F, Borlone C, Wittwer F, Bustamante H, Muller A, Ramirez A, et al. How to obtain and isolate equine sternal bone marrow mononuclear cells with limited resources. Arch Med Vet. 2014;46:471-6.

63. Menarim BC, Gillis KH, Oliver A, Mason C, Werre SR, Luo X, et al. Inflamed synovial fluid induces a homeostatic response in bone marrow mononuclear cells in vitro: Implications for joint therapy. FASEB J. 2020;34:4430-44.

64. Everett J. Bone marrow mononuclear cell therapy for equine joint disease. Proceedings, 66th Annual Convention, Am Assoc Equine Pract. Virtual. 2020. p. 226-7.

65. Fortier LN, Nixon AJ, Williams J, Cable CS. Isolation and chondrocytic differentiation of equine bone marrow-derived mesenchymal stem cells. Am J Vet Res. 1998;59:1182-7.

66. Bourzac C, Smith LC, Vincent P, Beauchamp G, Lavoie JP, Laverty S. Isolation of equine bone marrow-derived mesenchymal stem cells: a comparison between three protocols. Equine Vet J. 2010;42:519-27.

67. Zahedi M, Parham A, Dehghani H, Kazemi Mehrjerdi H. Equine bone marrow-derived mesenchymal stem cells: optimization of cell density in primary culture. Stem Cell Investig. 2018;5:31.

68. Lewis JS, Weinstein MP, Bobenchik AM, Campeau S, Cullen SK, Dingel T, Galas MF, Humphries RM. CLSI M100-ED33: 2023 Performance Standards for Antimicrobial Susceptibility Testing, 33rd Ed. CLSI. 2023.

69. Moser DK, Schoonover MJ, Holbrook TC, Payton ME. Effect of Regional Intravenous Limb Perfusate Volume on Synovial Fluid Concentration of Amikacin and Local Venous Blood Pressure in the Horse. Vet Surg. 2016;45:851-8.

70. Diaz De Rienzo MA, Stevenson P, Marchant R, Banat IM. Antibacterial properties of biosurfactants against selected Gram-positive and -negative bacteria. FEMS Microbiol Lett. 2016;363:fnv224.

71. Ueda Y, Mashima K, Miyazaki M, Hara S, Takata T, Kamimura H, et al. Inhibitory effects of polysorbate 80 on MRSA biofilm formed on different substrates including dermal tissue. Sci Rep. 2019;9:3128.

72. Li L, Molin S, Yang L, Ndoni S. Sodium Dodecyl Sulfate (SDS)-Loaded Nanoporous Polymer as Anti-Biofilm Surface Coating Material. Int J Mol Sci. 2013;14:3050-64.

73. Merritt JH, Kadouri DE, O'Toole GA. Growing and analyzing static biofilms. Curr Protoc Microbiol. 2005;Chapter 1:Unit 1B.

74. Gupta N, Sinha R, Krasnodembskaya A, Xu X, Nizet V, Matthay MA, et al. The TLR4-PAR1 Axis Regulates Bone Marrow Mesenchymal Stromal Cell Survival and Therapeutic Capacity in Experimental Bacterial Pneumonia. Stem Cells. 2018;36:796-806.

75. Kim SH, Das A, Chai JC, Binas B, Choi MR, Park KS, et al. Transcriptome sequencing wide functional analysis of human mesenchymal stem cells in response to TLR4 ligand. Sci Rep. 2016;6:30311.

76. Cassatella MA, Mosna F, Micheletti A, Lisi V, Tamassia N, Cont C, et al. Toll-like receptor-3-activated human mesenchymal stromal cells significantly prolong the survival and function of neutrophils. Stem Cells. 2011;29:1001-11.

77. *Staphylococcus aureus* subsp. aureus Rosenbach (ATCC® 29213™). American Type Culture Collection; 2020.

78. Crisostomo PR, Wang Y, Markel TA, Wang M, Lahm T, Meldrum DR. Human mesenchymal stem cells stimulated by TNF-alpha, LPS, or hypoxia produce growth factors by an NF kappa B- but not JNK-dependent mechanism. Am J Physiol Cell Physiol. 2008;294:C675-82.

79. Bogers SH, Barrett JG. Three-Dimensional Culture of Equine Bone Marrow-Derived Mesenchymal Stem Cells Enhances Anti-Inflammatory Properties in a Donor-Dependent Manner. Stem Cells Dev. 2022;31:777-86.

80. Park MJ, Lee J, Byeon JS, Jeong DU, Gu NY, Cho IS, et al. Effects of three-dimensional spheroid culture on equine mesenchymal stem cell plasticity. Vet Res Commun. 2018;42:171-81.

81. Jackson MV, Morrison TJ, Doherty DF, McAuley DF, Matthay MA, Kissenpfennig A, et al. Mitochondrial Transfer via Tunneling Nanotubes is an Important Mechanism by Which Mesenchymal Stem Cells Enhance Macrophage Phagocytosis in the *In Vitro* and *In Vivo* Models of ARDS. Stem Cells. 2016;34:2210-23.

82. Avellar HK, Lutter JD, Ganta CK, Beard W, Smith JR, Jonnalagadda N, et al. *In vitro* antimicrobial activity of equine platelet lysate and mesenchymal stromal cells against common clinical pathogens. Can J Vet Res. 2022;86:59-64.

83. Rashedi I, Gomez-Aristizabal A, Wang XH, Viswanathan S, Keating A. TLR3 or TLR4 Activation Enhances Mesenchymal Stromal Cell-Mediated Treg Induction via Notch Signaling. Stem Cells. 2017;35:265-75.

84. Sung DK, Chang YS, Sung SI, Yoo HS, Ahn SY, Park WS. Antibacterial effect of mesenchymal stem cells against *Escherichia coli* is mediated by secretion of beta-defensin-2 via toll-like receptor 4 signalling. Cell Microbiol. 2016;18:424-36.

85. Schwartbeck B, Birtel J, Treffon J, Langhanki L, Mellmann A, Kale D, et al. Dynamic *in vivo* mutations within the *ica* operon during persistence of *Staphylococcus aureus* in the airways of cystic fibrosis patients. PLoS Pathog. 2016;12:e1006024.

86. Buck LD, Paladino MM, Nagashima K, Brezel ER, Holtzman JS, Urso SJ, et al. Temperature-Dependent Influence of FliA Overexpression on PHL628 *E. coli* Biofilm Growth and Composition. Front Cell Infect Microbiol. 2021;11.

87. Barrachina L, Remacha AR, Romero A, Vazquez FJ, Albareda J, Prades M, et al. Priming Equine Bone Marrow-Derived Mesenchymal Stem Cells with Proinflammatory Cytokines: Implications in Immunomodulation-Immunogenicity Balance, Cell Viability, and Differentiation Potential. Stem Cells Dev. 2017;26:15-24.

88. Carter-Arnold JL, Neilsen NL, Amelse LL, Odoi A, Dhar MS. *In vitro* analysis of equine, bone marrow-derived mesenchymal stem cells demonstrates differences within age- and gender-matched horses. Equine Vet J. 2014;46:589-95.

89. Colleoni S, Bottani E, Tessaro I, Mari G, Merlo B, Romagnoli N, et al. Isolation, growth and differentiation of equine mesenchymal stem cells: effect of donor, source, amount of tissue and supplementation with basic fibroblast growth factor. Vet Res Commun. 2009;33:811-21.

90. Kim G, Jeon JH, Park K, Kim SW, Kim DH, Lee S. High throughput screening of mesenchymal stem cell lines using deep learning. Sci Rep. 2022;12:17507.

91. Huang AH, Motlekar NA, Stein A, Diamond SL, Shore EM, Mauck RL. High-throughput screening for modulators of mesenchymal stem cell chondrogenesis. Ann Biomed Eng. 2008;36:1909-21.

92. Russo A, Gatti A, Felici S, Gambardella A, Fini M, Neri MP, et al. Piezoelectric ultrasonic debridement as new tool for biofilm removal from orthopedic implants: A study *in vitro*. J Orthop Res. 2023.

93. Bohannon LK, Owens SD, Walker NJ, Carrade DD, Galuppo LD, Borjesson DL. The effects of therapeutic concentrations of gentamicin, amikacin and hyaluronic acid on cultured bone marrow-derived equine mesenchymal stem cells. Equine Vet J. 2013;45:732-6.

94. Song Y, Dou H, Li X, Zhao X, Li Y, Liu D, et al. Exosomal miR-146a Contributes to the Enhanced Therapeutic Efficacy of Interleukin-1 Beta-Primed Mesenchymal Stem Cells Against Sepsis. Stem Cells. 2017;35:1208-21.

95. Yuan W, Hu Q, Cheng H, Shang W, Liu N, Hua Z, et al. Cell wall thickening is associated with adaptive resistance to amikacin in methicillin-resistant *Staphylococcus aureus* clinical isolates. J Antimicrob Chemother. 2013;68:1089-96.

96. Masters EA, Trombetta RP, de Mesy Bentley KL, Boyce BF, Gill AL, Gill SR, et al. Evolving concepts in bone infection: redefining "biofilm," "acute vs. chronic osteomyelitis," "the immune proteome," and "local antibiotic therapy." Bone Res. 2019;7:20.

97. Saeed K, McLaren AC, Schwarz EM, Antoci V, Arnold WV, Chen AF, et al. 2018 international consensus meeting on musculoskeletal infection: Summary from the biofilm workgroup and consensus on biofilm related musculoskeletal infections. J Orthop Res. 2019;37:1007-17.

CHAPTER 5: EQUINE BONE MARROW-DERIVED MSC ALTER LIPIDOMIC AND CYTOKINE PROFILE DURING EXPOSURE TO *S. AUREUS* BIOFILMS *IN VITRO*

To be submitted for publication as:

Sarah M. Khatibzadeh, Linda A. Dahlgren, Clayton C. Caswell, William A. Ducker, Stephen R. Werre, Sophie H. Bogers. Equine bone-marrow derived MSC alter lipidomic and cytokine profile during exposure to *S. aureus* biofilms *in vitro*. *Stem Cells and Development*

Key words:

mesenchymal stromal cell, peripheral blood mononuclear cell, equine, biofilm, SPM, cytokine

Abbreviations:

MSC; equine bone marrow-derived mesenchymal stromal cells

PBMC; peripheral blood mononuclear cells

S. aureus; Staphylococcus aureus

CFU; colony-forming units

SPM; specialized pro-resolving mediators

AA; arachidonic acid

DHA; docosahexaenoic acid

EPA; eicosapentaenoic acid

PG; prostaglandin

TX; thromboxane

LT; leukotriene

LX; lipoxin

Rv; resolvin

MaR; maresin

PD; protectin

HEPE; hydroxyeicosapentaenoic acid

HETE; hydroxyeicosatetraenoic acid

DiHETE; dihydroxyeicosatetraenoic acid

DoHE; dihydroxydocosahexaenoic acid

FGF; fibroblastic growth factor

G-CSF; granulocyte colony stimulating factor

GM-CSF; granulocyte-macrophage colony stimulating factor

IL; interleukin

GRO; growth-regulated oncogene/keratinocyte chemoattractant

INF; interferon

IP; INF-γ inducible protein

TNF; tumor necrosis factor

RANTES; Regulated Upon Activation, T cell Expressed, and Secreted

ABSTRACT

Orthopedic biofilm infections exacerbate chronic inflammation and lead to tissue damage, clinical complications, and mortality in people and horses. Equine bone-marrow derived mesenchymal stromal cells (MSC) have immunomodulatory properties; however, their ability to modulate inflammation in biofilm infections is unknown. We evaluated the pro-resolving and anti-inflammatory response of MSC from 3 horses following transwell co-culture with autologous peripheral blood mononuclear cells (PBMC) and established *S. aureus* biofilms for 24 and 48 hours. Biofilm reduction was quantified photographically and by live bacterial colony-forming units. Co-culture medium was collected for quantification of specialized pro-resolving lipid mediators (SPM) by liquid chromatography-mass spectrometry and inflammatory cytokines and chemokines by multiplex bead ELISA. Co-culture significantly reduced biofilm pellicle area at both timepoints compared to untreated controls. Differences in SPM and inflammatory cytokines/chemokines were primarily detected at 48 hours. The pro-inflammatory mediator thromboxane B_2 was significantly reduced in MSC + PBMC + biofilm (MPB) co-culture compared to PBMC + biofilm controls at 48 hours. The metabolite 4-HDoHE was significantly reduced in MPB co-culture compared to MSC or PBMC alone at 48 hours. Significantly greater levels of arachidonic and eicosapentaenoic acid metabolites were detected in MPB co-cultures compared to either MSC or PBMC alone or individually co-cultured with biofilms. Cytokine/chemokine levels were not altered by MPB co-culture compared to PBMC + biofilm controls. Detection of inflammatory cytokines and chemokines was significantly increased when MSC and/or PBMC were co-cultured with biofilms compared to no biofilms at both timepoints, although were not different from biofilms alone. Our findings provide insight into MSC and

PBMC responses to *S. aureus* biofilms and supports continued investigation into the immunomodulatory potential of MSC against biofilm infections.

INTRODUCTION

Biofilms sustain a chronic inflammatory response during orthopedic infections by enabling infection persistence in the face of treatment [1-5] and by direct immune stimulation [6-9]. *Staphylococcus aureus* is a common causative agent of orthopedic biofilm infections leading to chronic, unresolved inflammation [5, 10]. Inflammation-exacerbated tissue damage, including peri-implant osteolysis, results in implant failure in infected fracture fixations and arthroplasties [11-15]. Such complications increase treatment duration and cost [11, 16, 17], reduce quality of life [17], and contribute to mortality rates as high as 55% in people [11-13, 18] and 56% in horses [12, 18-20]. A therapy capable of modulating the immune response to biofilms is urgently needed.

The immune response to infection is divided into two phases, an acute inflammatory phase and a reparative phase [21]. During inflammation, bacterial pathogen-associated molecular patterns bind to pattern recognition receptors on polymorphonuclear leukocytes (PMN), including neutrophils and inflammatory macrophages [22-24]. Pattern recognition receptor binding stimulates expression of pro-inflammatory cytokines and chemokines and enzymatic synthesis of pro-inflammatory lipid mediators, such as prostaglandins and thromboxane, from the ω-6 fatty acid arachidonic acid [8, 25-28]. These cellular signals enhance recruitment PMN to the site of infection and stimulate phagocytosis of pathogens and cellular debris, vasodilation, increased vascular permeability, and platelet activation [29-31]. Following clearance of pathogens and debris, the reparative phase promotes tissue healing, remodeling, and return to homeostasis [27, 32, 33]. Release of anti-inflammatory cytokines and growth factors from progenitor cells and regulatory macrophages reduce PMN infiltration and inflammatory cytokine expression, increase

anti-inflammatory cytokine and growth factor expression, and promote progenitor cell differentiation and division [27, 34, 35].

The transition from an inflammatory to a reparative state is driven by release of specialized pro-resolving lipid mediators (SPM) from progenitor cells and macrophages [36-38]. SPM are synthesized from arachidonic acid (lipoxins) [37] and from ω-3 fatty acids docosahexaenoic acid (D-series resolvins, protectins, maresins) [37, 39] and eicosapentaenoic acid (E-series resolvins) [40]. These SPM bind G protein-coupled receptors on macrophages [41] and MSC [38] to promote resolution of inflammation by increasing growth factor expression [38, 42], recruiting and promoting division of progenitor cells [36, 37], reducing PMN infiltration [30, 39] and limiting inflammatory cytokine expression [36, 38]. While SPM promote the transition to the reparative phase, SPM synthesis itself is triggered by inflammatory signals, including bacterial toxins [40, 43], complement [44], and prostaglandins [30]. SPM production is thereby an endogenous control mechanism to prevent chronic, dysregulated inflammation that leads to tissue damage and loss-of-function [45].

Strategies to mitigate inflammation targeted methods to inhibit acute inflammation and encourage resolution of inflammation. Mesenchymal stromal cells (MSC) from multiple species and tissue sources show promise as a therapy to modulate the inflammatory response to orthopedic biofilm infections based on their dual anti-inflammatory [35, 46, 47] and pro-resolving properties [36-38, 42]. MSC from horses and other species reduce inflammation by suppression of T-lymphocyte proliferation and inflammatory cytokine secretion [34, 35, 48-50] and promote healing following musculoskeletal injuries [51-54]. MSC reduced osteolysis and

inflammatory cytokine expression to a greater extent than antimicrobials alone during femoral implant *S. aureus* infection in a murine model, demonstrating immunomodulatory effects independent of reduced bacterial load [31]. MSC from people [36, 37, 42] and mice [38, 39, 43, 55] produce SPM, which may be integral to their ability to resolve inflammation and promote healing. MSC-derived SPM reduced pro-inflammatory cytokine expression and tissue damage, and promoted healing in models of diabetic nephropathy [38], periodontitis [36, 37], and peritonitis [39, 44], and are associated with disease resolution in COVID-19 patients [56]. The ability of equine MSC to reduce inflammation and/or promote resolution of inflammation via SPM production in response to orthopedic biofilms is unknown.

The objective of our study was to characterize the pro-resolving and anti-inflammatory response of equine bone marrow-derived MSC (MSC) to biofilms of the orthopedic pathogen *S. aureus in vitro*. We hypothesized that 1) MSC would produce SPM in response to *S. aureus* biofilms *in vitro*, with or without concurrent culture with peripheral blood mononuclear cells (PBMC), and that 2) co-culture of MSC and autologous PBMC with *S. aureus* biofilms *in vitro* would alter biofilm-induced production of inflammatory cytokines and chemokines by PBMC.

METHODS

Experimental Overview

Experiments were performed using passage 3 MSC and autologous PBMC from three donor horses (Table 5.1, Fig 5.1). Established 24-hour *S. aureus* biofilms were co-cultured in triplicate with MSC, PBMC, or both (autologous) in a transwell plate system as described previously (Chapter 3). Following co-culture for 24 or 48 hours, live bacterial counts were quantified on total well contents, including enzymatically digested biofilms. Biofilm pellicle reduction was quantified photographically. Conditioned medium was analyzed for the presence of SPM using lipidomics analysis and for equine inflammatory cytokines/chemokines using a commercial multiplex bead ELISA.

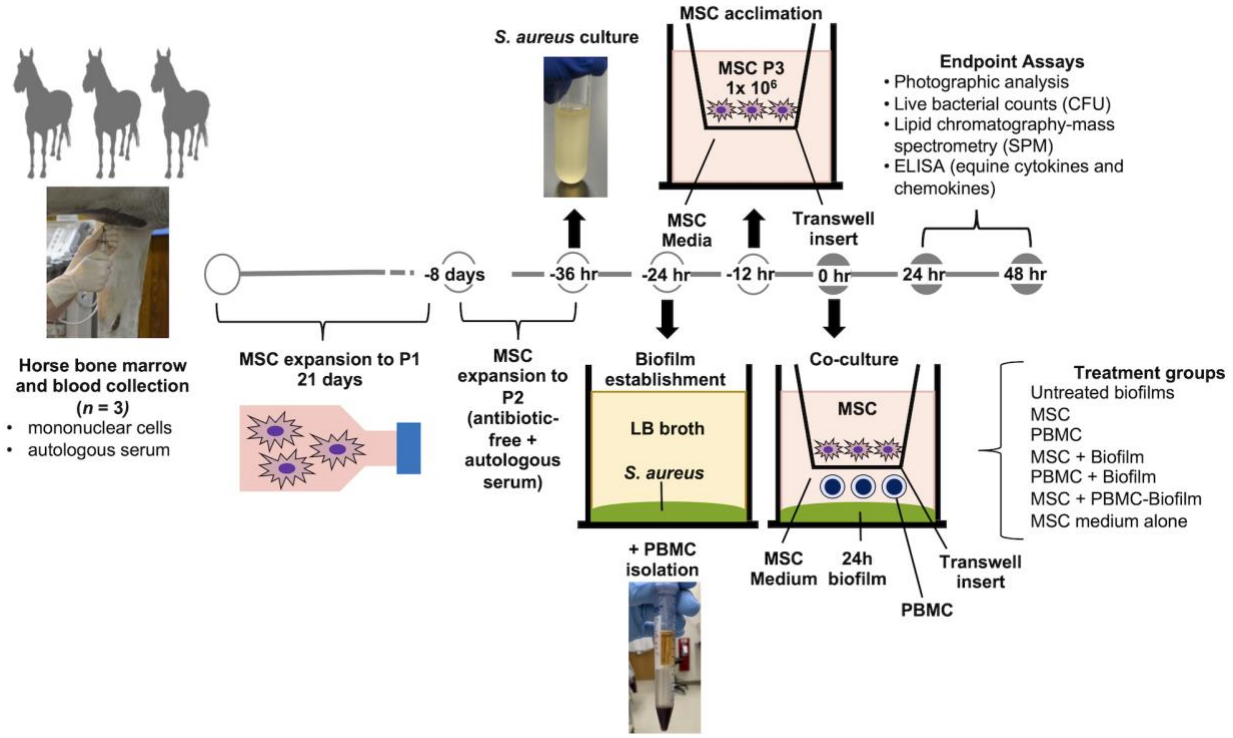

Figure 5.1: Experimental procedure for *in vitro* co-culture of equine bone marrow-derived mesenchymal stromal cells (MSC) and autologous peripheral blood mononuclear cells (PBMC) with *S. aureus* biofilms. Three healthy, adult equine donors were used for MSC, PBMC and autologous serum isolation.

Biofilm Preparation

Overnight Luria-Bertani broth cultures of *S. aureus* (ATCC® 2913) were grown at 37ºC, 200 rpm (Fisherbrand™ Incubating Mini-Shaker, Fisher Scientific™) and serially diluted to optical density (OD) at 600 nm of 0.05. Biofilms were established by inoculation of 2 x 10^5 CFU/well in 24-well, tissue-culture treated plates and growth at 37ºC, 5% CO_2, and 95% humidity for 24 hours to allow bacterial attachment and matrix production (Fig 5.1) [57, 58].

MSC Isolation and Culture

Under standing sedation and local anesthesia, 60 mL bone marrow was aspirated from the 4th and 5th sternebrae of 3 adult Thoroughbred horses (Table 5.1, Fig 5.1) into sodium heparinized syringes (200 units/mL marrow), following protocols approved by the Virginia Tech Institutional Animal Care and Use Committee. Mononuclear cells were isolated using gradient density separation (Ficoll® Paque PLUS), assessed by live-dead staining [27, 59], and plated at 350,000 live cells/cm^2 [60-62] in 175 cm^2 tissue culture flasks with MSC medium (low-glucose (l/g) GlutaMax DMEM, 110 µg/mL sodium pyruvate (Gibco™), 100 U/mL sodium penicillin, 100 µg/mL streptomycin sulfate (Sigma Aldrich®), 10% FBS (Gibco™) to isolate MSC. A 50% medium exchange was performed every 48 hours and MSC passaged at 70-80% to passage 1 prior to short-term cryopreservation at 1 x 10^7 cells/mL (Synth-a-freeze™, Gibco™) in liquid nitrogen, vapor phase.

Table 5.1: Bone marrow-derived MSC and blood PBMC donor horse information

Donor	Breed	Sex	Age (years)
1	TB	MC	10
2	TB	MC	12
3	TB	MC	10

Abbreviations: TB = Thoroughbred, MC = Male castrate

PBMC and Autologous Serum Isolation

For serum isolation, blood was aspirated from the jugular vein from the same 3 horses into borosilicate glass collection tubes, incubated for 30 minutes at room temperature (RT) to allow clot formation, and centrifuged at 1,000 x g, 10 minutes, RT. The serum aspirated, vacuum-filtered (Nalgene™ Rapid Flow™, 0.2 µm), and frozen at -20ºC until use. To isolate autologous PBMC, venous blood was collected into sodium heparinized syringes (200 units/mL blood). PBMC were isolated by gradient density centrifugation [63] using Lymphoprep™ (STEMCELL™ Technologies), viability assessed on live/dead staining, and resuspended in Roswell Park Institute Medium-1640, L-glutamine, HEPES (Gibco™) + 5% autologous serum at 2 x 10^6 cells/mL [64] and stored overnight at 4ºC prior to use in co-culture (Fig 5.1).

Biofilm Co-culture with MSC and PBMC

Thawed passage 2 MSC were expanded in antibiotic-free MSC medium (l/g DMEM, 10% FBS). A complete medium change to MSC medium + 10% autologous serum was performed 48 hours prior to trypsinization to allow shedding of FBS proteins that would interfere with downstream quantification assays. 1 x 10^6 passage 3 MSC were placed into 24-well transwell inserts (6.5 mm, 0.4 µm pore diameter, polyester, Corning®) in MSC medium + 5% autologous serum and acclimated overnight at 37ºC, 5% CO_2, and 95% humidity (Fig 5.1). PBMC viability

was confirmed following overnight storage and PBMC were resuspended in MSC medium + 5% autologous serum. To establish co-cultures, 24-hour *S. aureus* biofilms in 24-well plates were centrifuged at 1,400 x g, 10 minutes, RT, the overlying LB broth aspirated, and 500 µL MSC medium + 5% autologous serum alone (negative control) or containing 5 x 10^6 PBMC were added per well. MSC in transwell inserts were transferred to biofilm wells with MSC medium + 5% autologous serum alone or with 5 x 10^6 PBMC (Fig 5.1) for a starting ratio of 500 *S. aureus*:5 PBMC:1 MSC [49]. Biofilms were maintained in triplicate for 24 and 48 hours: untreated controls; MSC + biofilm (MSC co-culture); PBMC + biofilm (PBMC co-culture); MSC + PBMC + biofilm (combined co-culture) (Fig 5.1). MSC and PBMC culture media were collected prior to co-culture setup (0 hours) and at 24 and 48 hours to evaluate SPM and cytokine/chemokine production in the absence of biofilms. Unconditioned medium served as the control for the baseline analyte detection in serum.

Biofilm Photographic Analysis

Following co-culture, inserts containing MSC were removed and biofilms were photographed (iPhone XR, Apple, Inc) in a ring light booth with a black backdrop and the lens set to an object distance of 19 cm (PULUZ®). High resolution JPEG images were imported to ImageJ (NIH) and converted to 8-bit greyscale. Images that showed biofilm pellicles as white on a black background were obtained via default algorithm histogram thresholding. The number of white pixels (value 255) were recorded in an oval region of interest around the pellicle in triplicate. One independent, blinded reviewer (Jane Perkins) reviewed images from all horses. Pixel size was calibrated to reference lines of known distance (mm) and mean pellicle area (mm^2) was calculated.

Live Bacterial Quantification

Biofilm well contents were digested *in situ* with 20 µg/mL Proteinase K (Life Technologies, Inc) for 30 minutes at 37ºC,150 rpm (Fisherbrand™ Incubating Mini-Shaker) [4]. Digests were transferred to sterile microfuge tubes, serially diluted, plated in triplicate on tryptic soy agar, and incubated overnight at 37ºC. Isolated live colonies were counted, divided by the dilution factor, and the quotient multiplied by well volume to calculate total live bacteria (CFU/biofilm):

CFU/biofilm = (Live colonies / dilution factor) x well volume in mL

SPM Detection on Lipidomics Analysis

Conditioned medium samples were collected in polypropylene microfuge tubes, pooled across technical replicates, and stored immediately at -80°C. Samples were shipped on dry ice to the Lipidomics Core Facility, School of Medicine, Wayne State University (Detroit, Michigan) for SPM quantification by liquid chromatography-mass spectrometry [40] with a lower detection limit of 0.01 pg and a maximum acceptable signal:noise ratio of $\geq$ 3.

Equine Cytokine/Chemokine Quantification

Conditioned medium samples were collected in polypropylene microfuge tubes following biofilm centrifugation *in situ* at 1,400 x g, 10 minutes, RT, treated with a broad-spectrum protease inhibitor (HALT™, Thermo-Fisher Scientific™, 1x final concentration) and stored immediately at -80°C. Frozen samples were shipped on dry ice to the Respiratory TRACTS Core at the School of Medicine, University of North Carolina at Chapel Hill for quantification of equine immune cytokines and chemokines on the MILLIPLEX MAP Equine

Cytokine/Chemokine Magnetic Bead multiplex panel (EQCYTMAG-93K, Millipore-Sigma™, Merck©) [27, 65]. Cytokines and chemokines contributing to the pro-inflammatory (Table 5.2) and anti-inflammatory/regulatory responses to biofilms (Table 5.3) were measured. Medium + 5% equine serum (Corning®) was used for standard curve diluent.

Table 5.2: Pro-inflammatory cytokines and chemokines quantified in biofilm co-culture medium.

Cytokine/chemokine	Abbreviation	References
Interleukin-1α	IL-1α	[66, 67]
Interleukin-1β	IL-1β	[29, 68]
Interleukin-2	IL-2	[69]
Interleukin-6	IL-6	[9]
Interleukin-8	IL-8	[66, 67, 70]
Interleukin-13	IL-13	[71]
Interleukin-17A	IL-17A	[71]
Interleukin-18	IL-18	[72]
Interferon-γ	IFN- γ	[9, 69, 70]
Tumor necrosis factor (TNF)-α	TNF-α	[66, 70]
Eotaxin	Eotaxin	[73]
Fractalkine	CX3CL1	[74]
Growth-regulated oncogene/keratinocyte chemoattractant	GRO	[67]
Granulocyte-colony-stimulating factor	G-CSF	[75]
Granulocyte-macrophage colony-stimulating factor	GM-CSF	[75]
Regulated Upon Activation, T cell Expressed, and Secreted	RANTES	[76]

Table 5.3: Anti-inflammatory/regulatory cytokines and chemokines quantified in biofilm co-culture medium.

Cytokine/chemokine	Abbreviation	References
Fibroblastic growth factor-2	FGF-2	[77]
Interleukin-4	IL-4	[8]
Interleukin-5	IL-5	[71]
Interleukin-10	IL-10	[69]
Interleukin-12	IL-12	[72, 78]
Interferon-γ inducible protein-10	IP-10	[79]
Macrophage chemotactic protein-1	MCP-1	[80]

Statistical Analysis

Sample size was calculated (G*Power, University of Düsseldorf, Netherlands) based on serum SPM levels following endotoxin challenge in people [40]. Data distribution was assessed using normal probability plots, summarized as mean ± standard deviation or median ± interquartile range, and effects of treatment on outcomes were analyzed using a mixed model analysis of variance. The generalized linear model specified treatment, time, and the interaction between treatment and time as fixed effects, and horse was specified as a random effect. The treatment*time interaction was further analyzed to compare the treatment groups at each time point. Where appropriate, *p*-values were adjusted for multiple comparisons using Tukey's procedure. Statistical significance was set to $p < 0.05$. All analyses were performed using SAS version 9.4 (Cary, NC).

RESULTS

MSC and PBMC reduce biofilm size but not live bacterial counts

MSC maintained 75% of baseline viability following co-culture with *S. aureus* biofilms for 48 hours. PBMC viability remained at ≥ 99% following isolation and overnight storage. Live bacterial counts from all biofilm-cell co-cultures were unchanged compared to untreated biofilms (Table 5.4). Biofilm pellicle area was reduced by combined co-culture compared to biofilm controls at both timepoints (P = 0.016 at 24 hours; P = 0.004 at 48 hours) (Fig 5.2).

Table 5.4: Live bacterial CFU of *S. aureus* biofilms following co-culture with MSC and PBMC

Group	**Time (h)**	**CFU (mean ± SD)**	***P* value (compared to untreated control)**
Bf	24	$1.14 \pm 0.16 \times 10^9$	--
Bf	48	$1.15 \pm 0.20 \times 10^9$	--
MSC + Bf	24	$1.16 \pm 0.32 \times 10^9$	0.99
MSC + Bf	48	$1.15 \pm 0.16 \times 10^9$	>0.99
PBMC + Bf	24	$1.14 \pm 0.14 \times 10^9$	>0.99
PBMC + Bf	48	$0.93 \pm 0.33 \times 10^9$	0.78
MSC + PBMC + Bf	24	$1.03 \pm 0.28 \times 10^9$	0.96
MSC + PBMC + Bf	48	$1.16 \pm 0.47 \times 10^9$	>0.99

Abbreviations: MSC = equine bone marrow-derived mesenchymal stromal cells; PBMC = peripheral blood mononuclear cells; Bf = biofilm

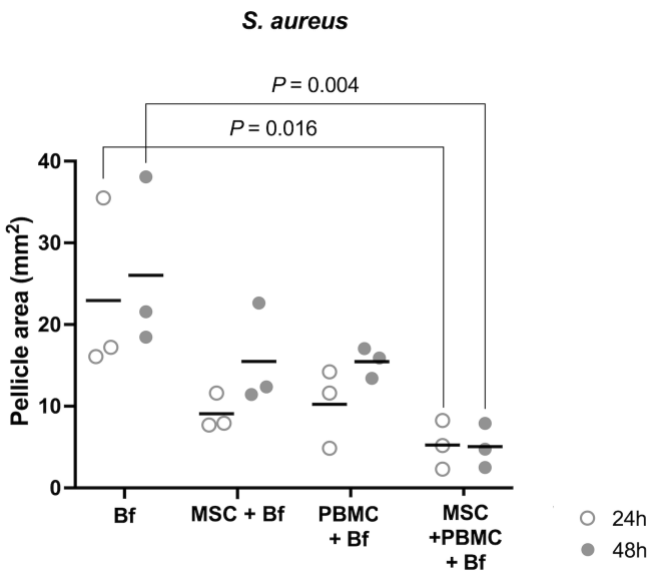

Figure 5.2: Dot-plots of normalized biofilm pellicle area (mm^2) from *n* = 3 horses. Horizontal black lines indicate mean pellicle size across horses, and circles indicate mean pellicle size for individual horses at 24 (open circles) or 48 hours (closed circles). Bf indicates untreated biofilm controls. Brackets and *P*-values indicate groups significantly different ($P < 0.05$) from each other.

MSC + PBMC + biofilm (combined) co-culture altered detection of lipid mediators

The pro-inflammatory mediator thromboxane (TX) B_2 was reduced in combined co-culture compared to PBMC co-culture at 48 hours ($P = 0.003$) (Fig 5.3A). PGE_2 and pro-resolving mediator LTB_4 were detected with an overall effect of treatment ($P = 0.034$) (Fig 5.3A). Multiple arachidonic acid metabolites (5-HETE, 11-HETE, 12-HETE, 5(S), 12(S)-DiHETE, 5(S), 6(R)-DiHETE) (Fig 5.3B) and eicosapentaenoic acid metabolites (11-HEPE, 15(S)-HEPE) (Fig 5.3C) were detected at greater levels in combined co-cultures ($P < 0.05$) compared to MSC or PBMC

alone. Additionally, PGE_2, LTB_4, and pro-resolving mediators LXA_4 (Fig 5.3A) and RvE1 (Fig 5.3C) were primarily observed in MSC co-cultures and MSC alone. The pro-inflammatory mediator PGF2-α (Fig 5.3A) and pro-resolving mediator RvE2 were primarily observed in PBMC co-cultures (Fig 5.3C), but did not show statistical differences between groups. The docosahexaenoic acid metabolite 4-HDoHE was reduced in combined co-culture compared to MSC ($P = 0.019$) and PBMC alone ($P = 0.024$) at 48 hours (Fig 5.3D). Additional arachidonic acid metabolites were increased in combined co-culture compared to MSC co-culture (5(S), 6(R)-DiHETE, (5(S), 6(R)-DiHETE), or compared to PBMC co-culture (12-HETE) at 48 hours (Fig 5.3B). Maresins, D-series resolvins, and multiple metabolites were not detected or were detected too inconsistently to analyze (Table 5.5)

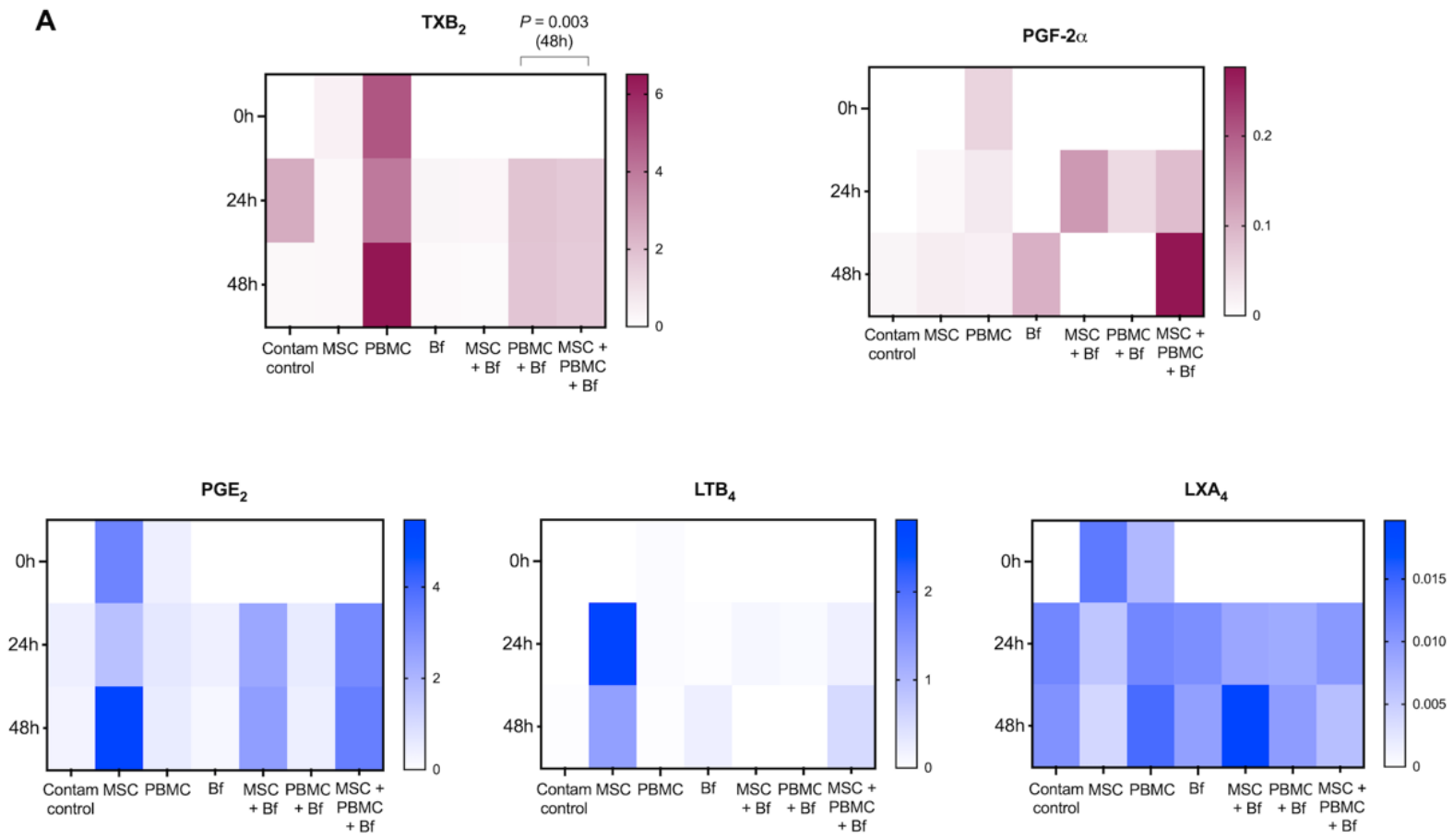
A
TXB2
P = 0.003
(48h)
PGF-2α
PGE2
LTB4
LXA4
0h
24h
48h
Contam control
MSC
PBMC
Bf
MSC + Bf
PBMC + Bf
MSC + PBMC + Bf

B

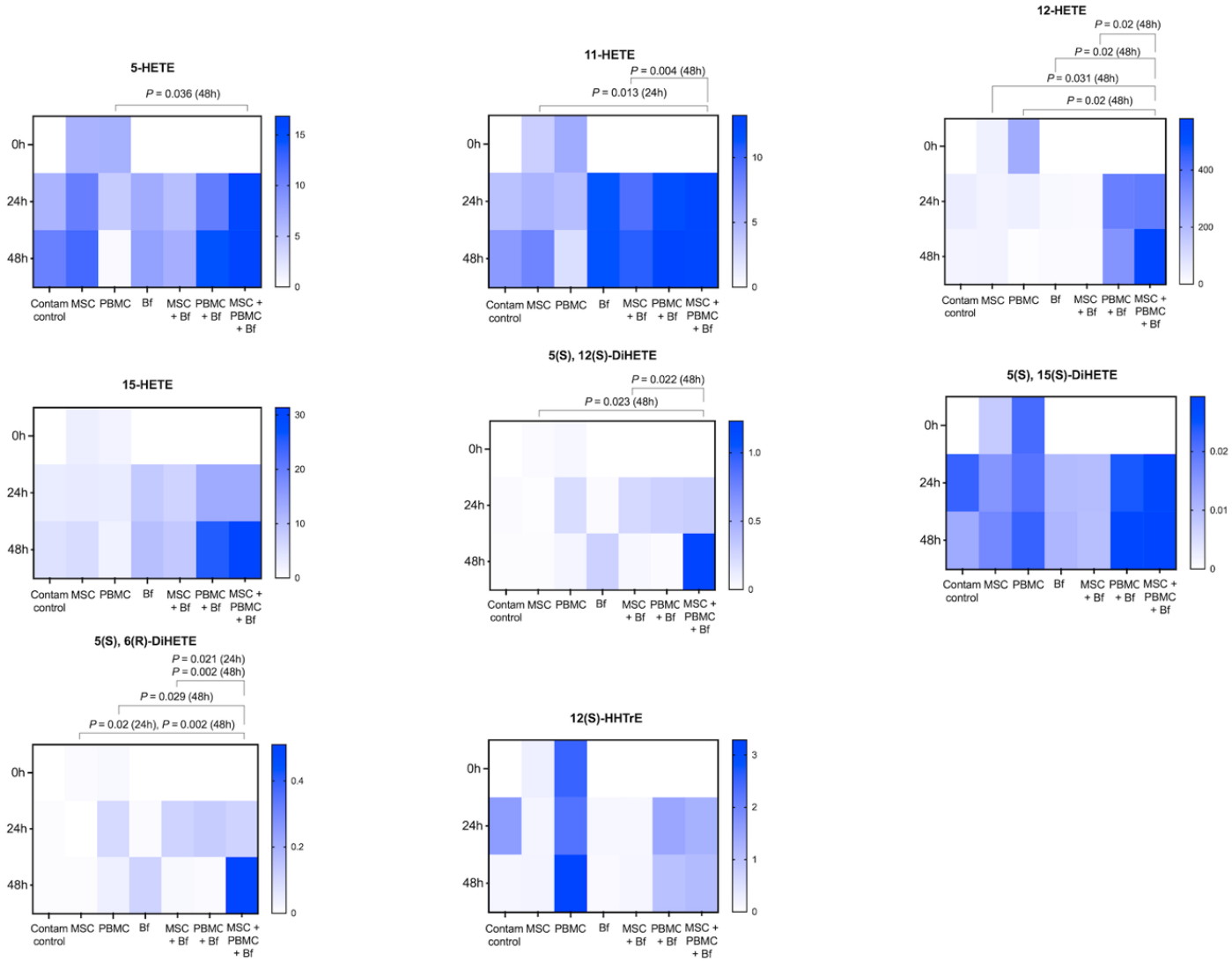
5-HETE
P = 0.036 (48h)
11-HETE
P = 0.004 (48h)
P = 0.013 (24h)
12-HETE
P = 0.02 (48h)
P = 0.02 (48h)
P = 0.031 (48h)
P = 0.02 (48h)
15-HETE
5(S), 12(S)-DiHETE
P = 0.022 (48h)
P = 0.023 (48h)
5(S), 15(S)-DiHETE
5(S), 6(R)-DiHETE
P = 0.021 (24h)
P = 0.002 (48h)
P = 0.029 (48h)
P = 0.02 (24h), P = 0.002 (48h)
12(S)-HHTrE
0h
24h
48h
Contam control
MSC
PBMC
Bf
MSC + Bf
PBMC + Bf
MSC + PBMC + Bf

C

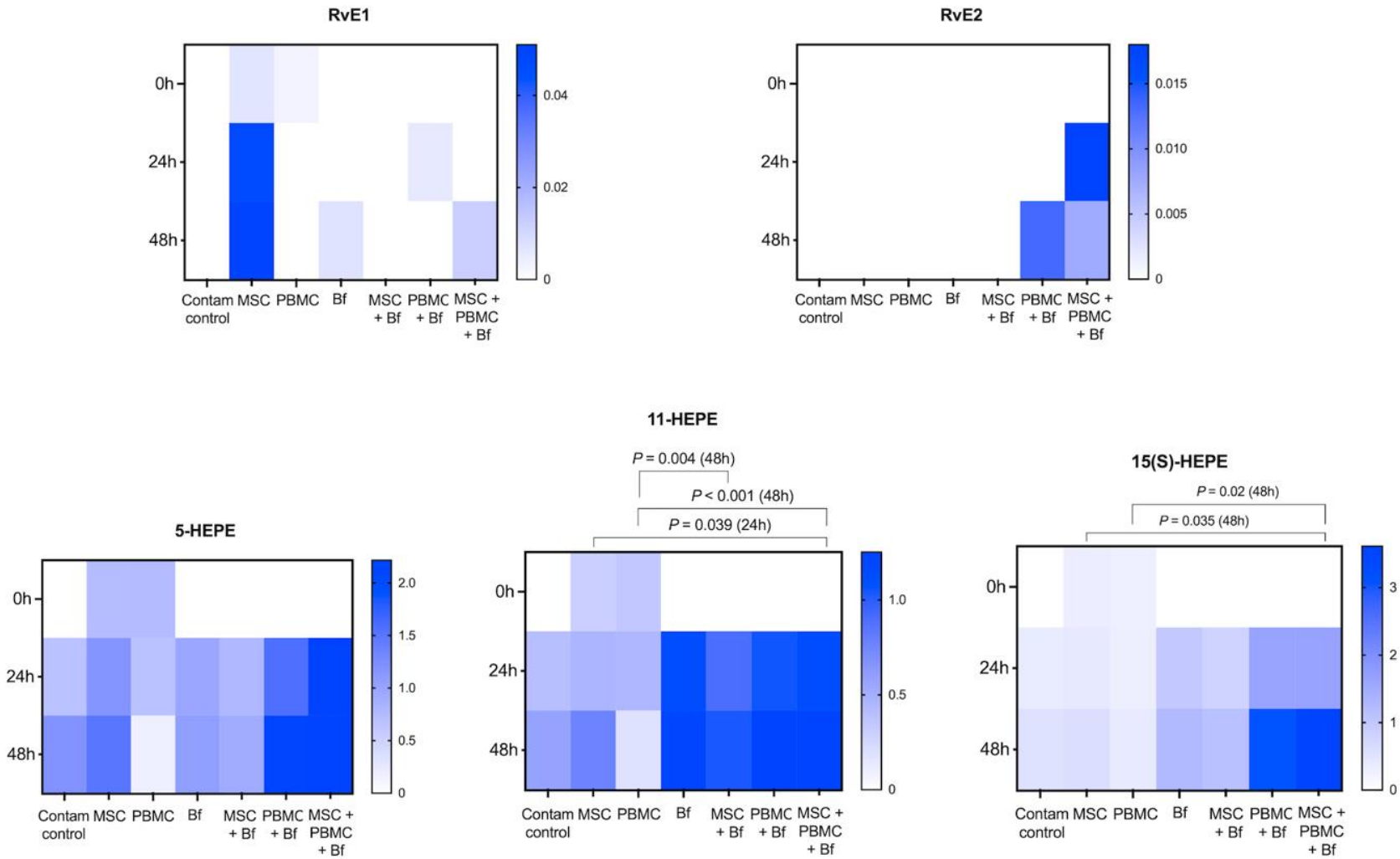
RvE1
0h
24h
48h
0.04
0.02
0
Contam control
MSC
PBMC
Bf
MSC + Bf
PBMC + Bf
MSC + PBMC + Bf
RvE2
0.015
0.010
0.005
0
5-HEPE
2.0
1.5
1.0
0.5
11-HEPE
P = 0.004 (48h)
P < 0.001 (48h)
P = 0.039 (24h)
15(S)-HEPE
P = 0.02 (48h)
P = 0.035 (48h)
3
2
1

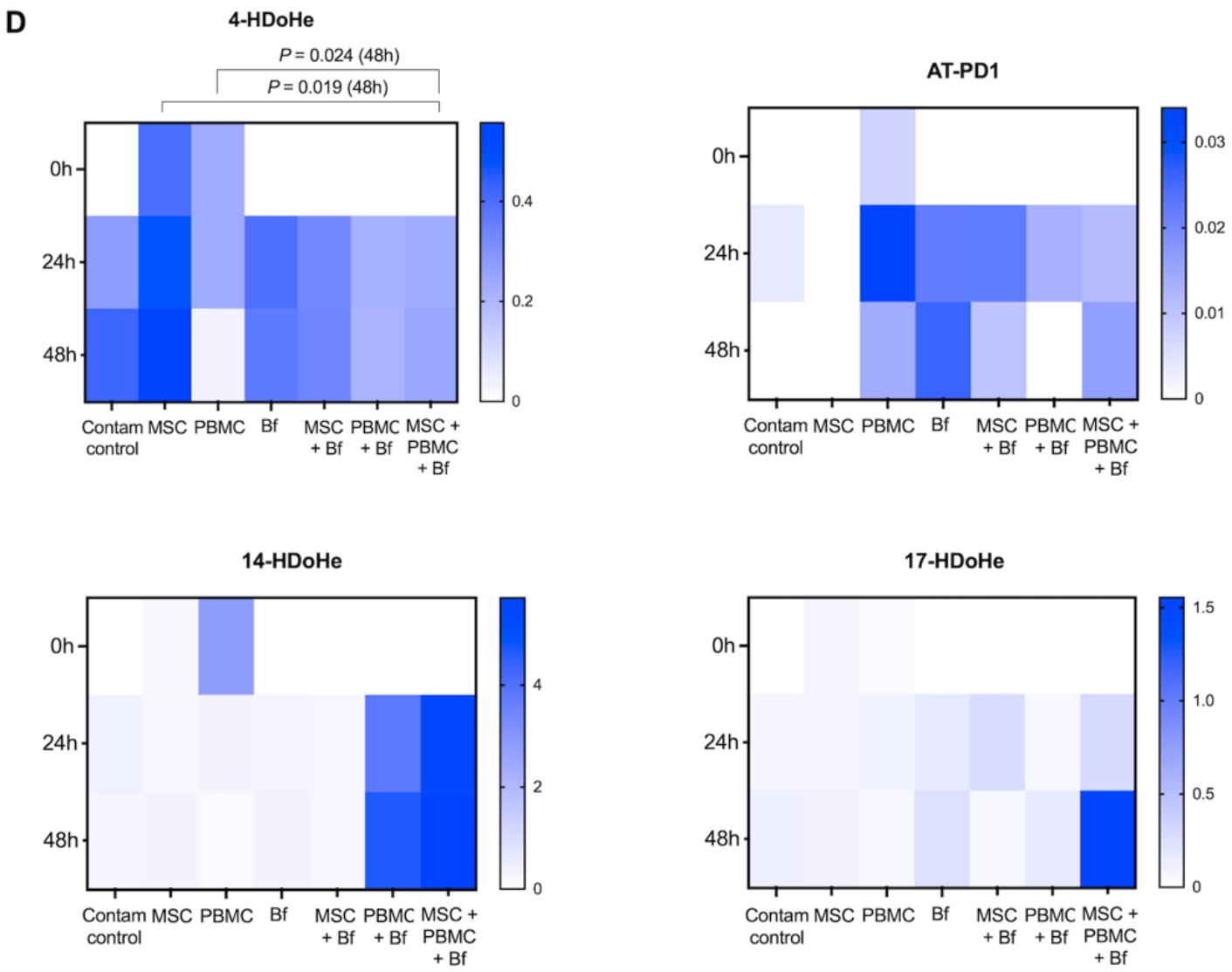
D
4-HDoHe
P = 0.024 (48h)
P = 0.019 (48h)
0h
24h
48h
0.4
0.2
0
Contam control
MSC
PBMC
Bf
MSC + Bf
PBMC + Bf
MSC + PBMC + Bf
AT-PD1
0.03
0.02
0.01
14-HDoHe
4
2
17-HDoHe
1.5
1.0
0.5

Figure 5.3: Specialized pro-resolving lipid mediators (SPM) detected on LC-MS following MPB co-culture.

Colorimetric representations of mean detected levels (ng/mL) of each mediator from $n = 3$ horses are on the right y-axis, co-culture time points are on the left y-axis, and treatment groups are on the x-axis. Bf indicates untreated biofilms. Maroon graphs indicate pro-inflammatory mediators and blue graphs indicate pro-resolving mediators and metabolites. SPM are grouped by arachidonic acid-derived mediators (A), arachidonic acid-derived metabolites (B), eicosapentaenoic acid-derived mediators and metabolites (C), and docosahexaenoic acid-derived metabolites (D). Brackets indicate groups significantly different ($P < 0.05$) from each other.

Table 5.3: Lipid mediators not detected or detected inconsistently following co-culture of MSC with *S. aureus* biofilms and PBMC. Lipids are organized by their fatty acid of origin.

Mediator class	Mediator	Detection
AA	20-COOH LTB_4	ND
AA	20-OH-LTB_4	DI
AA	PGD_2	ND
AA	LXA_5	ND
AA	LXB_4	ND
AA	15-epi-LXB_4	ND
AA	5(S),12(S)-DiHETE	DI
AA	5(S),6(R)-DiHETE	DI
AA	PGF-2α	DI
AA	LTB4	DI
DHA	PD1	ND
DHA	n-3, PD1	ND
DHA	22-OH-PD1	DI
DHA	MaR1	ND
DHA	7(S)-MaR1	ND
DHA	n-3, MaR1	ND
DHA	AT-RvD1	ND
DHA	RvD3	ND
DHA	AT-RvD3	ND
DHA	RvD4	ND
DHA	RvD5	ND
DHA	n-3, RvD5	DI
DHA	RvD6	ND
DHA	RvE1	DI
DHA	RvE2	DI
DHA	10(S)-DiHDoHE	ND
DHA	17(S)-DiHDoHE	ND
DHA	17-DoHE	DI
EPA	RvE3	ND

Abbreviations: AA = arachidonic acid; DHA = docosahexaenoic acid; EPA = eicosapentaenoic acid; ND = Not detected; DI = detected inconsistently

Cytokine and chemokine levels were not significantly affected by co-culture with MSC or PBMC compared to biofilms alone

Levels of multiple inflammatory cytokines and chemokines were increased in MSC co-culture, PBMC co-culture, or combined co-culture versus MSC or PBMC alone ($P < 0.05$, all comparisons) (Table 5.6, Fig 5.4A and B) but were not different from biofilm controls. Anti-inflammatory cytokines IL-4 ($P < 0.001$) and IL-10 ($P = 0.003$) were detected in all co-culture groups with an overall effect of treatment but with no relevant post-hoc differences (Fig 5.4C). No differences were detected in inflammatory cytokines or chemokines in combined co-culture compared to PBMC co-culture (Fig 5.4B). Concentrations of fractalkine, IL-1α, IL-1β, and INF-γ, were not detected in enough samples for statistical analysis (Fig 5.4A and B).

Table 5.6: Pairwise comparisons of equine inflammatory cytokines and chemokines quantified following co-culture of MSC with *S. aureus* biofilms and PBMC.

Cytokine/chemokine	Comparison	Time (h)	*P*-value
Eotaxin	MSC vs. MSC + biofilm	24	= 0.001
	MSC vs. MSC + biofilm	48	< 0.001
	PBMC vs. PBMC + biofilm	48	< 0.001
FGF-2	MSC vs. MSC + biofilm	24	< 0.001
	MSC vs. MSC + biofilm	48	< 0.001
	PBMC vs. PBMC + biofilm	24	< 0.001
	PBMC vs. PBMC + biofilm	48	< 0.001
	PBMC vs. MSC + PBMC + biofilm	24	< 0.001
	PBMC vs. MSC + PBMC + biofilm	48	< 0.001
G-CSF	MSC vs. MSC + biofilm	24	= 0.036
	MSC vs. MSC + biofilm	48	< 0.001
	PBMC vs. MSC + PBMC + biofilm	24	= 0.009
	PBMC vs. MSC + PBMC + biofilm	48	= 0.002
	PBMC vs. PBMC + biofilm	48	= 0.004
GM-CSF	PBMC vs. MSC + PBMC + biofilm	48	= 0.01
	PBMC vs. PBMC + biofilm	48	= 0.015
CXCL-1	MSC vs. MSC + biofilm	48	= 0.002
	MSC vs. MSC + PBMC + biofilm	48	= 0.002
IL-2	MSC vs. MSC + biofilm	24	= 0.046
	MSC vs. MSC + biofilm	48	= 0.009
	MSC vs. MSC + PBMC + biofilm	48	= 0.006
	PBMC vs. MSC + PBMC + biofilm	48	= 0.015
	PBMC vs. PBMC + biofilm	48	= 0.019
IL-5	PBMC vs. MSC + PBMC + biofilm	48	< 0.001
	PBMC vs. PBMC + biofilm	48	< 0.001
IL-6	PBMC vs. MSC + PBMC + biofilm	48	= 0.014
	PBMC vs. PBMC + biofilm	48	= 0.016
IL-8	MSC vs. MSC + PBMC + biofilm	48	= 0.025
	MSC + biofilm vs. MSC + PBMC + biofilm	48	= 0.036
IL-12	PBMC vs. MSC + PBMC + biofilm	48	= 0.003
	PBMC vs. PBMC + biofilm	48	= 0.003
IL-13	MSC vs. MSC + biofilm	48	= 0.025
	MSC vs. MSC + PBMC + biofilm	48	= 0.017
IL-17A	MSC vs. MSC + biofilm	24	< 0.001
	PBMC vs. PBMC + biofilm	24	< 0.001
	MSC vs. MSC + biofilm	48	< 0.001
	PBMC vs. PBMC + biofilm	48	< 0.001
IL-18	MSC vs. MSC + biofilm	48	= 0.018
	MSC vs. MSC + PBMC + biofilm	48	= 0.009
	PBMC vs. MSC + PBMC + biofilm	48	= 0.005

	PBMC vs. PBMC + biofilm	48	= 0.004
IP-10	MSC vs. MSC + biofilm	24	= 0.012
	PBMC vs. MSC + PBMC + biofilm	24	= 0.046
	MSC vs. MSC + biofilm	48	< 0.001
	PBMC vs. MSC + PBMC + biofilm	48	= 0.015
	PBMC vs. PBMC + biofilm	48	= 0.015
MCP-1	MSC vs. MSC + biofilm	24	< 0.001
	MSC vs. MSC + PBMC + biofilm	24	< 0.001
	PBMC vs. PBMC + biofilm	24	< 0.001
	MSC vs. MSC + biofilm	48	< 0.001
	MSC vs. MSC + PBMC + biofilm	48	< 0.001
	PBMC vs. PBMC + biofilm	48	< 0.001
TNF-α	MSC vs. MSC + PBMC + biofilm	24	= 0.028
	MSC vs. MSC + PBMC + biofilm	48	= 0.001

Abbreviations: MSC = equine bone marrow-derived mesenchymal stromal cells; PBMC = peripheral blood mononuclear cells; FGF = fibroblastic growth factor; G-CSF = granulocyte-colony stimulating factor; GM-CSF = granulocyte-macrophage colony stimulating factor; GRO =. growth-regulated oncogene/keratinocyte chemoattractant; IP = interferon inducible protein; IL = interleukin; MCP = macrophage chemotactic protein; TNF = tumor necrosis factor

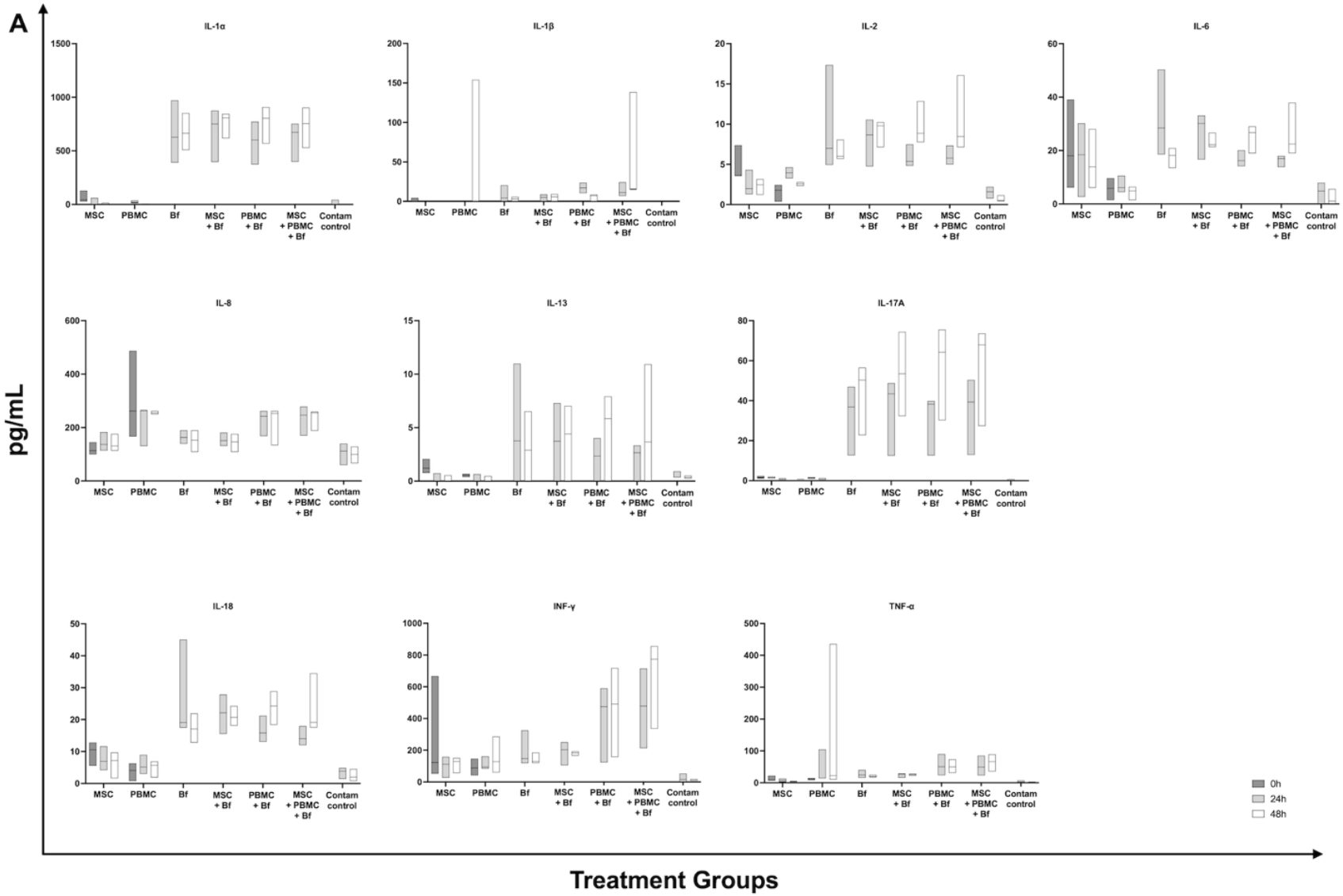
A
pg/mL
IL-1α
IL-1β
IL-2
IL-6
IL-8
IL-13
IL-17A
IL-18
INF-γ
TNF-α
MSC
PBMC
Bf
MSC + Bf
PBMC + Bf
MSC + PBMC + Bf
Contam control
0h
24h
48h
Treatment Groups

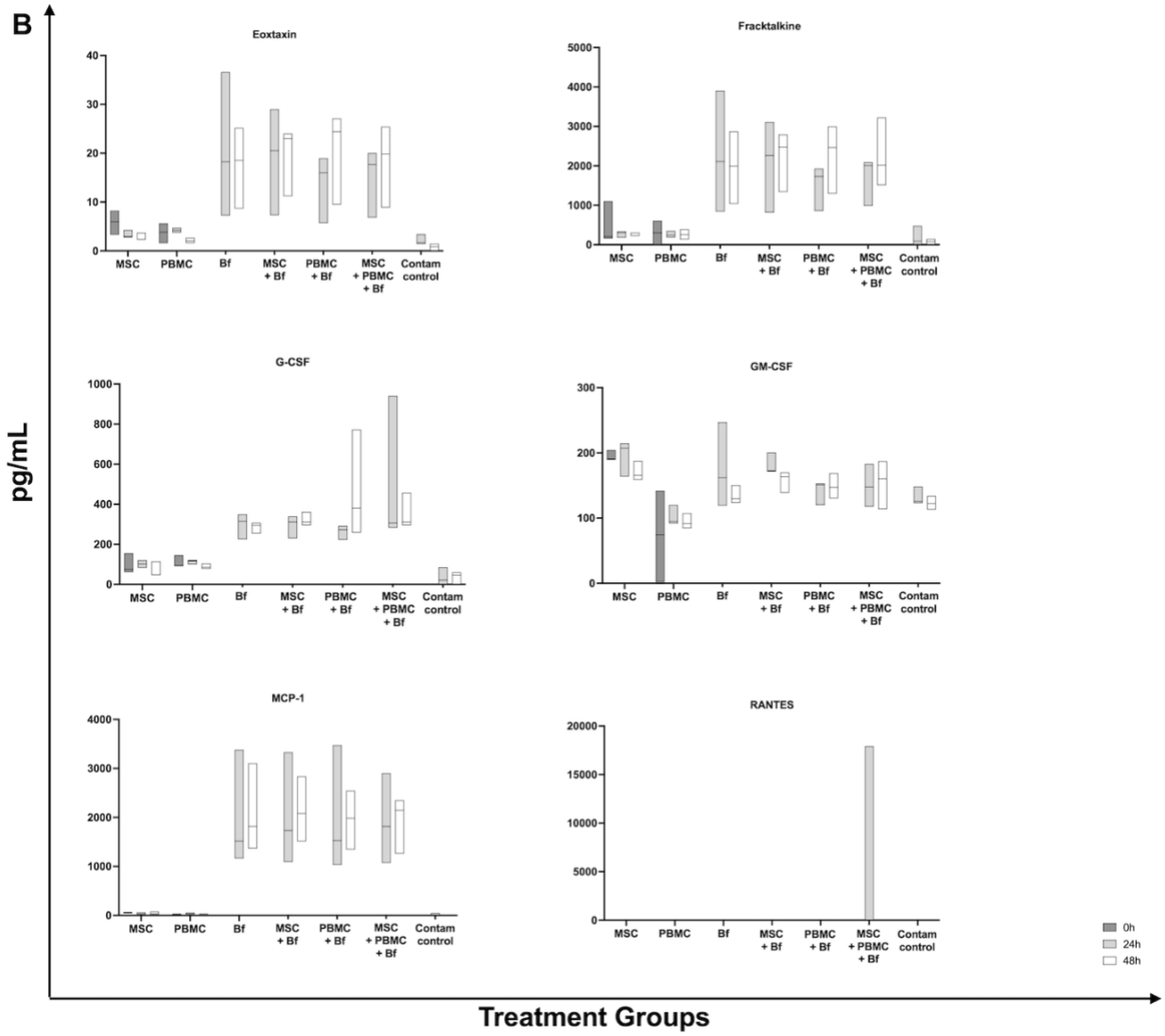
B
pg/mL
Eoxtaxin
Fracktalkine
G-CSF
GM-CSF
MCP-1
RANTES
MSC
PBMC
Bf
MSC + Bf
PBMC + Bf
MSC + PBMC + Bf
Contam control
0h
24h
48h
Treatment Groups

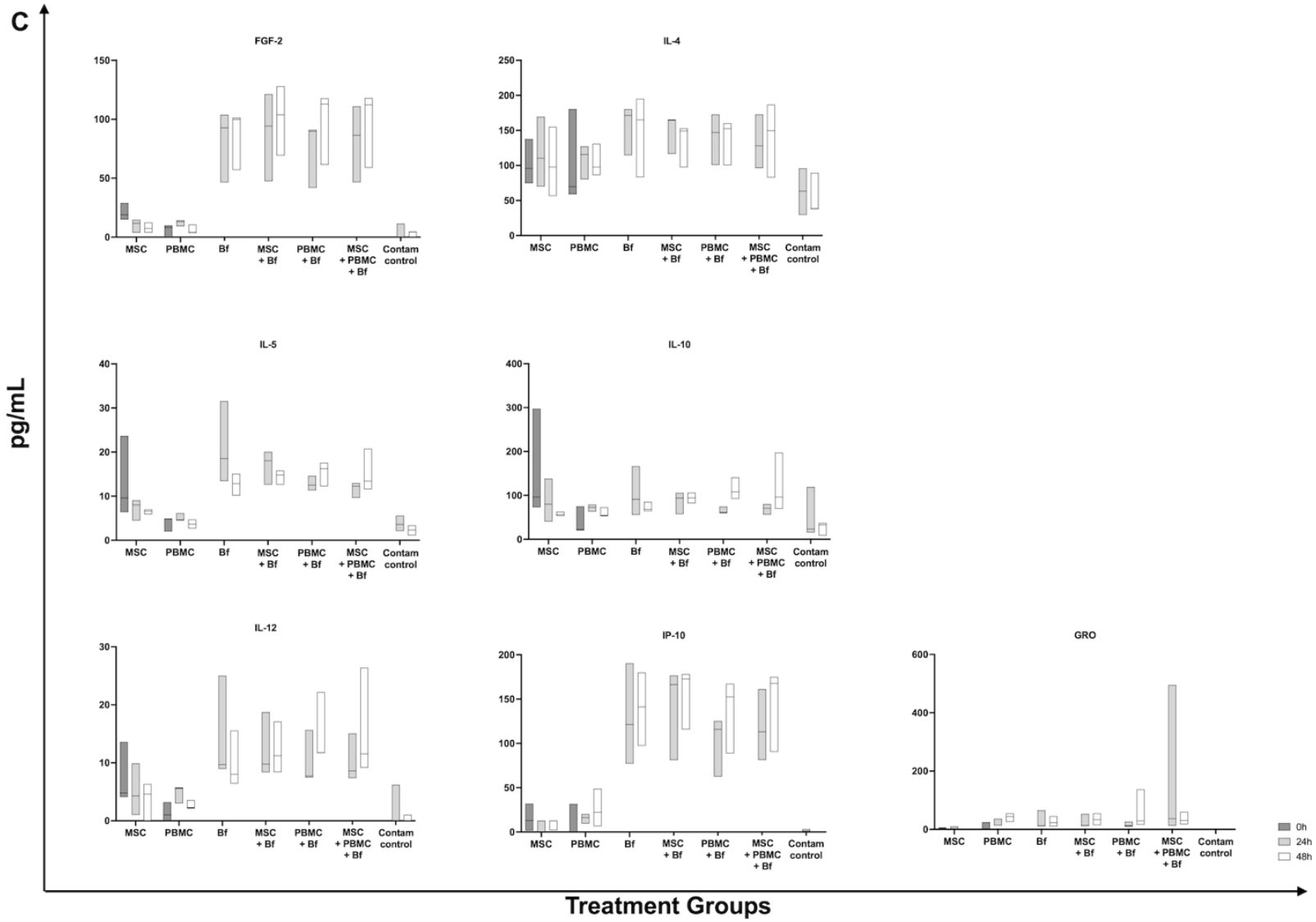
C
pg/mL
FGF-2
IL-4
IL-5
IL-10
IL-12
IP-10
GRO
MSC
PBMC
Bf
MSC + Bf
PBMC + Bf
MSC + PBMC + Bf
Contam control
0h
24h
48h
Treatment Groups

Figure 5.4: The inflammatory cytokine and chemokine response to co-culture of MSC and PBMC with *S. aureus* biofilms. Cytokines and chemokines were quantified on the MILLIPLEX MAP Equine Cytokine/Chemokine Magnetic Bead Panel (Millipore Sigma™, Merck©). Bf indicates untreated biofilms. Mediators are grouped by cytokines (A) and chemokines (B) contributing to the inflammatory response to biofilms and cytokines and chemokines contributing to the anti-inflammatory/regulatory response to biofilms (C). Box plots represent medians (center lines) ± minima and maxima (box edges) of cytokine and chemokine levels (pg/mL) from $n = 3$ horses.

DISCUSSION

This is the first equine study to investigate the lipidomic and cytokine/chemokine profile alterations of MSC and PBMC in response to established biofilms. These *in vitro* results demonstrated that alteration in SPM profile is likely a key response of MSC to *S. aureus* biofilms. The SPM response, in conjunction with biofilm pellicle reduction by MSC and PBMC compared to untreated controls, indicate interaction of both cell types in mounting a coordinated response to *S. aureus* biofilms [29, 81]. The ability of MSC to alter the profile of cytokines and chemokines remains unclear. Increased levels of multiple inflammatory cytokine and chemokines were detected on multiplex ELISA in biofilm co-cultures with MSC and/or PBMC compared to MSC or PBMC cultures alone. However, equivalent cytokine levels were detected in medium from *S. aureus* biofilms alone, which would not be expected to produce these cytokines. Our findings offer a basis for further mechanistic studies of MSC-mediated immunomodulation in the presence of biofilms.

The reduction of pro-inflammatory mediator TXB_2 observed in MPB co-culture versus PB co-culture is consistent with our first hypothesis that MSC would produce SPM in response to *S. aureus* biofilms *in vitro,* with or without concurrent culture with PBMC. The pattern of detection of multiple pro-resolving mediators (PGE_2, resolvins) in groups containing MSC, while not achieving post-hoc significance, also indicate that SPM may be a key mechanism for MSC to resolve biofilm-mediated inflammation. PGE_2 has dual pro-inflammatory and regulatory effects [34, 37, 82-86]. PGE_2 is elevated in serum during systemic inflammation and promotes expression of pro-inflammatory cytokines [87-89]. PGE_2 is also elevated in the synovial fluid of osteoarthritic joints [83, 84] and mediates pain signaling [82, 85] and subchondral bone

remodeling via osteoclast activation [85]. Conversely, PGE_2 secreted by MSC mediates key immunomodulatory functions, including T-lymphocyte suppression [34], reduction in pro-inflammatory cytokine secretion [46], macrophage polarization to a regulatory phenotype [86, 90], and SPM secretion [37]. The significance of increased detection of multiple arachidonic acid and docosahexaenoic acid metabolites in combined co-cultures compared to cell cultures alone is unknown. While these metabolites are intermediaries for synthesis of pro-resolving lipoxins (HETE, DiHETE) [91, 92] and E-series resolvins (HEPE) [93], they also have direct pro-resolving functions in supporting physiologic tissue remodeling [94], reducing neutrophil chemotaxis [95], and reducing pain pathway signaling [96]. Detection of these intermediates in co-culture may also reflect increased activity of lipoxin and resolvin-generating pathways, given that SPM are rapidly metabolized by target cells following synthesis [97-100] (Maddipatti, personal communication). Our findings support continued investigation of SPM as a key mechanism for MSC immunomodulation via autocrine signaling [37, 101], paracrine signaling between MSC and PBMC [34, 44], or interaction of MSC and PBMC with other immune cells (Fig 5.5) [37, 46, 102].

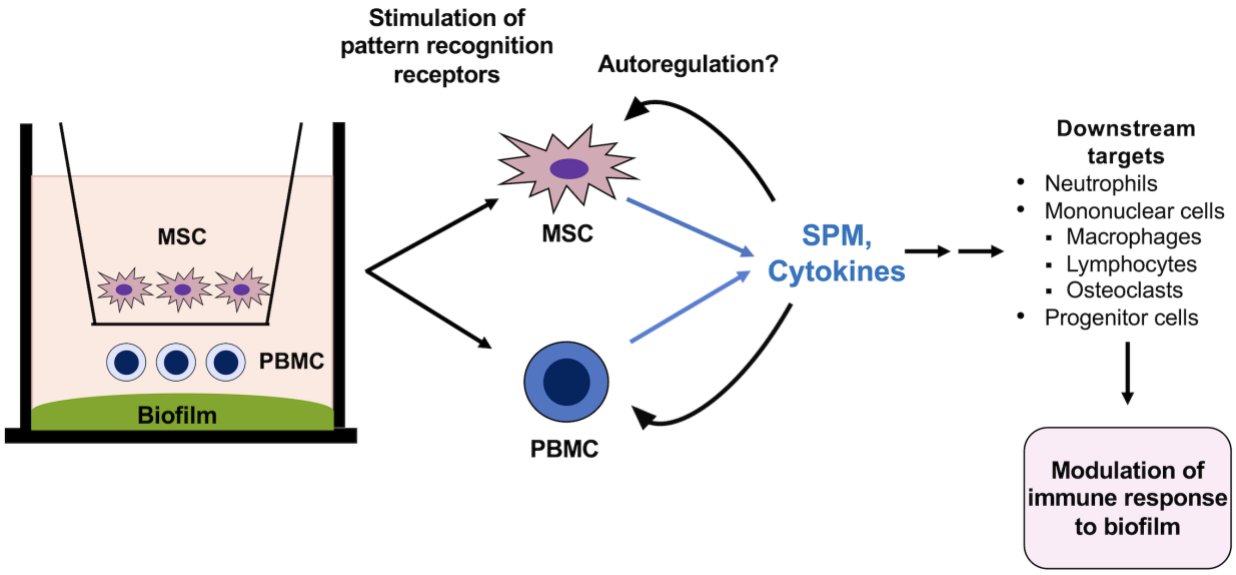

Figure 5.5: Possible pathways for modulation of the immune response to *S. aureus* biofilms. Stimulation of pattern recognition receptors on MSC and PBMC may generate secretion of SPM and inflammatory cytokines, which may influence either cell type in an autocrine or paracrine fashion or downstream immune cell effectors in the response to *S. aureus* biofilm infections.

Quantification of SPM produced by equine cells in this study is a novel approach to investigating the immunomodulatory properties MSC. Our LC-MS system utilizes internal standards that match the chemical structure and column retention times of the targets of interest as closely as possible, as lipid mediators are highly conserved between species [36, 37, 39, 55]. While calibration is often performed using pure standards that are each based on a specific isomer, chromatographic peaks of unknown lipids of interest may contain several isomers and vary between species [97]. Development of equine-specific standards may thereby help improve sensitivity of SPM detection in samples from equine cell culture. Lipidomic and cytokine/chemokine quantification are sensitive to variation between heterogenous individuals

[35, 40, 56, 103] and may be an additional source of sample variation seen in this study. Inclusion of a larger sample size may have improved detection of differences in lipids or cytokines/chemokines between groups (Maddipati, personal communication). While our conditioned medium collection process was tightly controlled, lipidomics and cytokine/chemokine quantification on ELISA are highly sensitive to small temperature changes [104] and storage time [105] and may be an additional source of variation in our results. Background presence of some SPM in our MSC medium, which contained autologous serum, is consistent with SPM detection in human serum [40] and may have masked some changes in SPM between groups.

We measured SPM following 24 and 48 hours of co-culture based on reported times of peak serum SPM levels following endotoxin challenge in people [40] and peak inflammatory cytokine levels in MSC culture [35]. Detection of changes in SPM and cytokines/chemokines following a 48-hour co-culture in our model indicates exposure time of biofilms to MSC and PBMC may be important to achieve immunomodulation. Measurement of SPM and cytokines/chemokines at earlier time points may have provided additional insight into the MSC immunomodulatory potential against *S. aureus* biofilms. SPM were detected in sera from people in early (< 12 hours) septic shock [98]. The peak detection time may also vary between mediator classes. Pro-inflammatory mediators PG and TX peaked at 8 hours, while pro-resolving resolvins, lipoxins peaked at 24 hours, post-endotoxin challenge in people [40]. Peak detection times for SPM and their metabolites may also vary between species. The arachidonic acid metabolite HETE peaked at 4 hours post-inflammatory challenge in people [106]. In comparison, the eicosapentaenoic acid metabolite HEPE peaked 1 hour following oxidative challenge but persisted for up to 7 days

post-challenge in mice [107]. Measurement of our analytes at additional time points is thereby necessary to further characterize the pro-resolving and anti-inflammatory responses of MSC to *S. aureus* biofilms and the potential for MSC to be utilized as an immunomodulatory therapy in equine orthopedic biofilm infections.

The cytokine/chemokine responses in our co-culture system warrant further investigation. While no cytokines or chemokines were altered when biofilms were co-cultured with MSC and PBMC versus PBMC alone, multiple pro-inflammatory cytokines were elevated in biofilm co-cultures compared to cell cultures alone. These findings are consistent with elevations in inflammatory cytokines produced by MSC and PBMC co-cultured with *S. aureus in vitro* [6, 7, 29, 108, 109]. While pre-stimulation of PBMC with phytohemagglutinin has been utilized to generate an MSC immunomodulatory response *in vitro* [48], we did not pre-stimulate PBMC in our study to reflect how PBMC may respond to MSC treatment in a clinical *S. aureus* biofilm infection. Pre-stimulation of MSC with toll like receptor ligands [102, 110-112], hypoxia [112-114], or three-dimensional culture [35, 115] enhances immunomodulatory function and may have improved the ability of MSC to reduce inflammatory cytokines and chemokines in our model. The MSC:PBMC ratio used in this study may also have influenced PBMC cytokine/chemokine production. We used an MSC:PBMC ratio of 1:5, which elicited PBMC inflammatory cytokine production [108] and an MSC immunomodulatory response in other studies [50]. Given that MSC immunomodulatory effects have been reported with MSC:PBMC ratios of 1:2 [116] to 1:10 [34, 48], evaluation of the cytokine/chemokine response to *S. aureus* biofilms over multiple MSC:PBMC ratios is warranted.

The reason for apparent detection of pro-inflammatory cytokines and chemokines in medium from untreated biofilms is unclear. Immune cytokines or chemokines are produced by eukaryotic cells in response to infectious/inflammatory stimuli [21] and would not be expected in purely bacterial culture systems. The minute detection levels of these mediators in unconditioned culture medium indicates a negligible baseline presence in the autologous sera used in the medium. Contamination of autologous serum with cells that would generate a cytokine response to biofilms is unlikely given that sera were filtered during preparation and frozen prior to use. The detection of inflammatory cytokines and chemokines from untreated biofilms may reflect a low level of cross-reaction of *S. aureus* secreted factors with ELISA reactions, combined with low overall cytokine/chemokine detection levels in co-culture groups. While circulating inflammatory cytokine responses to systemic *S. aureus* infections in mice [117], people [118], and cattle [68] have been successfully quantified, the cytokine response to *S. aureus* biofilms *in vitro* using an equine-specific assay has not been reported. The potential for cross-reaction of *S. aureus*-secreted factors with the equine multiplex ELISA warrants further investigation.

CONCLUSIONS

Co-culture of MSC and PBMC with *S. aureus* biofilms generated a visible antibiofilm response by pellicle area reduction and gross organizational loss. MSC altered production of multiple lipid mediators in response to *S. aureus* biofilms. The changes in SPM profile in response to *S. aureus* biofilms in our study are consistent with SPM responses to bacterial challenge in people [40, 98] and support the role of SPM as a key mechanism for MSC modulation of the immune response to biofilms. Conversely, the effect of MSC on the PBMC cytokine/chemokine response to

biofilms in this co-culture model requires further investigation. The results of our study give an initial basis on which to continue investigation of the SPM and cytokine/chemokine response of MSC to *S. aureus* biofilms.

Acknowledgements

The authors would like to thank the technical specialists at the Center for One Health Research (Nancy Tenpenny) and at the Collaborative Multidisciplinary Research Laboratory (Michelle Todd), the members of the Caswell Laboratory (Tristan Stoyanof, Dr. Mitchell Caudill), and numerous undergraduate students (Elanagh Smith, Olivia Brown, Breanna Murray, Emma Stewart, Kayla Hackler, Jacq Field, Hannah Elshafie, Sidney Schumaker, Jane Perkins), for their invaluable assistance and support.

Authors Disclosure

The authors have no conflicts of interest to disclose.

Funding Statement

Funding for this project was provided by the Morris Animal Foundation Large Animal Training Fellowship, the Regenerative Medicine Interdisciplinary Graduate Education Program and the Office of Research and Graduate Studies (Virginia Tech), and the Equine Research Competition (Virginia-Maryland College of Veterinary Medicine).

BIBLIOGRAPHY

1. Crawford EC, Singh A, Gibson TW, Scott Weese J. Biofilm-Associated Gene Expression in *Staphylococcus pseudintermedius* on a Variety of Implant Materials. Vet Surg. 2016;45:499-506.
2. Walker M, Singh A, Nazarali A, Gibson TW, Rousseau J, Weese JS. Evaluation of the Impact of Methicillin-Resistant *Staphylococcus pseudintermedius* Biofilm Formation on Antimicrobial Susceptibility. Vet Surg. 2016;45:968-71.
3. Pestrak MJ, Gupta TT, Dusane DH, Guzior DV, Staats A, Harro J, et al. Investigation of synovial fluid induced *Staphylococcus aureus* aggregate development and its impact on surface attachment and biofilm formation. PLoS One. 2020;15:e0231791.
4. Gilbertie JM, Schnabel LV, Hickok NJ, Jacob ME, Conlon BP, Shapiro IM, et al. Equine or porcine synovial fluid as a novel *ex vivo* model for the study of bacterial free-floating biofilms that form in human joint infections. PLoS One. 2019;14:e0221012.
5. Mandell JB, Orr S, Koch J, Nourie B, Ma D, Bonar DD, et al. Large variations in clinical antibiotic activity against *Staphylococcus aureus* biofilms of periprosthetic joint infection isolates. J Orthop Res. 2019;37:1604-9.
6. Wang X, Du J, Zhao C. Bacterial biofilms are associated with inflammatory cells infiltration and the innate immunity in chronic rhinosinusitis with or without nasal polyps. Inflammation. 2014;37:871-9.
7. Forestier C, Billard E, Milon G, Gueirard P. Unveiling and Characterizing Early Bilateral Interactions between Biofilm and the Mouse Innate Immune System. Front Microbiol. 2017;8:2309.

8. Prabhakara R, Harro JM, Leid JG, Keegan AD, Prior ML, Shirtliff ME. Suppression of the inflammatory immune response prevents the development of chronic biofilm infection due to methicillin-resistant *Staphylococcus aureus*. Infect Immun. 2011;79:5010-8.

9. Di Domenico EG, Cavallo I, Bordignon V, Prignano G, Sperduti I, Gurtner A, et al. Inflammatory cytokines and biofilm production sustain *Staphylococcus aureus* outgrowth and persistence: a pivotal interplay in the pathogenesis of atopic dermatitis. Sci Rep. 2018;8:9573.

10. Bidossi A, Bottagisio M, Savadori P, De Vecchi E. Identification and Characterization of Planktonic Biofilm-Like Aggregates in Infected Synovial Fluids From Joint Infections. Front Microbiol. 2020;11:1368.

11. Teterycz D, Ferry T, Lew D, Stern R, Assal M, Hoffmeyer P, et al. Outcome of orthopedic implant infections due to different staphylococci. Int J Infect Dis. 2010;14:e913-8.

12. Ahern BJ, Richardson DW, Boston RC, Schaer TP. Orthopedic infections in equine long bone fractures and arthrodeses treated by internal fixation: 192 cases (1990-2006). Vet Surg. 2010;39:588-93.

13. Pollmann CT, Dahl FA, Rotterud JHM, Gjertsen JE, Aroen A. Surgical site infection after hip fracture - mortality and risk factors: an observational cohort study of 1,709 patients. Acta Orthop. 2020;91:347-52.

14. Gomez E, Cazanave C, Cunningham SA, Greenwood-Quaintance KE, Steckelberg JM, Uhl JR, et al. Prosthetic joint infection diagnosis using broad-range PCR of biofilms dislodged from knee and hip arthroplasty surfaces using sonication. J Clin Microbiol. 2012;50:3501-8.

15. Shukla SK, Ward JP, Jacofsky MC, Sporer SM, Paprosky WG, Della Valle CJ. Perioperative testing for persistent sepsis following resection arthroplasty of the hip for periprosthetic infection. J Arthroplasty. 2010;25:87-91.

16. Kurtz SM, Lau E, Watson H, Schmier JK, Parvizi J. Economic burden of periprosthetic joint infection in the United States. J Arthroplasty. 2012;27:61-5 e1.

17. Goodrich LR. Osteomyelitis in horses. Vet Clin North Am Equine Pract. 2006;22:389-417, viii-ix.

18. Schneider RK, Bramlage LR, Moore RN, Mecklenburg LM, Kohn KW, Gabel AA. A retrospective of 192 horses affected with septic arthritis/tenosynovitis. Equine Vet J. 1992;24:436-42.

19. Curtiss AL, Stefanovski D, Richardson DW. Surgical site infection associated with equine orthopedic internal fixation: 155 cases (2008-2016). Vet Surg. 2019;48:685-93.

20. Rinnovati R, Butina BB, Lanci A, Mariella J. Diagnosis, Treatment, Surgical Management, and Outcome of Septic Arthritis of Tarsocrural Joint in 16 Foals. J Equine Vet Sci. 2018;67:128-32.

21. Tizard I. Veterinary Immunology, 10th ed. Saunders Elsevier, Ltd. Philadelphia, Pennsylvania, USA. 2019.

22. Tukel C, Nishimori JH, Wilson RP, Winter MG, Keestra AM, van Putten JP, et al. Toll-like receptors 1 and 2 cooperatively mediate immune responses to curli, a common amyloid from enterobacterial biofilms. Cell Microbiol. 2010;12:1495-505.

23. Varoga D, Klostermeier E, Paulsen F, Wruck C, Lippross S, Brandenburg LO, et al. The antimicrobial peptide HBD-2 and the Toll-like receptors-2 and -4 are induced in synovial membranes in case of septic arthritis. Virchows Arch. 2009;454:685-94.

24. Vedrine M, Berthault C, Leroux C, Reperant-Ferter M, Gitton C, Barbey S, et al. Sensing of *Escherichia coli* and LPS by mammary epithelial cells is modulated by O-antigen chain and CD14. PLoS One. 2018;13:e0202664.

25. Smith WL, Urade Y, Jakobsson PJ. Enzymes of the cyclooxygenase pathways of prostanoid biosynthesis. Chem Rev. 2011;111:5821-65.

26. Menarim B, Gillis K, Oliver A, Ngo Y, Mason C, Byron C, et al. Autologous bone marrow mononuclear cells modulate joint homeostasis in an equine *in vivo* model of synovitis. Orthopedic Research Society Annual Meeting. Austin, TX2019.

27. Menarim BC, Gillis KH, Oliver A, Mason C, Werre SR, Luo X, et al. Inflamed synovial fluid induces a homeostatic response in bone marrow mononuclear cells *in vitro*: Implications for joint therapy. FASEB J. 2020;34:4430-44.

28. Rieger AM, Hall BE, Barreda DR. Macrophage activation differentially modulates particle binding, phagocytosis and downstream antimicrobial mechanisms. Dev Comp Immunol. 2010;34:1144-59.

29. Leid JG, Shirtliff ME, Costerton JW, Stoodley P. Human leukocytes adhere to, penetrate, and respond to *Staphylococcus aureus* biofilms. Infect Immun. 2002;70:6339-45.

30. Levy BD, Clish, C. B., Schmidt, B., Gronert, K., Serhan, C. N. Lipid mediator class switching during acute inflammation: signals in resolution. Nat Immunol. 2001;2:612-9.

31. Yamamuro Y, Kabata T, Nojima T, Hayashi K, Tokoro M, Kajino Y, et al. Combined adipose-derived mesenchymal stem cell and antibiotic therapy can effectively treat periprosthetic joint infection in rats. Sci Rep. 2023;13:3949.

32. Menarim BC, El-Sheikh Ali H, Loux SC, Scoggin KE, Kalbfleisch TS, MacLeod JN, et al. Transcriptional and Histochemical Signatures of Bone Marrow Mononuclear Cell-Mediated Resolution of Synovitis. Front Immunol. 2021;12:734322.

33. Everett J. Bone marrow mononuclear cell therapy for equine joint disease. Proceedings: 66th Annual Convention, Am Assoc Equine Pract. Virtual. 2020. p. 226-7.

34. Colbath AC, Dow SW, Phillips JN, McIlwraith CW, Goodrich LR. Autologous and Allogeneic Equine Mesenchymal Stem Cells Exhibit Equivalent Immunomodulatory Properties *In Vitro*. Stem Cells Dev. 2017;26:503-11.

35. Bogers SH, Barrett JG. Three-Dimensional Culture of Equine Bone Marrow-Derived Mesenchymal Stem Cells Enhances Anti-Inflammatory Properties in a Donor-Dependent Manner. Stem Cells Dev. 2022;31:777-86.

36. Chen J, Xu H, Xia K, Cheng S, Zhang Q. Resolvin E1 accelerates pulp repair by regulating inflammation and stimulating dentin regeneration in dental pulp stem cells. Stem Cell Res Ther. 2021;12:75.

37. Cianci E, Recchiuti A, Trubiani O, Diomede F, Marchisio M, Miscia S, et al. Human Periodontal Stem Cells Release Specialized Proresolving Mediators and Carry Immunomodulatory and Prohealing Properties Regulated by Lipoxins. Stem Cells Transl Med. 2016;5:20-32.

38. Bai Y, Wang J, He Z, Yang M, Li L, Jiang H. Mesenchymal Stem Cells Reverse Diabetic Nephropathy Disease via Lipoxin A4 by Targeting Transforming Growth Factor beta (TGF-beta)/smad Pathway and Pro-Inflammatory Cytokines. Med Sci Monit. 2019;25:3069-76.

39. Schwab JM, Chiang N, Arita M, Serhan CN. Resolvin E1 and protectin D1 activate inflammation-resolution programmes. Nature. 2007;447:869-74.

40. Norris PC, Skulas-Ray AC, Riley I, Richter CK, Kris-Etherton PM, Jensen GL, et al. Identification of specialized pro-resolving mediator clusters from healthy adults after intravenous low-dose endotoxin and omega-3 supplementation: a methodological validation. Sci Rep. 2018;8:18050.

41. Fiore S, Ryeom SW, Weller PF, Serhan CN. Lipoxin recognition sites. Specific binding of labeled lipoxin A4 with human neutrophils. J Biol Chem. 1992;267:16168-76.

42. Gaudin A, Tolar M, Peters OA. Lipoxin A4 Attenuates the Inflammatory Response in Stem Cells of the Apical Papilla via ALX/FPR2. Sci Rep. 2018;8:8921.

43. Jordan PM, Gerstmeier J, Pace S, Bilancia R, Rao Z, Borner F, et al. *Staphylococcus aureus*-Derived alpha-Hemolysin Evokes Generation of Specialized Pro-resolving Mediators Promoting Inflammation Resolution. Cell Rep. 2020;33:108247.

44. Liu T, Xiang A, Peng T, Doran AC, Tracey KJ, Barnes BJ, et al. HMGB1-C1q complexes regulate macrophage function by switching between leukotriene and specialized proresolving mediator biosynthesis. Proc Natl Acad Sci U S A. 2019;116:23254-63.

45. Sugimoto MA, Sousa LP, Pinho V, Perretti M, Teixeira MM. Resolution of Inflammation: What Controls Its Onset? Front Immunol. 2016;7:160.

46. Aggarwal S, Pittenger MF. Human mesenchymal stem cells modulate allogeneic immune cell responses. Blood. 2005;105:1815-22.

47. Barrachina L, Remacha AR, Romero A, Vazquez FJ, Albareda J, Prades M, et al. Priming Equine Bone Marrow-Derived Mesenchymal Stem Cells with Proinflammatory Cytokines: Implications in Immunomodulation-Immunogenicity Balance, Cell Viability, and Differentiation Potential. Stem Cells Dev. 2017;26:15-24.

48. Ranera B, Antczak D, Miller D, Doroshenkova T, Ryan A, McIlwraith CW, et al. Donor-derived equine mesenchymal stem cells suppress proliferation of mismatched lymphocytes. Equine Vet J. 2016;48:253-60.

49. Carrade Holt DD, Wood JA, Granick JL, Walker NJ, Clark KC, Borjesson DL. Equine mesenchymal stem cells inhibit T cell proliferation through different mechanisms depending on tissue source. Stem Cells Dev. 2014;23:1258-65.

50. Carrade DD, Lame MW, Kent MS, Clark KC, Walker NJ, Borjesson DL. Comparative Analysis of the Immunomodulatory Properties of Equine Adult-Derived Mesenchymal Stem Cells. Cell Med. 2012;4:1-11.

51. Ferris DJ, Frisbie DD, Kisiday JD, McIlwraith CW, Hague BA, Major MD, et al. Clinical Outcome After Intra-Articular Administration of Bone Marrow Derived Mesenchymal Stem Cells in 33 Horses With Stifle Injury. Vet Surg 2014;43:255-65.

52. McCoy AM, Smith RL, Herrera S, Kawcak CE, McIlwraith CW, Goodrich LR. Long-term outcome after stifle arthroscopy in 82 Western performance horses (2003-2010). Vet Surg. 2019;48:956-65.

53. Crovace A, Lacitignola L, Rossi G, Francioso E. Histological and immunohistochemical evaluation of autologous cultured bone marrow mesenchymal stem cells and bone marrow mononucleated cells in collagenase-induced tendinitis of equine superficial digital flexor tendon. Vet Med Int. 2010;2010:250978.

54. Depuydt E, Broeckx SY, Van Hecke L, Chiers K, Van Brantegem L, van Schie H, et al. The Evaluation of Equine Allogeneic Tenogenic Primed Mesenchymal Stem Cells in a Surgically Induced Superficial Digital Flexor Tendon Lesion Model. Front Vet Sci. 2021;8:641441.

55. Yamada T, Tani Y, Nakanishi H, Taguchi R, Arita M, Arai H. Eosinophils promote resolution of acute peritonitis by producing proresolving mediators in mice. FASEB J. 2011;25:561-8.

56. Bai Y, Huang W, Li Y, Lai C, Huang S, Wang G, et al. Lipidomic alteration of plasma in cured COVID-19 patients using ultra high-performance liquid chromatography with high-resolution mass spectrometry. Biosci Rep. 2021;41.

57. Zhang XY, Sun K, Abulimiti A, Xu PP, Li ZY. Microfluidic System for Observation of Bacterial Culture and Effects on Biofilm Formation at Microscale. Micromachines (Basel). 2019;10.

58. Buzzo JR, Devaraj A, Gloag ES, Jurcisek JA, Robledo-Avila F, Kesler T, et al. Z-form extracellular DNA is a structural component of the bacterial biofilm matrix. Cell. 2021;184:5740-58 e17.

59. Correa F, Borlone C, Wittwer F, Bustamante H, Muller A, Ramirez A, et al. How to obtain and isolate equine sternal bone marrow mononuclear cells with limited resources. Arch Med Vet. 2014;46:471-6.

60. Fortier LN, Nixon AJ, Williams J, Cable CS. Isolation and chondrocytic differentiation of equine bone marrow-derived mesenchymal stem cells. Am J Vet Res. 1998;59:1182-7.

61. Bourzac C, Smith LC, Vincent P, Beauchamp G, Lavoie JP, Laverty S. Isolation of equine bone marrow-derived mesenchymal stem cells: a comparison between three protocols. Equine Vet J. 2010;42:519-27.

62. Zahedi M, Parham A, Dehghani H, Kazemi Mehrjerdi H. Equine bone marrow-derived mesenchymal stem cells: optimization of cell density in primary culture. Stem Cell Investig. 2018;5:31.

63. Mustafa A, Gillmeister L, Hernandez WP, Larsen CT, Witonsky S, Holladay SD, et al. Viability and function in lymphocytes cultured from the horse, chicken, and mouse: effects of different leukocyte enrichment techniques. J Immunoassay Immunochem. 2008;29:370-89.

64. Nazarpour RZ, Zabihi E, Alijanpour E, Abedian Z, Mehdizadeh H, Rahimi F. Optimization of Human Peripheral Blood Mononuclear Cells (PBMCs) Cryopreservation. Int J Mol Cell Med. 2012;1:88-93.

65. Gilbertie JM, Schaer TP, Engiles JB, Seiler GS, Deddens BL, Schubert AG, et al. A Platelet-Rich Plasma-Derived Biologic Clears *Staphylococcus aureus* Biofilms While Mitigating Cartilage Degeneration and Joint Inflammation in a Clinically Relevant Large Animal Infectious Arthritis Model. Front Cell Infect Microbiol. 2022;12:895022.

66. Wu X, Zhang Y, Chen X, Chen J, Jia M. Inflammatory immune response in rabbits with *Staphylococcus aureus* biofilm-associated sinusitis. Int Forum Allergy Rhinol. 2018;8:1226-32.

67. Ebersole JL, Peyyala R, Gonzalez OA. Biofilm-induced profiles of immune response gene expression by oral epithelial cells. Mol Oral Microbiol. 2019;34.

68. Lesueur J, Walachowski S, Barbey S, Cebron N, Lefebvre R, Launay F, et al. Standardized Whole Blood Assay and Bead-Based Cytokine Profiling Reveal Commonalities and Diversity of the Response to Bacteria and TLR Ligands in Cattle. Front Immunol. 2022;13:871780.

69. Assenmacher M, Löhning M, Scheffold A, Manz RA, Schmitz J, Radbruch A. Sequential production of IL-2, IFN-γ and IL-10 by individual staphylococcal enterotoxin B-activated T helper lymphocytes. Euro J Immunol. 1998;28:1534-43.

70. Gutierrez Jauregui R, Fleige H, Bubke A, Rohde M, Weiss S, Forster R. IL-1 beta Promotes *Staphylococcus aureus* Biofilms on Implants *in vivo*. Front Immunol. 2019;10:1082.

71. Bielen K, Jongers B, Boddaert J, Raju TK, Lammens C, Malhotra-Kumar S, et al. Biofilm-Induced Type 2 Innate Immunity in a Cystic Fibrosis Model of *Pseudomonas aeruginosa*. Front Cell Infect Microbiol. 2017;7:274.

72. Buzás K, Megyeri A, Miczák AF, Degré M, Mándi Y, Rosztóczy I. Different Staphylococcal Strains Elicit Different Levels of Production of T-helper 1-inducing Cytokines. Acta Microbiol Immunol Hung. 2004;51:371-84.

73. Maina IW, Patel NN, Cohen NA. Understanding the Role of Biofilms and Superantigens in Chronic Rhinosinusitis. Curr Otorhinolaryngol Rep. 2018;6:253-62.

74. Mariani E, Filardo G, Canella V, Berlingeri A, Bielli A, Cattini L, et al. Platelet-rich plasma affects bacterial growth *in vitro*. Cytotherapy. 2014;16:1294-304.

75. Saba S, Soong G, Greenberg S, Prince A. Bacterial stimulation of epithelial G-CSF and GM-CSF expression promotes PMN survival in CF airways. Am J Respir Cell Mol Biol. 2002;27:561-7.

76. Rammal A, Tewfik M, Rousseau S. Differences in RANTES and IL-6 levels among chronic rhinosinusitis patients with predominant Gram-negative and Gram-positive infection. J Otolaryngol Head Neck Surg. 2017;46:7.

77. Afami ME, El Karim I, About I, Coulter SM, Laverty G, Lundy FT. Ultrashort Peptide Hydrogels Display Antimicrobial Activity and Enhance Angiogenic Growth Factor Release by Dental Pulp Stem/Stromal Cells. Materials (Basel). 2021;14.

78. Heim CE, Vidlak D, Scherr TD, Hartman CW, Garvin KL, Kielian T. IL-12 promotes myeloid-derived suppressor cell recruitment and bacterial persistence during *Staphylococcus aureus* orthopedic implant infection. J Immunol. 2015;194:3861-72.

79. Dufour JH, Dziejman M, Liu MT, Leung JH, Lane TE, Luster AD. IFN-gamma-inducible protein 10 (IP-10; CXCL10)-deficient mice reveal a role for IP-10 in effector T cell generation and trafficking. J Immunol. 2002;168:3195-204.

80. de la Fuente-Nunez C, Mansour SC, Wang Z, Jiang L, Breidenstein EB, Elliott M, et al. Anti-Biofilm and Immunomodulatory Activities of Peptides That Inhibit Biofilms Formed by Pathogens Isolated from Cystic Fibrosis Patients. Antibiotics (Basel). 2014;3:509-26.

81. Gunther F, Wabnitz GH, Stroh P, Prior B, Obst U, Samstag Y, et al. Host defence against *Staphylococcus aureus* biofilms infection: phagocytosis of biofilms by polymorphonuclear neutrophils (PMN). Mol Immunol. 2009;46:1805-13.

82. May SA, Hooke RE, Lees P. Adverse conditions *in vitro* stimulate chondrocytes to produce prostaglandin E2 and stromelysin. Equine Vet J. 1991;23:380-2.

83. Frisbie DD, Kisiday JD, Kawcak CE, Werpy NM, McIlwraith CW. Evaluation of adipose-derived stromal vascular fraction or bone marrow-derived mesenchymal stem cells for treatment of osteoarthritis. J Orthop Res. 2009;27:1675-80.

84. Kirker-Head C, Chandna V, Agarwal R, Morris E, A T, MW OC, et al. Concentrations of substance P and prostaglandin E2 in synovial fluid of normal and abnormal joints of horses. Am J Vet Res. 2000;61:714-18.

85. Jiang W, Jin Y, Zhang S, Ding Y, Huo K, Yang J, et al. PGE2 activates EP4 in subchondral bone osteoclasts to regulate osteoarthritis. Bone Res. 2022;10:27.

86. Manferdini C, Paolella F, Gabusi E, Gambari L, Piacentini A, Filardo G, et al. Adipose stromal cells mediated switching of the pro-inflammatory profile of M1-like macrophages is facilitated by PGE_2: *in vitro* evaluation. Osteoarthritis Cartilage. 2017;25:1161-71.

87. Mangal D, Uboh CE, Soma LR, Liu Y. Inhibitory effect of triamcinolone acetonide on synthesis of inflammatory mediators in the equine. Eur J Pharmacol. 2014;736:1-9.

88. Janeway's Immunobiology, 4th ed. Garland Science, Taylor and Francis Group, LLC, New York New York, USA. 2012.

89. Strong VE, Mackrell PJ, Concannon EM, Naama HA, Schaefer PA, Shaftan GW, et al. Blocking prostaglandin E2 after trauma attenuates pro-inflammatory cytokines and improves survival. Shock. 2000;14:374-9.

90. Hyvarinen K, Holopainen M, Skirdenko V, Ruhanen H, Lehenkari P, Korhonen M, et al. Mesenchymal Stromal Cells and Their Extracellular Vesicles Enhance the Anti-Inflammatory Phenotype of Regulatory Macrophages by Downregulating the Production of Interleukin (IL)-23 and IL-22. Front Immunol. 2018;9:771.

91. Mainka M, George S, Angioni C, Ebert R, Goebel T, Kampschulte N, et al. On the biosynthesis of specialized pro-resolving mediators in human neutrophils and the influence of cell integrity. Biochim Biophys Acta Mol Cell Biol Lipids. 2022;1867:159093.

92. Wang B, Wu L, Chen J, Dong L, Chen C, Wen Z, et al. Metabolism pathways of arachidonic acids: mechanisms and potential therapeutic targets. Signal Transduct Target Ther. 2021;6:94.

93. Serhan CN, Chiang N, Dalli J. New pro-resolving n-3 mediators bridge resolution of infectious inflammation to tissue regeneration. Mol Aspects Med. 2018;64:1-17.

94. Endo J, Sano M, Isobe Y, Fukuda K, Kang JX, Arai H, et al. 18-HEPE, an n-3 fatty acid metabolite released by macrophages, prevents pressure overload-induced maladaptive cardiac remodeling. J Exp Med. 2014;211:1673-87.

95. von Schacky C, Marcus AJ, Safier LB, Ullman HL, Islam N, Broekman MJ, et al. Platelet-neutrophil interactions. 12S,20- and 5S,12S-dihydroxyeicosapentaenoic acids: two novel neutrophil metabolites from platelet-derived 12S-hydroxyeicosapentaenoic acid. J Lipid Res. 1990;31:801-10.

96. Callan N, Hanes D, Bradley R. Early evidence of efficacy for orally administered SPM-enriched marine lipid fraction on quality of life and pain in a sample of adults with chronic pain. J Transl Med. 2020;18:401.

97. Schebb NH, Kuhn H, Kahnt AS, Rund KM, O'Donnell VB, Flamand N, et al. Formation, Signaling and Occurrence of Specialized Pro-Resolving Lipid Mediators-What is the Evidence so far? Front Pharmacol. 2022;13:838782.

98. Kutzner L, Rund KM, Ostermann AI, Hartung NM, Galano JM, Balas L, et al. Development of an Optimized LC-MS Method for the Detection of Specialized Pro-Resolving Mediators in Biological Samples. Front Pharmacol. 2019;10:169.

99. Holopainen M, Colas RA, Valkonen S, Tigistu-Sahle F, Hyvarinen K, Mazzacuva F, et al. Polyunsaturated fatty acids modify the extracellular vesicle membranes and increase the production of proresolving lipid mediators of human mesenchymal stromal cells. Biochim Biophys Acta Mol Cell Biol Lipids. 2019;1864:1350-62.

100. Tai HH, Ensor CM, Tong M, Zhou H, Yan F. Prostaglandin catabolizing enzymes. Prostaglandins Other Lipid Mediat. 2002;68-69:483-93.

101. Lavy M, Gauttier V, Poirier N, Barille-Nion S, Blanquart C. Specialized Pro-Resolving Mediators Mitigate Cancer-Related Inflammation: Role of Tumor-Associated Macrophages and Therapeutic Opportunities. Front Immunol. 2021;12:702785.

102. Pezzanite LM, Chow L, Johnson V, Griffenhagen GM, Goodrich L, Dow S. Toll-like receptor activation of equine mesenchymal stromal cells to enhance antibacterial activity and immunomodulatory cytokine secretion. Vet Surg. 2021;50:858-71.

103. Sun X, Qu T, Wang W, Li C, Yang X, He X, et al. Untargeted lipidomics analysis in women with intrahepatic cholestasis of pregnancy: a cross-sectional study. BJOG. 2022;129:880-8.

104. Lupo S. LC-MS Sensitivity: Practical Strategies to Boost Your Signal and Lower Your Noise. LCGC North America. 2018;36:652-60.

105. de Jager W, Bourcier K, Rijkers GT, Prakken BJ, Seyfert-Margolis V. Prerequisites for cytokine measurements in clinical trials with multiplex immunoassays. BMC Immunol. 2009;10:52.

106. Mazaleuskaya LL, Salamatipour A, Sarantopoulou D, Weng L, FitzGerald GA, Blair IA, et al. Analysis of HETEs in human whole blood by chiral UHPLC-ECAPCI/HRMS. J Lipid Res. 2018;59:564-75.

107. Leiria LO, Wang CH, Lynes MD, Yang K, Shamsi F, Sato M, et al. 12-Lipoxygenase Regulates Cold Adaptation and Glucose Metabolism by Producing the Omega-3 Lipid 12-HEPE from Brown Fat. Cell Metab. 2019;30:768-83 e7.

108. Liu T, Nerren J, Liu M, Martens R, Cohen N. Basal and stimulus-induced cytokine expression is selectively impaired in peripheral blood mononuclear cells of newborn foals. Vaccine. 2009;27:674-83.

109. Peres AG, Stegen C, Li J, Xu AQ, Levast B, Surette MG, et al. Uncoupling of pro- and anti-inflammatory properties of *Staphylococcus aureus*. Infect Immun. 2015;83:1587-97.

110. Gupta N, Sinha R, Krasnodembskaya A, Xu X, Nizet V, Matthay MA, et al. The TLR4-PAR1 Axis Regulates Bone Marrow Mesenchymal Stromal Cell Survival and Therapeutic Capacity in Experimental Bacterial Pneumonia. Stem Cells. 2018;36:796-806.

111. Monsel A, Zhu YG, Gennai S, Hao Q, Hu S, Rouby JJ, et al. Therapeutic Effects of Human Mesenchymal Stem Cell-derived Microvesicles in Severe Pneumonia in Mice. Am J Respir Crit Care Med. 2015;192:324-36.

112. Crisostomo PR, Wang Y, Markel TA, Wang M, Lahm T, Meldrum DR. Human mesenchymal stem cells stimulated by TNF-alpha, LPS, or hypoxia produce growth factors by an NF kappa B- but not JNK-dependent mechanism. Am J Physiol Cell Physiol. 2008;294:C675-82.

113. Wang D, Chen D, Yu J, Liu J, Shi X, Sun Y, et al. Impact of Oxygen Concentration on Metabolic Profile of Human Placenta-Derived Mesenchymal Stem Cells As Determined by Chemical Isotope Labeling LC-MS. J Proteome Res. 2018;17:1866-78.

114. Ohnishi S, Yasuda T, Kitamura S, Nagaya N. Effect of hypoxia on gene expression of bone marrow-derived mesenchymal stem cells and mononuclear cells. Stem Cells. 2007;25:1166-77.

115. Park MJ, Lee J, Byeon JS, Jeong DU, Gu NY, Cho IS, et al. Effects of three-dimensional spheroid culture on equine mesenchymal stem cell plasticity. Vet Res Commun. 2018;42:171-81.

116. Paterson Y, Rash, N., Garvican, E. R., Paillot, R., Guest, D. J. Equine mesenchymal stromal cells and embryo-derived stem cells are immune privileged *in vitro*. Stem Cell Res Ther. 2014;5:1-13.

117. van den Berg S, Bowden MG, Bosma T, Buist G, van Dijl JM, van Wamel WJ, et al. A multiplex assay for the quantification of antibody responses in *Staphylococcus aureus* infections in mice. J Immunol Methods. 2011;365:142-8.

118. Leuzzi R, Bodini M, Thomsen IP, Soldaini E, Bartolini E, Muzzi A, et al. Dissecting the Human Response to *Staphylococcus aureus* Systemic Infections. Front Immunol. 2021;12:749432.

CHAPTER 6: CONCLUSIONS AND FUTURE DIRECTIONS

Orthopedic biofilm infections pose a significant health risk to people and horses. Biofilm infections can persist in the face of multimodal surgical debridement and long-term systemic and antimicrobial therapy. Moreover, biofilms can simultaneously avoid the host immune response and aggravate chronic inflammation and cause secondary tissue damage. Available treatments for orthopedic infections have yet to achieve both biofilm elimination and modulation of the immune response to biofilms. In order to address this unmet need, the overarching objectives of this dissertation were to investigate the ability of equine bone marrow-derived MSC to disrupt biofilms of orthopedic pathogens and modulate the immune response to orthopedic biofilms *in vitro*.

An *in vitro* model was developed in Chapter 3 that allowed MSC-biofilm interaction and quantification of biofilm biomass, pellicle size, and live bacterial counts. This model provided a novel yet simple approach to evaluate the mechanisms of MSC-biofilm interactions and evaluate MSC antibiofilm efficacy. Previous models combined biofilms with MSC conditioned medium [1-3], which does not allow MSC-biofilm interactions. Other models added MSC directly to biofilms [1], which would complicate downstream quantification of biofilm biomass and pellicle area. Therefore, our model represents a valuable tool with which to investigate further mechanisms of MSC to combat established biofilms of *S. aureus* and *E. coli*.

Utilizing the model developed in Chapter 3, we sought to evaluate MSC-mediated reduction of biofilms of common orthopedic pathogens and immune response modulation by MSC in Chapters 4 and 5. We demonstrated that the primary anti-biofilm mechanism of MSC was

disruption of the biofilm matrix, as evidenced by *S. aureus* biomass reduction and *S. aureus* and *E. coli* pellicle area reduction. However, MSC did not consistently reduce biofilm live bacterial counts across both bacteria and timepoints. This finding may reflect the need to separately quantify live bacteria within the adhered biofilm versus in the medium and/or pre-stimulate MSC with pattern recognition receptor ligands, such as lipopolysaccharide, to improve bacterial killing [3, 6]. In Chapter 5, co-culture of MSC with *S. aureus* biofilms and PBMC reduced biofilm pellicle area, consistent with findings in Chapter 4. MSC + PBMC + biofilm co-culture also increased detection of multiple pro-inflammatory and pro-resolving lipid mediators, including PGE_2, compared to MSC or PBMC cultures alone. This finding suggests that SPM release may be a mechanism by which MSC modulate the immune response to biofilms. Levels of multiple inflammatory cytokines on multiplex bead ELISA were also increased in MSC + PBMC + biofilm co-culture but were not different from untreated biofilms. The apparent and unexpected detection of inflammatory cytokines in medium from biofilms suggests possible interference between factors secreted by *S. aureus* and the ELISA that warrants further investigation.

The results of this dissertation provide useful initial mechanistic information on how MSC may combat orthopedic biofilms and open multiple avenues for continued investigation. Before MSC can be translated into an antibiofilm therapy, it is imperative to determine the optimal MSC dose for biofilm matrix disruption *and* live bacterial reduction. It is also essential to evaluate whether the effective MSC dose varies between bacterial strains, species, or even MSC source tissue.

Polymicrobial biofilms are common *in vivo* and enhance survival of indwelling bacteria by facilitating bacterial co-aggregation and secretion of matrix [6]. They may be more resistant to

disruption by MSC than biofilms of a single species and strain. The ability of MSC to disrupt polymicrobial biofilms therefore requires further investigation. It is possible that MSC manipulations discussed in Chapters 4 and 5, including pre-stimulation with pattern recognition receptor ligands [3, 6], hypoxia [7], or spheroid culture [4] may be essential for MSC to achieve any efficacy against polymicrobial biofilms.

Another crucial question is whether MSC-mediated biofilm matrix disruption is due to inhibition of bacterial quorum sensing. Quorum sensing is important in all stages of biofilm formation as outlined in Chapter 1 [8]. Natural antimicrobial peptides derived from plant extracts [9, 10] and synthetic antimicrobial peptides modeled after mammalian peptides [11, 12] have recently been shown to reduce biofilms by interrupting quorum sensing. Given that equine MSC secrete multiple antimicrobial peptides, the potential for MSC to disrupt quorum sensing is worth investigating. Utilization of a microfluidics system to evaluate parallel changes in biofilm growth and in expression of quorum sensing-related genes during co-culture with MSC would provide useful mechanistic insights.

Finally, the importance of identifying and isolating the active MSC-derived factor(s) that disrupt biofilms and modulate the immune response to biofilms cannot be overstated. Infected orthopedic structures represent true emergencies that require prompt and aggressive surgical and antimicrobial treatment to resolve. Unfortunately, delays in infection diagnosis and treatment are all too common in horses and lead to development of recalcitrant biofilm infections that recur in the face of treatment and cause crippling and life-threatening bone and joint destruction. Isolation of MSC for autologous treatment is time-intensive and delays timely initiation of

treatment. The ability to isolate the active antibiofilm factor(s) as a commercially available allogeneic treatment is therefore an attractive option. Direct isolation of MSC-secreted antimicrobial peptides or design of synthetic homologous peptides may be options for treatment translation. Alternatively, the ability to harness MSC-secreted extracellular vesicles as a treatment modality may provide a dual antibacterial and immunomodulatory therapy for orthopedic biofilm infections. Human MSC have recently been discovered to secrete both AMP [13] and immunoregulatory lipid mediators, such as PGE_2, in extracellular vesicles [14, 15]. Whether equine MSC also secrete their antimicrobial peptides and/or SPM via extracellular vesicles, and the safety of administering these vesicles as an allogeneic anti-biofilm therapy, is worthy of investigation. Isolation of MSC-secreted extracellular vesicles on a large scale would also facilitate pooling of vesicles across horses to reduce the effect of inter-donor variation on treatment efficacy. This approach is similar to the pooling of samples used in the production of equine platelet-rich plasma lysate (BIO-PLY™) [16].

The primary contribution of this dissertation is to provide the basis for continued investigation into the mechanisms of MSC-mediated biofilm reduction and immunomodulation that is required for eventual translation into an effective treatment for orthopedic infections. The potential to harness MSC as an anti-biofilm therapy would not only improve the overall ability of clinicians to treat orthopedic infections, but would also provide horses with chronic orthopedic infections the hope of a cure and a second chance at life.

References

1. Harman RM, Yang S, He MK, Van de Walle GR. Antimicrobial peptides secreted by equine mesenchymal stromal cells inhibit the growth of bacteria commonly found in skin wounds. Stem Cell Res Ther. 2017;8:157.
2. Marx C, Gardner S, Harman RM, Van de Walle GR. The mesenchymal stromal cell secretome impairs methicillin-resistant *Staphylococcus aureus* biofilms via cysteine protease activity in the equine model. Stem Cells Transl Med. 2020.
3. Cortes-Araya Y, Amilon K, Rink BE, Black G, Lisowski Z, Donadeu FX, et al. Comparison of Antibacterial and Immunological Properties of Mesenchymal Stem/Stromal Cells from Equine Bone Marrow, Endometrium, and Adipose Tissue. Stem Cells Dev. 2018;27:1518-25.
4. Bogers SH, Barrett JG. Three-Dimensional Culture of Equine Bone Marrow-Derived Mesenchymal Stem Cells Enhances Anti-Inflammatory Properties in a Donor-Dependent Manner. Stem Cells Dev. 2022;31:777-86.
5. Carter-Arnold JL, Neilsen NL, Amelse LL, Odoi A, Dhar MS. *In vitro* analysis of equine, bone marrow-derived mesenchymal stem cells demonstrates differences within age- and gender-matched horses. Equine Vet J. 2014;46:589-95.
6. Pezzanite LM, Chow L, Johnson V, Griffenhagen GM, Goodrich L, Dow S. Toll-like receptor activation of equine mesenchymal stromal cells to enhance antibacterial activity and immunomodulatory cytokine secretion. Vet Surg. 2021;50:858-71.
7. Crisostomo PR, Wang Y, Markel TA, Wang M, Lahm T, Meldrum DR. Human mesenchymal stem cells stimulated by TNF-alpha, LPS, or hypoxia produce growth factors

by an NF kappa B- but not JNK-dependent mechanism. Am J Physiol Cell Physiol. 2008;294:C675-82.

8. Solano C, Echeverz M, Lasa I. Biofilm dispersion and quorum sensing. Curr Opin Microbiol. 2014;18:96-104.
9. Dettweiler M, Lyles JT, Nelson K, Dale B, Reddinger RM, Zurawski DV, et al. American Civil War plant medicines inhibit growth, biofilm formation, and quorum sensing by multidrug-resistant bacteria. Sci Rep. 2019;9:7692.
10. Caceres M, Hidalgo W, Stashenko E, Torres R, Ortiz C. Essential Oils of Aromatic Plants with Antibacterial, Anti-Biofilm and Anti-Quorum Sensing Activities against Pathogenic Bacteria. Antibiotics (Basel). 2020;9.
11. Oliveira JTA, Souza PFN, Vasconcelos IM, Dias LP, Martins TF, Van Tilburg MF, et al. Mo-CBP3-PepI, Mo-CBP3-PepII, and Mo-CBP3-PepIII are synthetic antimicrobial peptides active against human pathogens by stimulating ROS generation and increasing plasma membrane permeability. Biochimie. 2019;157:10-21.
12. Amirkhanov NV, Tikunova NV, Pyshnyi DV. Synthetic Antimicrobial Peptides: I. Antimicrobial Activity of Amphiphilic and Nonamphiphilic Cationic Peptides. Russian J Bioorg Chem. 2018;44:492-503.
13. Alcayaga-Miranda F, Cuenca J, Khoury M. Antimicrobial Activity of Mesenchymal Stem Cells: Current Status and New Perspectives of Antimicrobial Peptide-Based Therapies. Front Immunol. 2017;8:339.
14. Hyvarinen K, Holopainen M, Skirdenko V, Ruhanen H, Lehenkari P, Korhonen M, et al. Mesenchymal Stromal Cells and Their Extracellular Vesicles Enhance the Anti-

Inflammatory Phenotype of Regulatory Macrophages by Downregulating the Production of Interleukin (IL)-23 and IL-22. Front Immunol. 2018;9:771.

15. Mocchi M, Dotti S, Bue MD, Villa R, Bari E, Perteghella S, et al. Veterinary Regenerative Medicine for Musculoskeletal Disorders: Can Mesenchymal Stem/Stromal Cells and Their Secretome Be the New Frontier? Cells. 2020;9.
16. Gilbertie JM, Schaer TP, Engiles JB, Seiler GS, Deddens BL, Schubert AG, et al. A Platelet-Rich Plasma-Derived Biologic Clears *Staphylococcus aureus* Biofilms While Mitigating Cartilage Degeneration and Joint Inflammation in a Clinically Relevant Large Animal Infectious Arthritis Model. Front Cell Infect Microbiol. 2022;12:895022.